

Characterization of Tgl2, a putative lipase in the IMS of yeast mitochondria

Dissertation

der Mathematisch-Naturwissenschaftlichen Fakultät
der Eberhard-Karls-Universität Tübingen
zur Erlangung des Grades eines
Doktors der Naturwissenschaften
(Dr. rer. nat.)

vorgelegt von

Vitasta Tiku
aus Noida, Indien

Tübingen
2024

Gedruckt mit Genehmigung der Mathematisch-Naturwissenschaftlichen Fakultät der
Eberhard-Karls-Universität Tübingen.

Tag der mündlichen Qualifikation: **15.08.24**

Dekan der Math.-Nat. Fakultät: Prof. Dr. Thilo Stehle

1. Berichterstatter: PD Kai Stefan Dimmer

2. Berichterstatter: Prof. Dr. Ralf-Peter Jansen

Erklärung/Declaration

Ich erkläre, dass ich die zur Promotion eingereichte Arbeit mit dem Titel:

"Characterization of Tgl2, a putative lipase in the intermembrane space of yeast mitochondria"

selbständig verfasst, nur die angegebenen Quellen und Hilfsmittel benutzt und wörtlich oder inhaltlich übernommene Stellen als solche gekennzeichnet habe. Ich versichere an Eides statt, dass diese Angaben wahr sind und dass ich nichts verschwiegen habe. Mir ist bekannt, dass die falsche Abgabe einer Versicherung an Eides statt mit Freiheitsstrafe bis zu drei Jahren oder mit Geldstrafe bestraft wird.

I hereby declare that I have produced the work entitled:

"Characterization of Tgl2, a putative lipase in the intermembrane space of yeast mitochondria"

Submitted for the award of a doctorate, on my own (without external help), have used only the sources and aids indicated and have marked passages included from other works, whether verbatim or in content, as such. I swear upon oath that these statements are true and that I have not concealed anything. I am aware that making a false declaration under oath is punishable by a term of imprisonment of up to three years or by a fine.

Tübingen, den

.....

Datum / Date

.....

Unterschrift / Signature

„If you wish to make an apple pie from scratch, you must first invent the universe“

- Carl Sagan

Contents

List of abbreviations.....	
Summary	
Zusammenfassung	
List of publications contained in this thesis	
Introduction	1
1.1 Mitochondria: Origin and structure	1
1.2 Mitochondrial Targeting Signals.....	2
1.2.1 Matrix targeting signals: pre-sequence and its variations	2
1.2.2 Mitochondrial Inner Membrane targeting signals	3
1.2.3 Mitochondrial Outer Membrane targeting signals	4
1.2.4 Intermembrane Space targeting signals	4
1.3 Mitochondrial import pathways	5
1.3.1 TOM Complex: Main entry gate for mitochondrial proteins.....	5
1.3.2 TIM23 Complex: Translocation through the MIM.....	5
1.3.3 ATP-driven import into the matrix	6
1.3.4 Import and integration into the MIM.....	6
1.3.5 Import into the IMS.....	7
1.3.6 Import and integration into the MOM	8
1.3.6.1 Biogenesis of β -barrel proteins.....	8
1.3.6.2 Biogenesis of α -helical proteins.....	9
1.4 Crosstalk between mitochondria and other organelles.....	11
1.4.1 ERMES: ER-mitochondria encounter structures	11
1.4.2 vCLAMP: Vacuolar-mitochondria patch	12
1.4.3 Mitochondria and peroxisomes	12
1.4.4 Mitochondria and lipid droplets (LDs).....	12
1.5 Lipid biosynthesis in yeast cells.....	13
1.5.1 Neutral lipids are stored in LDs	14
1.5.2 Mitochondria have limited contribution to lipid biosynthesis	16
1.5.2.1 Cardiolipin biosynthesis	16
1.5.2.2 PE biosynthesis.....	16
1.5.2.3 Ups/PRELI complex mediated PL trafficking.....	16
1.5.2.4 Possible alternative routes.....	17

2 Research Objectives	19
Characterization of Tgl2, a putative lipase in yeast mitochondria.....	20
3.1 Introduction	21
3.2 Results.....	25
3.2.1 Tgl2 forms homodimers in the absence of a reducing agent.....	25
3.2.2 Tgl2 is a soluble protein associating with the mitochondrial inner membrane	27
3.2.3 Tgl2 is a subunit of a higher molecular weight complex.....	28
3.2.4 The MIM protease Yme1 mediates the quality control of Tgl2.....	31
3.2.5 Analysis of single cysteine residues of Tgl2.....	33
3.2.6 The predicted catalytic triad of Tgl2 is required for its functionality	35
3.2.7 Disruption of the catalytic triad affects protein stability	37
3.2.8 Genetic interactions of <i>MCP2</i> , <i>TGL2</i> , and <i>YME1</i> (performed by Dr Kai S Dimmer).....	39
3.2.9 Mitochondria lacking Tgl2 have elevated levels of neutral lipids	42
3.3 Discussion.....	44
Yeast mitochondria can process <i>de novo</i> designed β - barrel proteins	50
4.1 Introduction	51
4.2 Results.....	53
4.2.1 The assembly of the TMBs depends to a variable extent on the TOB/SAM complex.....	53
4.2.2 The POTRA domain is necessary for the oligomerization of Tmb2.3	55
4.2.3 Point mutation in the β -signal does not significantly alter the biogenesis of both TMBs	56
4.2.4 Absence of the small TIMs - Tim8 and Tim13, does not affect the import of the TMBs.....	57
4.3 Discussion.....	59
Acknowledgments.....	
References	
Appendix	

List of abbreviations

MIM	Inner mitochondrial membrane
IMS	Intermembrane space
MOM	Outer mitochondrial membrane
mtDNA	Mitochondrial DNA
TIM	Translocase of the inner membrane
TOM	Translocase of the outer membrane
TOB	Topogenesis of the outer membrane β -barrel protein
SAM	Sorting and assembling machinery
MPP	Mitochondrial processing peptidase
sTIMs	Small TIM chaperones
PAM	Presequence translocase-associated motor
MTS	Mitochondria targeting signal
OXA	Oxidase assembly
WT	Wild type
WCL	Whole cell lysate
C	Cytosol
SDS-PAGE	Sodium dodecyl sulfate polyacrylamide gel electrophoresis
BN-PAGE	Blue native-polyacrylamide gel electrophoresis
PL	Phospholipids
PA	Phosphatidic acid
CL	Cardiolipin
DAG	Diacylglycerol
TAG	Triacylglycerol
FA	Fatty acids
MS	Mass Spectrometry
PS	Phosphatidylserine
PE	Phosphatidylethanolamine
TLC	Thin layer chromatography

Summary

Yeast cells store excess lipids as steryl esters (SEs) and triacylglycerols (TAGs) in lipid droplets, preventing lipotoxicity and serving as energy reservoirs. When required, TAG lipases hydrolyze these TAGs into diacylglycerols (DAGs) and free fatty acids which can be used in various cellular pathways as signaling molecules, precursors for phospholipid biosynthesis, and more.

The yeast Tgl (triacylglycerol lipase) family of lipases includes Tgl1 through Tgl5, of which all members except Tgl2 are found in lipid droplets. While Tgl3, Tgl4 and Tgl5 have dual functions of a TAG lipase as well as an acyltransferase, Tgl1 is primarily an SE hydrolase with minimal lipase activity.

Tgl2 is an unusual member of the Tgl family due to its smaller size and mitochondrial localization. Predominantly homologous to bacterial lipases, Tgl2 shows lipolytic activity toward DAGs and TAGs and can complement for the loss of a DAG kinase in *E. coli*. The protein contains the conserved A/GXSXG lipase motif with a catalytically active serine, loss of which abrogates protein activity. Within the mitochondria, the protein localizes to the intermembrane space (IMS) and its import is regulated by the Mia40-dependent disulfide relay pathway. While a single deletion of *TGL2* has no growth defect, a combined Loss of *TGL2* and *MCP2*, an ERMES suppressor and was recently shown to be involved in CoQ metabolism, results in increased cellular TAG levels and a growth phenotype that can be rescued by reintroducing Tgl2.

In this study, we tried to characterize the protein in greater detail to get a better understanding of its molecular function. Tgl2 was found to homodimerize in the absence of reducing agents, likely due to disulfide bridges. Additionally, Tgl2 also forms a thiol-dependent complex in native PAGE. The lipase motif (A/GXSXG) mutant, S144A, which was previously reported to be essential for the protein's lipolytic activity was further characterized where the mutated protein behaved like the native variant on SDS- and native PAGE but fails to rescue the growth phenotype of $\Delta mcp2/\Delta tgl2$. We also identified the catalytic triad of Tgl2, consisting of Ser-Asp-His, and observed that mutating the aspartate residue (D259) in the active site resulted in protein instability as well as loss of enzymatic activity. Steady-state level analyses of non-functional Tgl2 variants revealed that Yme1 is the protease responsible for Tgl2's quality control. Finally, mitochondria lacking both *MCP2* and *TGL2* have increased TAG levels, indicating Tgl2's role as a TAG lipase. The contribution of *MCP2* to these observations remains an open question.

Collectively, these results provide greater insight into the structure-function relationship of Tgl2 and suggest evidence towards its role in lipid metabolism.

Zusammenfassung

Hefezellen speichern überschüssige Lipide als Sterylester (SEs) und Triacylglycerine (TAGs) in Lipidtröpfchen, um Lipotoxizität zu verhindern und als Energiereservoir zu dienen. Bei Bedarf hydrolysieren TAG-Lipasen diese TAGs zu Diacylglycerinen (DAGs) und freien Fettsäuren, die in verschiedenen zellulären Stoffwechselwegen als Signalmoleküle, Vorstufen für die Phospholipidbiosynthese und mehr verwendet werden können.

Zur Familie der Hefe-Tgl-Lipasen (Triacylglycerol-Lipase) gehören die Lipasen Tgl1 bis Tgl5, von denen alle Mitglieder außer Tgl2 in Lipidtröpfchen zu finden sind. Während Tgl3, Tgl4 und Tgl5 sowohl die Funktion einer TAG-Lipase als auch einer Acyltransferase haben, ist Tgl1 in erster Linie eine SE-Hydrolase mit minimaler Lipaseaktivität.

Tgl2 ist aufgrund seiner geringen Größe und seiner mitochondrialen Lokalisierung ein ungewöhnliches Mitglied der Tgl-Familie. Tgl2 ist überwiegend homolog zu bakteriellen Lipasen und zeigt lipolytische Aktivität gegenüber DAGs und TAGs und kann eine DAG-Kinase in *E. coli* ergänzen. Das Protein enthält das konservierte A/GXSXG-Lipase-Motiv mit einem katalytisch aktiven Serin, dessen Verlust die Proteinaktivität aufhebt. In den Mitochondrien ist das Protein im Intermembranraum (IMS) lokalisiert, und sein Import wird durch den Mia40-abhängigen Disulfid-Relais-Weg reguliert. Während eine einzelne Deletion von *TGL2* keinen Wachstumsdefekt verursacht, führt ein kombinierter Verlust von *TGL2* und *MCP2*, einem ERMES-Suppressor, von dem kürzlich gezeigt wurde, dass er am CoQ-Stoffwechsel beteiligt ist, zu

In dieser Studie haben wir versucht, das Protein genauer zu charakterisieren, um ein besseres Verständnis seiner molekularen Funktion zu erhalten. Es wurde festgestellt, dass Tgl2 in Abwesenheit von Reduktionsmitteln homodimerisiert, wahrscheinlich aufgrund von Disulfidbrücken. Darüber hinaus bildet Tgl2 in nativer PAGE auch einen thiolabhängigen Komplex. Die Lipase-Motiv (A/GXSXG)-Mutante S144A, von der zuvor berichtet wurde, dass sie für die lipolytische Aktivität des Proteins wesentlich ist, wurde weiter charakterisiert, wobei sich das mutierte Protein auf SDS- und nativer PAGE wie die native Variante verhielt, aber den Wachstumsphänotyp von $\Delta mcp2/\Delta tgl2$ nicht retten konnte. Wir identifizierten auch die katalytische Triade von Tgl2, die aus Ser-Asp-His besteht, und beobachteten, dass die Mutation des Aspartatrests (D259) im aktiven Zentrum zur Instabilität des Proteins und zum Verlust der enzymatischen Aktivität führte. Analysen von nicht-funktionellen Tgl2-Varianten im stationären Zustand zeigten, dass Yme1 die für die Qualitätskontrolle von Tgl2 verantwortliche Protease ist. Schließlich weisen Mitochondrien, denen sowohl *MCP2* als auch *TGL2* fehlt, erhöhte TAG-Spiegel auf, was auf die Rolle von Tgl2 als TAG-Lipase hinweist. Der Beitrag von *MCP2* zu diesen Beobachtungen bleibt eine offene Frage.

Insgesamt bieten meine Ergebnisse einen besseren Einblick in die Struktur-Funktions-Beziehung von Tgl2 und deuten auf seine Rolle im Lipidstoffwechsel hin.

List of publications contained in this thesis

Tiku, V., Tatsuta, T., Jung, M., Rapaport, D., Dimmer, K., (submitted, pre-print on BioRxiv).
Characterization of Tgl2, a putative lipase in yeast mitochondria. 10.1101/2024.05.08.593122.

Moitra, A., Tiku, V., Rapaport, D. (2024), Yeast mitochondria can process de novo designed β -barrel proteins. FEBS J, 291: 292-307. <https://doi.org/10.1111/febs.16950>

Introduction

1.1 Mitochondria: Origin and structure

Mitochondria have evolved from a bacterial progenitor through symbiosis wherein an α -proteobacterium was engulfed by a host cell. This event was followed by or accompanied with the evolution of the eukaryotic cell (Gray, 2012). During the course of evolution, most mitochondrial genes were transferred to the eukaryotic nucleus, leaving behind only a small subset in the mitochondrial DNA, all of which are essential for normal mitochondrial function (Petrungaro & Kornmann, 2019). Mitochondria were first described in the early 1800s as distinct granular structures in the cell. Improvements in staining and microscopy resolution revealed more accurate morphological features like the presence of 'threads' as well as a membrane (Physiologische Gesellschaft zu Berlin., 1898).

The ultrastructure of mitochondria was first revealed by electron tomography (ET) and has undergone massive refinement over the years with the development of cryo-ET (Palade, 1953; Petrungaro & Kornmann, 2019). As bilayered organelles separated from the cytoplasm by its inner (MIM) and outer (MOM) membranes, mitochondria consist of 2 distinct compartments. Each compartment has its own defined role and composition. The innermost compartment – matrix, is the equivalent of the bacterial cytoplasm and the intermembrane space, which separates the two membranes, is the equivalent of the periplasm (Hoffmann & Avers, 1973; Pellegrini, 1980).

The outer mitochondrial membrane (MOM) is rather porous and allows free diffusion of ions as well as small, uncharged molecules. This movement is facilitated by pore-forming membrane proteins like Porin/VDAC (voltage-dependent anion channel) that form channels in the MOM (Campo et al., 2017; Mertins et al., 2014; Petrungaro & Kornmann, 2019). Some MOM proteins form contact sites with other organelles. These contact sites are crucial for exchanging metabolites, lipids, and for maintaining mitochondrial morphology and inheritance (Eisenberg-Bord et al., 2016; Helle et al., 2013).

The inner mitochondrial membrane (MIM) is highly convoluted, and in contrast to the MOM, has a more selective diffusion barrier. Typically tubular and lamellar, these invaginations of the MIM, called cristae, house most of the proteins responsible for oxidative phosphorylation (Gupta & Becker, 2021; Rampelt et al., 2017). Movement across the MIM requires very specific and selective transport proteins. This ion-selective nature of the MIM is key for maintaining the electrochemical gradient in mitochondria (Petrungaro & Kornmann, 2019).

The intermembrane space (IMS) is the smallest and most constricted mitochondrial compartment, consisting of only ~5% of the mitochondrial proteome. IMS proteins show great variability in their structures, functions, and import mechanisms (Edwards et al., 2020). The IMS environment is considerably more oxidizing than the cytoplasm and matrix, which is conducive to a substantial number of IMS proteins that have functionally essential disulfide bonds (Gabriel et al., 2007; Hell, 2008; Herrmann & Köhl, 2007; Nakamoto & Bardwell, 2004).

The matrix is the innermost compartment and is also the site of mtDNA replication, transcription, protein biosynthesis, and a wide array of enzymatic reactions including the citric acid cycle (Petrungaro & Kornmann, 2019). The matrix has a mild alkaline environment (pH 7.9-8) and the difference in pH contributes to the electrochemical across the MIM required for driving ATP synthesis (Llopis et al., 1998).

The central role of mitochondria in bioenergetics, calcium signaling, apoptosis, and vital metabolic pathways including lipids, amino acids, and the biosynthesis of Fe-S clusters is proof that they are more than just the powerhouses of the cell. While the classical role of mitochondria is oxidative phosphorylation, disruption of the other functions has also been shown to have severe consequences for the cell. In humans, mitochondrial pathologies mostly affect tissues with a high-energy demand, leading to a wide spectrum of diseases affecting cardiovascular health, neurological and skeletal function, and more (Javadov et al., 2020).

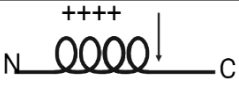

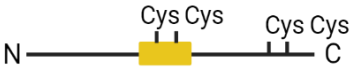

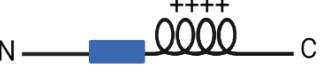



1.2 Mitochondrial Targeting Signals

Most mitochondrial proteins are synthesized in the cytosol as precursor proteins and are targeted to the mitochondria through distinct mitochondrial targeting signals (MTS). While the N-terminal, cleavable pre-sequence is the classical MTS, a considerable variety of internal and non-cleavable MTS have also been described over the years. Briefly, these targeting signals can be categorized into 1) linear targeting sequences either at the N-terminus or internal positions 2) multiple targeting sequences distributed across the protein sequence, allowing import in a loop-like fashion 3) distinct cysteine motifs enabling redox-mediated import. Table 1 gives a brief overview of different MTS and their characteristic features.

1.2.1 Matrix targeting signals: pre-sequence and its variations

The pre-sequence for matrix targeted proteins does not have any conserved residues but it does have a few characteristic features. The pre-sequence is typically 15-50 amino acids long (longer and shorter variations have been reported) and forms an amphipathic α -helix with a hydrophobic surface (Moberg et al., 2004; Petrungaro & Kornmann, 2019; Yamano et al., 2008). The pre-sequence presents its hydrophobic surface for recognition by Tom20 and the positively charged surface for recognition by Tom22. This is essential for the protein to be translocated across the MIM (Dekker et al., 1998). The pre-protein transverses across the TOM complex with the help of binding sites that have successively increasing affinity for the pre-sequence, with the highest affinity for the binding site at the IMS (Lee et al., 2012; Schatz, 1997). Once in the IMS, the pre-protein is threaded across the MIM through the TIM23 complex, with the help of membrane potential. Finally in the matrix, the pre-sequence is now cleaved by a soluble matrix protein, matrix pre-sequence peptidase (MPP), yielding the mature form of the protein. The MPP is essentially a heterodimer of Mas1 and Mas2, whose cleavage motif consists of 2 arginine residues and an aromatic residue (Taylor et al., 2001; Vögtle et al., 2017). Other matrix peptidases include IDE (in

Table 1: Targeting signals of mitochondrial precursor proteins (Adapted from Chacinska et al, 2005)

Type	Schematic	Import machinery	Cleavable/ Non-cleavable
Matrix proteins			
Amphipathic α -helical		TOM, TIM23, and PAM	Cleaved by MPP
Intermembrane Space proteins			
Bipartite sequence		TOM, TIM23, and PAM	Cleaved by MPP (1) and IMP (2)
Conserved cys motifs		TOM and MIA	Non-cleavable
Inner Membrane proteins			
Sorting pathway		TOM, TIM23, and PAM	Cleaved by MPP
Internal sorting signal		TOM and TIM23	Non-cleavable
Multiple internal sorting signals		TOM and TIM22	Non-cleavable
Outer Membrane proteins			
β -signal (■)		TOM and SAM/TOB	Non-cleavable
Signal anchor N-terminus (■), internal (■), C-terminus (■)		<ul style="list-style-type: none"> ■ MIM ■ TOM and SAM ■ Unknown 	Non-cleavable

humans) and Ste23 in yeast. Impairment in MPP function causes protein aggregation in mitochondria resulting in severe cellular defects (Küçükköse et al., 2020; Leissring et al., 2004).

1.2.2 Mitochondrial Inner Membrane targeting signals

MIM pre-proteins are imported through the TOM complex in a loop-like fashion, and their import is driven by IMS chaperones (Neupert & Herrmann, 2007). A number of MIM proteins contain the N-terminal MTS (cleavable or non-cleavable) and are imported like matrix-targeted proteins, arrested by the TIM23 complex, and finally directed into the MIM (Neupert, 1997; Schatz & Dobberstein, 1996; Voos et al., 1999). MIM proteins of the carrier proteins family consist of six α -

helical transmembrane domains and contain internal, non-cleavable targeting signals. This targeting information is distributed throughout the protein sequence and potentially recruits import receptors, facilitating membrane translocation (Curran et al., 2002; Vasiljev et al., 2004; Wiedemann et al., 2001). Moreover, these proteins also contain signals at their C-termini that are important for membrane insertion (Brandner et al., 2005). In the case of MIM proteins, the MTS is cleaved off by MPP and the sorting signal typically remains a part of the mature protein.

1.2.3 Mitochondrial Outer Membrane targeting signals

The MOM consists of two types of membrane proteins - α -helical and β -barrel proteins, neither of which has cleavable targeting signals. The β -barrel proteins contain a targeting signal at their C-terminus, called the β -signal, that allows recognition by Tom20 and subsequent translocation through the TOM complex (Jores et al., 2016; Kutik et al., 2008). While no characteristic targeting signals have been identified in α -helical MOM proteins, experimental data suggest that their positive charge and moderate hydrophobicity direct them towards the MOM. Depending on where one can find these sequences, α -helical MOM proteins can be divided into three classes – signal anchored (N-terminal MTS), tail anchored (C-terminal MTS), and polytopic (multiple transmembrane domains) proteins (Beilharz et al., 2003; Leissring et al., 2004; Setoguchi et al., 2006).

1.2.4 Intermembrane Space targeting signals

Proteins imported into the IMS constitute a wide range of targeting signals of which the bipartite sequence is the best-characterized one. Another commonly found targeting signal among IMS proteins are non-cleavable cysteine motifs. The bipartite sequence consists of an N-terminal pre-sequence followed by a hydrophobic stop-transfer domain. The stop-transfer domain arrests protein translocation by getting integrated into the MIM, further pulling the pre-protein through the TOM complex. The pre-sequence is then cleaved in the matrix by MPP, and the mature soluble protein is released into the IMS by a second cleavage event by IMP – inner membrane peptidase. (Esaki et al., 1999; Glick et al., 1992; Herrmann & Hell, 2005; Neupert, 1997). The IMP is a heterodimer of two N-terminally anchored proteins, Imp1 and Imp2, and requires a third protein – Som1 for proper proteolytic activity (Nunnari et al., 1993). For some IMS proteins like Mgm1, the sorting signal is cleaved by MIM proteases like the rhomboid protease Pcp1/Rbd1/Mdm37 (Esser et al., 2002; Herlan et al., 2003). Another peptidase, Oct1, cleaves an octapeptide sequence but its biological importance is unknown (Gakh et al., 2002)

A more commonly found targeting signal in IMS proteins is the mitochondrial intermembrane space signal (MISS). These are non-cleavable internal sequences, typically consisting of a characteristic CX₃C or CX₉C motif wherein the cysteine residues can form disulfide bonds with the IMS receptor, Mia40 (Milenkovic et al., 2007; Petrunger & Kornmann, 2019; Sideris & Tokatlidis, 2007). In addition to these covalent interactions, the pre-proteins possess a conserved hydrophobic residue which is crucial for substrate recognition by receptors (Banci et al., 2009; Petrunger & Kornmann, 2019).

Some IMS proteins like Cytb2 and Gpx3 have atypical targeting signals and are also imported differently.

1.3 Mitochondrial import pathways

1.3.1 TOM Complex: Main entry gate for mitochondrial proteins

The translocase of the outer membrane (TOM complex) is responsible for the recognition and translocation of most of the mitochondrial proteome. Figure 1 gives a brief overview of the different protein import pathways into mitochondria. The TOM complex consists of three receptors – Tom20, Tom22, and Tom70/Tom71 and has additional subunits – Tom5, Tom6, and Tom7, which are responsible for its stability (Brix et al., 1997). The central component of the TOM complex is Tom40, an integral membrane β -barrel protein that allows translocation of pre-proteins through its pore. Tom40 oligomerizes to form two or three channels per TOM complex, and its core is lined with hydrophilic and hydrophobic residues that are used differentially by pre-proteins to be translocated through the MOM (Kiebler et al., 1993; van Wilpe et al., 1999; Wiedemann & Pfanner, 2017; Yamano et al., 2008).

Broadly, there are two different mechanisms for translocation through the TOM complex. Pre-sequence containing proteins are translocated as loosely-folded, linear peptides whose amphipathic helix is recognized by Tom20 followed by recognition of the conserved positively charged surface by Tom22. The pre-protein then sequentially binds to Tom5, Tom6, and Tom7 and is finally received by the IMS domain of Tom22 (Chacinska et al., 2005; Endo et al., 2003; Kanamori et al., 1999; Komiya et al., 1998). On the other hand, Tom70/Tom71 recognize proteins containing internal targeting sequences (like those of the carrier proteins family) and then transfers them to Tom22. These pre-proteins are translocated in a looped formation with both the termini facing the cytosol (Brix et al., 1997; Kiebler et al., 1993; van Wilpe et al., 1999).

1.3.2 TIM23 Complex: Translocation through the MIM

Once the pre-proteins have translocated through the TOM complex, they are further processed by the TIM23 complex which can direct the pre-proteins either to the matrix or to the MIM (Schulz et al., 2015; van der Laan et al., 2013). Of the subunits of the TIM23 complex, Tim50 serves as a receptor that binds to the incoming pre-protein from the IMS side of Tom40-Tom22 and, in cooperation with Tim21, activates the pore-forming Tim23. In the absence of a pre-protein, Tim50 keeps the TIM23 channel closed to prevent ion leakage (Meinecke et al., 2006). The negative membrane potential on the matrix side exerts an electrophoretic effect on the positively charged pre-protein, driving translocation through the Tim23 channel (Alder et al., 2008; Chacinska et al., 2005; Meinecke et al., 2006; Mokranjac et al., 2009; Tamura, Harada, et al., 2009). Another subunit of this complex, Tim17, is involved in the sorting of the pre-protein into the lipid membrane (Chacinska et al., 2005; Martinez-Caballero et al., 2007). Very recently performed structural and biochemical analyses of the TIM23 complex report that Tim17, and not Tim23, is the major component for protein import through this complex. Crosslinking-based approaches revealed that a negatively- charged stretch on Tim17 engages with the pre-protein, and the

hydrophobic cavity of the protein allows translocation across the MIM. This model also suggests that Tim23 merely stabilizes the TIM23 translocase (Fielden et al., 2023; Sim et al., 2023; Wasilewski et al., 2023).

Proteins that are sorted into the MIM contains a hydrophobic sorting or stop-transfer sequence which is recognized by Mgr2 – a lateral gatekeeper that enables the release of these proteins into the membrane. Tim21 also links the TIM23 complex (associated with Mgr2) and Complex III and Complex IV of the respiratory chain complex to promote the release of the pre-protein (Glick et al., 1992; Ieva et al., 2014).

1.3.3 ATP-driven import into the matrix

While membrane potential is sufficient for translocation through the TIM23 channel and lateral insertion into the MIM, pre-proteins of the matrix require an ATP driven molecular motor for their import (van der Laan et al., 2007). The pre-sequence translocase-associated motor (PAM) consists of several essential components. Tim44 couples the mitochondrial heat-shock protein 70 (mtHsp70) to the Tim23 channel, transferring the unfolded peptide to the chaperone. Once with mtHsp70, the release of the pre-protein is stimulated by two membrane bound co-chaperones Pam16/Tim16 and Pam18/Tim14 that regulate the ATP activity of mtHsp70. Finally, Mge1 – a nucleotide exchange factor, promotes the release of ADP from mtHsp70 to initiate a new reaction cycle (Banerjee et al., 2015; Popov-Čeleketić et al., 2008; Ting et al., 2014). So far, two models have been proposed to describe the mechanism of PAM: The Brownian ratchet suggests that the tight binding of mtHsp70 to the pre-protein prevents backtracking through the import channels and allows the polypeptide to slide inwards until another molecular of mtHsp70 binds to it. This sequential ATP-dependent binding and release of mtHsp70 imports the polypeptide into the matrix. The pulling model suggests that mtHsp70 is bound to Tim44 and interacts with the transiting polypeptide. The ATP dependent conformational changes in mtHsp70 generate an inwards force so that another molecular of the chaperone can bind to the polypeptide. This binding and pulling motion continues until the pre-protein is imported into the matrix (Banerjee et al., 2015; De Los Rios et al., 2006; Horst et al., 1997; Kang et al., 1990).

The pre-sequences of matrix and MIM proteins are processed by the MPP and the residual pre-sequence peptide is degraded by the matrix peptidosome – PreP or Cym1 (Johnson et al., 2006; Mossmann et al., 2014). Some MIM sorted pre-proteins undergo two cleavage events – by MPP in the matrix and by IMP to remove the hydrophobic sorting sequence that releases the mature protein in the IMS or leaves it anchored in the MIM (Glick et al., 1992).

1.3.4 Import and integration into the MIM

Protein import and membrane integration of MIM proteins is divided into two models: the stop transfer pathway (as described in 1.3.2) or conservative sorting. Pre-proteins encoded by the mitochondria genome follow the conservative sorting mechanism and are exported into the MIM by Oxa1. These pre-proteins are co-translationally inserted into the MIM by Oxa1 and Mba1 (Pfeffer et al., 2015). More recently, Oxa1 has been shown to also sort nuclear-encoded proteins

including precursors of the TOM and TIM23 complex, as well as the carrier translocase TIM22. These proteins are imported via the TOM40 and TIM23-PAM complexes, and inserted into the MIM with the help of Oxa1 (Hildenbeutel et al., 2012; Stiller et al., 2016). More thorough systematic analyses concluded that single-spanning cleavable MIM proteins are inserted via the stop-transfer pathway and multi-spanning cleavable ones use a combination of stop-transfer and conservative sorting mechanisms (Park et al., 2013; Stiller et al., 2016).

The import of MIM carrier proteins relies on the TIM22 complex. These metabolite carriers have internal targeting sequences and six α -helices. Due to their high hydrophobicity, cytosolic chaperones like Hsp90 and Hsp70 maintain these proteins in an import competent formation and recruit them to the mitochondrial receptor, Tom70 (Young et al., 2003). The import of some carrier proteins is regulated by the cellular energy levels that can affect the phosphorylation status of Tom70, rendering them active or inactive (Kliza et al., 2021; O. Schmidt et al., 2011). Once these pre-proteins are through the TOM complex, they are bound by a helical wheel-like complex of Tim9 and Tim10 at the IMS which further interacts with MIM-bound Tim12 (Neupert & Herrmann, 2007). This complex of Tim9, Tim10, and Tim12 is suggested to tether to Tim54, the membrane integrated subunit of the TIM22 complex with a large IMS exposed domain (Petrungaro & Kornmann, 2019; Rehling et al., 2003, 2004; Sirrenberg et al., 1998). Tim22 serves as the central pore of this complex and allows for membrane potential dependent release of the carrier proteins into the MIM.

1.3.5 Import into the IMS

All IMS proteins are encoded by nuclear DNA. These proteins are recognized by and imported via either characteristic bipartite sequence or distinct cysteine motifs. Proteins with these cysteine motifs also contain a 9 amino acids long ITS (MISS) which is essential for protein targeting into the IMS. While proteins with a bipartite sequence are imported in an ATP independent manner wherein two cleavage events – by MPP in the matrix and IMP in the IMS, releases the mature protein in the IMS, the population with characteristic cysteine motifs relies on the disulfide relay or Mia40 import pathway (Petrungaro & Kornmann, 2019; Sideris et al., 2009).

Mia40 is bound to the MIM with its C-terminus accessibly protruding into the IMS. The C-terminus of Mia40 contains a CPC (cys-pro-cys) motif that forms transient disulfide bonds with precursors, trapping them in the IMS (Chacinska et al., 2004; Müller et al., 2008). In yeast, Fcj1 or Mitofilin recruits Mia40 to the IMS side of the TOM complex by structuring contact sites between the MOM and MIM (von der Malsburg et al., 2011). This increases the proximity of the incoming precursors with Mia40. In lower eukaryotes, Mia40 is a large protein with a cleavable presequence, but in higher eukaryotes it is rather small consisting of only the conserved C-terminal domain with active cysteines and no pre-sequence (Banci et al., 2009; Chacinska et al., 2004, 2008; Grumbt et al., 2007). For the incoming pre-protein to mature and release into the IMS, Mia40 catalyzes the formation of intramolecular disulfide bonds within the pre-protein, and in-turn gets re-oxidized by Erv1 with the help of Hot13 to initiate a new cycle (Chacinska et al., 2004; Grumbt et al., 2007; Müller et al., 2008). Erv1 is a FAD linked sulfhydryl oxidase that homodimerizes to enable electron

exchange. This dimerization is crucial for the activity of the protein. Erv1 accepts electrons from Mia40 via its shuttle cysteine motif. Next, the electrons are passed onto a central CXXC motif within Erv1, to covalently bound FAD, and finally shuttled to cytochrome c (cyt-c), cyt-c oxidase, and cyt-c peroxidase or O₂ is used resulting in hydrogen peroxide production (Dabir et al., 2007; Farrell & Thorpe, 2005). Erv1 directly associates with Mia40 and the precursor proteins to form a ternary complex that might be involved in assisting the formation of multiple cysteine bonds in the protein. This 'disulfide channeling' minimizes alternative contacts between the substrate, Mia40, and Erv1. (Banci et al., 2011; Bihlmaier et al., 2007; Mesecke et al., 2005; Stojanovski et al., 2008). Additionally, the yeast thiol peroxidase Gpx3 was also reported to maintain the redox state of Mia40 (Edwards et al., 2021)

Some substrates of the Mia40 pathway, like Tim22, do not contain canonical cysteine motifs but still solely depend on it for their import (Chatzi et al., 2016).

1.3.6 Import and integration into the MOM

All MOM proteins are synthesized on cytosolic ribosomes and are maintained in an import competent fashion by cytosolic chaperones like Hsp70 and their co-chaperones (Jores et al., 2018). These proteins can be divided into two major membrane protein classes, α -helical and β -barrel proteins.

1.3.6.1 Biogenesis of β -barrel proteins

β -Barrel proteins are inserted into the membrane with the help of multiple anti-parallel, transmembrane β -strands. These proteins are exclusively found in organelles originating from an endosymbiotic event. Some major MOM β -barrel proteins are Tom40, Porin, Sam50/Tob55, and Mdm10. Precursors of β -barrel proteins are targeted to the Tom40 channel where they are recognized by Tom20 and Tom70, translocated to the IMS, where Tim9-Tim10 and Tim8-Tim13 complexes guide these pre-proteins to the SAM (Sorting and Assembly Machinery) complex (Habib et al., 2005; Jores et al., 2016; Paschen et al., 2003; Wiedemann et al., 2003). The TOM and SAM complexes are linked by the cytosolic domains of their subunits Tom22 and Sam37, respectively, which makes substrate handover easier (Qiu et al., 2013; Wenz et al., 2015). Thus, the biogenesis of Tom40 requires a pre-existing mature TOM complex for its import.

Once in the membrane, these β -barrel proteins mature by oligomerizing (Porin) or by associating with the subunits of its complex (Tom40). Mdm10 is another MOM β -barrel protein involved in the assembly of MOM protein complexes. Found in association with two major protein complexes, ERMES and TOB/SAM, Mdm10 promotes the release of Tom40 from the TOB/SAM complex and promotes the integration of Tom22 into the MOM. This in turn enables the formation of the TOM complex (Meisinger et al., 2004; Petrunaro & Kornmann, 2019; Wideman et al., 2010; Yamano et al., 2010b). More recently, Porin/VDAC has also been shown to modulate the assembly of the TOM complex.

1.3.6.2 Biogenesis of α -helical proteins

α -helical MOM proteins are also synthesized on cytosolic ribosomes and brought to the mitochondrial receptors Tom20 and Tom70 with the help of chaperones (Cichocki et al., 2018; Opaliński et al., 2018; Papić et al., 2013). Mutations or loss of the targeting sequence in these proteins leads to mislocalization to the ER or peroxisomes (Cichocki et al., 2018; Okreglak & Walter, 2014; Vitali et al., 2018). So far, no clear import machinery has been identified for the insertion of these proteins. The MOM insertase Mim1 is suggested to promote the insertion of tail-anchored MOM proteins (Becker et al., 2008; Popov-Celeketić et al., 2008). Other mechanisms for membrane integration include contribution of the SAM complex as well (Otera et al., 2007; Petrunaro & Kornmann, 2019). For some tail-anchored proteins, membrane lipid composition has been shown to affect membrane targeting and insertion (Krumpe et al., 2012).

Multi-spanning MOM proteins like Ugo1 are recognized by Tom70 and transferred to the MIM complex that integrates them into the membrane (Becker et al., 2011; Dimmer et al., 2012). The MIM complex consists of Mim1 and Mim2, but the exact stoichiometry is still unknown. While mutational studies have confirmed that oligomerization of Mim1 is essential for the complex, the precise structure and molecular mechanism of the complex still need to be studied (Dimmer et al., 2012; Popov-Celeketić et al., 2008).

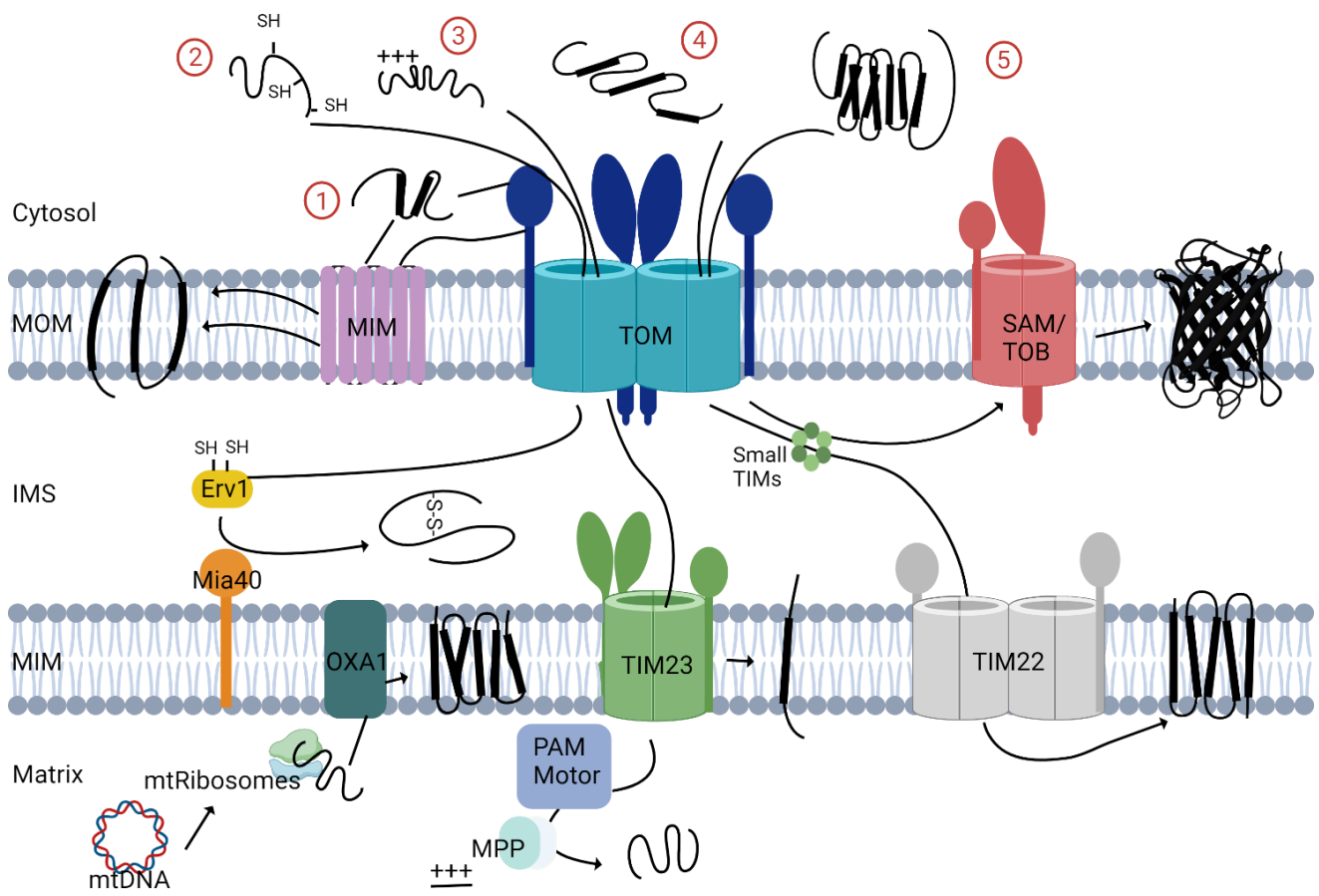


Figure 1. Protein import pathways of mitochondrial proteins.

Most mitochondrial proteins are synthesized on cytosolic ribosomes and translocated into the mitochondria through the TOM (translocase of the outer membrane) complex. After import, various protein translocases sort the precursor proteins into different mitochondrial subcompartments. The mitochondrial import (MIM) complex inserts proteins with α -helical membrane into the outer membrane (1). The mitochondrial intermembrane space import and assembly (MIA) pathway facilitates the uptake and oxidative folding of cysteine-rich proteins into the intermembrane space (2). The presequence translocase (TIM23 complex) transports precursors with a cleavable presequence across the inner membrane in a membrane potential-dependent manner ($\Delta\psi$). These pre-proteins are either inserted into the MIM or the presequence translocase-associated motor (PAM) uses ATP hydrolysis to drive them into the matrix where the mitochondrial processing peptidase (MPP) removes the presequence (3). Additionally, small TIM proteins transfer hydrophobic carriers to the carrier translocase (TIM22 complex), which then inserts these carrier proteins into the inner membrane, also in a membrane potential-dependent manner (4). The sorting assembly machinery (SAM complex) integrates β -barrel proteins into the outer membrane, with small TIM proteins assisting their transfer from the TOM complex to the SAM complex (5). MOM stands for mitochondrial outer membrane, IMS for intermembrane space, and MIM for mitochondrial inner membrane.

1.4 Crosstalk between mitochondria and other organelles

Mitochondria maintain their different functions by forming functionally essential contacts with most organelles in the cell. These contact sites are regions of very close apposition between the organellar membranes with a defined proteome and lipidome. In the past decades, several mitochondrial contact sites have been identified and/or suggested, existing in variable numbers and with distinct functions.

1.4.1 ERMES: ER-mitochondria encounter structures

The ER is the central hub of phospholipid synthesis in the cell. These lipids and lipid precursors are then distributed to other organelles as well as the plasma membrane, either through vesicular transport or through contact sites. While initial studies suggested the role of lipid transfer proteins (LTPs) in transporting lipids from one organelle to another by hosting them in a hydrophobic cavity, the discovery of ER-mitochondria contact sites suggests an alternative pathway for lipid exchange.

Initially identified in a high throughput screen in yeast, the ERMES (ER-mitochondria encounter structure) complex is made of both membrane-bound and soluble proteins and has a distinct role in mitochondrial distribution and physiology. Mutations in any component of this complex yield swollen, aggregated mitochondria (Berger et al., 1997; Petrunaro & Kornmann, 2019, 2019; Sogo & Yaffe, 1994). The core components of the complex are Mdm10, Mdm12, Mdm34, and Mmm1, all stably interacting at the interface of mitochondria and ER (Berger et al., 1997; Ellenrieder et al., 2016; Flinner et al., 2013; Sogo & Yaffe, 1994). Mdm10 is a β -barrel protein also associated with the SAM/TOB complex of the MOM and is suggested to aid protein assembly and insertion. Mdm12, Mdm34, and Mmm1 share a protein domain, the SMP (found in Synaptotagmin-like Mitochondrial and lipid-binding Protein) domain. As the name suggests, the SMP domain is essentially an elongated, hydrophobic cavity with an affinity for lipids (AhYoung et al., 2015). Multiple studies have confirmed the lipid binding and transporting activity of Mmm1 and Mdm12, at least in liposomes, and this feature of the ERMES complex components makes it a suitable candidate for lipid import into mitochondria (AhYoung et al., 2015; Petrunaro & Kornmann, 2019). However, ERMES mutants are still able to import lipids into the mitochondria, which can be attributed to the inconsistent rescue-ability of the different ERMES components. Mutants of *MDM12* and *MDM34* can be easily rescued by artificial tethers between ER and mitochondria. On the other hand, *MMM1* and *MDM10* mutants are only poorly rescued by this artificial protein (Petrunaro & Kornmann, 2019). These observations and the fact that mitochondria lacking ERMES components are viable and possess lipids in their membranes, suggests that there are alternative pathways for lipid import into the mitochondria (Petrunaro & Kornmann, 2019, 2019).

Over the years, many genes with the ability to suppress the phenotypes of ERMES mutations have been identified. Overexpressing *Mcp1*, a MOM protein, and *Mcp2*, a MIM protein, can suppress the phenotype of cells lacking *MDM10* (Tan et al., 2013). Both proteins have also been shown to restore the anomalous lipid composition of *mdm10* Δ cells (Tan et al., 2013). Other studies to identify ERMES suppressors yielded *Vps39* and *Vps13*, both involved in mitochondrial contact sites and will be discussed in the next section (Lang et al., 2015; Petrunaro & Kornmann, 2019).

MAMs (mitochondria-associated ER membranes) have been identified in mammalian cells but there is still some speculation about the composition of these sites. So far, the involvement of Mitofusin 2 (MFN2) – a MOM protein also localizing to the ER membrane as well as membrane structures consisting of VDAC1 and IP3R (inositol receptor on the ER membrane) have been reported (de Brito & Scorrano, 2008; Szabadkai et al., 2006).

1.4.2 vCLAMP: Vacuolar-mitochondria patch

The discovery of high-copy ERMES suppressors like Mcp1 and Mcp2 was an indication that mitochondria can receive lipids from potentially redundant pathways. In a high-throughput screen, Schuldiner et al discovered two vacuolar proteins – Vps39 and Vam7, whose absence led to an increase in ERMES sites in the cell (Hönscher et al., 2014; Petrunaro & Kornmann, 2019). Vps39 is a subunit of the HOPS (homotypic fusion and protein sorting) complex that facilitates fusion events at the vacuole (Bröcker et al., 2012; Seals et al., 2000). As a tethering protein, it was also reported to generate contact sites between vacuoles and mitochondria (with Tom40). This contact site, vCLAMP, is functionally and structurally distinct from the HOPS complex, as Vps39 was able to form the vCLAMP complex even in the absence of HOPS components (Hönscher et al., 2014; Petrunaro & Kornmann, 2019). Overexpression of Vps39 could rescue growth defects associated with the ERMES complex, and the absence of both vCLAMP and ERMES complexes yielded unviable cells (González Montoro et al., 2018; Petrunaro & Kornmann, 2019).

Mcp1 was also reported to interact with Vps13, an endosomal fusion protein. Overexpressing Vps13 could rescue the phenotype of ERMES mutants, suggesting its involvement in an ERMES bypass pathway (Lang et al., 2015). Since Vps13 is found in different organelle contact sites, it allows Mcp1 to interact with vacuoles and endosomes. Moreover, Vps13 harbors a lipid-transport domain which can accommodate several lipid molecules, indicating a potential contribution to lipid exchange (John Peter et al., 2017; Kumar et al., 2018).

1.4.3 Mitochondria and peroxisomes

Peroxisomes are very often found in close proximity to mitochondria or near ER-mitochondrial contact sites. Since mitochondria and peroxisomes are co-dependent for metabolic pathways including organelle division, there is much speculation about them sharing physical tethers (Delille et al., 2009; Fransen et al., 2012; Wanders, 2014). The localization of peroxisomes near ER-mitochondrial contact sites indicates a possibility of a three-way junction (Cohen et al., 2014). While proteins such as Pex11 and Mdm34 were initially suggested to form these tethers, recent split-Venus based discovered Fzo1 and Pex34 as contact sites proteins between mitochondria and peroxisomes (Mattiuzzi Ušaj et al., 2015; Shai et al., 2018).

1.4.4 Mitochondria and lipid droplets (LDs)

LDs store neutral lipids that can be utilized for energy production under conditions of stress. Since mitochondria house the enzymes responsible for energy metabolism, contact sites between the two organelles would ensure efficient substrate handover.

In mammalian cells, PLIN5 (Perilipin 5) has been suggested to act as a tether between LD and mitochondria in highly oxidative tissues (Wang et al., 2011; Boutant et al., 2017; Gemmink et al., 2018; Kimmel & Sztalryd, 2016). PLIN5 has been reported to interact with Mitofusin 2 (MFN2) and its overexpression induces recruitment of mitochondria and LDs towards each other (Boutant et al., 2017). Another protein that has been suggested to tether mitochondria and LDs is SNAP23, a SNARE protein in mouse fibroblasts. Depletion of this protein results in decreases organellar interaction, but the mechanism of this observation is unknown (Jägerström et al., 2009). The vacuolar protein Vps13 has also been shown to bind to LDs through its V-shaped alpha helices at the C-terminus and to mitochondria via its N-terminus (Li et al., 2020). Moreover, Vps13 has been shown to bind to fatty acids *in vitro*, but whether it's capable of doing the same *in vivo* is still unconfirmed (Kumar et al., 2018; Li et al., 2020). MIGA2, a MOM protein with a similar C-terminal structure as Vps13, is also suggested to facilitate LD-mitochondria contact sites (Freyre et al., 2019).

In yeast, several large-scale studies have been conducted to identify LD-mitochondria contact sites. One of these was a bimolecular fluorescence (BiFC) study which revealed Erg6 and Pet10 as putative subunits of tethering complexes between the two organelles (Pu et al., 2011). Meanwhile, Enkler et al have identified Arf1 as a regulator of contact sites between LD-mitochondria, LD-peroxisomes, or all three (Enkler et al., 2023). The same study reports that Arf1 can change membrane properties to regulate contact site formation, and its overexpression can recruit factors to increase these organellar junctions (Enkler et al., 2023).

1.5 Lipid biosynthesis in yeast cells

Lipids are not only important structural components of membranes but also play an important role in energy metabolism, apoptosis, as signaling molecules, and more. Cellular lipids can be broadly categorized into fatty acids, membrane lipids (phospholipids, sphingolipids, and sterols), and storage lipids (TAGs, steryl esters) (Klug & Daum, 2014).

Fatty acids (FAs) are the building blocks of most lipids. In yeast, FAs are either synthesized *de novo* or obtained from the hydrolysis of complex lipids. The most abundant FAs in yeast are palmitoleic acid, oleic acid, palmitic acid, and stearic acid (Tuller et al., 1999; Viljoen et al., 1986). Moreover, the composition of FAs varies between different organelles, and can also depend on growth conditions. The biosynthesis of FAs occurs primarily in the cytosol and selectively in mitochondria, and further modifications take place in the ER. Yeast can also take up FAs from their environment through diffusion or with the help of transporters. These FAs are then used for synthesizing phospholipids, stored as neutral lipids by the cell, or undergo β -oxidation in peroxisomes.

The major PLs in *S. cerevisiae* are phosphatidylcholine (PC), phosphatidylserine (PS), phosphatidylinositol (PI), and phosphatidylethanolamine (PE). Other than PLs, another class of membrane lipids that is essential for cells is sterols. Ergosterol is the predominant sterol in yeast, and cholesterol in mammals.

Phosphatidic acid (PA) is the central metabolite for the biosynthesis of phospholipids. Derived from glycerol-3-phosphate (from glucose metabolism), PA can either enter the lipid storage pathway or participate in PL biosynthesis (Athenstaedt & Daum, 1997; Horst et al., 1997). PA can be converted to cytidine di-phosphate diacylglycerol (CDP-DAG) by Cds1 (in ER) or Tam41 (in mitochondria) (Shen et al., 1996; Tamura et al., 2013). CDP-DAG is the main precursor molecular for other PLs, and depending on which head group it conjugates with, forms either PS, PI, or PGP (phosphatidylglycerolphosphate).

To form PE, PS is decarboxylated by Psd1 (in the MIM) or Psd2 (in Golgi/vacuoles) (E. Y. L. Chan & McQuibban, 2012; Trotter & Voelker, 1995). PE is then successively methylated, thrice, by Cho2 and Opi3 to yield PC (Kodaki & Yamashita, 1989). Both PE and PC can also be synthesized via the Kennedy pathway in the ER wherein exogenous ethanolamine or choline are taken up through specific transporters, phosphorylated, and conjugated with diacylglycerol. This final reaction is catalysed by phosphotransferases – Ept1 or Cpt1 (Bürgermeister et al., 2004; Hjelmstad & Bell, 1990). Interestingly, the formation of DAG from PA is a bi-directional reaction, and PA can be resynthesized from DAGs by the DAG kinase Dgk1 (Han et al., 2008).

The turnover of PLs is maintained by several enzymes including phospholipases, phosphatases, and remodeling enzymes like acyltransferases and transacylases.

1.5.1 Neutral lipids are stored in LDs

The term lipotoxicity was first used to describe the severe effects of free FAs overload on pancreatic islets. In yeast too, an excess of lipids can cause stress and eventually cell death. To circumvent this, free FAs and sterols are converted to neutral lipids like triacylglycerols (TAGs) and sterol esters (SEs) and stored in LDs (Obaseki et al., 2024).

Since the enzymes required for neutral lipid synthesis reside in the ER, LDs develop from or close to the ER membrane. Currently, there are several models to explain the formation of LDs from ER. The ER budding model proposes that LDs grow from the ER bilayer and eventually bud off, as TAGs begin to accumulate between the two leaflets. The bicelle formation model suggests that both leaflets of the ER membrane contribute to the formation of a PL monolayer by encasing neutral lipids. According to the lensing model, the outer leaflet stretches to accommodate neutral lipids until the lens buds off (Ploegh, 2007), and finally the vesicular budding model suggests the formation of a bilayer vesicle which is subsequently filled by neutral lipids (Walther & Farese, 2009) (Walther & Farese, 2012).

When not involved in PL biosynthesis, PA can be cleaved by phosphatases like Pah1 to generate DAGs, which are the precursors for TAG synthesis (Grimsey et al., 2008). DAGs can also be acquired from the degradation of phospholipids by phospholipases or deacylation of TAGs. Acyltransferases such as Dga1 and Lro1 can then create TAGs either using in an acyl-coA dependent reaction as for Dga1 or using PL, as is observed for Lro1 (Oelkers et al., 2000; Sorger & Daum, 2003).

The second major component of LDs are SEs which are synthesized by two enzymes – Are1 and Are2, both located at the ER. These enzymes catalyse a reaction between ergosterol (both Are1 and Are2) or lanosterol (only Are1) precursors with activated FAs to form SEs. Are1 and Are2 are the main SE synthases in yeast and have also been reported to show minor acyltransferases activity (Yang et al., 1996; C. Yu et al., 1996; Zweytick et al., 2000).

All the enzymes required for neutral lipids synthesis are found in the ER, or dually localized to LDs and ER. A quadruple deletion of *ARE1/ARE2/DGA1/LRO1*, while viable, is completely devoid of LDs (Sandager et al., 2002).

When required, TAGs and SE can be mobilized from LDs to provide DAGs, FAs, and sterols for various cellular processes. The degradation of TAGs is catalyzed by TAG lipases of the Tgl family: Tgl3, Tgl4, and Tgl5, all localizing to the LDs (Athenstaedt & Daum, 2003; Grillitsch & Daum, 2011). More recently, Ayr1, a bifunctional TAG lipase and acyltransferase has also been recognized and it localizes to LDs as well as the MOM (Ploier et al., 2013; Zahedi et al., 2006). SE hydrolysis is achieved by Tgl1, Yeh1, and Yeh2 of which Tgl1 and Yeh1 are found in LDs while Yeh2 is localized to the plasma membrane (Köffel et al., 2005).

A fifth TAG lipase, Tgl2, was identified in yeast mitochondrial fractions but its physiological relevance is still undefined (Ham et al., 2010).

1.5.2 Mitochondria have limited contribution to lipid biosynthesis

Mitochondrial lipid homeostasis depends on acquiring lipids from associated organelles such as ER and *in organello* synthesis of some PLs, primarily cardiolipin (CL). Once imported, these lipids have to be trafficked between the MIM and MOM as well the leaflets of the individual membranes (Tatsuta & Langer, 2017).

1.5.2.1 Cardiolipin biosynthesis

Cardiolipin (CL) is a PL exclusive to the mitochondria and is synthesized at the matrix site of the MIM using precursors from the ER. PA from the ER is transported from the MOM to the MIM by the heterodimeric Ups1/Mdm35 (yeast) or PRELID1-TRIAP1 (mammals) complex (Miliara et al., 2015; Potting et al., 2010; Tamura, Onguka, Hobbs, et al., 2012). The loss of these transporter proteins does not result in a complete loss of mitochondrial CL, suggesting a redundant mechanism.

A biosynthesis cascade converts PA to CL at the MIM, where the final step is a reaction between CDP-DAG and PG catalysed by Crd1 (Connerth et al., 2012; Tamura et al., 2013). The newly synthesized CL often contains saturated acyl chains which need to be remodeled. This is a reversible reaction catalyzed by Cld1 to yield mono-lyso CL (MLCL), and is reversed by Taz1 (Baile et al., 2013). Interestingly, Taz1 is found at both the mitochondrial membranes indicating that MLCL could be transported between the two membranes (Claypool et al., 2008; Y.-W. Lu et al., 2016). Defects in CL remodeling and biosynthesis causes severe defects in humans such as ataxia, Sengers syndrome, Barth syndrome, and several metabolic disorders (Bertero et al., 2020).

1.5.2.2 PE biosynthesis

Mitochondria also contain PE in notable amounts, especially in the MOM. It is either generated from decarboxylation of PS by Psd1, a MIM protein, or through the Kennedy pathway in the ER (E. Y. L. Chan & McQuibban, 2012; Trotter et al., 1995). To be decarboxylated, PS needs to be transported across the IMS by PS-specific lipid transporter protein complex, Ups2-Mdm35 (yeast) or SLMO2-TRIAP1 (mammals). PS can also be decarboxylated in the MOM, but this depends on efficient membrane apposition by the MICOS (mitochondria-cristae organization site) complex (Birner et al., 2001; Miyata et al., 2016; Trotter et al., 1995). The MICOS complex enables the MIM and MOM to be in close proximity and its disruption severely disturbs the mitochondrial ultrastructure as well as PE biosynthesis. In experiments employing artificial protein tethers to restore MICOS like MOM-MIM apposition, PE-related defects could be recovered (Aaltonen et al., 2016).

1.5.2.3 Ups/PRELI complex mediated PL trafficking

Ups1 was first identified as an important factor for the biogenesis of the mitochondrial fusion protein, Mgm1. The observation that the loss of Ups1 also leads to a decrease in mitochondrial CL amounts was an indication of its contribution to lipid metabolism (Osman et al., 2009; Tamura, Endo, et al., 2009). This was subsequently proven when Ups1 and Mdm35 were co-purified and tested for binding PLs in liposomes (Potting et al., 2010; Tamura et al., 2010). The complex could

bind to PA, CL, PG, PS, PI, and CDP-DAG and could also transfer PA between liposomes (Connerth et al., 2012). Ups1 has two homologues – Ups2 and Ups3, both capable of binding to Mdm35. Moreover, Ups2 can compensate for the CL decrease in cells lacking *UPS1* (Aaltonen et al., 2016; Miyata et al., 2016). Further biochemical analysis and pulse-chase experiments suggest that Ups1 and Ups2 regulate PE levels in the cell, perhaps even antagonistically. While Ups1 facilitates PE export from the MIM to the MOM, and accelerates the conversion of PE to PC, Ups2 prevents PE hydrolysis and export from the MIM (Horvath & Daum, 2013; Tamura, Onguka, Hobbs, et al., 2012; Tamura, Onguka, Itoh, et al., 2012). Despite its important lipid transport activity, Ups1 is dispensable for PA transport *in vivo*.

The Ups1/Mdm35 complex interacts with the membrane via the membrane binding residues of Ups1, and the transfer activity is mediated by very fine conformational changes in the proteins. Ups1 possesses a flexible loop and a long, mobile C-terminal helix that can function as a lid. As Ups1 binds to the membrane, it dissociates from Mdm35, allowing the lid domain to open and accommodate substrates (e.g. PA). Once loaded with PA, Ups1 forms a complex with Mdm35 to remain protected from MIM proteases like Yme1. The complex dissociates upon approaching the MIM and the substrate is released. Further substrate loading is controlled by several factors including CL concentration in the MIM, which prevents dissociation of Ups1, and the cycle is discontinued (J. Lu et al., 2020; Miliara et al., 2015; Watanabe et al., 2015; F. Yu et al., 2015).

1.5.2.4 Possible alternative routes

Lipid trafficking within and between the mitochondrial membranes is an active process, most likely mediated by PL scramblases. So far, the only known mitochondrial scramblase is PLSCR3 (PL scramblase 3), which can promote PL flipping and can increase CL levels at the mitochondrial surface (Liu et al., 2008).

Mdm31, a MIM protein has also been suggested to have lipid mediating/regulating activity between the MOM and MIM. Required for normal mitochondrial morphology and maintaining mtDNA, Mdm31 exhibits synthetic lethality with most ERMES genes (Dimmer et al., 2002, 2005; Tamura, Onguka, Hobbs, et al., 2012). Moreover, overexpression of the protein can restore the phenotypes of cells lacking ERMES and *UPS1* e.g. abnormal mitochondrial morphology, CL accumulation, growth defects, etc., which was not achievable when Ups1 was overexpressed in *MDM31* lacking cells (Dimmer et al., 2005; Tamura, Onguka, Hobbs, et al., 2012).

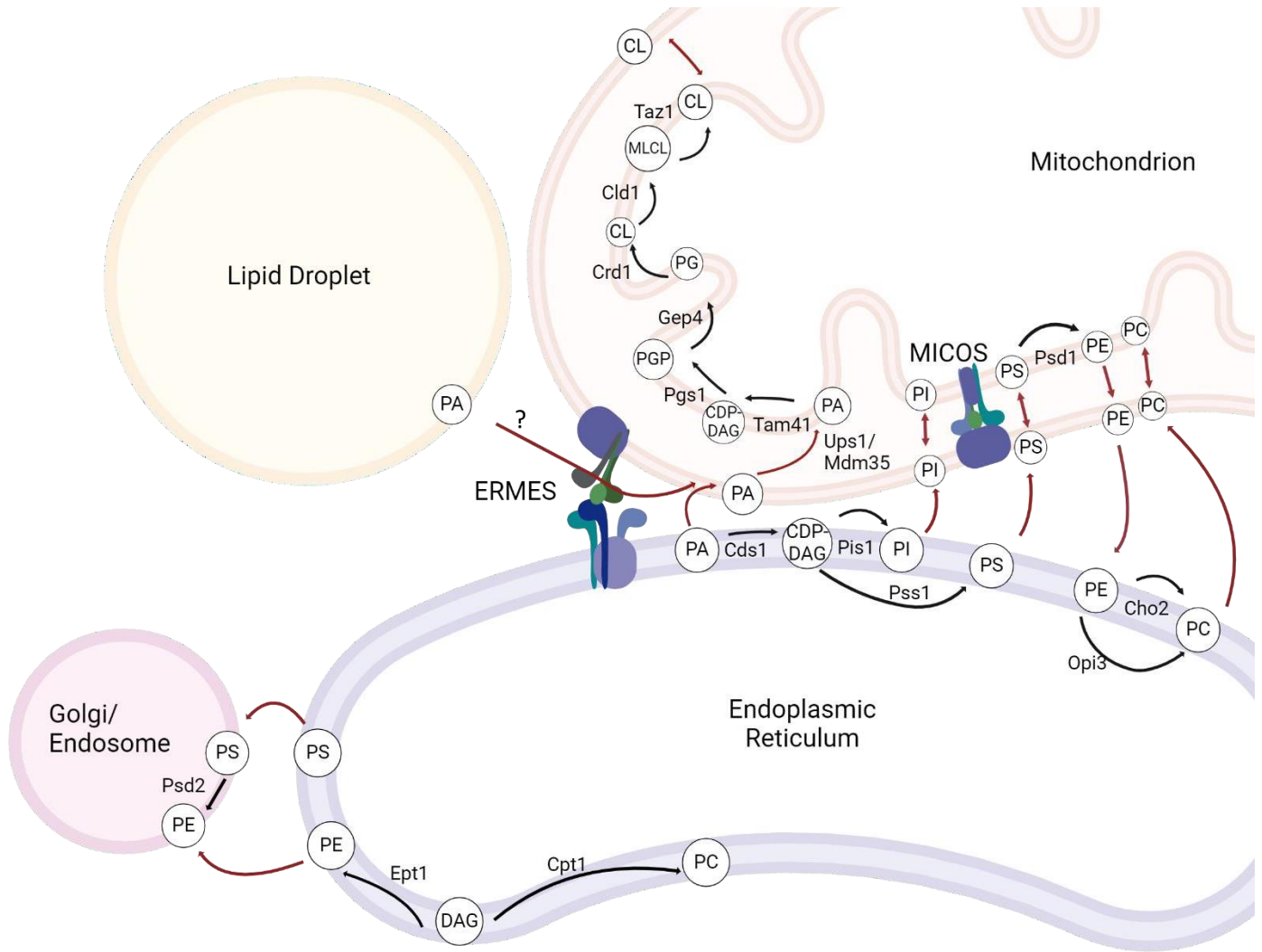


Figure 2. Phospholipid metabolism in yeast mitochondria

A brief overview of the biosynthesis of lipids in and in association with yeast mitochondria. Red arrows depict trafficking within or between organelles. Black arrows depict reactions catalyzed by corresponding enzymes. See text for details.

Adapted from Dimmer and Rapaport, 2016.

Research Objectives

The bacterial ancestry of mitochondria is made evident by their structure, protein machineries, and their ability to replicate semi-autonomously. These evolutionarily conserved features such as β -barrel proteins have been studied extensively and their physiological importance has ensured their conservation to higher eukaryotes. Other conserved features, while retained in yeast, are lost in higher eukaryotes.

In my thesis, I studied two evolutionarily conserved features of mitochondria. The first one is a putative lipase in the mitochondrial IMS which shares homology with primarily bacterial lipases and is not conserved in mammals. The second are β -barrel proteins which are highly conserved proteins in organelles with endosymbiotic origin.

Characterization of Tgl2, a putative lipase in yeast mitochondria

The research goals of this chapter are to characterize Tgl2 in greater detail and gain insight into its structure, molecular function, and understand its contribution to cellular lipid homeostasis.

Tiku, V., Tatsuta, T., Jung, M., Rapaport, D., Dimmer, K., (submitted, pre-print on BioRxiv). Characterization of Tgl2, a putative lipase in yeast mitochondria. 10.1101/2024.05.08.593122.

Yeast mitochondria can process *de novo* designed β - barrel proteins

The research objectives of this chapter are to express *de novo* designed synthetic β -barrel proteins in yeast cells, investigate their mitochondrial import behavior, and the role of key mitochondrial components in the biogenesis of these artificial proteins.

Moitra, A., Tiku, V. and Rapaport, D. (2024), Yeast mitochondria can process *de novo* designed β -barrel proteins. FEBS J, 291: 292-307. <https://doi.org/10.1111/febs.16950>

Characterization of Tgl2, a putative lipase in yeast mitochondria

Tiku, V., Tatsuta, T., Jung, M., Rapaport, D., Dimmer, K., (submitted, pre-print on BioRxiv). Characterization of Tgl2, a putative lipase in yeast mitochondria. 10.1101/2024.05.08.593122.

Personal Contribution

I studied the oligomerization behavior of Tgl2 where co-immunoprecipitation assays confirmed that it forms a homodimer under non-reducing conditions. I performed alkaline extraction to confirm the membrane topology of the homodimer, and sucrose gradient to determine the membrane tethering properties of monomeric Tgl2. Through antibody shift assays and non-denaturing PAGE, I found that the Tgl2 complex contains multiple copies of the protein. I also analyzed the quality control mechanism of the protein with the help of previously reported misfolded protein variants. I used disulfide bond prediction tools to predict the oxidative state of the cysteine residues of Tgl2 and used this to determine the impact of mutating 3 out of 8 cysteine residues on the stability of the protein. In addition to this, I compared the structure of Tgl2 with its closest structural homologue, LipA, and determined its catalytic triad using structure prediction tools. I performed site-directed mutagenesis to understand the contribution of the catalytically essential residues of Tgl2 to protein function and stability. Finally, I determined the neutral lipid composition of mitochondria isolated from cells lacking *TGL2* and *MCP2* through thin-layer chromatography. I co-wrote the manuscript and prepared all the figures.

Author Contributions

VT and KSD co-wrote the manuscript and designed and analysed the experiments. VT performed the experiments and prepared the figures. KSD supervised the project, acquired funding, and performed the tetrad dissection experiments. DR co-supervised the project and contributed to the manuscript. TT performed the lipidomics analysis and analysed the data. MJ and TT provided critical feedback on the manuscript.

Materials and methods

The materials and methods for this chapter can be found in the article – Characterization of Tgl2, a putative lipase in yeast mitochondria.

3.1 Introduction

Yeast cells store free sterols and fatty acids in their inert forms as SEs and TAGs, in lipid droplets. This prevents lipotoxicity and ensures an energy reservoir for high energy demanding situations. Enzymes like TAG lipases mobilize TAGs into DAGs and free fatty acids that can be used for various cellular pathways including phospholipid biosynthesis and even as signaling molecules (Grillitsch & Daum, 2011; Walther & Farese, 2012).

TAG lipases are hydrolytic enzymes relying on interfacial activation to carry out their function. This entails notable conformational changes that expose a hydrophobic pocket and the active site. The active site is buried under the lid domain, which is a short, mobile helical fragment. The lid domain is reported to be important for substrate specificity, and mutating it affects enzyme activity and specificity (Brady et al., 1990; Grillitsch & Daum, 2011; Ham et al., 2010; Khan et al., 2017; van Tilbeurgh et al., 1993).

The active site of lipases consists of a Ser-Asp-His catalytic triad, and this triad can also be found in α/β fold enzymes as well as serine proteases. While the serine and histidine residues are functionally essential, they do not contribute to protein stability. On the other hand, the aspartate residue is essential for protein stability as mutating it leads to a dramatic reduction in protein expression and/or function. This can be attributed to the stabilizing interactions of the carboxylate group (Brady et al., 1990; Jaeger et al., 1994; Lowe, 1992; Østerlund et al., 1997).

The only characteristic property of lipases is the conserved A/GXSXG motif where the serine is catalytically essential. Some lipases also possess the 'Patatin-domain', which was first identified in a plant protein with lipid acyl hydrolase activity (Mignery et al., 1988). In addition to this, some lipases are known to dimerize or contain intramolecular disulfide bridges that contribute to protein stability (Brady et al., 1990; Liebeton et al., 2001).

The Tgl family of lipases is a well-studied protein family of *S. cerevisiae*. It consists of 5 members found in LDs (Tgl1, Tgl3, Tgl4, and Tgl5) or mitochondria (Tgl2).

Tgl3 was the first member of the Tgl family to be discovered, and was found to be localized to LDs (Athenstaedt & Daum, 2003). A minor population of the protein can be found in the ER (C. Schmidt et al., 2013). Tgl3 possesses the canonical lipase motif and has a C-terminal hydrophobic domain which is a typical feature of LD proteins. The absence of *TGL3* was reported to have no growth phenotype but it does lead to a notable increase in cellular TAGs levels. Interestingly, the absence of *TGL3* causes hypersensitivity towards cerulenin – a FA synthesis inhibitor (Athenstaedt & Daum, 2003; I. Klein et al., 2016; C. Schmidt et al., 2013). Further sequence analysis revealed the H(X)₄D domain in Tgl3, which is the signature sequence of acyltransferases. Follow up enzyme assays confirmed lysophosphatidylethanolamine acyltransferase function of Tgl3, acting independent of its lipase function (Rajakumari & Daum, 2010a).

Tgl4 and Tgl5 were discovered when lipase activity was still detected in yeast cells lacking *TGL3*, suggesting redundancy. Predominantly found in LDs, Tgl4 can stably localize to the ER in the

absence of LDs. It is a multifunctional enzyme with TAG lipase, acyltransferase, and phospholipase activity (Rajakumari & Daum, 2010b). These observations were confirmed not only by the presence of the corresponding signature motifs but also through enzymatic assays which suggest specific lipase activity towards TAGs esterified with myristic acid (C14) and palmitic acid (C16). Moreover, the protein appears to be regulated by phosphorylation and cell cycle progression wherein phosphorylation by the cyclin-dependent kinase 1 (Cdk1) activates the protein, initiating lipolysis to support bud formation (Athenstaedt & Daum, 2005; Rajakumari & Daum, 2010b). The multifaceted nature of the protein can be confirmed by the phenotypes exhibited by yeast cells overexpressing the protein such as increased FFAs due to increased lipase activity as well as increased PL levels due to increase PL biosynthesis via acyltransferase activity (Athenstaedt & Daum, 2005; Grillitsch & Daum, 2011).

The third lipase, Tgl5, also exhibits dual function. Tgl5 is a lipase for TAGs containing long chain FAs like C26. The other function of Tgl5 is that of an acyltransferase, and like Tgl4, it acts on acylated phosphatidic acid. In the absence of LDs, Tgl5 localizes to the ER where it is highly unstable and is rapidly degraded. As with Tgl4, the lipase and acyltransferase activities of Tgl5 are regulated independent of each other. Additionally, both Tgl4 and Tgl5 are reported to be downregulated in the absence of non-polar lipids (Athenstaedt & Daum, 2005; I. Klein et al., 2016; Rajakumari & Daum, 2010a).

In yeast, SE hydrolase activity is collectively mediated by Yeh1, Yeh2, and Tgl1. Even though it contains the lipase motif, Tgl1 predominantly exhibits SE hydrolase activity. The protein co-localizes with Erg6, a LD marker protein as does Yeh1. On the other hand, Yeh2 can be found associated with the plasma membrane. A triple deletion of these genes leads to a complete loss of SE hydrolysis activity in yeast, but SE biosynthesis as well as TAG metabolism remain unaffected. Additionally, *in silico* structural analysis of Tgl1 predicted 1 – 3 transmembrane domains with the catalytically essential C-terminus extended inside the LD and the N-terminus exposed to the cytosol (Jandrositz et al., 2005; Köffel et al., 2005).

Tgl2 is also an unusual member of the Tgl family of yeast lipases. It is obviously smaller than the other Tgl proteins and is found in the mitochondrial fraction. Homologous to mostly bacterial lipases, the closest structural homologue of the protein is the periplasmic lipase, LipA, from *P. aeruginosa* (Figure 3). Tgl2 has been categorized as a lipase as it contains the conserved A/GXSXG lipase motif, where the serine is catalytically active (Ham et al., 2010). Initial studies with Tgl2 reported lipolytic activity towards DAGs and TAGs with short chain fatty acids and the ability to complement for the loss of a DAG kinase in *E. coli*. The phenotype observed upon DAG accumulation can be rescued by overexpressing Tgl2 (Van Heusden et al., 1998). In their study, Ham et al enriched Tgl2 from yeast and performed *in vitro* enzyme assays where they observed lipolytic activity towards long chain TAGs, with optimal activity for tributyrin. Moreover, they could confirm mitochondrial localization through fluorescence microscopy, and also showed that while cells lacking *TGL2* have no growth phenotype, they do exhibit decreased TAG mobilization (Ham et al., 2010). More recent studies have determined negative genetic interactions between *TGL2*

and *MCP2* (*CQD2*). *Mcp2* (*Cqd2*) is a MIM protein that was earlier reported to be a high-copy suppressors of the ERMES mutant *mdm10Δ* (Odendall et al., 2019; Tan et al., 2013). Kemmerer et al show that the protein regulates ubiquinone (CoQ) levels in the mitochondria (Kemmerer et al., 2021). The double deletion strain (*mcp2Δ/tgl2Δ*) shows a growth phenotype on non-fermentable carbon sources like glycerol which can be rescued when *Tgl2* is reintroduced (Odendall et al., 2019).

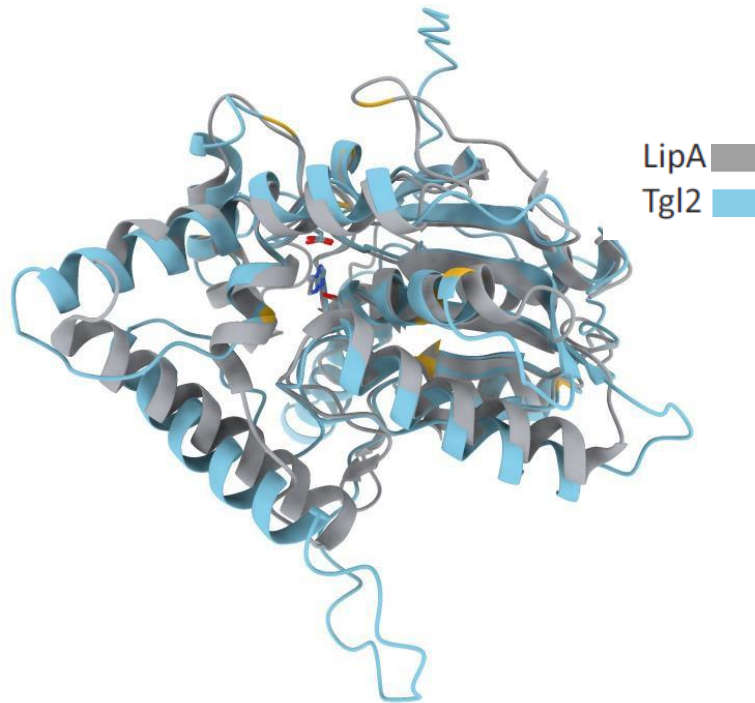


Figure 3. Structural homology between LipA and Tgl2

The crystal structure of LipA and AlphaFold prediction of Tgl2 compared using ChimeraX. The residues in yellow are cysteines and the residues with the highlighted side chains are the active sites of the two proteins.

Odendall et al also confirmed the subcellular localization of Tgl2 through differential centrifugation experiments, and showed that it's a soluble IMS protein (Odendall et al., 2019). Since Tgl2 contains 8 cysteine residues, it's a plausible candidate for import via the disulfide relay pathway (Hell, 2008). This was determined through radiolabeled import assays with WT and Mia40 depleted yeast cells. Indeed, protein import was inhibited in cells depleted for Mia40. Additionally, the import for a Tgl2 variant where all the cysteines are mutated to serine showed dramatically reduced kinetics as well as multiple proteolytic fragments (Odendall et al., 2019). It's important to note that the cysteine residues of Tgl2 do not exist in the conserved CX₃C or CX₉C motifs (Hell, 2008; Sideris & Tokatlidis, 2007).

The overarching aim of my thesis is to further characterize Tgl2 and form a comprehensive link between a TAG lipase in the IMS, where one lacks reportable amounts of TAGs, and cellular lipid metabolism.

I observed that Tgl2 can homodimerize in the absence of reducing agents, and this dimer is probably a result of disulfide bridges. Further, Tgl2 also forms a cysteine-dependent complex in native PAGE which can be disrupted using strong detergents. I also characterized the lipase motif mutant - S144A which was previously reported to be essential for lipolytic activity of the protein. The mutated protein was unable to rescue the growth phenotype of $\Delta mcp2/\Delta tgl2$ confirming loss of function. Additionally, I identified the catalytic triad of the protein and mutating the active site – D259A also led to loss of function as well as protein instability. Steady state levels analyses with unstable Tgl2 variants helped identify Yme1 as the protease responsible for the quality control of Tgl2. The mutants that were either undetectable or only weakly detectable in WT or $\Delta tgl2$ yeast could be detected like native Tgl2 in the absence of Yme1. Finally, I could show that mitochondria lacking *MCP2* and *TGL2* have more TAGs than WT mitochondria. This could be a direct consequence of the lack of Tgl2 – a TAG lipase. However, the contribution of Mcp2 to this phenotype is still puzzling.

Given the bacterial ancestry of mitochondria and the similarity of Tgl2 with mostly bacterial lipases, one could speculate that the protein was conserved to eukaryotes like yeast. However, why higher eukaryotes lack any such mitochondrial lipases is a question yet to be answered.

3.2 Results

3.2.1 Tgl2 forms homodimers in the absence of a reducing agent

All previous experiments with Tgl2 were performed under reducing conditions. Since the protein contains 8 cysteine residues, we were curious to study its behavior in the absence of a reducing agent. We isolated crude mitochondria from yeast cells over-expressing N-terminally HA tagged Tgl2 (HA-Tgl2) and omitted any reducing agents in the loading dye. The samples were analysed by SDS-PAGE and immunodecoration. A higher molecular weight species, approximately twice the size of Tgl2, was observed (Fig. 4A). Moreover, this species was lost over time since it was more easily detected in whole cell lysates and crude mitochondria isolated after mechanical rupturing than in mitochondria obtained from spheroplasting-based isolation protocols (Fig. 4B). This higher molecular weight species was quantified using the MOM protein Tom20 as a loading control and we observed that it contributes to almost half of the total protein in shorter isolation protocols whereas its appearance is noticeably reduced upon longer isolation protocols (Fig. 4B).

Next, we wanted to determine if this higher molecular weight variant is a homodimer of the protein, since its size corresponds to two molecules of the protein. To address this, we isolated mitochondria containing two variants of Tgl2 - N-terminally FLAG- or HA- tagged and performed co-immunoprecipitation assays using magnetic anti-FLAG beads. Samples from input, unbound, wash, and eluate fractions were collected and analyzed by SDS-PAGE and Western blotting using anti-HA and anti-FLAG antibodies. HA-tagged Tgl2 was detected only in the eluate fraction from mitochondria containing both tagged proteins. Moreover, we could confirm that the anti-FLAG beads do not unspecifically interact with HA-Tgl2 (Fig 4C).

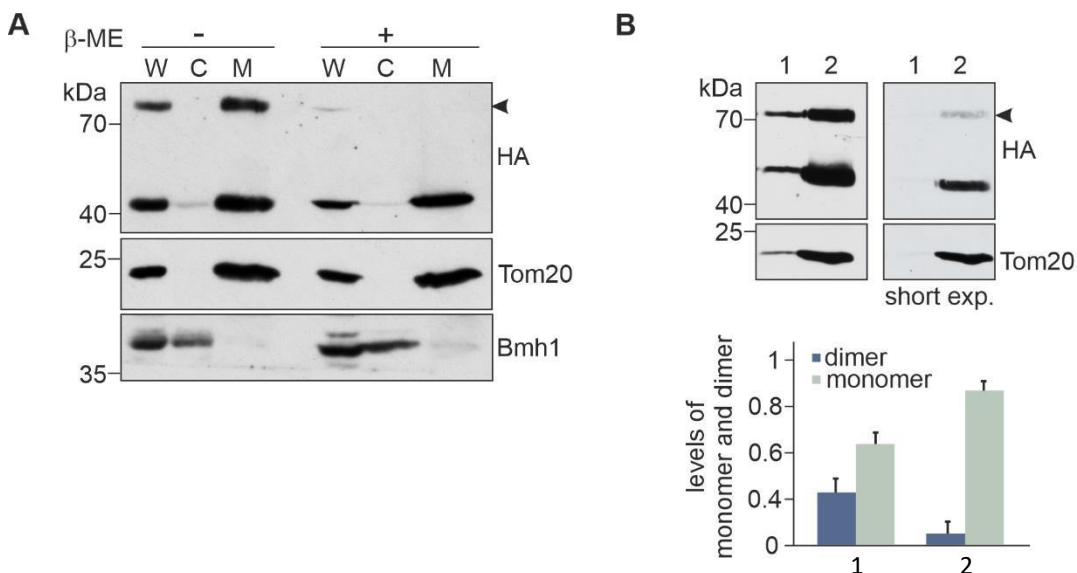
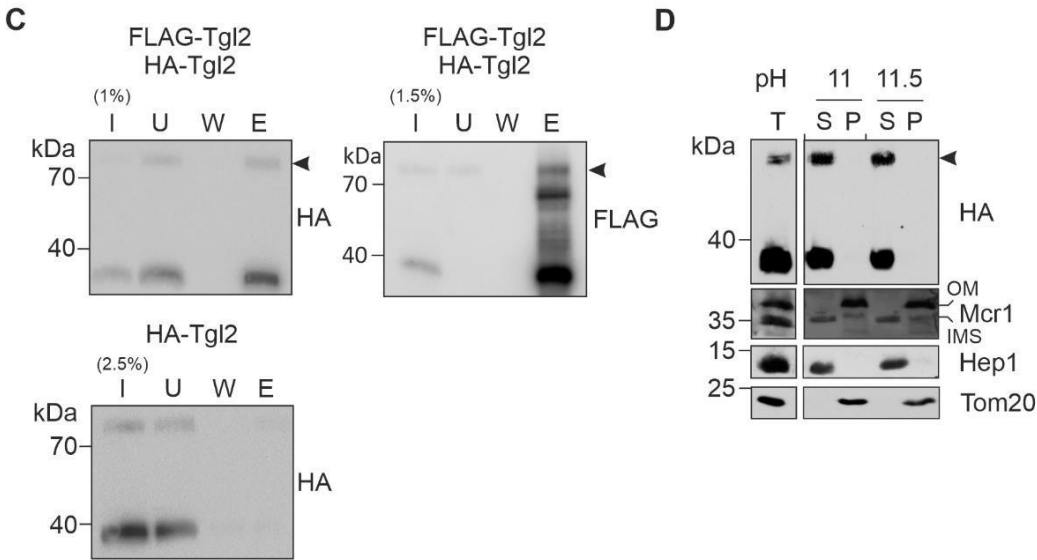


Figure 4. Tgl2 forms a homodimer that is sensitive to reducing agents.

(A) Tgl2 forms a higher molecular weight adduct under non-reducing conditions. Cells lacking TGL2 (*tgl2Δ*) were transformed with a plasmid encoding HA-Tgl2 and grown to mid-logarithmic



phase. Mechanical lysis was used to isolate whole cell (W), cytosolic (C), and mitochondrial (M) fractions. The samples were mixed with sample buffer with or without β -mercaptoethanol (β – ME) and analysed by SDS-PAGE and immunodecoration with antibodies against the HA-tag, as well as Tom20 (mitochondrial marker) and Bmhl (cytosolic marker). The higher molecular weight adduct is marked by an arrowhead. (B) The higher molecular weight adduct is more pronounced upon shorter isolation protocols. Cells expressing HA-Tgl2 were grown to mid-logarithmic phase and mitochondrial fractions were isolated afterwards either mechanical lysis (1) or spheroplasting (2). The samples were analysed by non-reducing SDS-PAGE and immunodecoration. Quantification of the adduct was done with Tom20 as a loading control and the total Tgl2 amounts were taken as 100%. The graph represents the mean values \pm SD of four independent experiments. (C) The adduct is a homodimer of Tgl2. Mitochondria were isolated from *tgl2* Δ cells expressing either HA-Tgl2 or co-expressing HA-Tgl2 and FLAG-Tgl2. The organelles were solubilized and subjected to co-immunoprecipitation with anti-FLAG beads. Samples from input (I), unbound (U, 5%), wash (W, 5%) and eluate fractions (E, 50%) were analyzed by SDS-PAGE and immunodecoration with antibodies against the FLAG-tag. (D) Tgl2 dimer is soluble. Mitochondria containing HA-Tgl2 were subjected to alkaline extraction at different pH values. The supernatant (S) and pellet (P) fractions were analysed by SDS-PAGE and immunodecoration with the indicated antibodies. Tom20 (membrane integrated protein), Hep1 (soluble matrix protein), Mcr1 (a protein with two isoforms, long 34 kDa form embedded in the MOM and shorter soluble form in the IMS).

3.2.2 Tgl2 is a soluble protein associating with the mitochondrial inner membrane

The solubility of Tgl2 was previously confirmed using alkaline extraction experiments. Since this experiment was performed for the monomeric form, we applied the same approach to analyse the solubility of the dimer. Isolated mitochondria were subjected to alkaline extraction assay and the pellet and supernatant fractions were analysed by SDS-PAGE and immunodecoration was performed with Tom20, Mcr1, and Hep1 as controls for membrane integrated and soluble proteins (Fig. 4D). We observed that the dimeric form is also found in the soluble fraction, indicating that both forms of the protein are soluble.

Since lipases are lipid-binding proteins, Tgl2 would need to access its potential substrates by binding to either or both mitochondrial membranes. To determine this, we performed a sucrose gradient centrifugation with mitochondrial vesicles containing HA-Tgl2 (Fig. 5A). Of note, the majority of the protein was found in the vesicle fraction (Fig 5A SG). The fractions were analyzed by immunodecoration where Tgl2 could be detected in fractions also containing Cox2, an MIM protein. The MOM marker protein Tom20 was completely absent in these fractions suggesting that a large population of Tgl2 associates with the MIM (Fig 5B and C).

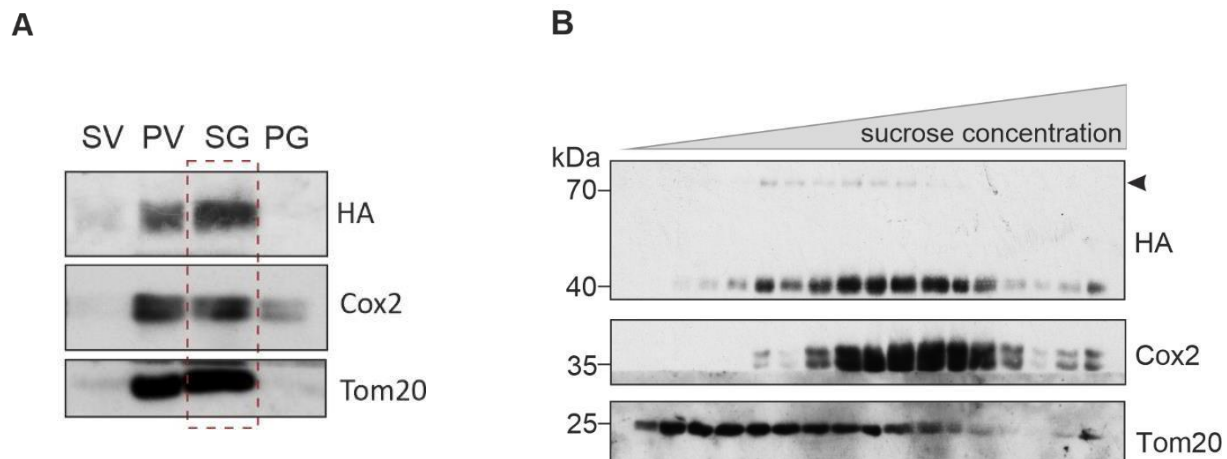
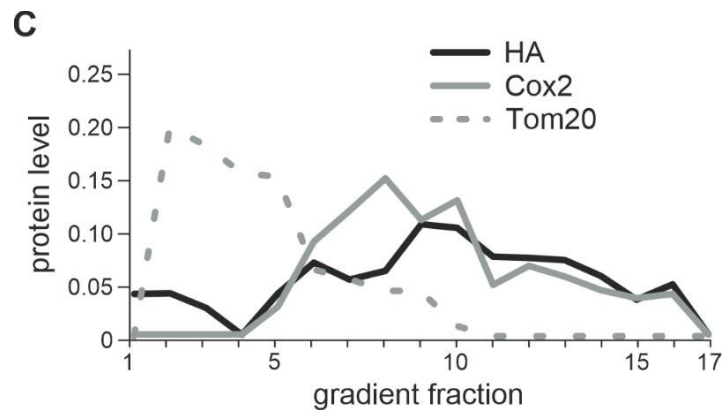


Figure 5. Tgl2 associates with the mitochondrial inner membrane.

(A) The majority of Tgl2 is found in mitochondrial vesicles. Mitochondrial vesicles were obtained after swelling and sonication of mitochondria from cells containing HA-Tgl2. The indicated control fractions were collected after swelling, vesicle generation, and clarifying spins. The sample was sonicated to form vesicles followed by clarifying spin to yield supernatant – SV and pellet – PV fractions. The vesicles in PV was sonicated again and subjected to a slower clarifying spin resulting in SG (supernatant) and PG (pellet). Fraction SG was further subjected to a sucrose gradient to separate the MOM and MIM vesicles. The fractions were analysed by SDS-PAGE and immunodecoration. (B) Tgl2 associates with MIM vesicles. The mitochondrial vesicles from SG fraction (depicted in panel A) were separated by sucrose density centrifugation. Fractions were collected and analysed by SDS-PAGE and immunodecorated with the indicated antibodies, Cox2 (MIM protein) and Tom20 (MOM protein).



(C) Tgl2 and Cox2 containing fractions coincide. Intensities corresponding to Tgl2, Cox2, and Tom20 were quantified and normalized to the total content of each protein

3.2.3 Tgl2 is a subunit of a higher molecular weight complex

Tgl2 was identified in a high throughput screen as a negative interactor of *MCP2*, an MIM protein suggested to be involved in lipid metabolism and CoQ homeostasis (Kemmerer et al., 2021; Odendall et al., 2019). Despite trying several different approaches, we could not establish any physical interaction between *Mcp2* and Tgl2. We enriched HA-Tgl2 through performed co-immunoprecipitation assays and subjected this to proteomics analyses. The data failed to reveal *Mcp2* as an interaction partner and, moreover, no other protein of interest could be identified from the dataset (data not included).

Interestingly, Tgl2 does form a complex in native gels. We isolated mitochondria from yeast overexpressing HA-Tgl2, solubilized them with either digitonin or Triton X-100, and subjected them to blue native (BN)-PAGE followed by immunodecoration. We observed that Tgl2 migrates as part of a complex of 500kDa that was more stable upon mild solubilization using digitonin (Fig. 6A). We applied this approach to a wide range of deletion mutants where yeast deletion strains of potential physical interactors selected by educated guess, transformed with HA-Tgl2, and the isolated mitochondria were analysed by BN-PAGE. However, the Tgl2 complex was unaltered in these mutants (Figure 7A). In addition to this, we also compared the steady state levels of the protein in the same mutants but no notable variations were observed (Fig. 7B). Of note, the Tgl2 complex appears as a sharp solitary band in BN-PAGE unlike known mitochondrial membrane embedded complexes like TOM complex that displays a rather broad band in native gels. This behaviour further suggests that Tgl2 is indeed a soluble protein of defined quaternary structure without associated membrane lipids.

To understand the composition of the complex, we performed an antibody-shift assay with solubilized mitochondria containing both HA-Tgl2 and FLAG-Tgl2 or only FLAG-Tgl2. The mitochondrial lysate was incubated with anti-HA antibody, subjected to BN-PAGE, and

immunodecorated against anti-FLAG antibody. We observed a size shift only for the sample containing both tagged Tgl2 variants (Fig. 6B). As expected, the complex was not shifted in mitochondria containing only FLAG-Tgl2. These observations indicate that the complex contains at least two copies of Tgl2.

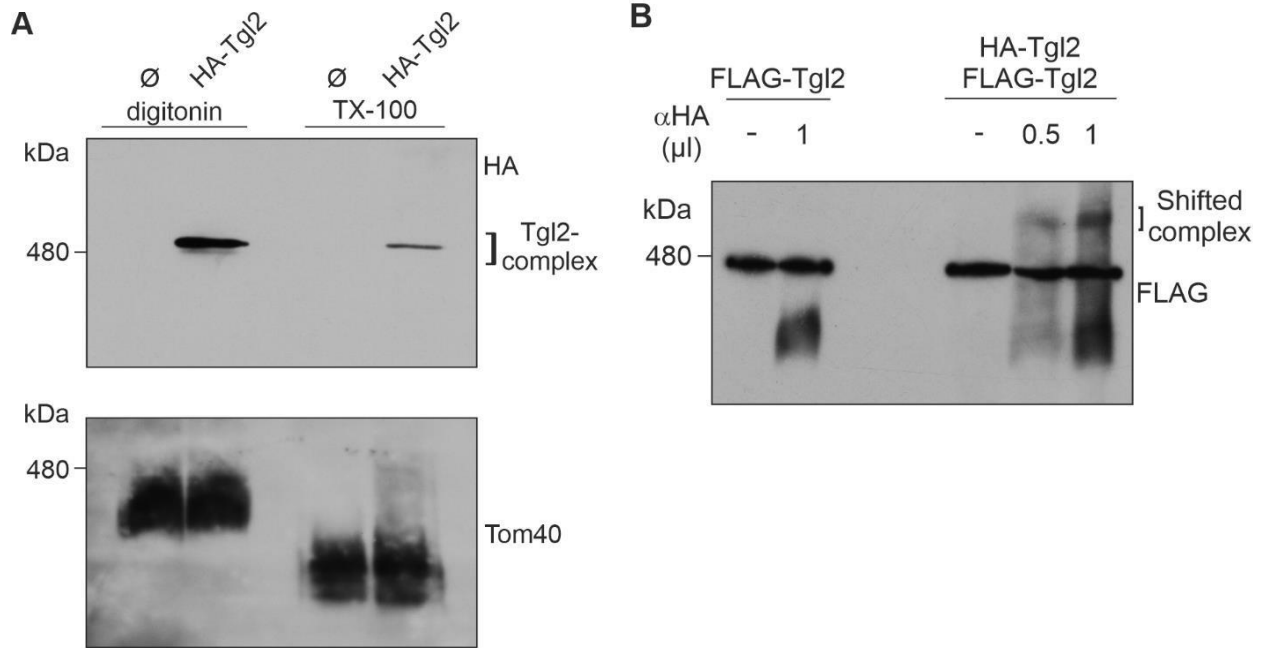


Figure 6. Tgl2 is a component of a higher molecular weight complex

(A) Tgl2 forms a higher molecular weight complex. Mitochondria containing HA-Tgl2 were solubilized with either digitonin or TritonX-100 (TX-100) and subjected to BN-PAGE (4-14%) and immunodecoration with antibodies against either HA-tag or Tom40, as a loading control. (B) Tgl2 complex contains at least 2 copies of the protein. Mitochondria containing either only HA-Tgl2 or HA-Tgl2 and FLAG-Tgl2 were solubilized with digitonin. The lysate was incubated with 0, 0.5, or 1 μL anti-HA antibody (α-HA) and analysed by BN-PAGE (4-14%) and immunodecoration with anti-FLAG antibody.

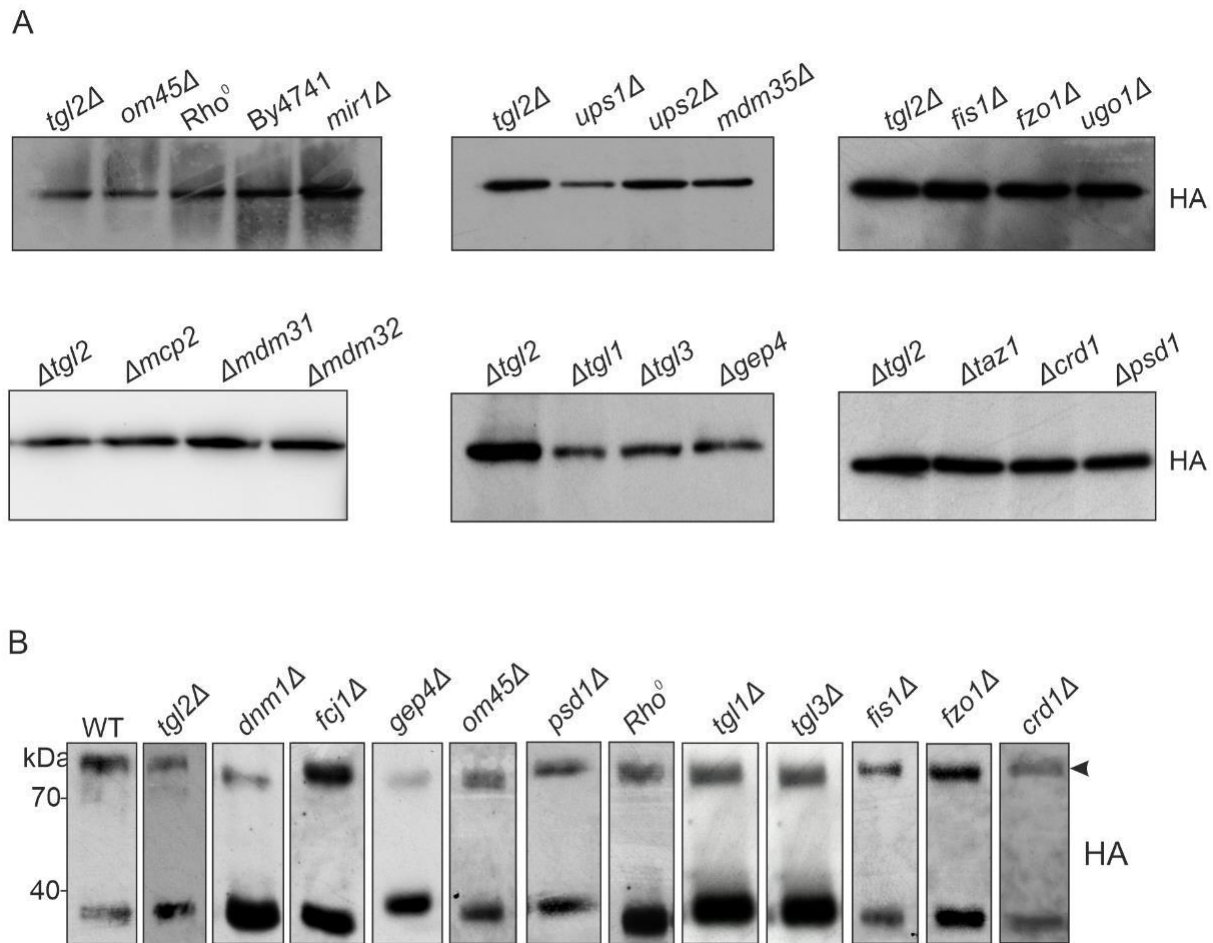


Figure 7. Tgl2 complex in different deletion mutants

(A) The Tgl2 complex is unaffected in the absence of the indicated strains. Mitochondria were isolated from the mentioned strains, solubilized with digitonin, and analysed by BN-PAGE (4-14%) and immunodecoration against HA-tag. There were no noticeable effects on the complex formation. (B) Steady state levels of Tgl2 in different deletion strains. Mitochondria were isolated from the indicated strains expressing HA-Tgl2 and analysed by SDS-PAGE and immunodecoration with an antibody against HA-tag. The Western blots are representative of some strains used in this experiment ($n = 3$).

3.2.4 The MIM protease Yme1 mediates the quality control of Tgl2

Previous studies on the quality control of IMS proteins have identified Yme1, an iAAA protease of the MIM, to be responsible for degrading misfolded or unstable proteins in the IMS (Leonhard et al., 1999; Schreiner et al., 2012). Many of these proteins are also substrates of the disulfide relay import pathway. We previously observed that C-terminally modified Tgl2 (Tgl2-HA) and Tgl2_{cys}, with all cysteine residues mutated to serine, were barely detectable in WT yeast cells and failed to rescue the growth defect in the *mcp2Δ/tgl2Δ* double mutant (Odendall et al., 2019). To test if non-functional and potentially misfolded Tgl2 variants are substrates of Yme1, we compared the steady-state levels of HA-Tgl2, Tgl2-HA, and HA-Tgl2_{cys} in *tgl2Δ* and *yme1Δ* cells. We previously reported that only a functional Tgl2 variant can rescue the growth phenotype in *mcp2Δ/tgl2Δ*, and used this system to assess the functionality of the different protein variants. A complementation assay on non-fermentable (glycerol) carbon sources confirmed these observations (Fig. 8A and (Odendall et al., 2019)). A significant growth defect was seen for *mcp2Δ/tgl2Δ* on glycerol medium, which could only be rescued by reintroducing HA-Tgl2, and not the other two variants, confirming that Tgl2-HA and HA-Tgl2_{cys} are indeed non-functional. To compare the steady-state levels of these variants, we obtained whole cell lysate, cytosolic, and crude mitochondrial fractions from either *tgl2Δ* or *yme1Δ* cells expressing these protein variants and analyzed them by Western blotting (Fig. 8B). Native-like HA-Tgl2 was detected in both *tgl2Δ* and *yme1Δ* cells, while Tgl2-HA and HA-Tgl2_{cys} were only detected in *yme1Δ* cell fractions. These results confirm that Yme1 eliminates non-functional Tgl2 variants. Interestingly, HA-Tgl2_{cys} cannot form a homodimer, supporting the hypothesis that the observed dimer is due to disulfide bridges.

Next, we wanted to analyse the complex formation of these non-functional variants of Tgl2. Mitochondria isolated from *tgl2Δ* or *yme1Δ* were subjected to BN-PAGE and immunodecoration. We could detect the complex for HA-Tgl2 in mitochondria isolated from either both *tgl2Δ* and *yme1Δ* cells. In contrast, a complex containing Tgl2-HA could be detected only in mitochondria lacking Yme1 (Fig. 8C). HA-Tgl2_{cys} is unable to form a complex even in the absence of Yme1 suggesting that the complex is dependent on cysteine residues. The levels of the loading control - TOM complex were detected with an antibody against Tom40, and are not altered (Fig. 8C). To confirm that the cells expressed the different proteins, a fraction of the solubilized mitochondria was also loaded on SDS-PAGE and analysed using the indicated antibodies (Fig. 8D).

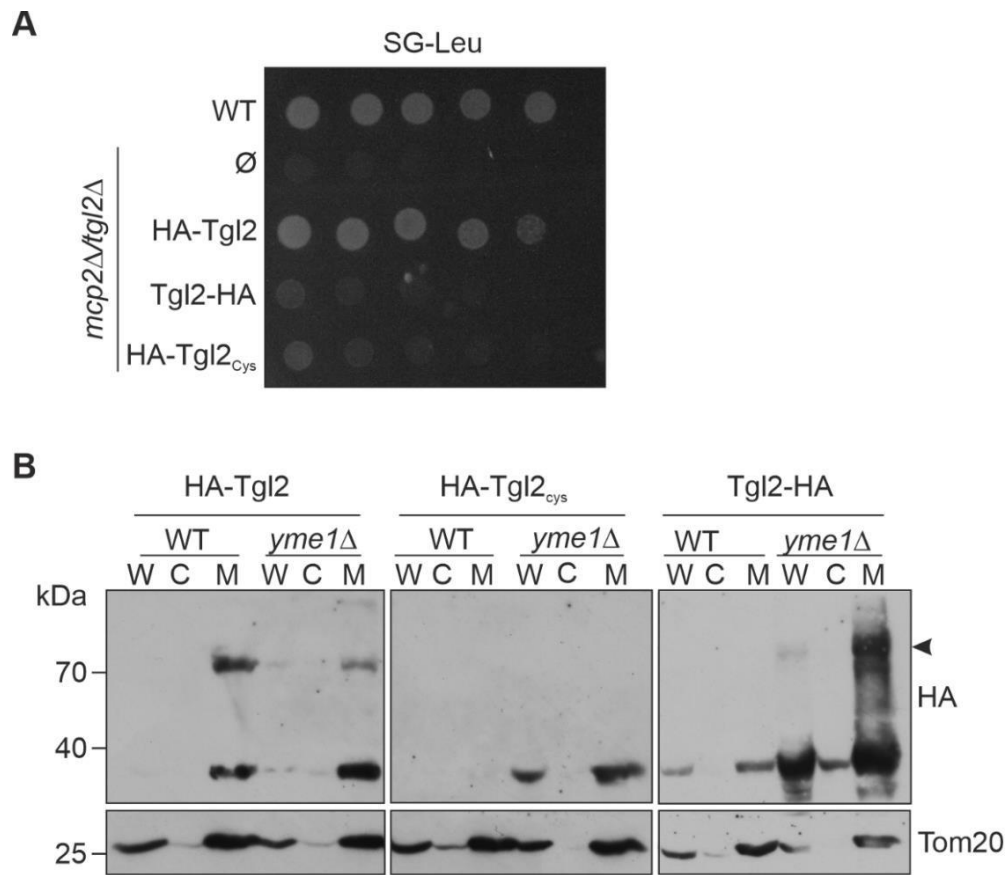
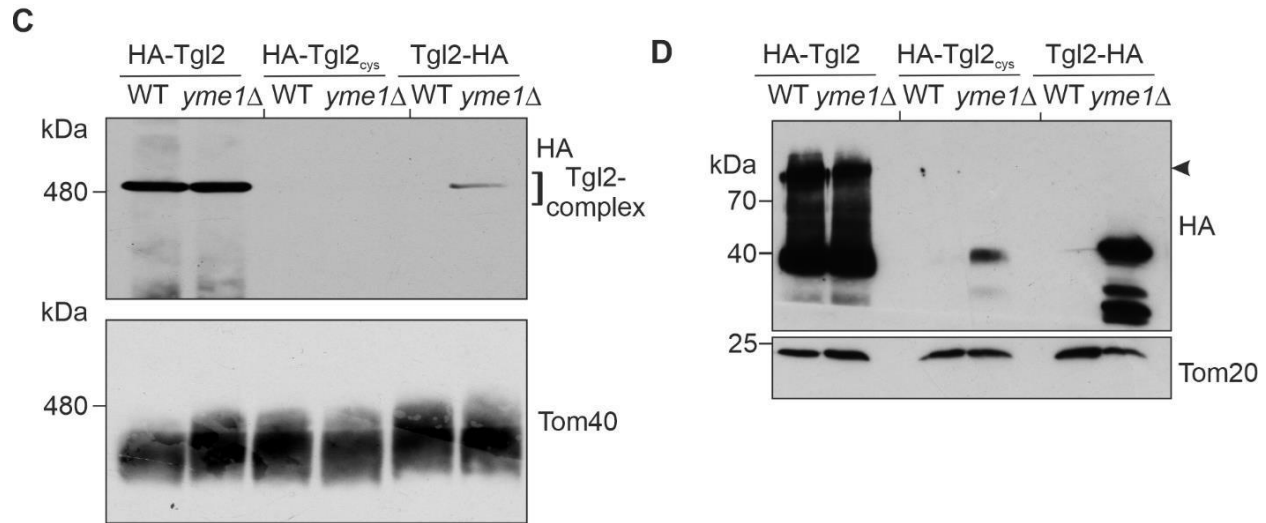


Figure 8. The MIM protease Yme1 mediates the quality control of Tgl2

(A) C-terminally tagged Tgl2 and a Tgl2 variant with all its cysteine residues mutated to serine do not rescue the growth defect of *mcp2Δ/tgl2Δ*. WT or *mcp2Δ/tgl2Δ* cells were transformed with an empty vector (\emptyset) or a plasmid encoding the indicated variants were grown to logarithmic phase, and dropped on SG-Leu plates in a 1:5 dilution series. Plates were incubated at 30°C and imaged after 5 days. (B) WT or *yme1Δ* cells encoding the indicated Tgl2 variants were grown to mid-logarithmic phase and whole cell (W), cytosolic (C), or mitochondrial (M) fractions were isolated by mechanical lysis. The samples were analysed by SDS-PAGE and immunodecoration with antibodies against HA and Tom20 as a loading control.



(C) Mitochondria isolated from either WT or *yme1* Δ cells expressing the indicated Tgl2 variants were solubilized with digitonin and analysed by BN-PAGE (4-14%) and immunodecoration with antibodies against HA or Tom40, as a loading control. (D) Aliquots (5%) of the solubilized mitochondria described in (C) were taken after the clarifying spin and analysed by SDS-PAGE and immunodecoration against HA and Tom20, as a loading control.

3.2.5 Analysis of single cysteine residues of Tgl2

The closest structural homologue of Tgl2 is a bacterial lipase – LipA, an extracellular lipase in the periplasmic space of *P. aeruginosa*. LipA has an intramolecular disulfide bond (between C183 and C235) which is important for the stability of the protein (Noble et al., 1993; Papadopoulos et al., 2022). Disruption of this disulfide bridge results in loss of lipolytic function as well as rapid degradation of the protein (Jaeger et al., 1994; Liebeton et al., 2001). We used AlphaFold for structural prediction of Tgl2 (Fig 9A and Jumper et al., 2021; Varadi et al., 2022) and bioinformatics tools ((Cheng et al., 2006; Ferrè & Clote, 2005a, 2005b) to predict the oxidation states of all the cysteine residues and to predict disulfide bridges between them (Fig 9B and C). Using these tools, we identified and selected three candidates – C31, C232, and C256, and performed site-directed mutagenesis to create HA-Tgl2_{C31A}, HA-Tgl2_{C232A}, and HA-Tgl2_{C256A}, and transformed them into Δ *tgl2*, Δ *mcp2*/ Δ *tgl2*, and Δ *yme1* strains. Our complementation assays revealed that all three mutants could rescue the growth defect of Δ *mcp2*/ Δ *tgl2* (Fig 9D). Thus, these cysteine residues are not essential for the functionality of the protein. To study the steady-state levels of the three mutants, we isolated crude mitochondrial fractions from Δ *tgl2* and Δ *yme1* yeast and analysed them by SDS-PAGE and immunodecoration. We observed expression levels comparable to the native protein, and, disappointingly, no impact on the stability of the protein. In addition to this, none of these point mutations had an impact on the homodimerization although C256 and C232 (partially) are exposed outwards and could be involved in intermolecular disulfide bridges (Fig 9E and F).

Since the Tgl2 complex is cysteine dependent (Fig 8C), we wanted to analyse if these cysteine residues are essential for its formation or stability. To achieve this, we performed native PAGE and immunodecoration with solubilized mitochondria containing either HA-Tgl2_{C31A}, HA-Tgl2_{C232A}, or HA-Tgl2_{C256A} (Fig 9F). We could not observe any difference in the complex formation or stability between the native protein and the cysteine mutants. From this we could conclude that these single point mutations by themselves are not sufficient to destabilize either the homodimer or oligomer formed by Tgl2 and therefore have no obvious impact on the functionality of the protein.

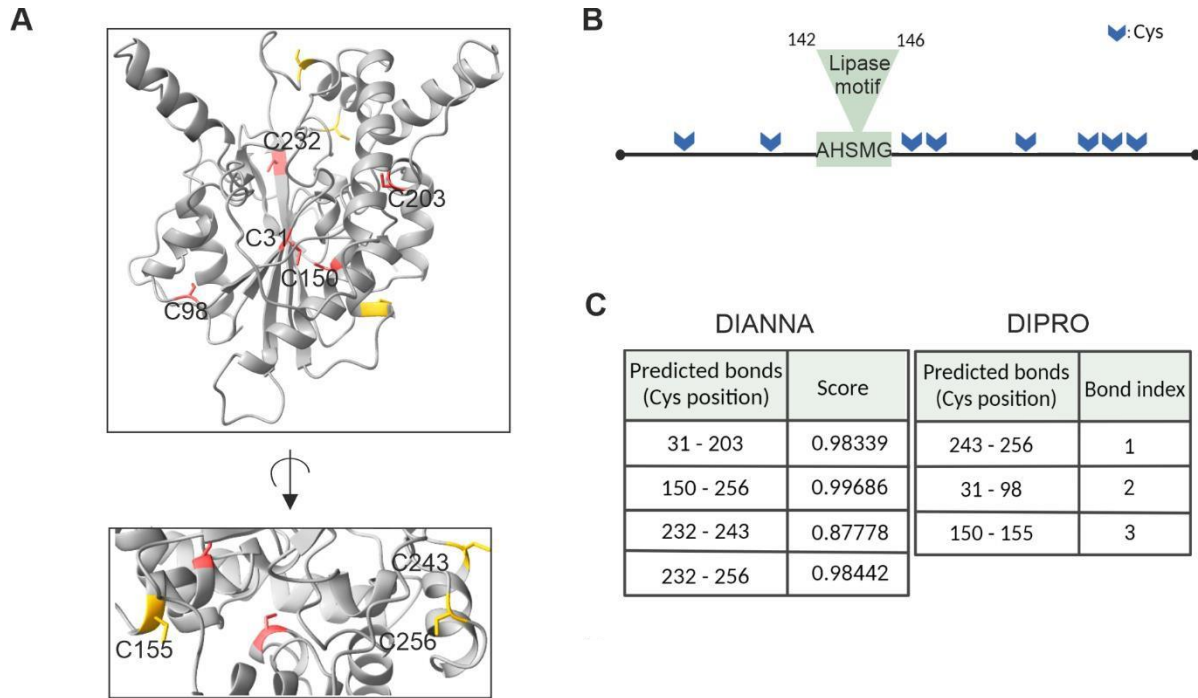
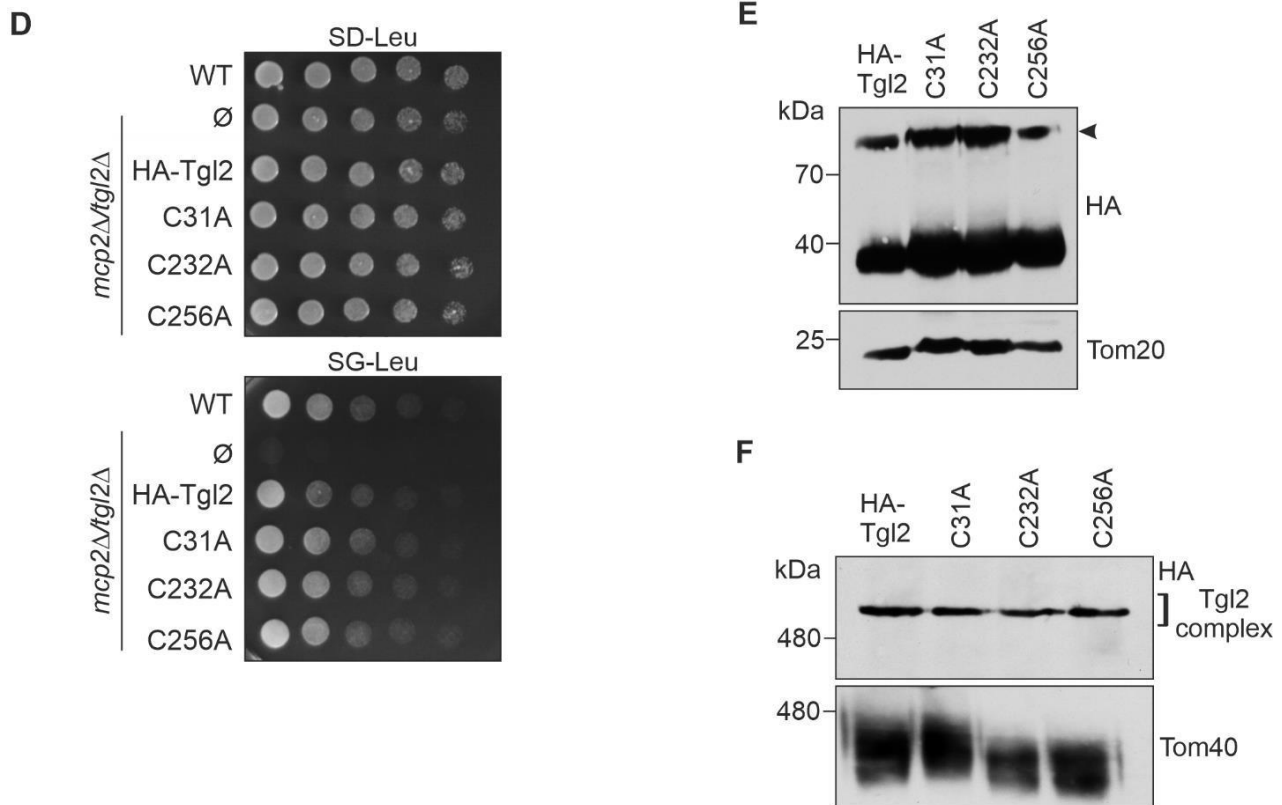


Figure 9. Analysis of the contribution of single cysteine residues of Tgl2

(A) Tgl2 has 8 cysteine residues that can potentially form intra or intermolecular disulfide bridges. Predicted structure of Tgl2 with the cysteine residues highlighted in red (functional group buried) or yellow (functional group exposed). (B) Schematic representation of the cysteine residues of Tgl2 marked with blue arrows and the canonical lipase motif marked in green (Created with Biorender). (C) Prediction of putative disulfide bonds within Tgl2 using using DiANNA and DIPRO. The cysteine pairs are in decreasing order of probability of disulfide bond formation.



(D) WT or *mcp2Δ/tgl2Δ* cells were transformed with an empty vector Φ or a plasmid encoding the indicated variants were grown to logarithmic phase, and dropped on SD-Leu or SG-Leu plates in a 1:5 dilution series. Plates were incubated at 30°C and imaged after several days. (E) *tgl2Δ* cells expressing the indicated variants of Tgl2 were grown to mid-logarithmic phase and the crude mitochondrial fractions were isolated. The samples were analysed by SDS-PAGE and immunodecoration with the indicated antibodies. (F) Mitochondria from *tgl2Δ* cells expressing the indicated protein variants were solubilized with digitonin and analysed by BN-PAGE (4-14%) and immunodecoration with antibodies against HA or Tom40.

3.2.6 The predicted catalytic triad of Tgl2 is required for its functionality

The canonical lipase motif - (G/A)XSXG of Tgl2 identifies it as a lipase. The serine residue of this motif is catalytically active (Fig 10A (Grillitsch & Daum, 2011)). In *in vitro* lipase assays using affinity tag-enriched protein extracts, Ham et al. report that mutating the Serine 144 to Alanine (HA-Tgl2_{S144A}) leads to loss of lipolytic activity of Tgl2. Moreover, prokaryotic and eukaryotic lipases typically contain a catalytic triad consisting of Ser-Asp-His, wherein the serine is often part of the conserved lipase motif. This triad is also analogous to the catalytic center of serine proteases as well as acyltransferases such as Tgl3 and Lro1 (Athenstaedt & Daum, 2003; Choudhary et al., 2011; Jaeger et al., 1994) (Fig 10B). We used the structural data of LipA as well as other bacterial lipases that share homology with Tgl2, to gain more insight into the catalytic triad of Tgl2. *In silico* analysis

of the predicted structure of Tgl2 suggest a catalytic triad comprising of Ser144, Asp259, and His281 (Fig 10B) (Jumper et al., 2021; Noble et al., 1993; Varadi et al., 2022).

We performed site-directed mutagenesis to mutate the catalytically active S144 and D259 to alanine, and used the resulting protein variants for our studies. In our complementation assays, HA-Tgl2_{S144A} was unable to complement the growth phenotype exhibited by $\Delta mcp2/\Delta tgl2$ on glycerol-containing medium (Fig 10C). Moreover, HA-Tgl2_{D259A} is also unable to rescue the growth phenotype of $\Delta mcp2/\Delta tgl2$ on non-fermentable carbon sources (Fig 10D). Therefore, the residues S144 and D259 are involved in the catalytic triad as loss of these residues leads to improper or loss of protein function.

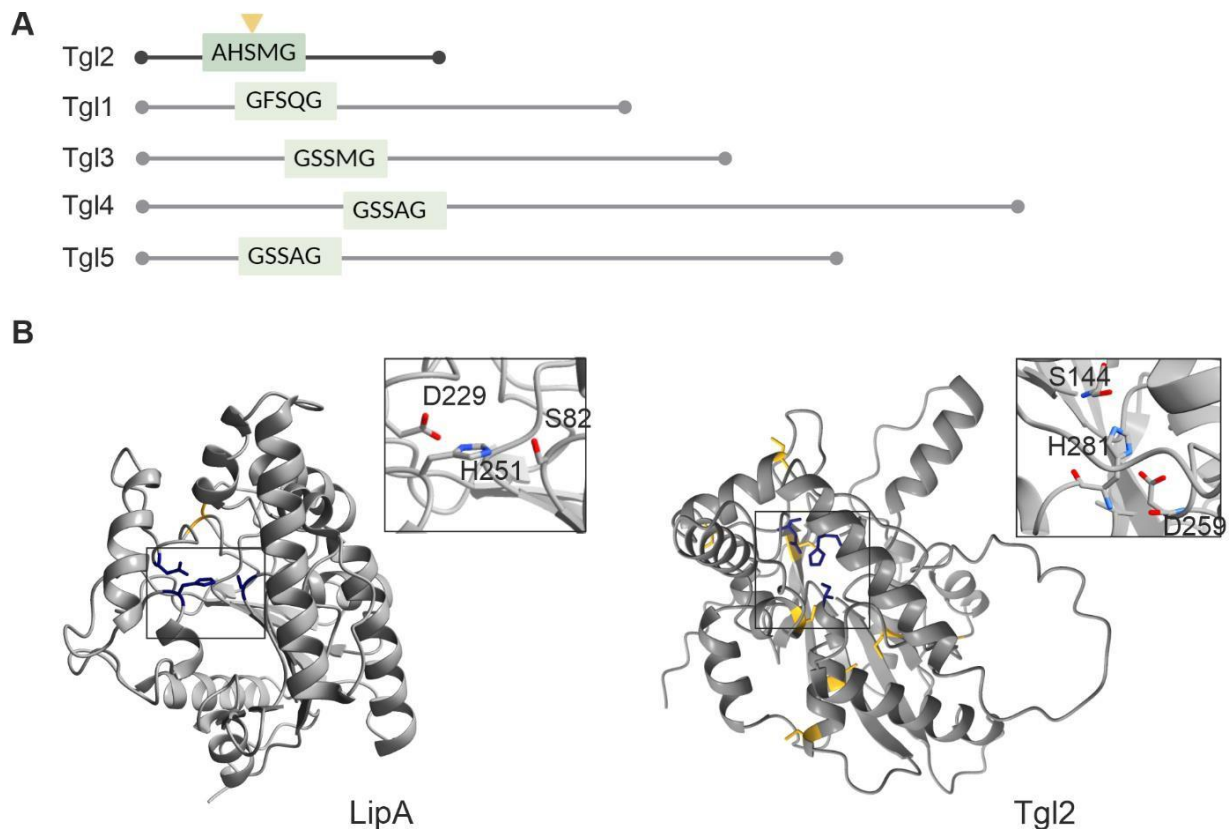
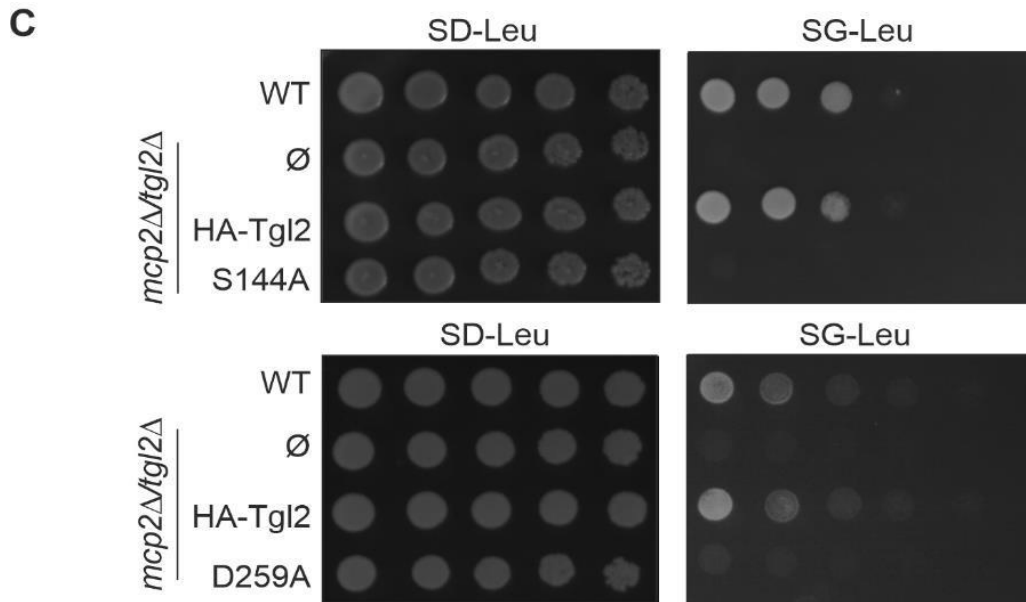


Figure 10. The predicted catalytic triad of Tgl2 is required for its functionality

(A) Tgl2 belongs to the Tgl family of yeast lipases and has a characteristic lipase motif (green) with a catalytically active serine (yellow arrow). Adapted from Papadopoulos et al 2022. (B) The predicted catalytic triad of Tgl2 (Ser-Asp-His). The crystal structure of LipA (left) with the intramolecular disulfide bond highlighted in yellow and the catalytic triad consisting of S82, D229, and H251 highlighted in blue (Noble et al 1993) was employed to predict the structure of Tgl2 (right) with its cysteine residues in yellow and the predicted catalytic triad (S144-D259-H281) in blue (Jumper et al., 2021; Varadi et al., 2022).



(C) WT or *mcp2 Δ /tgl2 Δ* cells transformed with the indicated variants were grown to logarithmic phase, and dropped on either SD-Leu or SG-Leu plates in a 1:5 dilution series. Plates were incubated at 30°C and imaged after several days.

3.2.7 Disruption of the catalytic triad affects protein stability

The HA-Tgl2_{S144A} variant is a non-functional mutant with expression levels comparable to the native protein (Fig 11A). To determine its ability to form the Tgl2 complex, we solubilized mitochondria isolated from $\Delta tgl2$ and $\Delta yme1$ cell harbouring HA-Tgl2 or HA-Tgl2_{S144A} and subjected them to native PAGE and immunodecoration. Fig 11B shows that the complex could be detected comparably for both variants. From this we could conclude the Ser144 is vital for the catalytic activity of the protein, but has no impact on the stability or structural integrity of the different forms of the protein.

To characterize the aspartate mutant, we analysed its steady-state levels in $\Delta tgl2$ and $\Delta yme1$ yeast strains. We found that in addition to losing its function, the aspartate mutant is expressed notably less than the native protein in $\Delta tgl2$ cells but to nearly the same extent in $\Delta yme1$ (Fig 11C). This was also observed for the protein complex, as the higher molecular weight complex is detectable only in very little amounts for the mutated protein in $\Delta tgl2$ cells, and comparably to the native complex in $\Delta yme1$ yeast (Fig 11D). In contrast to the S144A variant, perturbing the catalytic triad in mutating the aspartate residue leads to instability in complex formation in WT-like conditions, suggesting that the aspartate residue is critical for the stability of Tgl2.

These observations are in congruence with previous studies where the catalytically active aspartate residue was shown to be crucial for protein stability in lipases from *G. candidum* as well as human pancreatic lipase and choline esterase. These studies have also confirmed that while

mutating the serine leads to loss of function, it has no impact on protein stability (Østerlund et al., 1997).

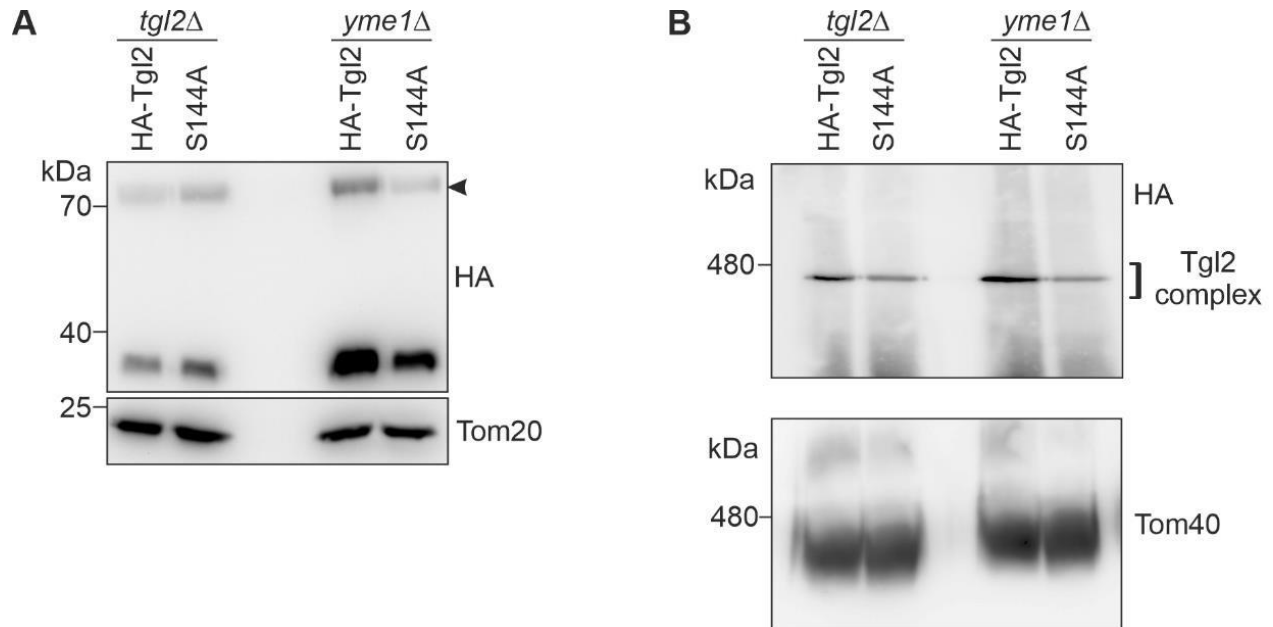
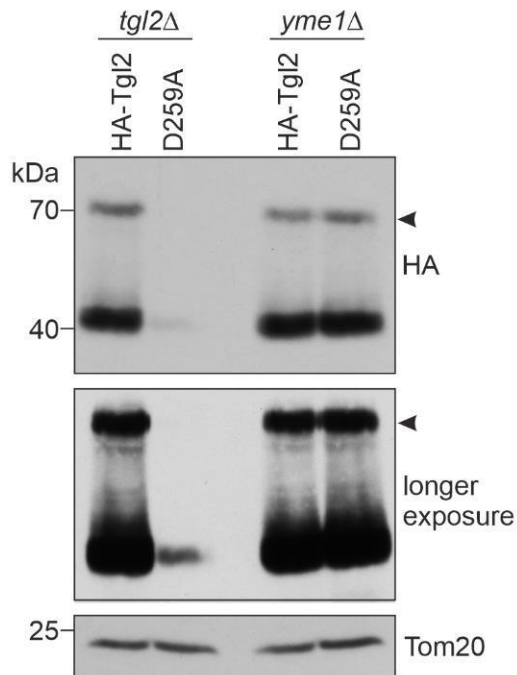
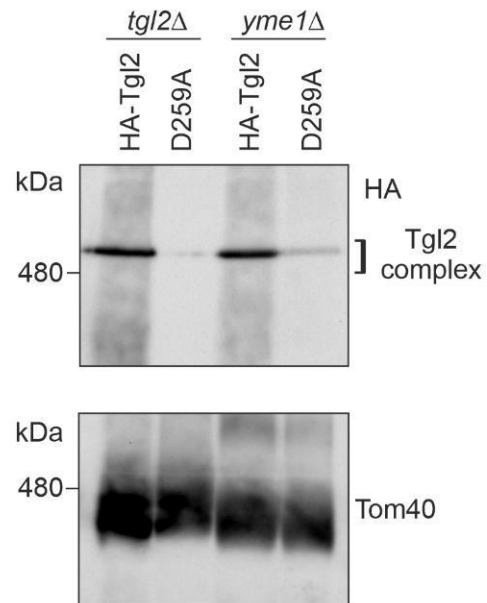


Figure 11. Disruption of the catalytic triad leads to protein instability

(A) and (C) *tgl2Δ* and *yme1Δ* cells expressing the indicated Tgl2 variants were grown to mid-logarithmic phase and crude mitochondrial fractions were isolated by mechanical lysis. The samples were analysed by SDS-PAGE and immunodecoration with antibodies against HA and Tom20, as a loading control.

C**D**

(B) and (D) Mitochondria isolated from *tgl2Δ* and *yme1Δ* cells expressing the indicated Tgl2 variants were solubilized with digitonin and analysed by BN-PAGE (4-14%) and immunodecoration with antibodies against HA and Tom40.

3.2.8 Genetic interactions of *MCP2*, *TGL2*, and *YME1* (performed by Dr Kai S Dimmer)

Of the mutants created in this study, the non-functional variants (HA-Tgl2_{Cys}, Tgl2-HA, HA-Tgl2_{S144A}, and HA-Tgl2_{D259A}) either could not be detected or were detected in very low amounts in $\Delta mcp2/\Delta tgl2$ (Fig. 12C). Thus, we needed to answer the question of whether these variants are indeed non-functional due to loss of enzymatic capacity or are unable to complement due to their low expression levels.

We attempted to create the triple mutant - $\Delta mcp2/\Delta tgl2/\Delta yme1$ to prevent degradation of the mutated Tgl2 variants and to monitor their rescue-ability. The triple mutant always yielded non-viable spores (Fig. 13A).

The lethality of the triple deletion is a consequence of the absence of all three genes, and not from a combination of the three individual genes since all three single deletion mutants as well as all combinations of double mutants show no growth defect on glucose at optimal temperatures. Moreover, the loss of *MCP2* or *TGL2* does not worsen the growth defect of *yme1Δ* cells at elevated temperatures. Finally, unlike *mcp2Δ/tgl2Δ*, *yme1Δ* cells do not show a growth defect on non-fermentable carbon sources (Fig. 13B). So far we cannot explain the lethality caused by the triple deletion of *MCP2*, *TGL2* and *YME1*. We assume that all three IMS proteins share a functional

relationship. As expected, when we express functional plasmid borne Tgl2 in heterozygous diploid triple mutant cells prior to tetrad dissection we can retrieve triple deletion cells expressing plasmid borne Tgl2. On the other hand, plasmids encoding non-functional Tgl2 variants (e.g. Ser144A mutant) fail to yield triple deletion cells expressing the mutant proteins (data not shown).

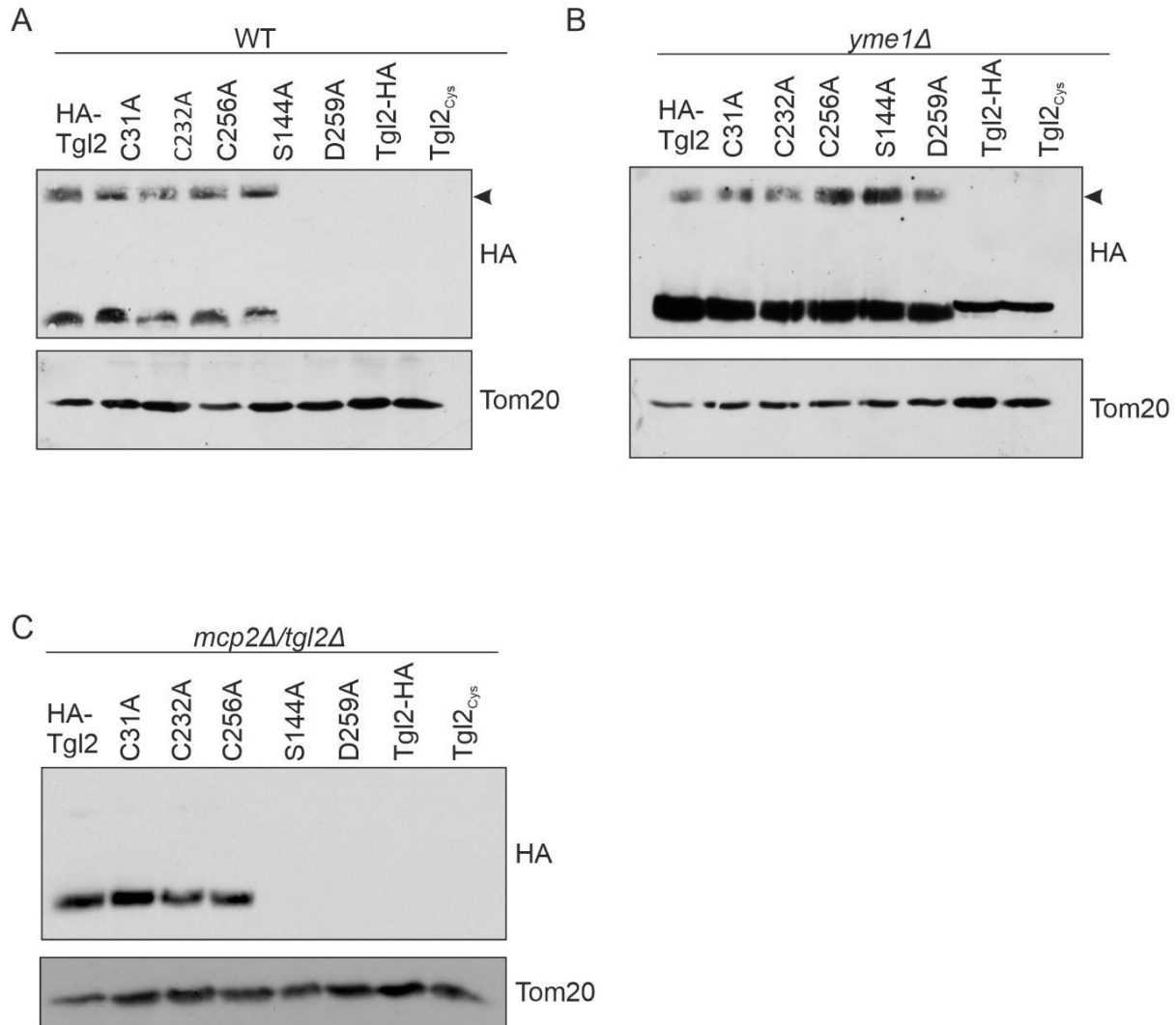
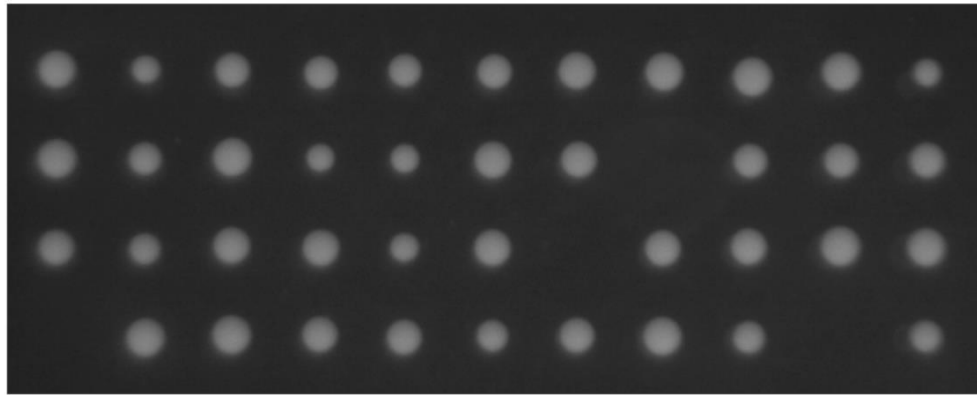


Figure 12. Steady state levels of Tgl2 mutants

(A-C) The expression Tgl2 mutants varies in WT, $\Delta yme1$, and $\Delta mcp2/\Delta tgl2$ cells. Cells expressing the the indicated variants of Tgl2 were grown to mid-logarithmic phase and crude mitochondrial fractions were isolated. The organelles were analysed by SDS-PAGE and immunodecoration with antibodies against the HA-Tag and Tom20, as a loading control. All variants of Tgl2 can be detected in $yme1\Delta$ cells. D259A is detectable in WT cells only in higher exposures. In $\Delta mcp2/\Delta tgl2$, only the functional variants can be detected at comparable levels to the native protein.

A



WT	<i>m t</i>	<i>m y</i>	<i>t y</i>	<i>y</i>	<i>t y</i>	<i>t</i>	<i>t</i>	<i>t</i>	<i>t</i>	<i>m t</i>
<i>t</i>	<i>y</i>	<i>t</i>	<i>m t</i>	<i>m t</i>	<i>m</i>	<i>m</i>	(3Δ)	<i>m y</i>	<i>m y</i>	<i>y</i>
<i>m y</i>	<i>m y</i>	<i>t y</i>	<i>m</i>	<i>m t</i>	<i>y</i>	(3Δ)	<i>y</i>	<i>y</i>	WT	<i>t</i>
(3Δ)	<i>t</i>	<i>m</i>	<i>y</i>	<i>y</i>	<i>m t</i>	<i>y</i>	<i>m</i>	<i>m t</i>	(3Δ)	<i>m y</i>

B

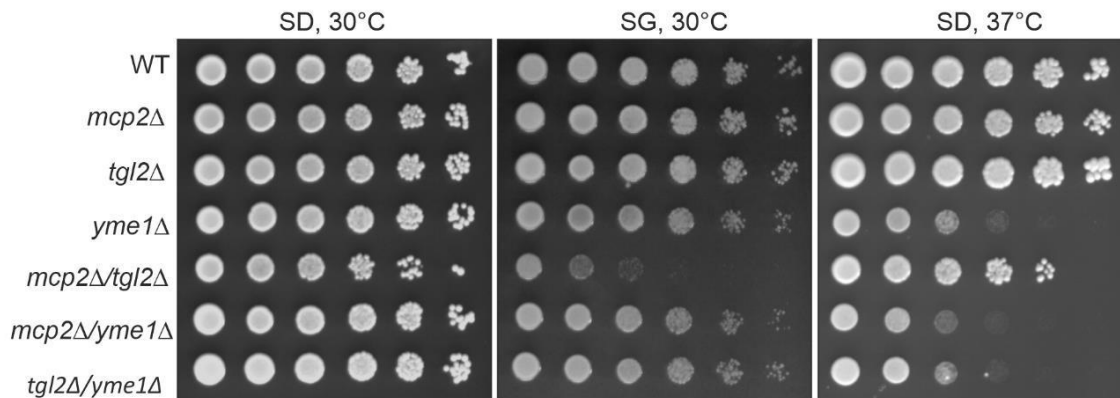


Figure 13. Genetic interactions of *MCP2*, *TGL2*, and *YME1*

Experiment performed by Dr Kai S Dimmer. (A) Excerpt of 11 out of more than 100 dissected tetrads of the heterozygous triple deletion mutant (*mcp2Δ/MCP2 - tgl2Δ/TGL2 - yme1Δ/YME1*). The table below the haploid clones shows the genotype analysis, *m*: *mcp2Δ*, *t*: *tgl2Δ*, *y*: *yme1Δ*, WT: wild type, (3Δ): triple deletion – not viable. (B) Growth analysis of single and double deletion strains of the three genes. Growth at either 30°C or 37°C was analysed by drop dilution assay of 1:5 serial dilutions on synthetic medium containing either glucose (SD) or glycerol (SG).

3.2.9 Mitochondria lacking Tgl2 have elevated levels of neutral lipids

Through lipidomics analysis from whole cell extracts, we previously reported elevated TAG and DAG levels in $\Delta mcp2/\Delta tgl2$ yeast cells (Odendall et al., 2019). Since Tgl2 and Mcp2 are mitochondrial proteins, we wondered if this perturbation is primarily caused by mitochondria. We isolated neutral lipids from mitochondria (WT, $\Delta mcp2$, $\Delta tgl2$, and $\Delta mcp2/\Delta tgl2$) and subjected them to TLC analysis (Fig. 14A). To assess this further, we isolated mitochondria from WT, $\Delta mcp2$, $\Delta tgl2$, and $\Delta mcp2/\Delta tgl2$, trypsinized them, and purified them by a density gradient. The purity of the mitochondria was confirmed by SDS-PAGE and immunodecoration against peroxisomal, ER, and cytosolic proteins. Fig. 14B confirms that the mitochondrial fractions were prepared uniformly with almost no indication of contact sites with the aforementioned organelles. Lipidomics analyses of mitochondria revealed elevated TAG and DAG levels in $\Delta mcp2/\Delta tgl2$ as well as $\Delta tgl2$. This suggests that the previously observations reflected the mitochondrial neutral lipid levels, as the effect appears to be amplified in our lipidomics analysis (Fig. 14C).

These results and the fact that TAG levels the increase observed from the cell lysates (Odendall et al., 2019) is enhanced in the mitochondrial fractions suggests that the increase in TAG levels is due to increased mitochondrial or mitochondria associated TAGs.

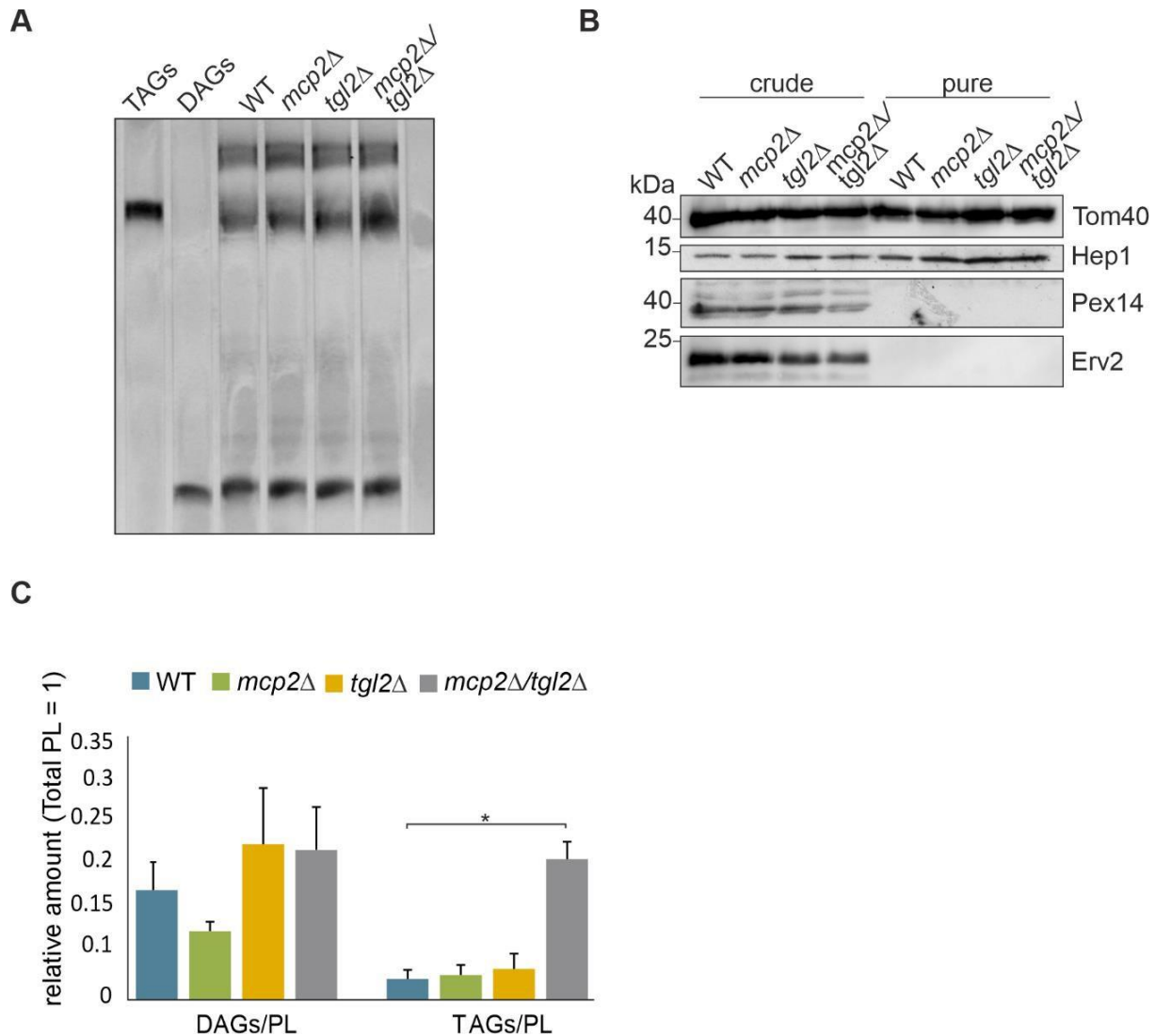


Figure 14. Mitochondrial fractions from *mcp2Δ/tgl2Δ* cells show increased TAG levels

(A) Neutral lipids were extracted from mitochondria of the indicated cells and analysed by thin-layer chromatography. The lipids were stained with a primuline solution and visualised under UV-light. The migration behaviour of standard neutral lipids is indicated on the left. (B) Mitochondria were isolated from the indicated strains, treated with trypsin and further purified by sucrose gradient. Crude and purified mitochondria (100 μ g) were analysed by SDS-PAGE and immunodecoration. Tom40 and Hep1, mitochondrial markers, Pex14, peroxisomal marker, and Erv2, ER marker. (C) Pure mitochondria from (B) were analysed by mass spectrometric analysis. The amounts of TAGs and DAGs versus total PL is shown as a mean with SD bars ($n = 3$, * $p < 0.05$, GraphPad T-test calculator). MS analysis was performed by Dr T. Tatsuta (MPI-AGE, Köln).

3.3 Discussion

Lipids are the main structural components of biological membranes and their metabolism is crucial for maintaining cellular health. Even in simpler model organisms like *S. cerevisiae*, deficiencies in lipid metabolism result in impaired cellular function and, in some cases, severe growth defects (Connerth et al., 2012; Enkler & Spang, 2024; Tatsuta & Langer, 2017). There have been significant advancements in the field of lipid metabolism in the last few years wherein the cross talk between mitochondria and other organelles has acquired a crucial role. Reports of protein tethers between the mitochondrial outer membrane (MOM) and membranes of proximal organelles laid the foundation of the concept of 'contact sites', which has become a topic of extensive research. The ERMES complex was the first of such mitochondrial tethers to be recognized, and has been now thoroughly elucidated ((AhYoung et al., 2015; Kawano et al., 2018; Kornmann & Walter, 2010). ERMES subunits have been shown to bind to and traffic phospholipids between the ER and mitochondria. The loss of these subunits results in severe growth phenotypes and anomalous mitochondrial morphology (Burgess et al., 1994; Dimmer et al., 2002; Kornmann et al., 2009; Youngman et al., 2004).

Communication between mitochondria and other organelles such as vacuoles and peroxisomes has also been described wherein vCLAMP – the contact sites between mitochondria and vacuoles have been implicated in endocytosis. It is also known that the loss of vCLAMP leads to impaired PL transport, suggesting its contribution towards lipid homeostasis (John Peter et al., 2017; Kakimoto et al., 2018). Rather recently, contact sites between mitochondria with peroxisomes and lipid droplets have also been suggested, but the exact mechanism of potential lipid transfer between and within these organelles still needs much exploration (Enkler et al., 2023; Kakimoto et al., 2018; Schuldiner & Bohnert, 2017; Shai et al., 2016).

In a previous study, we characterized a high copy suppressor of ERMES mutants – Mcp2 (now Cqd2) which was more recently shown to be involved in CoQ metabolism yeast (Kemmerer et al., 2021). We first identified Tgl2 in a high throughput screen of deletion of *MCP2* where the two genes displayed negative genetic interaction, more prominently on non-fermentable carbon sources (Odendall et al., 2019). This growth defect is lost after prolonged growth on fermentable carbon sources – a phenomenon often observed for lipid metabolism and ERMES mutants (Burgess et al., 1994; John Peter et al., 2017; Sogo & Yaffe, 1994). We could also show that both Mcp2 and Tgl2 are proteins located with their functional domains in the IMS (Kemmerer et al., 2021; Odendall et al., 2019). Of the two, Tgl2 is a soluble protein and relies on the disulfide relay pathway for its import into the IMS (Odendall et al., 2019).

In my work, we further characterized Tgl2 to gain a better understanding of its molecular function. We observed that Tgl2 can form homodimers under non-reducing conditions. We suggest that the dimer is a product of intermolecular disulfide bridges between two or more of the eight cysteine residues of the protein. We could also confirm an oligomeric form of the protein containing at least two copies of itself. Moreover, Tgl2 is not conserved amongst higher eukaryotes and has its closest structural homologues in prokaryotes. These bacterial lipases e.g. LipA from *P. aeruginosa*,

were shown to harbour intra as well as intermolecular disulfide bridges. Furthermore, extracellular lipases of higher eukaryotes like human pancreatic lipase, and lipoprotein lipase also contain disulfide bonds which are often essential for protein function, allowing dimerization that facilitates substrate binding or protein stability (Gunn & Neher, 2023; Liebeton et al., 2001). Since mutation of all cysteine residues of Tgl2 led to loss of function of the protein we decided to mutate three single cysteine residues that according to structure prediction programs are likely to be involved in intra- or intermolecular cysteine bridges. Taken together, mutation of cysteine 31, 232, or 256 had no influence on the quaternary structure or function of Tgl2.

The non-functional variants of Tgl2 like Tgl2-HA and Tgl2_{cys}, are undetectable in WT or $\Delta tgl2$ yeast, indicating a quality control mechanism for the protein. A vast majority of the IMS proteins rely on Yme1, an i-AAA protease in the MIM, for their folding and/or degradation (Schreiner et al., 2012). Yme1 has an IMS exposed catalytic domain which is suggested to have chaperone-like activity (Leonhard et al., 1999). More studies have successfully shown protein folding and assembling activity of Yme1 (Fiumera et al., 2009; Schreiner et al., 2012). By comparing the steady state levels of native and non-functional variants of Tgl2, we could confirm that its quality control is maintained by Yme1. The undetectable or weakly detectable protein mutants could be observed in $\Delta yme1$ yeast, and were expressed similar to the native Tgl2.

Ham et al. previously characterized the lipase motif of Tgl2. By mutating the conserved serine residue (S144), they could induce a loss of *in vitro* lipolytic activity (Ham et al., 2010). Our observations agree with these studies that despite native-like expression levels in WT and $\Delta yme1$ yeast strains, Tgl2_{S144A} is unable to rescue the growth defect of $\Delta mcp2/\Delta tgl2$. We also characterized the predicted Ser-Asp-His catalytic triad of Tgl2 and showed that disrupting the catalytically active aspartate (D259) to alanine leads to a non-functional, poorly expressing variant of the protein. Studies pertaining to other lipases and acyltransferases show that while a conservative mutation (aspartate to glutamate) results in only partial loss of function, mutating the aspartate to alanine or valine leads to loss of enzyme activity as well as stability. This is potentially due to a compensatory effect of the carboxylic group of glutamate. Since the carboxylic group is essential for stabilizing interactions with other residues in its vicinity, its loss can lead to protein misfolding and/or instability (Jiger & Demleitner, 1992; Østerlund et al., 1997).

The catalytic triad is a feature of several enzymes including proteases, acyltransferases, and lipases (Fig. 15). Some members of the Tgl family exhibit lipase as well as acyltransferase activity, suggesting that Tgl2 could be involved in transferring fatty acids between substrates rather than hydrolysing TAGs (Grillitsch & Daum, 2011; Klug & Daum, 2014).

The lipolytic activity of Tgl2 was shown through *in vitro* lipase assays wherein Tgl2 enriched lysate was used to hydrolyse different TAGs— of which tributyrin was the optimal substrate. *In vivo* analyses using cerulenin could also confirm TAG-specific activity of Tgl2 (Ham et al., 2010; Van Heusden et al., 1998). We performed lipidomics analysis using mitochondrial fractions devoid of contact sites and could detect elevated levels of neutral lipids in fractions isolated from $\Delta mcp2/\Delta tgl2$ yeast cells. This observation aligns with our previous lipidomics analysis from whole

cell lysate fractions of the same strains (Odendall et al., 2019). This observation could be corroborated by TLC assays where, again, we observed higher amounts of TAGs in the lipid fractions extracted from $\Delta mcp2/\Delta tgl2$ and $\Delta tgl2$ mitochondria. Notably, the neutral lipid content measured in the lipidomics analyses reflected primarily long chain fatty acids, which are the most abundant forms of TAGs and DAGs. In conclusion, our experiments could show that absence of Tgl2 results in increased neutral lipids in yeast mitochondria, and this phenotype is amplified in $\Delta mcp2/\Delta tgl2$ yeast.

To achieve a rounded understanding of Tgl2, we tried to ascertain its physical interaction partners through co-immunoprecipitation experiments. Despite using different affinity tags and experimental conditions, we were unable to find any proteins of interest in our proteomics data. In a recent mitochondrial complexome study, Tgl2 was shown to co-migrate with Ups1 and Ups3, both of which are lipid transfer proteins in the IMS (Schulte et al., 2023). To investigate further, we performed native PAGE with $\Delta ups1$ yeast expressing HA-Tgl2 but the complex remains unchanged in size and stability. We were also unable to detect any interaction partners in preliminary chemical crosslinking experiments (data not shown). We applied the same approach to $\Delta ups2$ and $\Delta mdm35$, proteins involved in the lipid transfer complex of the IMS, but the complex was still unchanged (Potting et al., 2010; Tamura, Onguka, Itoh, et al., 2012).

A suitable alternative to our methods could be a high throughput screen of *TGL2* using the deletion of *TGL2* as the bait, which could streamline the process of finding genetic or physical interactors. Another approach to determine interaction partners would be to identify the components of the Tgl2 complex through complexome analysis. The complex from BN-PAGE could also be analyzed by mass spectrometry using appropriate controls which might help us identify the components of the complex. Given the bacterial ancestry of mitochondria and the similarity of Tgl2 with mostly bacterial lipases, one could speculate that the protein was conserved to simpler eukaryotes like yeast. However, why higher eukaryotes lack any such mitochondrial lipases is a question yet to be answered. Finally, identification of the physiological substrates of Tgl2 would be the key to understanding its true role in the IMS.

The cysteine-rich sequence of Tgl2 posed a challenge for recombinant expression. Despite trying several affinity-tags and expression conditions, the protein was always insoluble or was co-purified along with GroEL (data not shown). Extensive washing steps to remove the chaperone led to destabilization of the protein leading to degradation. Table 2 gives a brief overview of the different constructs created. In the future, one could also try to purify the protein without its unstructured N-terminal region which could improve solubility (Fig. 16). Complementation assays with this construct show that the truncation does not disturb the ability of Tgl2 to rescue the growth phenotype of $\Delta mcp2/\Delta tgl2$ (data not shown).

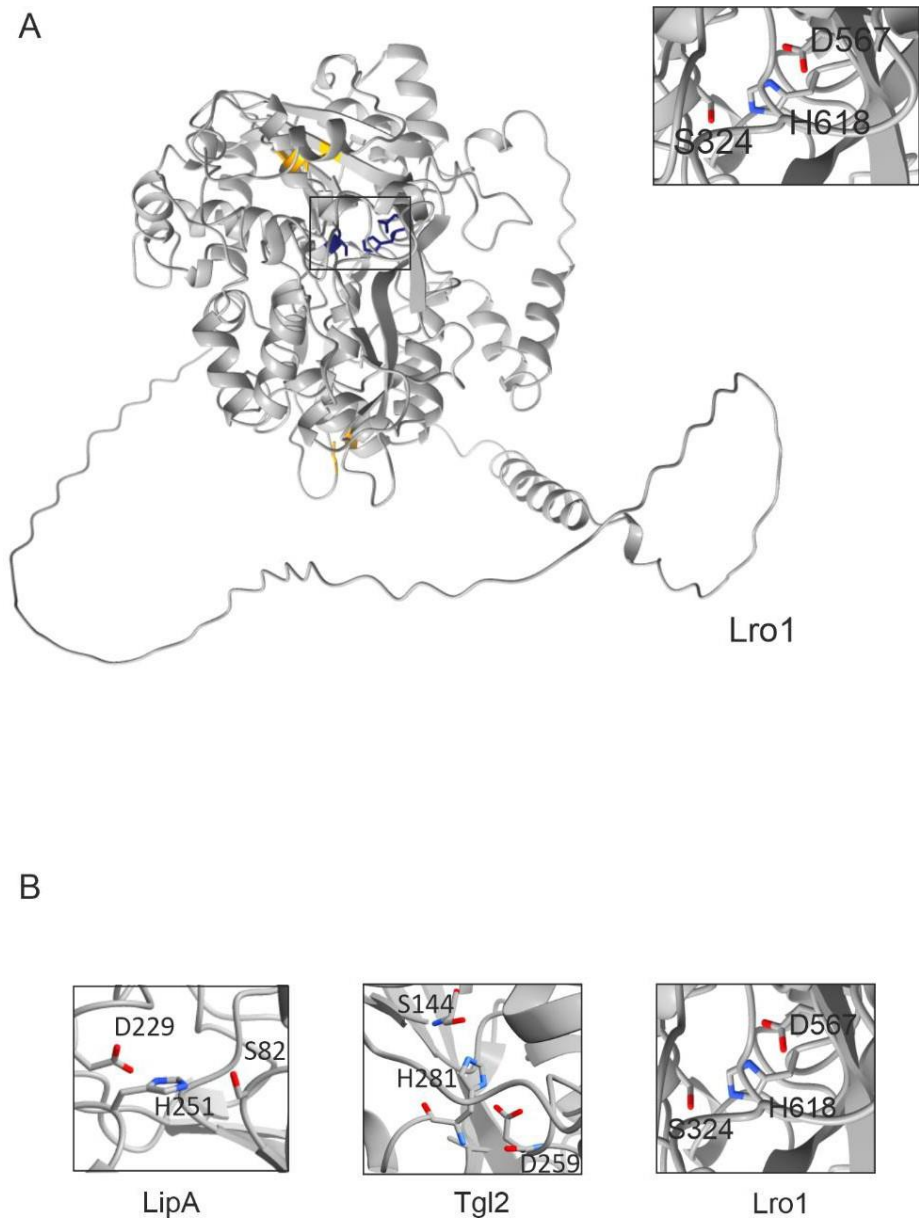


Figure 15. Catalytic triad of Lro1 – a yeast acyltransferase

(A) Acyltransferases contain a catalytic triad consisting of Ser-Asp-His. Predicted structure of Lro1 with the intramolecular disulfide bonds in yellow and the catalytic triad highlighted in blue. (B) The Ser-Asp-His catalytic triad of LipA (left, a bacterial lipase), Tgl2 (center, yeast putative TAG lipase), and Lro1 (right, yeast acyltransferase).

Table 2. Constructs used for recombinant expression of Tgl2

Construct	Organism	Comments
GST-Tgl2	- <i>E. coli</i> BL21 (DE3) - <i>E. coli</i> Origami B(DE3)	- The construct is soluble but co-elutes with GroEL which could not be removed. We were unable to accurately estimate the protein amounts because of this reason. - Construct was used to generate an antibody against Tgl2.
MBP-Tgl2	- <i>E. coli</i> BL21 (DE3) - <i>E. coli</i> Origami B(DE3) - <i>E. coli</i> Rosetta (DE3)	Solubility issues. Purification from inclusion bodies was not successful.
His-Tgl2	- <i>E. coli</i> - <i>S. cerevisiae</i>	- Could not be expressed in <i>E. coli</i> - Detection issues in both organisms
His-Sumo-Tgl2	- <i>E. coli</i> BL21 (DE3) - <i>E. coli</i> C41 (DE3)	- Solubility issues. We tried to purify from inclusion bodies, but the construct is highly susceptible to misfolding and could only be obtained as incorrectly refolded protein. - The soluble protein fraction (obtained in minor amounts) could not be enriched sufficiently.
Strep-Tgl2	- <i>E. coli</i> Shuffle Express - <i>E. coli</i> C41 (DE3) - <i>S. cerevisiae</i>	- The construct is soluble but co-elutes with GroEL.
His-Tgl2 _(Δ1-17)	- <i>E. coli</i> BL21 (DE3) - <i>S. cerevisiae</i>	- Truncated construct where the disordered N-terminal region (17 amino acids) is removed to improve solubility. - Solubility issues in <i>E. coli</i> so we did not pursue it. - We could purify it in very small amounts from yeast mitochondria.

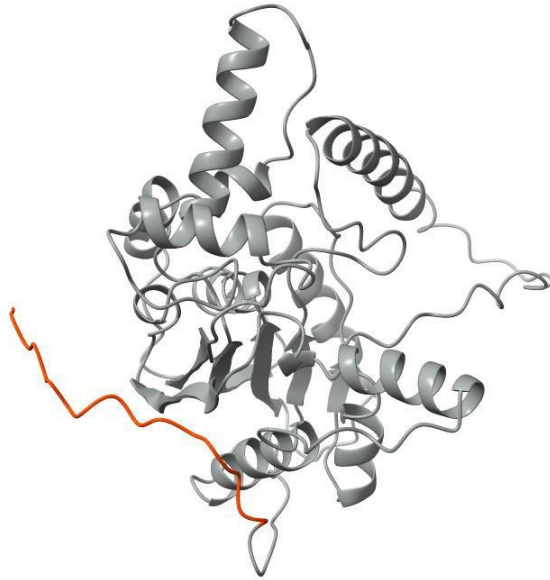


Figure 16. Unstructured N-terminal region of Tgl2

AlphaFold prediction of Tgl2 with the unstructured N-terminus (17 amino acids) highlighted in red.

Yeast mitochondria can process *de novo* designed β - barrel proteins

Moitra, A., Tiku, V., Rapaport, D. (2024), Yeast mitochondria can process *de novo* designed β -barrel proteins. FEBSJ, 291: 292-307. <https://doi.org/10.1111/febs.16950>

Personal Contribution

I performed sub-cellular fraction experiments to analyze the distribution of synthetic β -barrel proteins in cells lacking *SAM/MAS37*. To understand the impact of the Tob55/Sam50 on the oligomerization behavior of the β -barrel proteins, I performed native-PAGE with N-terminally truncated variants of Sam50/Tob55. I also performed site-directed mutagenesis to mutate the β -signal of these proteins and its impact on their oligomerization behavior through native-PAGE. Finally, I analyzed the steady state levels of the proteins in cells lacking the small TIMs- Tim8 and Tim13 (Data not shown).

Author Contributions

AM and DR co-wrote the manuscript, designed the experiments, and analysed the data. AM and VT performed the experiments and prepared the figures. DR supervised the project and acquired funding.

Materials and methods

The materials and methods for this section can be found in the article - Yeast mitochondria can process *de novo* designed β -barrel proteins.

4.1 Introduction

All β -barrel pre-proteins are synthesized by nuclear DNA and rely on cytosolic chaperones like Hsp70, and its co-chaperones, to hold them in an import competent fashion. Upon recognition by the TOM receptors Tom20 and Tom70, these precursor proteins are translocated through the TOM complex (van Wilpe et al., 1999; Yamamoto et al., 2009; Yamano et al., 2008). Yeast mitochondria consist of four main β -barrel proteins- Tom40 which is the main portal for all mitochondrial proteins, Tob55/Sam50 which enables insertion of β -barrel proteins, the main ion and metabolite channel VDAC, and Mdm10. Mdm10 exists in two populations, either associated with the ERMES or the SAM complex (Chacinska et al., 2009; Gupta & Becker, 2021).

The SAM (Sorting and Machinery) or TOB complex consists of 3 subunits, the central β -barrel subunit - Sam50/Tob55 and its peripheral subunits – Sam37/Tom37 and Sam35/Tob38. Sam50 belongs to the Omp85 protein family and is a 16-stranded β -barrel protein (Habib et al., 2005; A. Klein et al., 2012; Kozjak et al., 2003; Paschen et al., 2003). It possesses an N-terminal POTRA (Polypeptide transport associated) domain that protrudes into the IMS and is suggested to be involved in the recognition of β -barrel precursor proteins (Habib et al., 2006; Höhr et al., 2015; Noinaj et al., 2017). The last strand of Sam50 contains the canonical β -signal which mediates binding of incoming precursor proteins with the SAM machinery. Both Sam35 and Sam37 are known to interact with Sam50 but only Sam35 is in direct contact, capping the β -barrel (Diederichs et al., 2020). Sam37 is exposed to the cytosolic face of the MOM, and is reported to maintain the stability of the SAM complex (N. C. Chan & Lithgow, 2008). While the formation of the SAM complex is poorly understood, multiple studies have confirmed its contribution to the assembly of the TOM complex in cooperation with the MIM complex and Mdm10. The SAM-Mdm10 complex not only promotes the release of Tom40 precursors for further assembly, but also promotes Tom22 to integrate into the MIM aiding its assembly with the small Toms (Yamano et al., 2010b, 2010a).

Extensive structural and biochemical studies have uncovered how the SAM machinery inserts these pre-proteins into the MOM. The first and last strands of Sam50 form a lateral gate. The incoming precursor protein interrupts this lateral gate as it interacts with the sixth- β strand of Sam50, and undergoes a β -signal swap. The precursor protein is then sequentially inserted, folded, and accumulated at the lateral gate. As the first and last β -strands of the pre-proteins form H-bonds to form a β -barrel, it is released from the SAM complex into the MOM (N. C. Chan & Lithgow, 2008; Diederichs et al., 2020, 2020; Höhr et al., 2018). How the pre-protein is released exactly is still unknown. Two theories have been suggested to explain this mechanism – the lateral gate release theory suggests temporary membrane thinning at the vicinity of the gate which eases the release of the pre-protein from Sam50 (Höhr et al., 2018). The barrel-swapping theory suggests that the folded pre-protein forms a temporary complex with a Sam50, disrupting the dynamic Sam50 homodimer. As the protein develops and dissociates, it is replaced by a Sam50 molecule to restore the dimer (Takeda et al., 2021).

The *de novo* design of soluble, small β -barrel proteins (<70 amino acids) was only recently achieved as the small size poses a challenge to the overall stability of the protein. In their experiments, Vorobieva et al successfully designed, purified, and characterized two artificial β -barrel proteins – Tmb 2.3 and Tmb 2.17 using molecular simulation and x-ray crystallography (Vorobieva et al., 2021). In our studies, we wanted to understand if these small, artificial β -barrel proteins emulate the behavior of canonical β -barrel proteins. To achieve this, we expressed these proteins in yeast, assessed their integration into the mitochondria, and analyzed their behavior using biochemical methods typical for mitochondrial β -barrel proteins.

4.2 Results

4.2.1 The assembly of the TMBs depends to a variable extent on the TOB/SAM complex

Precursors of beta-barrel are received by the TOM receptors and processed through the TOM complex into the IMS. The small TIM chaperones in the IMS receive the pre-protein and prevent its aggregation. From here, insertion into the MOM is mediated by the TOB/SAM complex (Chacinska et al., 2009; Habib et al., 2005; Kozjak et al., 2003; Neupert & Herrmann, 2007; Wiedemann et al., 2003). Since we could confirm mitochondrial targeting of the TMBs, we wanted to assess if their insertion into the MOM is dependent on the TOB/SAM complex.

We transformed plasmids encoding either Tmb2.3-HA or Tmb2.17-HA into WT or cells lacking Mas37/Sam37. The cells were grown at 24°C to avoid accumulation of suppressors at elevated temperatures as Mas37/Sam37 is important for proper import by the TOB/SAM complex. Cytosolic, mitochondrial, and ER fractions were obtained by sub-cellular fractionation and the steady state levels of the TMBs were analyzed by SDS-PAGE and immunoblotting (Fig. 17A and B).

We observed that both Tmb2.3-HA and Tmb.217-HA behave like canonical mitochondrial β -barrel proteins such as Tom40. The mitochondrial levels of the TMBs as well as Tom40 were significantly reduced in *mas37/sam37* Δ cells as compared to those in WT cells. The steady state levels of the ER protein, Erv2, and the cytosolic protein, Hsp82, remain unaffected.

While the decrease in the mitochondrial amounts of the TMBs could be explained by mistargeting to another compartment such as ER, we could not detect any notable amounts of these proteins in the ER or cytosolic fractions. These observations could also be explained by the reduced amounts of Tom40 itself, and the lack of Sam37/Mas37 simply exaggerates this effect.

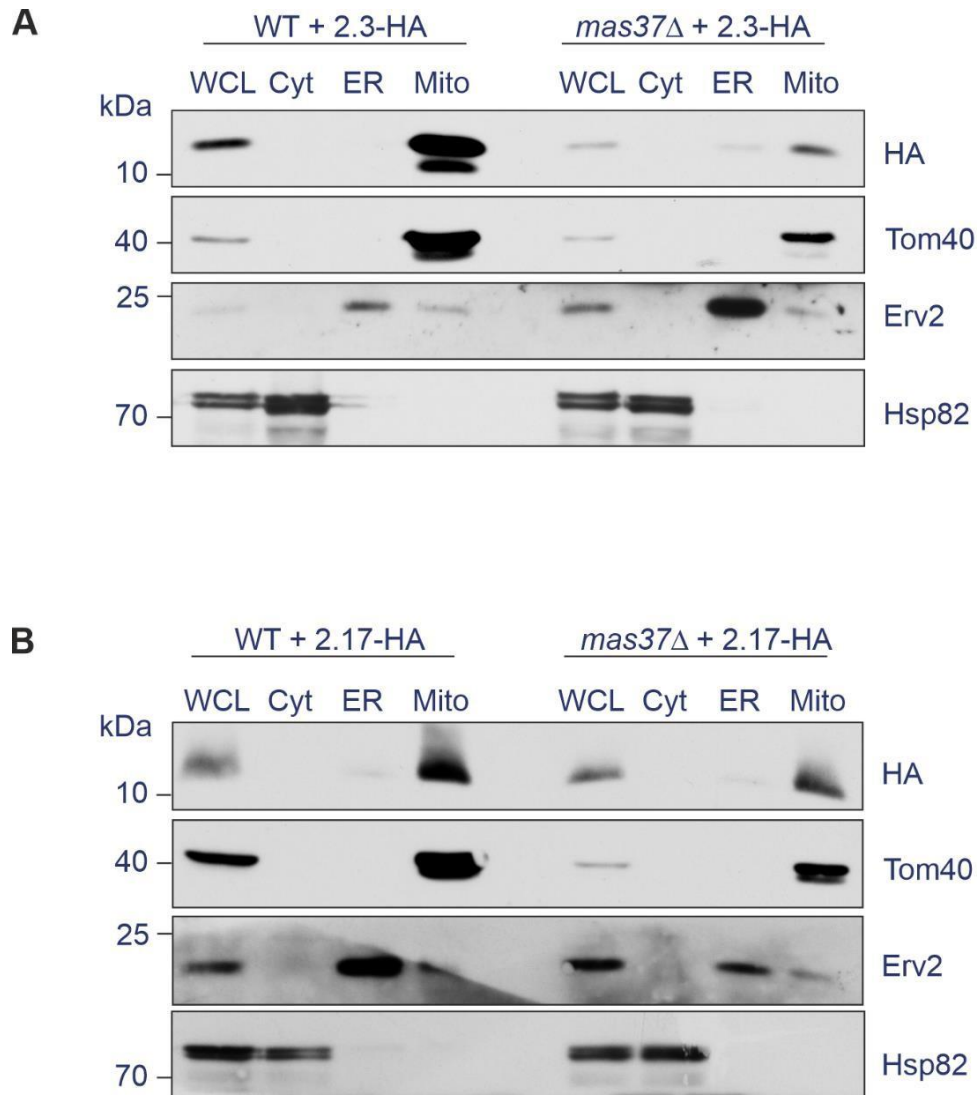


Figure 17. The membrane integration of both TMBs requires Mas37/Sam37

(A, B) WT and *mas37/sam37Δ* yeast cells were transformed with a plasmid encoding for either Tmb2.3-HA (A) or Tmb2.17-HA (B). Whole cell lysate (WCL), cytosol (Cyt), endoplasmic reticulum (ER) and mitochondrial (Mito) fractions isolated from the transformed cells were subjected to SDS-PAGE and immunoblotting with the indicated antibodies. Erv2 is an ER membrane protein, while Hsp82 is used as a cytosolic marker.

4.2.2 The POTRA domain is necessary for the oligomerization of Tmb2.3

Sam50/Tob55 is an essential component of the SAM complex. Itself a β -barrel protein, the N-terminus of the protein protrudes into the IMS, and contains a polypeptide transport-associated domain (POTRA) domain (Habib et al., 2006; Kutik et al., 2008). While there is contradicting evidence about the involvement of the POTRA domain in pre-protein recognition, the role of Sam50/Tob55 in the membrane integration of β -barrel precursors is indisputable.

Habib et al previously showed that the deletion of the POTRA domain results in impairment in the biogenesis of β -barrel proteins (Habib et al., 2006). To analyze the involvement of this domain in the biogenesis of the TMBs, we expressed Tmb2.3-HA in cells harboring truncated variants of Tob55/Sam50. The truncated versions lacked either 50 - *tob55*(Δ 50), or 102 - *tob55*(Δ 102), amino acid residues at the N terminus. BN-PAGE analyses of mitochondria isolated from these cells revealed that these truncations prevent oligomerization of Tmb2.3-HA. These findings demonstrate that the N-terminal region of Tob55/Sam50 is required for proper assembly of Tmb2.3-HA (Fig. 18).

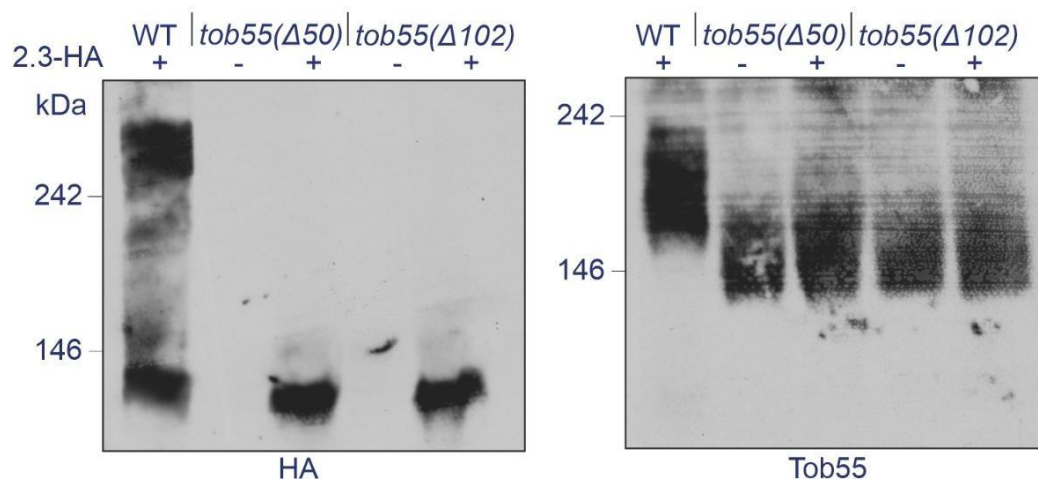


Figure 18. The POTRA domain is necessary for the oligomerization of Tmb2.3

Mitochondria were isolated from the indicated Tmb2.3-HA expressing cells harbouring either native Tob55/Sam50 or its N-terminally truncated variants. Samples were analysed by BN-PAGE and immunodecoration with antibodies against either the HA tag (left panel) or Tob55/Sam50 (right panel).

4.2.3 Point mutation in the β -signal does not significantly alter the biogenesis of both TMBs

The last β -strand of mitochondrial β -barrel proteins contains a motif termed ' β -signal' which facilitates their interaction with the TOB/SAM complex. This motif consists of Po-X-G-X-X-Hy-X-Hy-X, where Po stands for a polar residue, G for Glycine and Hy represents a hydrophobic residue. While alterations in the in the β -signal do not interfere with the initial targeting of newly synthesized β -barrel proteins to mitochondria, it does affect their interaction with the TOB/SAM complex (Kutik et al., 2008).

Since the TMBs differ in their targeting and oligomerization behaviours, we wanted to investigate whether they possess a sequence similar to the β -signal and if further examination of this motif could explain our observations. Sequence analysis of the TMBs revealed that Tmb2.3 indeed contained a canonical β -signal, whereas Tmb2.17 had only a partial consensus sequence, wherein the polar first residue was lacking (Q115 in Tmb2.3, A115 in Tmb2.17).

To assess whether this variation in their β -signals contributes to the differential dependence of the TMBs on the SAM/TOB complex, the following mutants were generated - Tmb2.3_{Q115A}-HA and Tmb2.17_{A115Q}-HA (Fig. 19A). BN-PAGE analysis of mitochondria harbouring these mutated TMBs showed that Tmb2.3_{Q115A}-HA was unable to form oligomers to the same extent as native Tmb2.3-HA. On the other hand, both Tmb2.18_{A115Q}-HA and Tmb2.17-HA were predominantly detected in their monomeric forms (Fig. 19B). This effect should be further investigating by altering the C-terminal end of the β -signal which also varies between the TMBs.

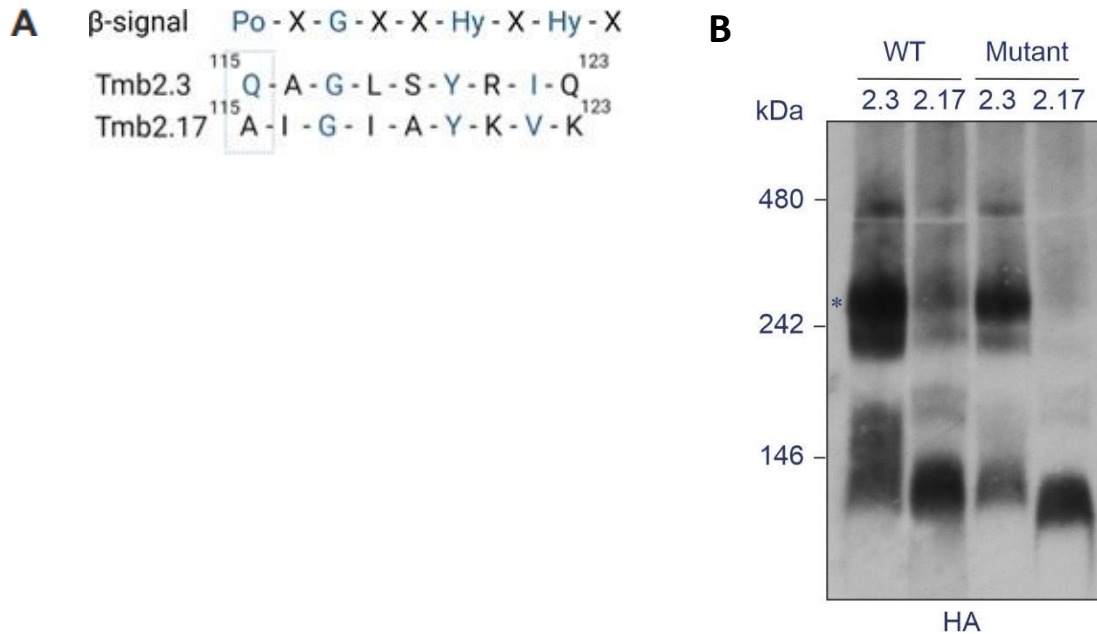


Figure 19. Point mutation in the β -signal does not alter the assembly of Tmb2.3 and Tmb2.17

(A) Conserved mitochondrial β -signal motif (top) and the corresponding β -signal motif in the TMBs (bottom). The β -signal residues are in red and the mutated residues in bold. Po, polar; Hy, hydrophobic. (B) Mitochondria isolated from WT cells expressing either wild type or mutant TMBs were subjected to BN-PAGE and immunoblotting with antibodies against the HA tag. A high molecular weight form of Tmb2.3-HA is indicated by an asterisk.

4.2.4 Absence of the small TIMs - Tim8 and Tim13, does not affect the import of the TMBs

The small TIM chaperones – Tim8, Tim9, Tim10, and Tim13, maintain the pre-protein in a soluble fashion in the IMS, and bring them to the TOB receptor for membrane integration (Mokranjac & Neupert, 2009). Since both Tim9 and Tim10 are essential proteins, the involvement of small TIMs in the import of the TMBs could only be tested in the *tim8Δ/tim13Δ* mutant (Curran et al., 2002, 2002; Davis et al., 2007; Vial et al., 2002). We expressed the TMBs in WT and *tim8Δ/tim13Δ*, and analyzed their steady state levels by SDS-PAGE and immunoblotting. We could not observe any alterations in the steady-state levels of the TMBs in the mutants. Moreover, there was no impact on the behaviour of canonical β -barrel proteins as well (Fig. 20). However, import via the IMS has some redundancy due to the presence of the other two TIM chaperones. Therefore, one cannot dismiss the argument that the import route of the TMBs is through the IMS, after which they are inserted into the MOM.

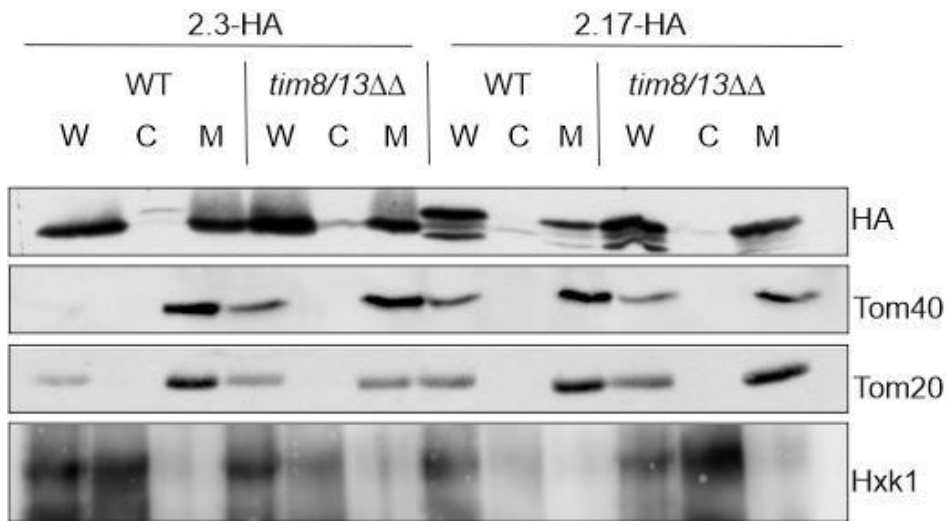


Figure 20. Absence of the small TIMs - Tim8 and Tim13, does not affect the import of the TMBs

The TMBs were expressed in WT and *tim8Δ/tim13Δ* yeast cells and the crude mitochondrial fractions were isolated by mechanical rupture. Whole cell lysate (W) and cytosolic (C) fractions were collected and subjected to TCA precipitation. The fractions – W, C, and mitochondrial (M) were analysed by SDS-PAGE and immunoblotting against the indicated antibodies.

4.3 Discussion

All β -barrel proteins are synthesized in the cytosol, maintained import competent by cytosolic chaperones and co-chaperones that bring them to the TOM receptors. After their translocation through the Tom40 pore, the β -barrel proteins are passed on to small TIM chaperones in the IMS which initiate MOM integration with the help of the TOB/SAM complex (Chacinska et al., 2009; Neupert, 1997; Neupert & Herrmann, 2007).

In our study, we examined the behavior of two synthetic β -barrel proteins in a physiological environment typical for β -barrel proteins (Vorobieva et al., 2021). We wanted to investigate the recognition and assembly of these proteins by the mitochondrial import machinery, and to also better understand the principles of β -barrel protein biogenesis.

We analyzed the role of the TOB/SAM complex in the assembly of the artificial TMBs by studying the steady state levels of these proteins in the absence of Sam37/Mas37, which is known to stabilize the TOB/SAM complex (Kozjak et al., 2003; Wenz et al., 2015). We observed a decrease in the steady state levels of the TMBs in the mitochondrial fraction in *sam37 Δ* cells. Previous studies have reported that destabilization of the complex affects the efficiency with which β -barrel proteins such as Tom40 are inserted into the MOM (N. C. Chan & Lithgow, 2008; Waizenegger et al., 2004; Wiedemann et al., 2003). Moreover, this decrease in Tom40 levels could also contribute to the observed decrease in steady state levels of the TMBs.

Since truncations in the N-terminal POTRA domain of Tob55/Sam50 has been reported to impair the biogenesis of β -barrel proteins (Habib et al., 2006), we performed BN-PAGE of mitochondria with N-terminal truncations of Sam50/Tob55. The observations that the higher oligomers of Tmb2.3 are dramatically reduced in the POTRA domain mutants demonstrate the importance of the TOB/SAM complex not only for the general import of Tmb2.3-HA, but also for its assembly into oligomers.

Throughout the course of our study, we observed subtle variations in the behaviours of the two TMBs - such as the partial mislocalization to the ER of 2.17 and its inability to form higher oligomers. Sequence analysis revealed variations in the putative β -signal of the two proteins, which we tried to compensate for by site-directed mutagenesis. Unfortunately, the point mutations in the β -signal of the proteins did not alter the behavior significantly, and the differential behavior of Tmb2.17 remained unchanged. The TMBs possess several other diverging properties such as variable hydrophobicities of the β -strands, thermodynamic stabilities, sequence dissimilarity, as well as differences in the putative β -signal that could be responsible for their differential behaviours.

Collectively, this study demonstrates that the biogenesis of *de novo* designed TMBs, Tmb2.17 and Tmb2.3, is independent of the TOM receptors and depends variably on the TOB/SAM complex.

Acknowledgments

I would like to thank Kai for giving me the opportunity to work on this exciting project. I am grateful to him as well as Doron for their critical input and mentorship throughout my PhD. I would also like to mention all my group members, old and new, without whom this journey would be unimaginable. Finally, I would like to acknowledge my friends and family for their endless patience and support.

References

- Aaltonen, M. J., Friedman, J. R., Osman, C., Salin, B., di Rago, J.-P., Nunnari, J., Langer, T., & Tatsuta, T. (2016). MICOS and phospholipid transfer by Ups2–Mdm35 organize membrane lipid synthesis in mitochondria. *Journal of Cell Biology*, *213*(5), 525–534. <https://doi.org/10.1083/jcb.201602007>
- AhYoung, A. P., Jiang, J., Zhang, J., Khoi Dang, X., Loo, J. A., Zhou, Z. H., & Egea, P. F. (2015). Conserved SMP domains of the ERMES complex bind phospholipids and mediate tether assembly. *Proceedings of the National Academy of Sciences*, *112*(25). <https://doi.org/10.1073/pnas.1422363112>
- Alder, N. N., Sutherland, J., Buhring, A. I., Jensen, R. E., & Johnson, A. E. (2008). Quaternary Structure of the Mitochondrial TIM23 Complex Reveals Dynamic Association between Tim23p and Other Subunits. *Molecular Biology of the Cell*, *19*(1), 159–170. <https://doi.org/10.1091/mbc.E07-07-0669>
- Athenstaedt, K., & Daum, G. (1997). Biosynthesis of phosphatidic acid in lipid particles and endoplasmic reticulum of *Saccharomyces cerevisiae*. *Journal of Bacteriology*, *179*(24), 7611–7616. <https://doi.org/10.1128/jb.179.24.7611-7616.1997>
- Athenstaedt, K., & Daum, G. (2003). YMR313c/TGL3 Encodes a Novel Triacylglycerol Lipase Located in Lipid Particles of *Saccharomyces cerevisiae**. *Journal of Biological Chemistry*, *278*(26), 23317–23323. <https://doi.org/10.1074/jbc.M302577200>
- Athenstaedt, K., & Daum, G. (2005). Tgl4p and Tgl5p, Two Triacylglycerol Lipases of the Yeast *Saccharomyces cerevisiae* Are Localized to Lipid Particles. *Journal of Biological Chemistry*, *280*(45), 37301–37309. <https://doi.org/10.1074/jbc.M507261200>

- Baile, M. G., Whited, K., & Claypool, S. M. (2013). Deacylation on the matrix side of the mitochondrial inner membrane regulates cardiolipin remodeling. *Molecular Biology of the Cell*, *24*(12), 2008–2020. <https://doi.org/10.1091/mbc.E13-03-0121>
- Banci, L., Bertini, I., Calderone, V., Cefaro, C., Ciofi-Baffoni, S., Gallo, A., Kallergi, E., Lionaki, E., Pozidis, C., & Tokatlidis, K. (2011). Molecular recognition and substrate mimicry drive the electron-transfer process between MIA40 and ALR. *Proceedings of the National Academy of Sciences of the United States of America*, *108*(12), 4811–4816. <https://doi.org/10.1073/pnas.1014542108>
- Banci, L., Bertini, I., Cefaro, C., Ciofi-Baffoni, S., Gallo, A., Martinelli, M., Sideris, D. P., Katrakili, N., & Tokatlidis, K. (2009). MIA40 is an oxidoreductase that catalyzes oxidative protein folding in mitochondria. *Nature Structural & Molecular Biology*, *16*(2), 198–206. <https://doi.org/10.1038/nsmb.1553>
- Banerjee, R., Gladkova, C., Mapa, K., Witte, G., & Mokranjac, D. (2015). Protein translocation channel of mitochondrial inner membrane and matrix-exposed import motor communicate via two-domain coupling protein. *eLife*, *4*, e11897. <https://doi.org/10.7554/eLife.11897>
- Becker, T., Pfannschmidt, S., Guiard, B., Stojanovski, D., Milenkovic, D., Kutik, S., Pfanner, N., Meisinger, C., & Wiedemann, N. (2008). Biogenesis of the mitochondrial TOM complex: Mim1 promotes insertion and assembly of signal-anchored receptors. *The Journal of Biological Chemistry*, *283*(1), 120–127. <https://doi.org/10.1074/jbc.M706997200>
- Becker, T., Wenz, L.-S., Krüger, V., Lehmann, W., Müller, J. M., Goroncy, L., Zufall, N., Lithgow, T., Guiard, B., Chacinska, A., Wagner, R., Meisinger, C., & Pfanner, N. (2011). The mitochondrial import protein Mim1 promotes biogenesis of multispinning outer membrane proteins. *The Journal of Cell Biology*, *194*(3), 387–395. <https://doi.org/10.1083/jcb.201102044>

- Beilharz, T., Egan, B., Silver, P. A., Hofmann, K., & Lithgow, T. (2003). Bipartite signals mediate subcellular targeting of tail-anchored membrane proteins in *Saccharomyces cerevisiae*. *The Journal of Biological Chemistry*, 278(10), 8219–8223. <https://doi.org/10.1074/jbc.M212725200>
- Berger, K. H., Sogo, L. F., & Yaffe, M. P. (1997). Mdm12p, a Component Required for Mitochondrial Inheritance That Is Conserved between Budding and Fission Yeast. *Journal of Cell Biology*, 136(3), 545–553. <https://doi.org/10.1083/jcb.136.3.545>
- Bertero, E., Kutschka, I., Maack, C., & Dudek, J. (2020). Cardiolipin remodeling in Barth syndrome and other hereditary cardiomyopathies. *Biochimica et Biophysica Acta (BBA) - Molecular Basis of Disease*, 1866(8), 165803. <https://doi.org/10.1016/j.bbadis.2020.165803>
- Bihlmaier, K., Mesecke, N., Terziyska, N., Bien, M., Hell, K., & Herrmann, J. M. (2007). The disulfide relay system of mitochondria is connected to the respiratory chain. *The Journal of Cell Biology*, 179(3), 389–395. <https://doi.org/10.1083/jcb.200707123>
- Birner, R., Bürgermeister, M., Schneiter, R., & Daum, G. (2001). Roles of Phosphatidylethanolamine and of Its Several Biosynthetic Pathways in *Saccharomyces cerevisiae*. *Molecular Biology of the Cell*, 12(4), 997–1007. <https://doi.org/10.1091/mbc.12.4.997>
- Boutant, M., Kulkarni, S. S., Joffraud, M., Ratajczak, J., Valera-Alberni, M., Combe, R., Zorzano, A., & Cantó, C. (2017). Mfn2 is critical for brown adipose tissue thermogenic function. *The EMBO Journal*, 36(11), 1543–1558. <https://doi.org/10.15252/embj.201694914>
- Brady, L., Brzozowski, A. M., Derewendat, Z. S., Dodson, E., Dodson, G., Tolley, S., Turkenburg, J. P., Christiansent, L., Hüge-Jensent, B., Norskovt, L., Thimt, L., & Menge, U. (1990). A serine protease triad forms the catalytic centre of a triacylglycerol lipase. 343.
- Brandner, K., Rehling, P., & Truscott, K. N. (2005). The carboxyl-terminal third of the dicarboxylate carrier is crucial for productive association with the inner membrane twin-pore translocase. *The Journal of Biological Chemistry*, 280(7), 6215–6221. <https://doi.org/10.1074/jbc.M412269200>

- Brix, J., Dietmeier, K., & Pfanner, N. (1997). Differential Recognition of Preproteins by the Purified Cytosolic Domains of the Mitochondrial Import Receptors Tom20, Tom22, and Tom70*. *Journal of Biological Chemistry*, 272(33), 20730–20735. <https://doi.org/10.1074/jbc.272.33.20730>
- Bröcker, C., Kuhlee, A., Gatsogiannis, C., kleine Balderhaar, H. J., Hönscher, C., Engelbrecht-Vandré, S., Ungermann, C., & Raunser, S. (2012). Molecular architecture of the multisubunit homotypic fusion and vacuole protein sorting (HOPS) tethering complex. *Proceedings of the National Academy of Sciences*, 109(6), 1991–1996. <https://doi.org/10.1073/pnas.1117797109>
- Bürgermeister, M., Birner-Grünberger, R., Nebauer, R., & Daum, G. (2004). Contribution of different pathways to the supply of phosphatidylethanolamine and phosphatidylcholine to mitochondrial membranes of the yeast *Saccharomyces cerevisiae*. *Biochimica et Biophysica Acta (BBA) - Molecular and Cell Biology of Lipids*, 1686(1), 161–168. <https://doi.org/10.1016/j.bbalip.2004.09.007>
- Burgess, S. M., Delannoy, M., & Jensen, R. E. (1994). MMM1 encodes a mitochondrial outer membrane protein essential for establishing and maintaining the structure of yeast mitochondria. *Journal of Cell Biology*, 126(6), 1375–1391. <https://doi.org/10.1083/jcb.126.6.1375>
- Campo, M. L., Peixoto, P. M., & Martínez-Caballero, S. (2017). Revisiting trends on mitochondrial mega-channels for the import of proteins and nucleic acids. *Journal of Bioenergetics and Biomembranes*, 49(1), 75–99. <https://doi.org/10.1007/s10863-016-9662-z>
- Chacinska, A., Guiard, B., Müller, J. M., Schulze-Specking, A., Gabriel, K., Kutik, S., & Pfanner, N. (2008). Mitochondrial Biogenesis, Switching the Sorting Pathway of the Intermembrane Space Receptor Mia40*. *Journal of Biological Chemistry*, 283(44), 29723–29729. <https://doi.org/10.1074/jbc.M805356200>

- Chacinska, A., Koehler, C. M., Milenkovic, D., Lithgow, T., & Pfanner, N. (2009). Importing Mitochondrial Proteins: Machineries and Mechanisms. *Cell*, *138*(4), 628–644.
<https://doi.org/10.1016/j.cell.2009.08.005>
- Chacinska, A., Lind, M., Frazier, A. E., Dudek, J., Meisinger, C., Geissler, A., Sickmann, A., Meyer, H. E., Truscott, K. N., Guiard, B., Pfanner, N., & Rehling, P. (2005). Mitochondrial presequence translocase: Switching between TOM tethering and motor recruitment involves Tim21 and Tim17. *Cell*, *120*(6), 817–829. <https://doi.org/10.1016/j.cell.2005.01.011>
- Chacinska, A., Pfannschmidt, S., Wiedemann, N., Kozjak, V., Sanjuán Szklarz, L. K., Schulze-Specking, A., Truscott, K. N., Guiard, B., Meisinger, C., & Pfanner, N. (2004). Essential role of Mia40 in import and assembly of mitochondrial intermembrane space proteins. *The EMBO Journal*, *23*(19), 3735–3746. <https://doi.org/10.1038/sj.emboj.7600389>
- Chan, E. Y. L., & McQuibban, G. A. (2012). Phosphatidylserine Decarboxylase 1 (Psd1) Promotes Mitochondrial Fusion by Regulating the Biophysical Properties of the Mitochondrial Membrane and Alternative Topogenesis of Mitochondrial Genome Maintenance Protein 1 (Mgm1) *. *Journal of Biological Chemistry*, *287*(48), 40131–40139.
<https://doi.org/10.1074/jbc.M112.399428>
- Chan, N. C., & Lithgow, T. (2008). The Peripheral Membrane Subunits of the SAM Complex Function Codependently in Mitochondrial Outer Membrane Biogenesis. *Molecular Biology of the Cell*, *19*(1), 126–136. <https://doi.org/10.1091/mbc.e07-08-0796>
- Chatzi, A., Manganas, P., & Tokatlidis, K. (2016). Oxidative folding in the mitochondrial intermembrane space: A regulated process important for cell physiology and disease. *Biochimica et Biophysica Acta*, *1863*(6Part A), 1298–1306. <https://doi.org/10.1016/j.bbamcr.2016.03.023>

- Cheng, J., Saigo, H., & Baldi, P. (2006). Large-scale prediction of disulphide bridges using kernel methods, two-dimensional recursive neural networks, and weighted graph matching. *Proteins: Structure, Function, and Bioinformatics*, 62(3), 617–629. <https://doi.org/10.1002/prot.20787>
- Choudhary, V., Jacquier, N., & Schneider, R. (2011). The topology of the triacylglycerol synthesizing enzyme Lro1 indicates that neutral lipids can be produced within the luminal compartment of the endoplasmatic reticulum. *Communicative & Integrative Biology*, 4(6), 781–784.
- Cichocki, B. A., Krumpke, K., Vitali, D. G., & Rapaport, D. (2018). Pex19 is involved in importing dually targeted tail-anchored proteins to both mitochondria and peroxisomes. *Traffic*, 19(10), 770–785. <https://doi.org/10.1111/tra.12604>
- Claypool, S. M., Boontheung, P., McCaffery, J. M., Loo, J. A., & Koehler, C. M. (2008). The Cardiolipin Transacylase, Tafazzin, Associates with Two Distinct Respiratory Components Providing Insight into Barth Syndrome. *Molecular Biology of the Cell*, 19(12), 5143–5155. <https://doi.org/10.1091/mbc.e08-09-0896>
- Cohen, Y., Klug, Y. A., Dimitrov, L., Erez, Z., Chuartzman, S. G., Elinger, D., Yofe, I., Soliman, K., Gärtner, J., Thoms, S., Schekman, R., Elbaz-Alon, Y., Zalckvar, E., & Schuldiner, M. (2014). Peroxisomes are juxtaposed to strategic sites on mitochondria. *Molecular bioSystems*, 10(7), 1742–1748. <https://doi.org/10.1039/c4mb00001c>
- Connerth, M., Tatsuta, T., Haag, M., Klecker, T., Westermann, B., & Langer, T. (2012). Intramitochondrial Transport of Phosphatidic Acid in Yeast by a Lipid Transfer Protein. *Science*, 338(6108), 815–818. <https://doi.org/10.1126/science.1225625>
- Curran, S. P., Leuenberger, D., Oppliger, W., & Koehler, C. M. (2002). The Tim9p–Tim10p complex binds to the transmembrane domains of the ADP/ATP carrier. *The EMBO Journal*, 21(5), 942–953. <https://doi.org/10.1093/emboj/21.5.942>

- Dabir, D. V., Leverich, E. P., Kim, S.-K., Tsai, F. D., Hirasawa, M., Knaff, D. B., & Koehler, C. M. (2007). A role for cytochrome c and cytochrome c peroxidase in electron shuttling from Erv1. *The EMBO Journal*, *26*(23), 4801–4811. <https://doi.org/10.1038/sj.emboj.7601909>
- Davis, A. J., Alder, N. N., Jensen, R. E., & Johnson, A. E. (2007). The Tim9p/10p and Tim8p/13p Complexes Bind to Specific Sites on Tim23p during Mitochondrial Protein Import. *Molecular Biology of the Cell*, *18*(2), 475–486. <https://doi.org/10.1091/mbc.e06-06-0546>
- de Brito, O. M., & Scorrano, L. (2008). Mitofusin 2 tethers endoplasmic reticulum to mitochondria. *Nature*, *456*(7222), 605–610. <https://doi.org/10.1038/nature07534>
- De Los Rios, P., Ben-Zvi, A., Slutsky, O., Azem, A., & Goloubinoff, P. (2006). Hsp70 chaperones accelerate protein translocation and the unfolding of stable protein aggregates by entropic pulling. *Proceedings of the National Academy of Sciences of the United States of America*, *103*(16), 6166–6171. <https://doi.org/10.1073/pnas.0510496103>
- Dekker, P. J., Ryan, M. T., Brix, J., Müller, H., Hönliger, A., & Pfanner, N. (1998). Preprotein translocase of the outer mitochondrial membrane: Molecular dissection and assembly of the general import pore complex. *Molecular and Cellular Biology*, *18*(11), 6515–6524. <https://doi.org/10.1128/MCB.18.11.6515>
- Delille, H. K., Alves, R., & Schrader, M. (2009). Biogenesis of peroxisomes and mitochondria: Linked by division. *Histochemistry and Cell Biology*, *131*(4), 441–446. <https://doi.org/10.1007/s00418-009-0561-9>
- Diederichs, K. A., Ni, X., Rollauer, S. E., Botos, I., Tan, X., King, M. S., Kunji, E. R. S., Jiang, J., & Buchanan, S. K. (2020). Structural insight into mitochondrial β -barrel outer membrane protein biogenesis. *Nature Communications*, *11*(1), 3290. <https://doi.org/10.1038/s41467-020-17144-1>

- Dimmer, K. S., Fritz, S., Fuchs, F., Messerschmitt, M., Weinbach, N., Neupert, W., & Westermann, B. (2002). Genetic Basis of Mitochondrial Function and Morphology in *Saccharomyces cerevisiae*. *Molecular Biology of the Cell*, *13*(3), 847–853. <https://doi.org/10.1091/mbc.01-12-0588>
- Dimmer, K. S., Jakobs, S., Vogel, F., Altmann, K., & Westermann, B. (2005). Mdm31 and Mdm32 are inner membrane proteins required for maintenance of mitochondrial shape and stability of mitochondrial DNA nucleoids in yeast. *The Journal of Cell Biology*, *168*(1), 103–115. <https://doi.org/10.1083/jcb.200410030>
- Dimmer, K. S., Papić, D., Schumann, B., Sperl, D., Krumpe, K., Walther, D. M., & Rapaport, D. (2012). A crucial role for Mim2 in the biogenesis of mitochondrial outer membrane proteins. *Journal of Cell Science*, *125*(Pt 14), 3464–3473. <https://doi.org/10.1242/jcs.103804>
- Diverse membrane-associated proteins contain a novel SMP domain.* (n.d.). <https://doi.org/10.1096/fj.05-4581hyp>
- Edwards, R., Eaglesfield, R., & Tokatlidis, K. (2021). The mitochondrial intermembrane space: The most constricted mitochondrial sub-compartment with the largest variety of protein import pathways. *Open Biology*, *11*(3), 210002. <https://doi.org/10.1098/rsob.210002>
- Edwards, R., Gerlich, S., & Tokatlidis, K. (2020). The biogenesis of mitochondrial intermembrane space proteins. *Biological Chemistry*, *401*(6–7), 737–747. <https://doi.org/10.1515/hsz-2020-0114>
- Eisenberg-Bord, M., Shai, N., Schuldiner, M., & Bohnert, M. (2016). A Tether Is a Tether Is a Tether: Tethering at Membrane Contact Sites. *Developmental Cell*, *39*(4), 395–409. <https://doi.org/10.1016/j.devcel.2016.10.022>
- Ellenrieder, L., Opaliński, Ł., Becker, L., Krüger, V., Mirus, O., Straub, S. P., Ebell, K., Flinner, N., Stiller, S. B., Guiard, B., Meisinger, C., Wiedemann, N., Schleiff, E., Wagner, R., Pfanner, N., & Becker, T. (2016). Separating mitochondrial protein assembly and endoplasmic reticulum tethering by

selective coupling of Mdm10. *Nature Communications*, 7, 13021.

<https://doi.org/10.1038/ncomms13021>

Endo, T., Yamamoto, H., & Esaki, M. (2003). Functional cooperation and separation of translocators in protein import into mitochondria, the double-membrane bounded organelles. *Journal of Cell Science*, 116(Pt 16), 3259–3267. <https://doi.org/10.1242/jcs.00667>

Enkler, L., & Spang, A. (2024). Functional interplay of lipid droplets and mitochondria. *FEBS Letters*, 598(10), 1235–1251. <https://doi.org/10.1002/1873-3468.14809>

Enkler, L., Szentgyörgyi, V., Pennauer, M., Prescianotto-Baschong, C., Riezman, I., Wiesyk, A., Avraham, R. E., Spiess, M., Zalckvar, E., Kucharczyk, R., Riezman, H., & Spang, A. (2023). Arf1 coordinates fatty acid metabolism and mitochondrial homeostasis. *Nature Cell Biology*, 25(8), Article 8. <https://doi.org/10.1038/s41556-023-01180-2>

Esaki, M., Kanamori, T., Nishikawa, S., & Endo, T. (1999). Two distinct mechanisms drive protein translocation across the mitochondrial outer membrane in the late step of the cytochrome b2 import pathway. *Proceedings of the National Academy of Sciences*, 96(21), 11770–11775. <https://doi.org/10.1073/pnas.96.21.11770>

Esser, K., Tursun, B., Ingenhoven, M., Michaelis, G., & Pratje, E. (2002). A Novel Two-step Mechanism for Removal of a Mitochondrial Signal Sequence Involves the mAAA Complex and the Putative Rhomboid Protease Pcp1. *Journal of Molecular Biology*, 323(5), 835–843. [https://doi.org/10.1016/S0022-2836\(02\)01000-8](https://doi.org/10.1016/S0022-2836(02)01000-8)

Farrell, S. R., & Thorpe, C. (2005). Augmenter of liver regeneration: A flavin-dependent sulfhydryl oxidase with cytochrome c reductase activity. *Biochemistry*, 44(5), 1532–1541. <https://doi.org/10.1021/bi0479555>

Ferrè, F., & Clote, P. (2005a). DiANNA: A web server for disulfide connectivity prediction. *Nucleic Acids Research*, 33(suppl_2), W230–W232. <https://doi.org/10.1093/nar/gki412>

- Ferrè, F., & Clote, P. (2005b). Disulfide connectivity prediction using secondary structure information and diresidue frequencies. *Bioinformatics*, *21*(10), 2336–2346.
<https://doi.org/10.1093/bioinformatics/bti328>
- Fielden, L. F., Busch, J. D., Merkt, S. G., Ganesan, I., Steiert, C., Hasselblatt, H. B., Busto, J. V., Wirth, C., Zufall, N., Jungbluth, S., Noll, K., Dung, J. M., Butenko, L., von der Malsburg, K., Koch, H.-G., Hunte, C., van der Laan, M., & Wiedemann, N. (2023). Central role of Tim17 in mitochondrial presequence protein translocation. *Nature*, *621*(7979), 627–634.
<https://doi.org/10.1038/s41586-023-06477-8>
- Fiumera, H. L., Dunham, M. J., Saracco, S. A., Butler, C. A., Kelly, J. A., & Fox, T. D. (2009). Translocation and Assembly of Mitochondrially Coded *Saccharomyces cerevisiae* Cytochrome *c* Oxidase Subunit Cox2 by Oxa1 and Yme1 in the Absence of Cox18. *Genetics*, *182*(2), 519–528.
<https://doi.org/10.1534/genetics.109.101196>
- Flinner, N., Ellenrieder, L., Stiller, S. B., Becker, T., Schleiff, E., & Mirus, O. (2013). Mdm10 is an ancient eukaryotic porin co-occurring with the ERMES complex. *Biochimica Et Biophysica Acta*, *1833*(12), 3314–3325. <https://doi.org/10.1016/j.bbamcr.2013.10.006>
- Fransen, M., Nordgren, M., Wang, B., & Apanasets, O. (2012). Role of peroxisomes in ROS/RNS-metabolism: Implications for human disease. *Biochimica et Biophysica Acta (BBA) - Molecular Basis of Disease*, *1822*(9), 1363–1373. <https://doi.org/10.1016/j.bbadis.2011.12.001>
- Freyre, C. A. C., Rauher, P. C., Ejsing, C. S., & Klemm, R. W. (2019). MIGA2 Links Mitochondria, the ER, and Lipid Droplets and Promotes *De Novo* Lipogenesis in Adipocytes. *Molecular Cell*, *76*(5), 811–825.e14. <https://doi.org/10.1016/j.molcel.2019.09.011>
- Gabriel, K., Milenkovic, D., Chacinska, A., Müller, J., Guiard, B., Pfanner, N., & Meisinger, C. (2007). Novel mitochondrial intermembrane space proteins as substrates of the MIA import pathway. *Journal of Molecular Biology*, *365*(3), 612–620. <https://doi.org/10.1016/j.jmb.2006.10.038>

- Gakh, O., Cavadini, P., & Isaya, G. (2002). Mitochondrial processing peptidases. *Biochimica et Biophysica Acta (BBA) - Molecular Cell Research*, 1592(1), 63–77. [https://doi.org/10.1016/S0167-4889\(02\)00265-3](https://doi.org/10.1016/S0167-4889(02)00265-3)
- Gemmink, A., Daemen, S., Kuijpers, H. J. H., Schaart, G., Duimel, H., López-Iglesias, C., van Zandvoort, M. A. M. J., Knoop, K., & Hesselink, M. K. C. (2018). Super-resolution microscopy localizes perilipin 5 at lipid droplet-mitochondria interaction sites and at lipid droplets juxtaposing to perilipin 2. *Biochimica et Biophysica Acta (BBA) - Molecular and Cell Biology of Lipids*, 1863(11), 1423–1432. <https://doi.org/10.1016/j.bbalip.2018.08.016>
- Glick, B. S., Brandt, A., Cunningham, K., Müller, S., Hallberg, R. L., & Schatz, G. (1992). Cytochromes *c1* and *b2* are sorted to the intermembrane space of yeast mitochondria by a stop-transfer mechanism. *Cell*, 69(5), 809–822. [https://doi.org/10.1016/0092-8674\(92\)90292-K](https://doi.org/10.1016/0092-8674(92)90292-K)
- González Montoro, A., Auffarth, K., Hönscher, C., Bohnert, M., Becker, T., Warscheid, B., Reggiori, F., van der Laan, M., Fröhlich, F., & Ungermann, C. (2018). Vps39 Interacts with Tom40 to Establish One of Two Functionally Distinct Vacuole-Mitochondria Contact Sites. *Developmental Cell*, 45(5), 621–636.e7. <https://doi.org/10.1016/j.devcel.2018.05.011>
- Gray, M. W. (2012). Mitochondrial Evolution. *Cold Spring Harbor Perspectives in Biology*, 4(9), a011403. <https://doi.org/10.1101/cshperspect.a011403>
- Grillitsch, K., & Daum, G. (2011). Triacylglycerol lipases of the yeast. *Frontiers in Biology*, 6(3), Article 3. <https://doi.org/10.1007/s11515-011-1142-6>
- Grimsey, N., Han, G.-S., O'Hara, L., Rochford, J. J., Carman, G. M., & Siniossoglou, S. (2008). Temporal and Spatial Regulation of the Phosphatidate Phosphatases Lipin 1 and 2. *The Journal of Biological Chemistry*, 283(43), 29166–29174. <https://doi.org/10.1074/jbc.M804278200>
- Grumbt, B., Stroobant, V., Terziyska, N., Israel, L., & Hell, K. (2007). Functional Characterization of Mia40p, the Central Component of the Disulfide Relay System of the Mitochondrial

- Intermembrane Space*. *Journal of Biological Chemistry*, 282(52), 37461–37470.
<https://doi.org/10.1074/jbc.M707439200>
- Gunn, K. H., & Neher, S. B. (2023). Structure of dimeric lipoprotein lipase reveals a pore adjacent to the active site. *Nature Communications*, 14(1), 2569. <https://doi.org/10.1038/s41467-023-38243-9>
- Gupta, A., & Becker, T. (2021). Mechanisms and pathways of mitochondrial outer membrane protein biogenesis. *Biochimica et Biophysica Acta (BBA) - Bioenergetics*, 1862(1), 148323.
<https://doi.org/10.1016/j.bbabi.2020.148323>
- Habib, S. J., Waizenegger, T., Lech, M., Neupert, W., & Rapaport, D. (2005). Assembly of the TOB complex of mitochondria. *The Journal of Biological Chemistry*, 280(8), 6434–6440.
<https://doi.org/10.1074/jbc.M411510200>
- Habib, S. J., Waizenegger, T., Niewianda, A., Paschen, S. A., Neupert, W., & Rapaport, D. (2006). The N-terminal domain of Tob55 has a receptor-like function in the biogenesis of mitochondrial β -barrel proteins. *Journal of Cell Biology*, 176(1), 77–88. <https://doi.org/10.1083/jcb.200602050>
- Ham, H. J., Rho, H. J., Shin, S. K., & Yoon, H.-J. (2010). The TGL2 Gene of *Saccharomyces cerevisiae* Encodes an Active Acylglycerol Lipase Located in the Mitochondria. *Journal of Biological Chemistry*, 285(5), 3005–3013. <https://doi.org/10.1074/jbc.M109.046946>
- Han, G.-S., O'Hara, L., Carman, G. M., & Siniosoglou, S. (2008). An Unconventional Diacylglycerol Kinase That Regulates Phospholipid Synthesis and Nuclear Membrane Growth *♦. *Journal of Biological Chemistry*, 283(29), 20433–20442. <https://doi.org/10.1074/jbc.M802903200>
- Hell, K. (2008). The Erv1-Mia40 disulfide relay system in the intermembrane space of mitochondria. *Biochimica Et Biophysica Acta*, 1783(4), 601–609. <https://doi.org/10.1016/j.bbamcr.2007.12.005>
- Helle, S. C. J., Kanfer, G., Kolar, K., Lang, A., Michel, A. H., & Kornmann, B. (2013). Organization and function of membrane contact sites. *Biochimica et Biophysica Acta (BBA) - Molecular Cell Research*, 1833(11), 2526–2541. <https://doi.org/10.1016/j.bbamcr.2013.01.028>

- Herlan, M., Vogel, F., Bornhövd, C., Neupert, W., & Reichert, A. S. (2003). Processing of Mgm1 by the Rhomboid-type Protease Pcp1 Is Required for Maintenance of Mitochondrial Morphology and of Mitochondrial DNA*. *Journal of Biological Chemistry*, 278(30), 27781–27788.
<https://doi.org/10.1074/jbc.M211311200>
- Herrmann, J. M., & Hell, K. (2005). Chopped, trapped or tacked – protein translocation into the IMS of mitochondria. *Trends in Biochemical Sciences*, 30(4), 205–212.
<https://doi.org/10.1016/j.tibs.2005.02.005>
- Herrmann, J. M., & Köhl, R. (2007). Catch me if you can! Oxidative protein trapping in the intermembrane space of mitochondria. *The Journal of Cell Biology*, 176(5), 559–563.
<https://doi.org/10.1083/jcb.200611060>
- Hildenbeutel, M., Theis, M., Geier, M., Haferkamp, I., Neuhaus, H. E., Herrmann, J. M., & Ott, M. (2012). The membrane insertase Oxa1 is required for efficient import of carrier proteins into mitochondria. *Journal of Molecular Biology*, 423(4), 590–599.
<https://doi.org/10.1016/j.jmb.2012.07.018>
- Hjelmstad, R. H., & Bell, R. M. (1990). The sn-1,2-diacylglycerol cholinephosphotransferase of *Saccharomyces cerevisiae*. Nucleotide sequence, transcriptional mapping, and gene product analysis of the CPT1 gene. *Journal of Biological Chemistry*, 265(3), 1755–1764.
[https://doi.org/10.1016/S0021-9258\(19\)40081-1](https://doi.org/10.1016/S0021-9258(19)40081-1)
- Hoffmann, H. P., & Avers, C. J. (1973). Mitochondrion of yeast: Ultrastructural evidence for one giant, branched organelle per cell. *Science (New York, N.Y.)*, 181(4101), 749–751.
<https://doi.org/10.1126/science.181.4101.749>
- Höhr, A. I. C., Lindau, C., Wirth, C., Qiu, J., Stroud, D. A., Kutik, S., Guiard, B., Hunte, C., Becker, T., Pfanner, N., & Wiedemann, N. (2018). Membrane protein insertion through a mitochondrial β -

barrel gate. *Science (New York, N.Y.)*, 359(6373), eaah6834.

<https://doi.org/10.1126/science.aah6834>

Höhr, A. I. C., Straub, S. P., Warscheid, B., Becker, T., & Wiedemann, N. (2015). Assembly of β -barrel proteins in the mitochondrial outer membrane. *Biochimica et Biophysica Acta (BBA) - Molecular Cell Research*, 1853(1), 74–88. <https://doi.org/10.1016/j.bbamcr.2014.10.006>

Hönscher, C., Mari, M., Auffarth, K., Bohnert, M., Griffith, J., Geerts, W., van der Laan, M., Cabrera, M., Reggiori, F., & Ungermann, C. (2014). Cellular Metabolism Regulates Contact Sites between Vacuoles and Mitochondria. *Developmental Cell*, 30(1), 86–94.

<https://doi.org/10.1016/j.devcel.2014.06.006>

Horst, M., Oppliger, W., Rospert, S., Schönfeld, H. J., Schatz, G., & Azem, A. (1997). Sequential action of two hsp70 complexes during protein import into mitochondria. *The EMBO Journal*, 16(8), 1842–1849. <https://doi.org/10.1093/emboj/16.8.1842>

Horvath, S. E., & Daum, G. (2013). Lipids of mitochondria. *Progress in Lipid Research*, 52(4), 590–614.

<https://doi.org/10.1016/j.plipres.2013.07.002>

Ieva, R., Schrempp, S. G., Opaliński, L., Wollweber, F., Höß, P., Heißwolf, A. K., Gebert, M., Zhang, Y., Guiard, B., Rospert, S., Becker, T., Chacinska, A., Pfanner, N., & van der Laan, M. (2014). Mgr2 functions as lateral gatekeeper for preprotein sorting in the mitochondrial inner membrane. *Molecular Cell*, 56(5), 641–652. <https://doi.org/10.1016/j.molcel.2014.10.010>

Jaeger, K.-E., Ransac, S., Dijkstra, B. W., Colson, C., van Heuvel, M., & Misset, O. (1994). Bacterial lipases☆. *FEMS Microbiology Reviews*, 15(1), 29–63. <https://doi.org/10.1111/j.1574-6976.1994.tb00121.x>

Jägerström, S., Polesie, S., Wickström, Y., Johansson, B. R., Schröder, H. D., Højlund, K., & Boström, P. (2009). Lipid droplets interact with mitochondria using SNAP23. *Cell Biology International*, 33(9), 934–940. <https://doi.org/10.1016/j.cellbi.2009.06.011>

- Jandrositz, A., Petschnigg, J., Zimmermann, R., Natter, K., Scholze, H., Hermetter, A., Kohlwein, S. D., & Leber, R. (2005). The lipid droplet enzyme Tgl1p hydrolyzes both steryl esters and triglycerides in the yeast, *Saccharomyces cerevisiae*. *Biochimica et Biophysica Acta (BBA) - Molecular and Cell Biology of Lipids*, *1735*(1), 50–58. <https://doi.org/10.1016/j.bbalip.2005.04.005>
- Javadov, S., Kozlov, A. V., & Camara, A. K. S. (2020). Mitochondria in Health and Diseases. *Cells*, *9*(5), 1177. <https://doi.org/10.3390/cells9051177>
- Jiger, S., & Demleitner, G. (n.d.). *Lipase of Staphylococcus hyicus: Analysis of the catalytic triad by site-directed mutagenesis*.
- John Peter, A. T., Herrmann, B., Antunes, D., Rapaport, D., Dimmer, K. S., & Kornmann, B. (2017). Vps13-Mcp1 interact at vacuole–mitochondria interfaces and bypass ER–mitochondria contact sites. *Journal of Cell Biology*, *216*(10), 3219–3229. <https://doi.org/10.1083/jcb.201610055>
- Johnson, K. A., Bhushan, S., Ståhl, A., Hallberg, B. M., Frohn, A., Glaser, E., & Eneqvist, T. (2006). The closed structure of presequence protease PreP forms a unique 10,000 Angstroms³ chamber for proteolysis. *The EMBO Journal*, *25*(9), 1977–1986. <https://doi.org/10.1038/sj.emboj.7601080>
- Jores, T., Klinger, A., Groß, L. E., Kawano, S., Flinner, N., Duchardt-Ferner, E., Wöhnert, J., Kalbacher, H., Endo, T., Schleiff, E., & Rapaport, D. (2016). Characterization of the targeting signal in mitochondrial β -barrel proteins. *Nature Communications*, *7*(1), 12036. <https://doi.org/10.1038/ncomms12036>
- Jores, T., Lawatscheck, J., Beke, V., Franz-Wachtel, M., Yunoki, K., Fitzgerald, J. C., Macek, B., Endo, T., Kalbacher, H., Buchner, J., & Rapaport, D. (2018). Cytosolic Hsp70 and Hsp40 chaperones enable the biogenesis of mitochondrial β -barrel proteins. *Journal of Cell Biology*, *217*(9), 3091–3108. <https://doi.org/10.1083/jcb.201712029>
- Jumper, J., Evans, R., Pritzel, A., Green, T., Figurnov, M., Ronneberger, O., Tunyasuvunakool, K., Bates, R., Žídek, A., Potapenko, A., Bridgland, A., Meyer, C., Kohl, S. A. A., Ballard, A. J., Cowie, A., Romera-

- Paredes, B., Nikolov, S., Jain, R., Adler, J., ... Hassabis, D. (2021). Highly accurate protein structure prediction with AlphaFold. *Nature*, *596*(7873), 583–589.
<https://doi.org/10.1038/s41586-021-03819-2>
- Kakimoto, Y., Tashiro, S., Kojima, R., Morozumi, Y., Endo, T., & Tamura, Y. (2018). Visualizing multiple inter-organelle contact sites using the organelle-targeted split-GFP system. *Scientific Reports*, *8*(1), 6175. <https://doi.org/10.1038/s41598-018-24466-0>
- Kanamori, T., Nishikawa, S., Nakai, M., Shin, I., Schultz, P. G., & Endo, T. (1999). Uncoupling of transfer of the presequence and unfolding of the mature domain in precursor translocation across the mitochondrial outer membrane. *Proceedings of the National Academy of Sciences of the United States of America*, *96*(7), 3634–3639. <https://doi.org/10.1073/pnas.96.7.3634>
- Kang, P. J., Ostermann, J., Shilling, J., Neupert, W., Craig, E. A., & Pfanner, N. (1990). Requirement for hsp70 in the mitochondrial matrix for translocation and folding of precursor proteins. *Nature*, *348*(6297), 137–143. <https://doi.org/10.1038/348137a0>
- Kawano, S., Tamura, Y., Kojima, R., Bala, S., Asai, E., Michel, A. H., Kornmann, B., Riezman, I., Riezman, H., Sakae, Y., Okamoto, Y., & Endo, T. (2018). Structure-function insights into direct lipid transfer between membranes by Mmm1-Mdm12 of ERMES. *The Journal of Cell Biology*, *217*(3), 959–974. <https://doi.org/10.1083/jcb.201704119>
- Kemmerer, Z. A., Robinson, K. P., Schmitz, J. M., Manicki, M., Paulson, B. R., Jochem, A., Hutchins, P. D., Coon, J. J., & Pagliarini, D. J. (2021). UbiB proteins regulate cellular CoQ distribution in *Saccharomyces cerevisiae*. *Nature Communications*, *12*(1), Article 1.
<https://doi.org/10.1038/s41467-021-25084-7>
- Khan, F. I., Lan, D., Durrani, R., Huan, W., Zhao, Z., & Wang, Y. (2017). The Lid Domain in Lipases: Structural and Functional Determinant of Enzymatic Properties. *Frontiers in Bioengineering and Biotechnology*, *5*. <https://doi.org/10.3389/fbioe.2017.00016>

- Kiebler, M., Keil, P., Schneider, H., van der Klei, I. J., Pfanner, N., & Neupert, W. (1993). The mitochondrial receptor complex: A central role of MOM22 in mediating preprotein transfer from receptors to the general insertion pore. *Cell*, *74*(3), 483–492. [https://doi.org/10.1016/0092-8674\(93\)80050-O](https://doi.org/10.1016/0092-8674(93)80050-O)
- Kimmel, A. R., & Sztalryd, C. (2016). The Perilipins: Major Cytosolic Lipid Droplet–Associated Proteins and Their Roles in Cellular Lipid Storage, Mobilization, and Systemic Homeostasis*. *Annual Review of Nutrition*, *36*(Volume 36, 2016), 471–509. <https://doi.org/10.1146/annurev-nutr-071813-105410>
- Klein, A., Israel, L., Lackey, S. W. K., Nargang, F. E., Imhof, A., Baumeister, W., Neupert, W., & Thomas, D. R. (2012). Characterization of the insertase for β -barrel proteins of the outer mitochondrial membrane. *Journal of Cell Biology*, *199*(4), 599–611. <https://doi.org/10.1083/jcb.201207161>
- Klein, I., Klug, L., Schmidt, C., Zandl, M., Korber, M., Daum, G., & Athenstaedt, K. (2016). Regulation of the yeast triacylglycerol lipases Tgl4p and Tgl5p by the presence/absence of nonpolar lipids. *Molecular Biology of the Cell*, *27*(13), 2014–2024. <https://doi.org/10.1091/mbc.E15-09-0633>
- Kliza, K. W., Liu, Q., Roosenboom, L. W. M., Jansen, P. W. T. C., Filippov, D. V., & Vermeulen, M. (2021). Reading ADP-ribosylation signaling using chemical biology and interaction proteomics. *Molecular Cell*, *81*(21), 4552–4567.e8. <https://doi.org/10.1016/j.molcel.2021.08.037>
- Klug, L., & Daum, G. (2014). Yeast lipid metabolism at a glance. *FEMS Yeast Research*, *14*(3), 369–388. <https://doi.org/10.1111/1567-1364.12141>
- Kodaki, T., & Yamashita, S. (1989). Characterization of the methyltransferases in the yeast phosphatidylethanolamine methylation pathway by selective gene disruption. *European Journal of Biochemistry*, *185*(2), 243–251. <https://doi.org/10.1111/j.1432-1033.1989.tb15109.x>
- Köffel, R., Tiwari, R., Falquet, L., & Schneiter, R. (2005). The *Saccharomyces cerevisiae* YLL012/YEH1, YLR020/YEH2, and TGL1 Genes Encode a Novel Family of Membrane-Anchored Lipases That Are

Required for Steryl Ester Hydrolysis. *Molecular and Cellular Biology*, 25(5), 1655–1668.

<https://doi.org/10.1128/MCB.25.5.1655-1668.2005>

Komiya, T., Rospert, S., Koehler, C., Looser, R., Schatz, G., & Mihara, K. (1998). Interaction of mitochondrial targeting signals with acidic receptor domains along the protein import pathway: Evidence for the “acid chain” hypothesis. *The EMBO Journal*, 17(14), 3886–3898.

<https://doi.org/10.1093/emboj/17.14.3886>

Kornmann, B., Currie, E., Collins, S. R., Schuldiner, M., Nunnari, J., Weissman, J. S., & Walter, P. (2009).

An ER-Mitochondria Tethering Complex Revealed by a Synthetic Biology Screen. *Science*, 325(5939), 477–481. <https://doi.org/10.1126/science.1175088>

Kornmann, B., & Walter, P. (2010). ERMES-mediated ER-mitochondria contacts: Molecular hubs for the regulation of mitochondrial biology. *Journal of Cell Science*, 123(9), 1389–1393.

<https://doi.org/10.1242/jcs.058636>

Kozjak, V., Wiedemann, N., Milenkovic, D., Lohaus, C., Meyer, H. E., Guiard, B., Meisinger, C., & Pfanner, N. (2003). An Essential Role of Sam50 in the Protein Sorting and Assembly Machinery of the Mitochondrial Outer Membrane*. *Journal of Biological Chemistry*, 278(49), 48520–48523.

<https://doi.org/10.1074/jbc.C300442200>

Krumpe, K., Frumkin, I., Herzig, Y., Rimon, N., Özbalci, C., Brügger, B., Rapaport, D., & Schuldiner, M.

(2012). Ergosterol content specifies targeting of tail-anchored proteins to mitochondrial outer membranes. *Molecular Biology of the Cell*, 23(20), 3927–3935.

<https://doi.org/10.1091/mbc.e11-12-0994>

Küçükköse, C., Taskin, A., Marada, A., Dennerlein, S., Brummer, T., & Vögtle, F. (2020). Functional coupling of presequence processing and degradation in human mitochondria. *FEBS Journal*.

Kumar, N., Leonzino, M., Hancock-Cerutti, W., Horenkamp, F. A., Li, P., Lees, J. A., Wheeler, H., Reinisch, K. M., & De Camilli, P. (2018). VPS13A and VPS13C are lipid transport proteins differentially

localized at ER contact sites. *The Journal of Cell Biology*, 217(10), 3625–3639.

<https://doi.org/10.1083/jcb.201807019>

Kutik, S., Stojanovski, D., Becker, L., Becker, T., Meinecke, M., Krüger, V., Prinz, C., Meisinger, C., Guiard, B., Wagner, R., Pfanner, N., & Wiedemann, N. (2008). Dissecting membrane insertion of mitochondrial beta-barrel proteins. *Cell*, 132(6), 1011–1024.

<https://doi.org/10.1016/j.cell.2008.01.028>

Lang, A. B., John Peter, A. T., Walter, P., & Kornmann, B. (2015). ER-mitochondrial junctions can be bypassed by dominant mutations in the endosomal protein Vps13. *The Journal of Cell Biology*, 210(6), 883–890. <https://doi.org/10.1083/jcb.201502105>

Lee, S., Lee, D. W., Yoo, Y.-J., Duncan, O., Oh, Y. J., Lee, Y. J., Lee, G., Whelan, J., & Hwang, I. (2012).

Mitochondrial Targeting of the Arabidopsis F1-ATPase γ -Subunit via Multiple Compensatory and Synergistic Presequence Motifs. *The Plant Cell*, 24(12), 5037–5057.

Leissring, M. A., Farris, W., Wu, X., Christodoulou, D. C., Haigis, M. C., Guarente, L., & Selkoe, D. J. (2004). Alternative translation initiation generates a novel isoform of insulin-degrading enzyme targeted to mitochondria. *The Biochemical Journal*, 383(Pt. 3), 439–446.

<https://doi.org/10.1042/bj20041081>

Leonhard, K., Stiegler, A., Neupert, W., & Langer, T. (1999). Chaperone-like activity of the AAA domain of the yeast Yme1 AAA protease. *Nature*, 398(6725), 348–351. <https://doi.org/10.1038/18704>

Li, P., Lees, J. A., Lusk, C. P., & Reinisch, K. M. (2020). Cryo-EM reconstruction of a VPS13 fragment reveals a long groove to channel lipids between membranes. *The Journal of Cell Biology*, 219(5), e202001161. <https://doi.org/10.1083/jcb.202001161>

Liebeton, K., Zacharias, A., & Jaeger, K.-E. (2001). Disulfide Bond in *Pseudomonas aeruginosa* Lipase Stabilizes the Structure but Is Not Required for Interaction with Its Foldase. *Journal of Bacteriology*, 183(2), 597. <https://doi.org/10.1128/JB.183.2.597-603.2001>

- Liu, J., Epand, R. F., Durrant, D., Grossman, D., Chi, N., Epand, R. M., & Lee, R. M. (2008). Role of phospholipid scramblase 3 in the regulation of tumor necrosis factor- α -induced apoptosis. *Biochemistry*, *47*(15), 4518–4529. <https://doi.org/10.1021/bi701962c>
- Llopis, J., McCaffery, J. M., Miyawaki, A., Farquhar, M. G., & Tsien, R. Y. (1998). Measurement of cytosolic, mitochondrial, and Golgi pH in single living cells with green fluorescent proteins. *Proceedings of the National Academy of Sciences*, *95*(12), 6803–6808. <https://doi.org/10.1073/pnas.95.12.6803>
- Lowe, M. E. (1992). The catalytic site residues and interfacial binding of human pancreatic lipase. *Journal of Biological Chemistry*, *267*(24), 17069–17073. [https://doi.org/10.1016/S0021-9258\(18\)41893-5](https://doi.org/10.1016/S0021-9258(18)41893-5)
- Lu, J., Chan, C., Yu, L., Fan, J., Sun, F., & Zhai, Y. (2020). Molecular mechanism of mitochondrial phosphatidate transfer by Ups1. *Communications Biology*, *3*(1), 1–14. <https://doi.org/10.1038/s42003-020-01121-x>
- Lu, Y.-W., Galbraith, L., Herndon, J. D., Lu, Y.-L., Pras-Raves, M., Vervaart, M., Van Kampen, A., Luyf, A., Koehler, C. M., McCaffery, J. M., Gottlieb, E., Vaz, F. M., & Claypool, S. M. (2016). Defining functional classes of Barth syndrome mutation in humans. *Human Molecular Genetics*, *25*(9), 1754–1770. <https://doi.org/10.1093/hmg/ddw046>
- Martinez-Caballero, S., Peixoto, P. M. V., Kinnally, K. W., & Campo, M. L. (2007). A fluorescence assay for peptide translocation into mitochondria. *Analytical Biochemistry*, *362*(1), 76–82. <https://doi.org/10.1016/j.ab.2006.12.015>
- Mattiazzi Ušaj, M., Brložnik, M., Kaferle, P., Žitnik, M., Wolinski, H., Leitner, F., Kohlwein, S. D., Zupan, B., & Petrovič, U. (2015). Genome-Wide Localization Study of Yeast Pex11 Identifies Peroxisome–Mitochondria Interactions through the ERMES Complex. *Journal of Molecular Biology*, *427*(11), 2072–2087. <https://doi.org/10.1016/j.jmb.2015.03.004>

- Meinecke, M., Wagner, R., Kovermann, P., Guiard, B., Mick, D. U., Hutu, D. P., Voos, W., Truscott, K. N., Chacinska, A., Pfanner, N., & Rehling, P. (2006). Tim50 maintains the permeability barrier of the mitochondrial inner membrane. *Science (New York, N.Y.)*, *312*(5779), 1523–1526.
<https://doi.org/10.1126/science.1127628>
- Meisinger, C., Rissler, M., Chacinska, A., Szklarz, L. K. S., Milenkovic, D., Kozjak, V., Schönfisch, B., Lohaus, C., Meyer, H. E., Yaffe, M. P., Guiard, B., Wiedemann, N., & Pfanner, N. (2004). The Mitochondrial Morphology Protein Mdm10 Functions in Assembly of the Preprotein Translocase of the Outer Membrane. *Developmental Cell*, *7*(1), 61–71.
<https://doi.org/10.1016/j.devcel.2004.06.003>
- Mertins, B., Psakis, G., & Essen, L.-O. (2014). Voltage-dependent anion channels: The wizard of the mitochondrial outer membrane. *Biological Chemistry*, *395*(12), 1435–1442.
<https://doi.org/10.1515/hsz-2014-0203>
- Mesecke, N., Terziyska, N., Kozany, C., Baumann, F., Neupert, W., Hell, K., & Herrmann, J. M. (2005). A disulfide relay system in the intermembrane space of mitochondria that mediates protein import. *Cell*, *121*(7), 1059–1069. <https://doi.org/10.1016/j.cell.2005.04.011>
- Mignery, G. A., Pikaard, C. S., & Park, W. D. (1988). Molecular characterization of the patatin multigene family of potato. *Gene*, *62*(1), 27–44. [https://doi.org/10.1016/0378-1119\(88\)90577-x](https://doi.org/10.1016/0378-1119(88)90577-x)
- Milenkovic, D., Gabriel, K., Guiard, B., Schulze-Specking, A., Pfanner, N., & Chacinska, A. (2007). Biogenesis of the essential Tim9-Tim10 chaperone complex of mitochondria: Site-specific recognition of cysteine residues by the intermembrane space receptor Mia40. *The Journal of Biological Chemistry*, *282*(31), 22472–22480. <https://doi.org/10.1074/jbc.M703294200>
- Miliara, X., Garnett, J. A., Tatsuta, T., Abid Ali, F., Baldie, H., Pérez-Dorado, I., Simpson, P., Yague, E., Langer, T., & Matthews, S. (2015). Structural insight into the TRIAP1/PRELI-like domain family of

- mitochondrial phospholipid transfer complexes. *EMBO Reports*, 16(7), 824–835.
<https://doi.org/10.15252/embr.201540229>
- Miyata, N., Watanabe, Y., Tamura, Y., Endo, T., & Kuge, O. (2016). Phosphatidylserine transport by Ups2-Mdm35 in respiration-active mitochondria. *The Journal of Cell Biology*, 214(1), 77–88.
<https://doi.org/10.1083/jcb.201601082>
- Moberg, P., Nilsson, S., Ståhl, A., Eriksson, A.-C., Glaser, E., & Måler, L. (2004). NMR solution structure of the mitochondrial F1beta presequence from *Nicotiana plumbaginifolia*. *Journal of Molecular Biology*, 336(5), 1129–1140. <https://doi.org/10.1016/j.jmb.2004.01.006>
- Mokranjac, D., & Neupert, W. (2009). Thirty years of protein translocation into mitochondria: Unexpectedly complex and still puzzling. *Biochimica et Biophysica Acta (BBA) - Molecular Cell Research*, 1793(1), 33–41. <https://doi.org/10.1016/j.bbamcr.2008.06.021>
- Mokranjac, D., Sichtung, M., Popov-Celeketić, D., Mapa, K., Gevorkyan-Airapetov, L., Zohary, K., Hell, K., Azem, A., & Neupert, W. (2009). Role of Tim50 in the transfer of precursor proteins from the outer to the inner membrane of mitochondria. *Molecular Biology of the Cell*, 20(5), 1400–1407.
<https://doi.org/10.1091/mbc.e08-09-0934>
- Mossmann, D., Vögtle, F.-N., Taskin, A. A., Teixeira, P. F., Ring, J., Burkhart, J. M., Burger, N., Pinho, C. M., Tadic, J., Loreth, D., Graff, C., Metzger, F., Sickmann, A., Kretz, O., Wiedemann, N., Zahedi, R. P., Madeo, F., Glaser, E., & Meisinger, C. (2014). Amyloid- β peptide induces mitochondrial dysfunction by inhibition of preprotein maturation. *Cell Metabolism*, 20(4), 662–669.
<https://doi.org/10.1016/j.cmet.2014.07.024>
- Müller, J. M., Milenkovic, D., Guiard, B., Pfanner, N., & Chacinska, A. (2008). Precursor oxidation by Mia40 and Erv1 promotes vectorial transport of proteins into the mitochondrial intermembrane space. *Molecular Biology of the Cell*, 19(1), 226–236. <https://doi.org/10.1091/mbc.e07-08-0814>

- Nakamoto, H., & Bardwell, J. C. A. (2004). Catalysis of disulfide bond formation and isomerization in the *Escherichia coli* periplasm. *Biochimica Et Biophysica Acta*, *1694*(1–3), 111–119.
<https://doi.org/10.1016/j.bbamcr.2004.02.012>
- Neupert, W. (1997). PROTEIN IMPORT INTO MITOCHONDRIA. *Annual Review of Biochemistry*, *66*(Volume 66, 1997), 863–917. <https://doi.org/10.1146/annurev.biochem.66.1.863>
- Neupert, W., & Herrmann, J. M. (2007). Translocation of proteins into mitochondria. *Annual Review of Biochemistry*, *76*, 723–749. <https://doi.org/10.1146/annurev.biochem.76.052705.163409>
- Noble, M. E., Cleasby, A., Johnson, L. N., Egmond, M. R., & Frenken, L. G. (1993). The crystal structure of triacylglycerol lipase from *Pseudomonas glumae* reveals a partially redundant catalytic aspartate. *FEBS Letters*, *331*(1–2), 123–128. [https://doi.org/10.1016/0014-5793\(93\)80310-q](https://doi.org/10.1016/0014-5793(93)80310-q)
- Noinaj, N., Gumbart, J. C., & Buchanan, S. K. (2017). The β -barrel assembly machinery in motion. *Nature Reviews Microbiology*, *15*(4), 197–204. <https://doi.org/10.1038/nrmicro.2016.191>
- Nunnari, J., Fox, T. D., & Walter, P. (1993). A mitochondrial protease with two catalytic subunits of nonoverlapping specificities. *Science (New York, N.Y.)*, *262*(5142), 1997–2004.
<https://doi.org/10.1126/science.8266095>
- Obaseki, E., Adebayo, D., Bandyopadhyay, S., & Hariri, H. (n.d.). Lipid droplets and fatty acid-induced lipotoxicity: In a nutshell. *FEBS Letters*, *n/a*(n/a). <https://doi.org/10.1002/1873-3468.14808>
- Odendall, F., Backes, S., Tatsuta, T., Weill, U., Schuldiner, M., Langer, T., Herrmann, J. M., Rapaport, D., & Dimer, K. S. (2019). The mitochondrial intermembrane space-facing proteins Mcp2 and Tgl2 are involved in yeast lipid metabolism. *Molecular Biology of the Cell*, *30*(21), 2681–2694.
<https://doi.org/10.1091/mbc.E19-03-0166>
- Oelkers, P., Tinkelenberg, A., Erdeniz, N., Cromley, D., Billheimer, J. T., & Sturley, S. L. (2000). A Lecithin Cholesterol Acyltransferase-like Gene Mediates Diacylglycerol Esterification in Yeast*. *Journal of Biological Chemistry*, *275*(21), 15609–15612. <https://doi.org/10.1074/jbc.C000144200>

- Okreglak, V., & Walter, P. (2014). The conserved AAA-ATPase Msp1 confers organelle specificity to tail-anchored proteins. *Proceedings of the National Academy of Sciences*, *111*(22), 8019–8024.
<https://doi.org/10.1073/pnas.1405755111>
- Opaliński, Ł., Song, J., Priesnitz, C., Wenz, L.-S., Oeljeklaus, S., Warscheid, B., Pfanner, N., & Becker, T. (2018). Recruitment of Cytosolic J-Proteins by TOM Receptors Promotes Mitochondrial Protein Biogenesis. *Cell Reports*, *25*(8), 2036–2043.e5. <https://doi.org/10.1016/j.celrep.2018.10.083>
- Osman, C., Haag, M., Potting, C., Rodenfels, J., Dip, P. V., Wieland, F. T., Brügger, B., Westermann, B., & Langer, T. (2009). The genetic interactome of prohibitins: Coordinated control of cardiolipin and phosphatidylethanolamine by conserved regulators in mitochondria. *The Journal of Cell Biology*, *184*(4), 583–596. <https://doi.org/10.1083/jcb.200810189>
- Østerlund, T., Contreras, J. A., & Holm, C. (1997). Identification of essential aspartic acid and histidine residues of hormone-sensitive lipase: Apparent residues of the catalytic triad. *FEBS Letters*, *403*(3), 259–262. [https://doi.org/10.1016/S0014-5793\(97\)00063-X](https://doi.org/10.1016/S0014-5793(97)00063-X)
- Otera, H., Taira, Y., Horie, C., Suzuki, Y., Suzuki, H., Setoguchi, K., Kato, H., Oka, T., & Mihara, K. (2007). A novel insertion pathway of mitochondrial outer membrane proteins with multiple transmembrane segments. *The Journal of Cell Biology*, *179*(7), 1355–1363.
<https://doi.org/10.1083/jcb.200702143>
- Palade, G. E. (1953). An electron microscope study of the mitochondrial structure. *The Journal of Histochemistry and Cytochemistry: Official Journal of the Histochemistry Society*, *1*(4), 188–211.
<https://doi.org/10.1177/1.4.188>
- Papadopoulos, A., Busch, M., Reiners, J., Hachani, E., Baeumers, M., Berger, J., Schmitt, L., Jaeger, K.-E., Kovacic, F., Smits, S. H. J., & Kedrov, A. (2022). The periplasmic chaperone Skp prevents misfolding of the secretory lipase A from *Pseudomonas aeruginosa*. *Frontiers in Molecular Biosciences*, *9*. <https://www.frontiersin.org/articles/10.3389/fmolb.2022.1026724>

- Papić, D., Elbaz-Alon, Y., Koerdt, S. N., Leopold, K., Worm, D., Jung, M., Schuldiner, M., & Rapaport, D. (2013). The role of Dj1 in import of the mitochondrial protein Mim1 demonstrates specificity between a cochaperone and its substrate protein. *Molecular and Cellular Biology*, 33(20), 4083–4094. <https://doi.org/10.1128/MCB.00227-13>
- Park, K., Botelho, S. C., Hong, J., Österberg, M., & Kim, H. (2013). Dissecting stop transfer versus conservative sorting pathways for mitochondrial inner membrane proteins in vivo. *The Journal of Biological Chemistry*, 288(3), 1521–1532. <https://doi.org/10.1074/jbc.M112.409748>
- Paschen, S. A., Waizenegger, T., Stan, T., Preuss, M., Cyrklaff, M., Hell, K., Rapaport, D., & Neupert, W. (2003). Evolutionary conservation of biogenesis of β -barrel membrane proteins. *Nature*, 426(6968), 862–866. <https://doi.org/10.1038/nature02208>
- Pellegrini, M. (1980). Three-dimensional reconstruction of organelles in *Euglena gracilis* Z. II. Qualitative and quantitative changes of chloroplasts and mitochondrial reticulum in synchronous cultures during bleaching. *Journal of Cell Science*, 46, 313–340. <https://doi.org/10.1242/jcs.46.1.313>
- Petrungaro, C., & Kornmann, B. (2019). Lipid exchange at ER-mitochondria contact sites: A puzzle falling into place with quite a few pieces missing. *Current Opinion in Cell Biology*, 57, 71–76. <https://doi.org/10.1016/j.ceb.2018.11.005>
- Pfeffer, S., Woellhaf, M. W., Herrmann, J. M., & Förster, F. (2015). Organization of the mitochondrial translation machinery studied in situ by cryoelectron tomography. *Nature Communications*, 6(1), 6019. <https://doi.org/10.1038/ncomms7019>
- Physiologische Gesellschaft zu Berlin. (1898). *Archiv für Physiologie: Vol. Jahrg.1898*. Veit & Comp. <https://www.biodiversitylibrary.org/item/109725>
- Ploegh, H. L. (2007). A lipid-based model for the creation of an escape hatch from the endoplasmic reticulum. *Nature*, 448(7152), 435–438. <https://doi.org/10.1038/nature06004>

- Ploier, B., Scharwey, M., Koch, B., Schmidt, C., Schatte, J., Rechberger, G., Kollroser, M., Hermetter, A., & Daum, G. (2013). Screening for Hydrolytic Enzymes Reveals Ayr1p as a Novel Triacylglycerol Lipase in *Saccharomyces cerevisiae*. *The Journal of Biological Chemistry*, *288*(50), 36061–36072. <https://doi.org/10.1074/jbc.M113.509927>
- Popov-Čeleketić, D., Mapa, K., Neupert, W., & Mokranjac, D. (2008). Active remodelling of the TIM23 complex during translocation of preproteins into mitochondria. *The EMBO Journal*, *27*(10), 1469–1480. <https://doi.org/10.1038/emboj.2008.79>
- Popov-Celeketić, J., Waizenegger, T., & Rapaport, D. (2008). Mim1 functions in an oligomeric form to facilitate the integration of Tom20 into the mitochondrial outer membrane. *Journal of Molecular Biology*, *376*(3), 671–680. <https://doi.org/10.1016/j.jmb.2007.12.006>
- Potting, C., Wilmes, C., Engmann, T., Osman, C., & Langer, T. (2010). Regulation of mitochondrial phospholipids by Ups1/PRELI-like proteins depends on proteolysis and Mdm35. *The EMBO Journal*, *29*(17), 2888–2898. <https://doi.org/10.1038/emboj.2010.169>
- Pu, J., Ha, C. W., Zhang, S., Jung, J. P., Huh, W.-K., & Liu, P. (2011). Interactomic study on interaction between lipid droplets and mitochondria. *Protein & Cell*, *2*(6), 487–496. <https://doi.org/10.1007/s13238-011-1061-y>
- Qiu, J., Wenz, L.-S., Zerbes, R. M., Oeljeklaus, S., Bohnert, M., Stroud, D. A., Wirth, C., Ellenrieder, L., Thornton, N., Kutik, S., Wiese, S., Schulze-Specking, A., Zufall, N., Chacinska, A., Guiard, B., Hunte, C., Warscheid, B., van der Laan, M., Pfanner, N., ... Becker, T. (2013). Coupling of Mitochondrial Import and Export Translocases by Receptor-Mediated Supercomplex Formation. *Cell*, *154*(3), 596–608. <https://doi.org/10.1016/j.cell.2013.06.033>
- Rajakumari, S., & Daum, G. (2010a). Janus-faced Enzymes Yeast Tgl3p and Tgl5p Catalyze Lipase and Acyltransferase Reactions. *Molecular Biology of the Cell*, *21*(4), 501–510. <https://doi.org/10.1091/mbc.E09-09-0775>

- Rajakumari, S., & Daum, G. (2010b). Multiple Functions as Lipase, Steryl Ester Hydrolase, Phospholipase, and Acyltransferase of Tgl4p from the Yeast *Saccharomyces cerevisiae*. *Journal of Biological Chemistry*, 285(21), 15769–15776. <https://doi.org/10.1074/jbc.M109.076331>
- Rampelt, H., Zerbes, R. M., van der Laan, M., & Pfanner, N. (2017). Role of the mitochondrial contact site and cristae organizing system in membrane architecture and dynamics. *Biochimica et Biophysica Acta (BBA) - Molecular Cell Research*, 1864(4), 737–746. <https://doi.org/10.1016/j.bbamcr.2016.05.020>
- Rehling, P., Brandner, K., & Pfanner, N. (2004). Mitochondrial import and the twin-pore translocase. *Nature Reviews Molecular Cell Biology*, 5(7), 519–530. <https://doi.org/10.1038/nrm1426>
- Rehling, P., Model, K., Brandner, K., Kovermann, P., Sickmann, A., Meyer, H. E., Kühlbrandt, W., Wagner, R., Truscott, K. N., & Pfanner, N. (2003). Protein insertion into the mitochondrial inner membrane by a twin-pore translocase. *Science (New York, N.Y.)*, 299(5613), 1747–1751. <https://doi.org/10.1126/science.1080945>
- Sandager, L., Gustavsson, M. H., Ståhl, U., Dahlqvist, A., Wiberg, E., Banas, A., Lenman, M., Ronne, H., & Stymne, S. (2002). Storage lipid synthesis is non-essential in yeast. *The Journal of Biological Chemistry*, 277(8), 6478–6482. <https://doi.org/10.1074/jbc.M109109200>
- Schatz, G. (1997). Just follow the acid chain. *Nature*, 388(6638), 121–122. <https://doi.org/10.1038/40510>
- Schatz, G., & Dobberstein, B. (1996). Common principles of protein translocation across membranes. *Science (New York, N.Y.)*, 271(5255), 1519–1526. <https://doi.org/10.1126/science.271.5255.1519>
- Schmidt, C., Athenstaedt, K., Koch, B., Ploier, B., & Daum, G. (2013). Regulation of the Yeast Triacylglycerol Lipase Tgl3p by Formation of Nonpolar Lipids. *Journal of Biological Chemistry*, 288(27), 19939–19948. <https://doi.org/10.1074/jbc.M113.459610>

- Schmidt, O., Harbauer, A. B., Rao, S., Eyrich, B., Zahedi, R. P., Stojanovski, D., Schönfisch, B., Guiard, B., Sickmann, A., Pfanner, N., & Meisinger, C. (2011). Regulation of mitochondrial protein import by cytosolic kinases. *Cell*, *144*(2), 227–239. <https://doi.org/10.1016/j.cell.2010.12.015>
- Schreiner, B., Westerburg, H., Forné, I., Imhof, A., Neupert, W., & Mokranjac, D. (2012). Role of the AAA protease Yme1 in folding of proteins in the intermembrane space of mitochondria. *Molecular Biology of the Cell*, *23*(22), 4335–4346. <https://doi.org/10.1091/mbc.e12-05-0420>
- Schuldiner, M., & Bohnert, M. (2017). A different kind of love – lipid droplet contact sites. *Biochimica et Biophysica Acta (BBA) - Molecular and Cell Biology of Lipids*, *1862*(10, Part B), 1188–1196. <https://doi.org/10.1016/j.bbalip.2017.06.005>
- Schulte, U., Den Brave, F., Haupt, A., Gupta, A., Song, J., Müller, C. S., Engelke, J., Mishra, S., Mårtensson, C., Ellenrieder, L., Priesnitz, C., Straub, S. P., Doan, K. N., Kulawiak, B., Bildl, W., Rampelt, H., Wiedemann, N., Pfanner, N., Fakler, B., & Becker, T. (2023). Mitochondrial complexome reveals quality-control pathways of protein import. *Nature*, *614*(7946), 153–159. <https://doi.org/10.1038/s41586-022-05641-w>
- Schulz, C., Schendzielorz, A., & Rehling, P. (2015). Unlocking the presequence import pathway. *Trends in Cell Biology*, *25*(5), 265–275. <https://doi.org/10.1016/j.tcb.2014.12.001>
- Seals, D. F., Eitzen, G., Margolis, N., Wickner, W. T., & Price, A. (2000). A Ypt/Rab effector complex containing the Sec1 homolog Vps33p is required for homotypic vacuole fusion. *Proceedings of the National Academy of Sciences*, *97*(17), 9402–9407. <https://doi.org/10.1073/pnas.97.17.9402>
- Setoguchi, K., Otera, H., & Mihara, K. (2006). Cytosolic factor- and TOM-independent import of C-tail-anchored mitochondrial outer membrane proteins. *The EMBO Journal*, *25*(24), 5635–5647. <https://doi.org/10.1038/sj.emboj.7601438>

- Shai, N., Schuldiner, M., & Zalckvar, E. (2016). No peroxisome is an island—Peroxisome contact sites. *Biochimica et Biophysica Acta (BBA) - Molecular Cell Research*, *1863*(5), 1061–1069.
<https://doi.org/10.1016/j.bbamcr.2015.09.016>
- Shai, N., Yifrach, E., van Roermund, C. W. T., Cohen, N., Bibi, C., IJlst, L., Cavellini, L., Meurisse, J., Schuster, R., Zada, L., Mari, M. C., Reggiori, F. M., Hughes, A. L., Escobar-Henriques, M., Cohen, M. M., Waterham, H. R., Wanders, R. J. A., Schuldiner, M., & Zalckvar, E. (2018). Systematic mapping of contact sites reveals tethers and a function for the peroxisome-mitochondria contact. *Nature Communications*, *9*(1), 1761. <https://doi.org/10.1038/s41467-018-03957-8>
- Shen, H., Heacock, P. N., Clancey, C. J., & Dowhan, W. (1996). The CDS1 Gene Encoding CDP-diacylglycerol Synthase In *Saccharomyces cerevisiae* Is Essential for Cell Growth (*). *Journal of Biological Chemistry*, *271*(2), 789–795. <https://doi.org/10.1074/jbc.271.2.789>
- Sideris, D. P., Petrakis, N., Katrakili, N., Mikropoulou, D., Gallo, A., Ciofi-Baffoni, S., Banci, L., Bertini, I., & Tokatlidis, K. (2009). A novel intermembrane space–targeting signal docks cysteines onto Mia40 during mitochondrial oxidative folding. *The Journal of Cell Biology*, *187*(7), 1007–1022.
<https://doi.org/10.1083/jcb.200905134>
- Sideris, D. P., & Tokatlidis, K. (2007). Oxidative folding of small Tims is mediated by site-specific docking onto Mia40 in the mitochondrial intermembrane space. *Molecular Microbiology*, *65*(5), 1360–1373. <https://doi.org/10.1111/j.1365-2958.2007.05880.x>
- Sim, S. I., Chen, Y., Lynch, D. L., Gumbart, J. C., & Park, E. (2023). Structural basis of mitochondrial protein import by the TIM23 complex. *Nature*, *621*(7979), 620–626.
<https://doi.org/10.1038/s41586-023-06239-6>
- Sirrenberg, C., Endres, M., Folsch, H., Stuart, R. A., Neupert, W., & Brunner, M. (1998). Carrier protein import into mitochondria mediated by the intermembrane proteins Tim10/Mrs11 and Tim12/Mrs5. *Nature*, *391*(6670), 912–915. <https://doi.org/10.1038/36136>

- Sogo, L. F., & Yaffe, M. P. (1994). Regulation of mitochondrial morphology and inheritance by Mdm10p, a protein of the mitochondrial outer membrane. *Journal of Cell Biology*, *126*(6), 1361–1373.
<https://doi.org/10.1083/jcb.126.6.1361>
- Sorger, D., & Daum, G. (2003). Triacylglycerol biosynthesis in yeast. *Applied Microbiology and Biotechnology*, *61*(4), 289–299. <https://doi.org/10.1007/s00253-002-1212-4>
- Stiller, S. B., Höpker, J., Oeljeklaus, S., Schütze, C., Schrempp, S. G., Vent-Schmidt, J., Horvath, S. E., Frazier, A. E., Gebert, N., van der Laan, M., Bohnert, M., Warscheid, B., Pfanner, N., & Wiedemann, N. (2016). Mitochondrial OXA Translocase Plays a Major Role in Biogenesis of Inner-Membrane Proteins. *Cell Metabolism*, *23*(5), 901–908.
<https://doi.org/10.1016/j.cmet.2016.04.005>
- Stojanovski, D., Milenkovic, D., Müller, J. M., Gabriel, K., Schulze-Specking, A., Baker, M. J., Ryan, M. T., Guiard, B., Pfanner, N., & Chacinska, A. (2008). Mitochondrial protein import: Precursor oxidation in a ternary complex with disulfide carrier and sulfhydryl oxidase. *The Journal of Cell Biology*, *183*(2), 195–202. <https://doi.org/10.1083/jcb.200804095>
- Szabadkai, G., Bianchi, K., Várnai, P., De Stefani, D., Wieckowski, M. R., Cavagna, D., Nagy, A. I., Balla, T., & Rizzuto, R. (2006). Chaperone-mediated coupling of endoplasmic reticulum and mitochondrial Ca²⁺ channels. *The Journal of Cell Biology*, *175*(6), 901–911.
<https://doi.org/10.1083/jcb.200608073>
- Takeda, H., Tsutsumi, A., Nishizawa, T., Lindau, C., Busto, J. V., Wenz, L.-S., Ellenrieder, L., Imai, K., Straub, S. P., Mossmann, W., Qiu, J., Yamamori, Y., Tomii, K., Suzuki, J., Murata, T., Ogasawara, S., Nureki, O., Becker, T., Pfanner, N., ... Endo, T. (2021). Mitochondrial sorting and assembly machinery operates by β -barrel switching. *Nature*, *590*(7844), 163–169.
<https://doi.org/10.1038/s41586-020-03113-7>

- Tamura, Y., Endo, T., Iijima, M., & Sesaki, H. (2009). Ups1p and Ups2p antagonistically regulate cardiolipin metabolism in mitochondria. *The Journal of Cell Biology*, *185*(6), 1029–1045.
<https://doi.org/10.1083/jcb.200812018>
- Tamura, Y., Harada, Y., Nishikawa, S., Yamano, K., Kamiya, M., Shiota, T., Kuroda, T., Kuge, O., Sesaki, H., Imai, K., Tomii, K., & Endo, T. (2013). Tam41 Is a CDP-Diacylglycerol Synthase Required for Cardiolipin Biosynthesis in Mitochondria. *Cell Metabolism*, *17*(5), 709–718.
<https://doi.org/10.1016/j.cmet.2013.03.018>
- Tamura, Y., Harada, Y., Shiota, T., Yamano, K., Watanabe, K., Yokota, M., Yamamoto, H., Sesaki, H., & Endo, T. (2009). Tim23–Tim50 pair coordinates functions of translocators and motor proteins in mitochondrial protein import. *The Journal of Cell Biology*, *184*(1), 129–141.
<https://doi.org/10.1083/jcb.200808068>
- Tamura, Y., Iijima, M., & Sesaki, H. (2010). Mdm35p imports Ups proteins into the mitochondrial intermembrane space by functional complex formation. *The EMBO Journal*, *29*(17), 2875–2887.
<https://doi.org/10.1038/emboj.2010.149>
- Tamura, Y., Onguka, O., Hobbs, A. E. A., Jensen, R. E., Iijima, M., Claypool, S. M., & Sesaki, H. (2012). Role for Two Conserved Intermembrane Space Proteins, Ups1p and Up2p, in Intra-mitochondrial Phospholipid Trafficking*. *Journal of Biological Chemistry*, *287*(19), 15205–15218.
<https://doi.org/10.1074/jbc.M111.338665>
- Tamura, Y., Onguka, O., Itoh, K., Endo, T., Iijima, M., Claypool, S. M., & Sesaki, H. (2012). Phosphatidylethanolamine Biosynthesis in Mitochondria: PHOSPHATIDYLSERINE (PS) TRAFFICKING IS INDEPENDENT OF A PS DECARBOXYLASE AND INTERMEMBRANE SPACE PROTEINS UPS1P AND UPS2P*. *Journal of Biological Chemistry*, *287*(52), 43961–43971.
<https://doi.org/10.1074/jbc.M112.390997>

- Tan, T., Özbalci, C., Brügger, B., Rapaport, D., & Dimmer, K. S. (2013). Mcp1 and Mcp2, two novel proteins involved in mitochondrial lipid homeostasis. *Journal of Cell Science*, jcs.121244. <https://doi.org/10.1242/jcs.121244>
- Tatsuta, T., & Langer, T. (2017). Intramitochondrial phospholipid trafficking. *Biochimica et Biophysica Acta (BBA) - Molecular and Cell Biology of Lipids*, 1862(1), 81–89. <https://doi.org/10.1016/j.bbalip.2016.08.006>
- Taylor, A. B., Smith, B. S., Kitada, S., Kojima, K., Miyaura, H., Otwinowski, Z., Ito, A., & Deisenhofer, J. (2001). Crystal structures of mitochondrial processing peptidase reveal the mode for specific cleavage of import signal sequences. *Structure (London, England: 1993)*, 9(7), 615–625. [https://doi.org/10.1016/s0969-2126\(01\)00621-9](https://doi.org/10.1016/s0969-2126(01)00621-9)
- Ting, S.-Y., Schilke, B. A., Hayashi, M., & Craig, E. A. (2014). Architecture of the TIM23 inner mitochondrial translocon and interactions with the matrix import motor. *The Journal of Biological Chemistry*, 289(41), 28689–28696. <https://doi.org/10.1074/jbc.M114.588152>
- Trotter, P. J., Pedretti, J., Yates, R., & Voelker, D. R. (1995). Phosphatidylserine Decarboxylase 2 of *Saccharomyces cerevisiae*. *Journal of Biological Chemistry*, 270(11), 6071–6080. <https://doi.org/10.1074/jbc.270.11.6071>
- Trotter, P. J., & Voelker, D. R. (1995). Identification of a Non-mitochondrial Phosphatidylserine Decarboxylase Activity (PSD2) in the Yeast *Saccharomyces cerevisiae*(*). *Journal of Biological Chemistry*, 270(11), 6062–6070. <https://doi.org/10.1074/jbc.270.11.6062>
- Tuller, G., Nemeč, T., Hrastnik, C., & Daum, G. (1999). Lipid composition of subcellular membranes of an FY1679-derived haploid yeast wild-type strain grown on different carbon sources. *Yeast*, 15(14), 1555–1564. [https://doi.org/10.1002/\(SICI\)1097-0061\(199910\)15:14<1555::AID-YEA479>3.0.CO;2-Z](https://doi.org/10.1002/(SICI)1097-0061(199910)15:14<1555::AID-YEA479>3.0.CO;2-Z)

- van der Laan, M., Meinecke, M., Dudek, J., Hutu, D. P., Lind, M., Perschil, I., Guiard, B., Wagner, R., Pfanner, N., & Rehling, P. (2007). Motor-free mitochondrial presequence translocase drives membrane integration of preproteins. *Nature Cell Biology*, *9*(10), 1152–1159. <https://doi.org/10.1038/ncb1635>
- van der Laan, M., Schrempp, S. G., & Pfanner, N. (2013). Voltage-coupled conformational dynamics of mitochondrial protein-import channel. *Nature Structural & Molecular Biology*, *20*(8), 915–917. <https://doi.org/10.1038/nsmb.2643>
- Van Heusden, G. P. H., Nebohâcovâ, M., Overbeeke, T. L. A., & Steensma, H. Y. (1998). The *Saccharomyces cerevisiae* TGL2 gene encodes a protein with lipolytic activity and can complement an *Escherichia coli* diacylglycerol kinase disruptant. *Yeast*, *14*(3), 225–232. [https://doi.org/10.1002/\(SICI\)1097-0061\(199802\)14:3<225::AID-YEA215>3.0.CO;2-#](https://doi.org/10.1002/(SICI)1097-0061(199802)14:3<225::AID-YEA215>3.0.CO;2-#)
- van Tilbeurgh, H., Egloff, M.-P., Martinez, C., Rugani, N., Verger, R., & Cambillau, C. (1993). Interfacial activation of the lipase–procolipase complex by mixed micelles revealed by X-ray crystallography. *Nature*, *362*(6423), 814–820. <https://doi.org/10.1038/362814a0>
- van Wilpe, S., Ryan, M. T., Hill, K., Maarse, A. C., Meisinger, C., Brix, J., Dekker, P. J., Moczko, M., Wagner, R., Meijer, M., Guiard, B., Hönlinger, A., & Pfanner, N. (1999). Tom22 is a multifunctional organizer of the mitochondrial preprotein translocase. *Nature*, *401*(6752), 485–489. <https://doi.org/10.1038/46802>
- Varadi, M., Anyango, S., Deshpande, M., Nair, S., Natassia, C., Yordanova, G., Yuan, D., Stroe, O., Wood, G., Laydon, A., Žídek, A., Green, T., Tunyasuvunakool, K., Petersen, S., Jumper, J., Clancy, E., Green, R., Vora, A., Lutfi, M., ... Velankar, S. (2022). AlphaFold Protein Structure Database: Massively expanding the structural coverage of protein-sequence space with high-accuracy models. *Nucleic Acids Research*, *50*(D1), D439–D444. <https://doi.org/10.1093/nar/gkab1061>

Vasiljev, A., Ahting, U., Nargang, F. E., Go, N. E., Habib, S. J., Kozany, C., Panneels, V., Sinning, I., Prokisch, H., Neupert, W., Nussberger, S., & Rapaport, D. (2004). Reconstituted TOM Core Complex and Tim9/Tim10 Complex of Mitochondria Are Sufficient for Translocation of the ADP/ATP Carrier across Membranes. *Molecular Biology of the Cell*, *15*(3), 1445–1458.

<https://doi.org/10.1091/mbc.E03-05-0272>

Vial, S., Lu, H., Allen, S., Savory, P., Thornton, D., Sheehan, J., & Tokatlidis, K. (2002). Assembly of Tim9 and Tim10 into a Functional Chaperone*. *Journal of Biological Chemistry*, *277*(39), 36100–36108. <https://doi.org/10.1074/jbc.M202310200>

Viljoen, B. C., Kock, J. L. F., & Lategan, P. M. (1986). Fatty Acid Composition as a Guide to the Classification of Selected Genera of Yeasts Belonging to the Endomycetales. *Microbiology*, *132*(8), 2397–2400. <https://doi.org/10.1099/00221287-132-8-2397>

Vitali, D. G., Sinzel, M., Bulthuis, E. P., Kolb, A., Zabel, S., Mehlhorn, D. G., Figueiredo Costa, B., Farkas, Á., Clancy, A., Schuldiner, M., Grefen, C., Schwappach, B., Borgese, N., & Rapaport, D. (2018). The GET pathway can increase the risk of mitochondrial outer membrane proteins to be mistargeted to the ER. *Journal of Cell Science*, *131*(10), jcs211110. <https://doi.org/10.1242/jcs.211110>

Vögtle, F.-N., Burkhart, J. M., Gonczarowska-Jorge, H., Kücükköse, C., Taskin, A. A., Kopczynski, D., Ahrends, R., Mossmann, D., Sickmann, A., Zahedi, R. P., & Meisinger, C. (2017). Landscape of submitochondrial protein distribution. *Nature Communications*, *8*(1), 290.

<https://doi.org/10.1038/s41467-017-00359-0>

von der Malsburg, K., Müller, J. M., Bohnert, M., Oeljeklaus, S., Kwiatkowska, P., Becker, T., Loniewska-Lwowska, A., Wiese, S., Rao, S., Milenkovic, D., Hutu, D. P., Zerbes, R. M., Schulze-Specking, A., Meyer, H. E., Martinou, J.-C., Rospert, S., Rehling, P., Meisinger, C., Veenhuis, M., ... van der Laan, M. (2011). Dual Role of Mitofilin in Mitochondrial Membrane Organization and Protein Biogenesis. *Developmental Cell*, *21*(4), 694–707. <https://doi.org/10.1016/j.devcel.2011.08.026>

- Voos, W., Martin, H., Krimmer, T., & Pfanner, N. (1999). Mechanisms of protein translocation into mitochondria. *Biochimica et Biophysica Acta (BBA) - Reviews on Biomembranes*, 1422(3), 235–254. [https://doi.org/10.1016/S0304-4157\(99\)00007-6](https://doi.org/10.1016/S0304-4157(99)00007-6)
- Vorobieva, A. A., White, P., Liang, B., Horne, J. E., Bera, A. K., Chow, C. M., Gerben, S., Marx, S., Kang, A., Stiving, A. Q., Harvey, S. R., Marx, D. C., Khan, G. N., Fleming, K. G., Wysocki, V. H., Brockwell, D. J., Tamm, L. K., Radford, S. E., & Baker, D. (2021). De novo design of transmembrane β barrels. *Science (New York, N.Y.)*, 371(6531), eabc8182. <https://doi.org/10.1126/science.abc8182>
- Waizenegger, T., Habib, S. J., Lech, M., Mokranjac, D., Paschen, S. A., Hell, K., Neupert, W., & Rapaport, D. (2004). Tob38, a novel essential component in the biogenesis of β -barrel proteins of mitochondria. *EMBO Reports*, 5(7), 704–709. <https://doi.org/10.1038/sj.embor.7400183>
- Walther, T. C., & Farese, R. V. (2009). The life of lipid droplets. *Biochimica et Biophysica Acta (BBA) - Molecular and Cell Biology of Lipids*, 1791(6), 459–466. <https://doi.org/10.1016/j.bbalip.2008.10.009>
- Walther, T. C., & Farese, R. V. (2012). Lipid Droplets and Cellular Lipid Metabolism. *Annual Review of Biochemistry*, 81(1), 687–714. <https://doi.org/10.1146/annurev-biochem-061009-102430>
- Wanders, R. J. A. (2014). Metabolic functions of peroxisomes in health and disease. *Biochimie*, 98, 36–44. <https://doi.org/10.1016/j.biochi.2013.08.022>
- Wasilewski, M., Draczkowski, P., & Chacinska, A. (2023). Protein import into mitochondria—A new path through the membranes. *Nature Structural & Molecular Biology*, 30(12), Article 12. <https://doi.org/10.1038/s41594-023-01170-w>
- Watanabe, Y., Tamura, Y., Kawano, S., & Endo, T. (2015). Structural and mechanistic insights into phospholipid transfer by Ups1–Mdm35 in mitochondria. *Nature Communications*, 6(1), 7922. <https://doi.org/10.1038/ncomms8922>

- Wenz, L.-S., Ellenrieder, L., Qiu, J., Bohnert, M., Zufall, N., van der Laan, M., Pfanner, N., Wiedemann, N., & Becker, T. (2015). Sam37 is crucial for formation of the mitochondrial TOM–SAM supercomplex, thereby promoting β -barrel biogenesis. *Journal of Cell Biology*, *210*(7), 1047–1054. <https://doi.org/10.1083/jcb.201504119>
- Wideman, J. G., Go, N. E., Klein, A., Redmond, E., Lackey, S. W. K., Tao, T., Kalbacher, H., Rapaport, D., Neupert, W., & Nargang, F. E. (2010). Roles of the Mdm10, Tom7, Mdm12, and Mmm1 Proteins in the Assembly of Mitochondrial Outer Membrane Proteins in *Neurospora crassa*. *Molecular Biology of the Cell*, *21*(10), 1725–1736. <https://doi.org/10.1091/mbc.E09-10-0844>
- Wiedemann, N., Kozjak, V., Chacinska, A., Schönfisch, B., Rospert, S., Ryan, M. T., Pfanner, N., & Meisinger, C. (2003). Machinery for protein sorting and assembly in the mitochondrial outer membrane. *Nature*, *424*(6948), 565–571. <https://doi.org/10.1038/nature01753>
- Wiedemann, N., & Pfanner, N. (2017). Mitochondrial Machineries for Protein Import and Assembly. *Annual Review of Biochemistry*, *86*(Volume 86, 2017), 685–714. <https://doi.org/10.1146/annurev-biochem-060815-014352>
- Wiedemann, N., Pfanner, N., & Ryan, M. T. (2001). The three modules of ADP/ATP carrier cooperate in receptor recruitment and translocation into mitochondria. *The EMBO Journal*, *20*(5), 951–960. <https://doi.org/10.1093/emboj/20.5.951>
- Yamamoto, H., Fukui, K., Takahashi, H., Kitamura, S., Shiota, T., Terao, K., Uchida, M., Esaki, M., Nishikawa, S., Yoshihisa, T., Yamano, K., & Endo, T. (2009). Roles of Tom70 in Import of Presequence-containing Mitochondrial Proteins*. *Journal of Biological Chemistry*, *284*(46), 31635–31646. <https://doi.org/10.1074/jbc.M109.041756>
- Yamano, K., Tanaka-Yamano, S., & Endo, T. (2010a). Mdm10 as a dynamic constituent of the TOB/SAM complex directs coordinated assembly of Tom40. *EMBO Reports*, *11*(3), 187–193. <https://doi.org/10.1038/embor.2009.283>

- Yamano, K., Tanaka-Yamano, S., & Endo, T. (2010b). Tom7 Regulates Mdm10-mediated Assembly of the Mitochondrial Import Channel Protein Tom40*. *Journal of Biological Chemistry*, 285(53), 41222–41231. <https://doi.org/10.1074/jbc.M110.163238>
- Yamano, K., Yatsukawa, Y., Esaki, M., Hobbs, A. E. A., Jensen, R. E., & Endo, T. (2008). Tom20 and Tom22 Share the Common Signal Recognition Pathway in Mitochondrial Protein Import*. *Journal of Biological Chemistry*, 283(7), 3799–3807. <https://doi.org/10.1074/jbc.M708339200>
- Yang, H., Bard, M., Bruner, D. A., Gleeson, A., Deckelbaum, R. J., Aljinovic, G., Pohl, T. M., Rothstein, R., & Sturley, S. L. (1996). Sterol esterification in yeast: A two-gene process. *Science (New York, N.Y.)*, 272(5266), 1353–1356. <https://doi.org/10.1126/science.272.5266.1353>
- Young, J. C., Hoogenraad, N. J., & Hartl, F. U. (2003). Molecular chaperones Hsp90 and Hsp70 deliver preproteins to the mitochondrial import receptor Tom70. *Cell*, 112(1), 41–50. [https://doi.org/10.1016/s0092-8674\(02\)01250-3](https://doi.org/10.1016/s0092-8674(02)01250-3)
- Youngman, M. J., Hobbs, A. E. A., Burgess, S. M., Srinivasan, M., & Jensen, R. E. (2004). Mmm2p, a mitochondrial outer membrane protein required for yeast mitochondrial shape and maintenance of mtDNA nucleoids. *The Journal of Cell Biology*, 164(5), 677–688. <https://doi.org/10.1083/jcb.200308012>
- Yu, C., Kennedy, N. J., Chang, C. C. Y., & Rothblatt, J. A. (1996). Molecular Cloning and Characterization of Two Isoforms of *Saccharomyces cerevisiae* Acyl-CoA: Sterol Acyltransferase*. *Journal of Biological Chemistry*, 271(39), 24157–24163. <https://doi.org/10.1074/jbc.271.39.24157>
- Yu, F., He, F., Yao, H., Wang, C., Wang, J., Li, J., Qi, X., Xue, H., Ding, J., & Zhang, P. (2015). Structural basis of intramitochondrial phosphatidic acid transport mediated by Ups1-Mdm35 complex. *EMBO Reports*, 16(7), 813–823. <https://doi.org/10.15252/embr.201540137>
- Zahedi, R. P., Sickmann, A., Boehm, A. M., Winkler, C., Zufall, N., Schönfisch, B., Guiard, B., Pfanner, N., & Meisinger, C. (2006). Proteomic analysis of the yeast mitochondrial outer membrane reveals

accumulation of a subclass of preproteins. *Molecular Biology of the Cell*, 17(3), 1436–1450.

<https://doi.org/10.1091/mbc.e05-08-0740>

Zweytick, D., Athenstaedt, K., & Daum, G. (2000). Intracellular lipid particles of eukaryotic cells.

Biochimica Et Biophysica Acta, 1469(2), 101–120. <https://doi.org/10.1016/s0005->

2736(00)00294-7

Characterization of Tgl2, a putative lipase in yeast mitochondria

Vitasta Tiku¹, Takashi Tatsuta², Martin Jung³, Doron Rapaport¹, and Kai Stefan Dimmer^{1*}

¹Interfaculty Institute of Biochemistry, University of Tübingen, Tübingen, Germany

²Max Planck Institute for Biology of Ageing, Köln, Germany

³University of Saarland, Homburg, Germany

* To whom correspondence should be addressed:

Interfaculty Institute of Biochemistry

University of Tübingen

72076 Tübingen

Germany

Tel: +49-7071-2974174

Fax: +49-7071-294016

E-mail: kai-stefan.dimmer@uni-tuebingen.de

Running title: Characterization of Tgl2

Key words: mitochondria / intermembrane space / lipids / lipases

Abstract

Mitochondria derive the majority of their lipids from other organelles through contact sites. These lipids, primarily phosphoglycerolipids, are the main components of mitochondrial membranes. In the cell, neutral lipids like triacylglycerides (TAGs) are stored in lipid droplets, playing an important role in maintaining cellular health. Enzymes like lipases mobilize these TAGs according to cellular needs. Neutral lipids have not yet been reported to play an important role in mitochondria so the presence of a putative TAG lipase – Tgl2, in yeast mitochondria is surprising. Moreover, *TGL2* and *MCP2*, a high-copy suppressor for *ERMES* deficient cells, display genetic interactions suggesting a potential link to lipid metabolism. In this study, we characterize in detail Tgl2. We show that Tgl2 forms dimers through intermolecular disulfide bridges and a cysteine-dependent high molecular weight complex. Furthermore, we could identify the lipase motif and catalytic triad of Tgl2 through *in silico* comparison with other lipases and mutated the catalytically active residues accordingly. Both mutants failed to rescue the growth phenotype of *mcp2Δ/tgl2Δ* double deletion strain suggesting that the residues are indeed essential for the protein's function. Additionally, we discovered that the catalytically active aspartate residue is important for protein stability. Steady state level analyses with non-functional variants of Tgl2 led to the identification of Yme1 as the protease responsible for its quality control. Finally, we provide evidence that the overall increase in TAGs in cells lacking *Mcp2* and Tgl2 originates from the mitochondria. Collectively, our study provides new insights into a key player in mitochondrial lipid homeostasis.

Introduction

Mitochondria are complex organelles with a wide array of functions. Their endosymbiotic bacterial ancestry has enabled them to evolve into semi-autonomous, bilayered entities consisting of an outer (MOM) and an inner mitochondrial membrane (MIM) (1, 2). These membranes are distinct in their protein content and lipid composition, separating the organelle into two aqueous sub-compartments – the matrix and the intermembrane space (IMS) (1).

Mitochondrial membranes have a dynamic architecture which is enabled by a continuous supply of lipids and proteins. While some lipids like cardiolipin are synthesized *in organello* from its precursor phosphatidic acid, mitochondria predominantly acquire lipids from the ER. Contact sites facilitating lipid exchange between mitochondria and lipid droplets (LDs), have also been suggested (3, 4). Once imported, these lipids need to be re-distributed between the two membranes, but the exact mechanism for this is still unknown. Alterations in the MICOS (mitochondrial contact site) complex have been shown to disturb mitochondrial ultrastructure and disrupt cristae morphology, suggesting a potential contribution to lipid metabolism (5–7). Further, lipid transfer proteins (LTPs) mediating a constant exchange of precursor lipids between the MIM and MOM, by shuttling them across the IMS have also been reported (8, 9).

The IMS is a small and rather crowded sub-compartment, housing ~50 proteins in yeast and humans (10, 11). While these numbers account for the soluble protein population, there is also a considerable fraction of MIM and MOM proteins that protrude into the IMS. As a buffer between the two membranes, the IMS allows for exchange of lipids, metabolites, and movement of proteins to maintain mitochondrial function. These proteins are typically small and are imported through either the disulfide relay pathway or the stop-transfer pathway. Additionally, some proteins such as CytC, Prx1, and Adk1 to name a few, are imported through atypical pathways some of which are yet to be fully elucidated (12, 13).

Tgl2 is a TAG lipase localized to the mitochondrial intermembrane space (14, 15). It belongs to the Tgl family of lipases in *S. cerevisiae* of which Tgl1, Tgl3, Tgl4, and Tgl5 can be found in LDs or cytosol (16). A previous study suggested lipolytic activity of Tgl2 towards short-chain TAGs and DAGs and long-chain TAGs (14). The protein has also been shown to compensate for the absence of DAG Kinase in *E. coli* (17). While deletion of *TGL2* does not result in a detectable phenotype, we previously reported negative genetic interactions of *TGL2* with *MCP2* (15). Elevated levels of Mcp2 appear to maintain lipid trafficking to and from mitochondria in ERMES (ER mitochondria encounter structure) deficient yeast (18), and the protein was more recently suggested to be involved in CoQ mobilization from the MIM (19).

Phosphatidylethanolamine (PE) and cardiolipin (CL), which is exclusive to mitochondria, are synthesized in mitochondria from precursor phosphoglycerolipids (PGL) that not only need to be imported but also have to be transported across the IMS, since certain biosynthesis steps take place in the MIM. PE is

synthesized from phosphatidylserine (PS) by the MIM decarboxylase Psd1 (20). CL is assembled from the precursor phosphatidic acid (PA) in the MIM, before maturation of the unique lipid takes place in the MOM (9). Of the repertoire of IMS proteins, the only evolutionarily conserved lipid transfer system is the Ups1/Ups2/Mdm35 complex (9, 21–23). This system is involved in the trafficking of the aforementioned lipids PA and PS (9, 20, 22, 23). Therefore, and since neutral lipids like TAGs are primarily stored in and mobilized from LDs, reports on the presence of a putative TAG lipase in the IMS are of high interest. In this study, we characterized Tgl2 and study its quality control. We identified its putative catalytic site and investigated its effect on cellular neutral lipid content.

Results

Tgl2 forms a homodimer that is sensitive to reducing agents

Tgl2 harbours 8 cysteine residues that are essential for its import through the Mia40 pathway (15). Since all our previous studies about Tgl2 were performed under reducing conditions, we asked whether the protein would behave differently under non-reducing conditions, especially since the IMS has a more oxidizing environment than the cytosol or matrix (24). We isolated crude mitochondria from yeast cells over-expressing N-terminally HA tagged Tgl2 (HA-Tgl2) and omitted any reducing agents during SDS-PAGE. A higher molecular weight species, approximately twice the size of Tgl2, was observed (Fig. 1A). Further, this species was lost over time as it could be detected more evidently in whole cell lysates and crude mitochondria isolated after mechanical rupturing but to a lesser extent in mitochondria obtained from spheroplasting-based isolation protocols (Fig. 1B). We further quantified this higher molecular weight species using the MOM protein Tom20 as a loading control. We observed that after shorter isolation protocols, this species contributes to almost half of the total protein whereas its appearance is noticeably reduced upon longer isolation protocols (Fig. 1B). Therefore, we assume that the species is not a consequence of oxidation, which would be expected to increase over time.

Since the size of this higher molecular weight species is twice that of Tgl2, we assumed that it could be a homodimer of Tgl2. To test our hypothesis, we isolated mitochondria containing two variants of Tgl2 – N-terminally tagged with either HA- or FLAG-tag and performed co-immunoprecipitation with beads containing antibodies against the FLAG-tag. We analysed the fractions by Western blotting and immunodecoration with antibodies against the two different tags. HA-tagged Tgl2 was detected only in the eluate fraction from mitochondria containing both tagged proteins. As a control, we could verify that the anti-FLAG beads do not unspecifically interact with HA-Tgl2. Furthermore, we could also detect the higher molecular weight species of both variants in the eluate fraction (Fig. 1C, arrowhead). Taken together, the two tagged Tg2 species are indeed interacting with each other, and the higher molecular species is a homodimer.

The submitochondrial localization of Tgl2 was previously determined through hypo-osmotic lysis assays. We previously showed by alkaline extraction that monomeric Tgl2 is not embedded in a mitochondrial membrane (15). However, we wondered if varying the pH could alter the response of the either the monomeric or the dimeric forms of the protein to alkaline extraction, by retaining any membrane interactions. Isolated mitochondria were subjected to alkaline extraction assay and the pellet and supernatant fractions were analysed by SDS-PAGE and immunodecoration was performed with Tom20, Mcr1, and Hep1 as controls for membrane integrated and soluble proteins (Fig. 1D). We observed that the dimeric form is also found in the soluble fraction, indicating that both forms of the protein are soluble.

Tgl2 is associated with the mitochondrial inner membrane

A protein like Tgl2, with a suggested affinity for lipids, would need to bind to either of the mitochondrial membranes to gain access to potential substrates. We asked whether we could observe a specific interaction of Tgl2 with vesicles of one of the mitochondrial membranes. To ascertain this, we performed a sucrose gradient centrifugation with mitochondrial vesicles containing HA-Tgl2 (Fig. 2A). The fractions of the gradient with increasing density were analysed by Western blotting. Tgl2 was found in vesicles of higher density that also contained the *bona fide* MIM protein Cox2 and was almost completely absent in lighter fractions marked by the presence of the MOM protein Tom20 (Fig. 2B and C). These observations suggest that the vast majority of Tgl2 tends to associate with the MIM.

Tgl2 is a component of a higher molecular weight complex

We previously identified *TGL2* in a synthetic genetic array as a negative interactor of *MCP2* - encoding the kinase Mcp2, an IMS facing protein involved in mitochondrial lipid and coenzyme Q homeostasis (15, 18, 19). Although we tried several different experimental approaches, we could not observe any physical interaction between Tgl2 and Mcp2. (data not shown). Furthermore, co-immunoprecipitation experiments with tagged Tgl2 (HA-Tgl2) and subsequent proteomic analysis failed to reveal Mcp2 as a putative interactor. Of note, no other prominent putative interaction partner(s) could be identified through proteomics analysis (data not shown). The proteomics analysis revealed as hits, ribosomal proteins and abundant mitochondrial proteins such as Porin and Om45. The dataset also contained MIM proteins like Mir1, Cox2 and Cyc1.

Even though we could not identify any promising putative interactors, we wanted to know if Tgl2 forms a higher molecular weight complex. To address this, we isolated mitochondria from yeast overexpressing HA-Tgl2, solubilized them with either digitonin or Triton X-100, and subjected them to blue native (BN)-PAGE followed by immunodecoration. We observed that Tgl2 migrates as part of a complex of 500kDa that was more stable upon mild solubilization using digitonin (Fig. 3A). As expected, and to verify that the anti-HA does not display any cross-reactivity, no signal was detected in cells transformed with an empty vector. This approach was also used to analyse the Tgl2-complex in yeast deletion strains of potential physical interactors selected by educated guess. Table S1 provides an overview of the different deletion mutants analysed and the roles of the respective proteins in mitochondrial physiology. We did not observe a reduction in size or loss of the Tgl2-complex in any of these mutants. We also monitored the steady state levels of monomeric and dimeric Tgl2 in the various deletion strains and the dimeric protein was always detected (Fig. S1). Of note, the Tgl2 complex appears as a sharp solitary band unlike known mitochondrial membrane embedded complexes like TOM complex that displays a rather broad band in native gels (Fig. 3A). The precise apparent complex of Tgl2 is supported also by a recent high throughput complexome

study (25). This behaviour further suggests that Tgl2 is indeed a soluble protein of defined quaternary structure without associated membrane lipids.

We next asked if the Tgl2-containing complex contains multiple copies of the protein. To address this, we performed an antibody shift assay with solubilised mitochondria containing one or two differently tagged variants of Tgl2. Prior to the BN-PAGE analysis we incubated the mitochondrial lysate with an antibody against the HA-tag and immunodecorated against the FLAG-tag. We observed a size shift only for the sample containing both tagged Tgl2 variants (Fig. 3B). In contrast, the complex was not shifted when mitochondria containing only FLAG-Tgl2 were used. These observations indicate that the complex contains at least two copies of Tgl2.

The MIM protease Yme1 mediates the quality control of Tgl2

Previous studies regarding quality control of IMS proteins have reported that Yme1 – an iAAA protease of the MIM, is responsible for degrading misfolded or unstable proteins in the IMS (26, 27). Many of these proteins are also substrates of the disulfide relay import pathway. We previously observed that C-terminally modified Tgl2 and Tgl2_{Cys}, whose cysteine residues were mutated to serine, were hardly detectable in WT yeast cells. These protein variants were also unable to rescue the growth defect exhibited by the *mcp2Δ/tgl2Δ* double mutant (15). To test whether non-functional and potentially misfolded Tgl2 variants are substrates of Yme1, we compared the steady state levels of N-terminally tagged Tgl2 (HA-Tgl2), C-terminally tagged Tgl2 (Tgl2-HA), and a variant of Tgl2 wherein all the cysteines are mutated to serine (HA-Tgl2_{cys}) in *tgl2Δ* to those in *yme1Δ* cells. We previously reported that only a functional variant of Tgl2 can rescue the growth phenotype exhibited by *mcp2Δ/tgl2Δ*, and consequently used this as a system to assess the functionality of HA-Tgl2, Tgl2-HA, and HA-Tgl2_{cys}. We performed a drop-dilution assay on non-fermentable (glycerol) carbon sources and could confirm these observations (Fig. 4A and (15)). A stark growth defect was observed for *mcp2Δ/tgl2Δ* on glycerol-containing medium which could only be rescued by introducing HA-Tgl2 but not the other two variants, further confirming that Tgl2-HA and HA-Tgl2_{cys} are non-functional. To compare the steady state levels of these variants, we obtained whole cell lysate, cytosolic, and crude mitochondrial fractions from either *tgl2Δ* or *yme1Δ* expressing these protein variants, and analysed them Western blotting (Fig. 4B). We could detect the native-like HA-Tgl2 in *tgl2Δ* as well as *yme1Δ* cells. However, Tgl2-HA and HA-Tgl2_{cys} were only detected in the fractions from *yme1Δ* cells. These findings confirm the notion that Yme1 is involved in the elimination of non-functional variants of Tgl2. Interestingly, HA-Tgl2_{cys} is unable to form a homodimer, strengthening the hypothesis that the observed dimer is indeed due to disulfide bridges.

Next, we wanted to analyse if non-functional Tgl2 variants form higher molecular weight complexes, and if these complexes behave similar to the native one. We isolated mitochondria from *tgl2* Δ and *yme1* Δ cells expressing the variants of interest, solubilized them with digitonin, and analysed them by native PAGE and immunodecoration (Fig. 4C). We could detect the complex for HA-Tgl2 in mitochondria isolated from either both *tgl2* Δ and *yme1* Δ cells. In contrast, a complex containing Tgl2-HA could be detected only in mitochondria lacking Yme1 (Fig. 4C). Of note, HA-Tgl2_{cys} is unable to form a complex even in the absence of Yme1 indicating that the complex is dependent on the cysteine residues. As a control, the levels of the TOM complex, detected with an antibody against Tom40, are not altered (Fig. 4C). To confirm that the cells expressed the different proteins, a fraction the solubilized mitochondria was also loaded on SDS-PAGE and analysed using the indicated antibodies (Fig. 4D).

Analysis of the contribution of single cysteine residues of Tgl2

The closest structural homologue of Tgl2 is a bacterial lipase – LipA, in the periplasmic space of *P. aeruginosa*. LipA has an intramolecular disulfide bond (between C183 and C235) which is important for the stability of the protein (28, 29). Disruption of this disulfide bridge results in loss of lipolytic function as well as rapid degradation of the protein (28). Since the Tgl2_{cys} variant is highly unstable (Fig. 4B), we wondered if Tgl2 has any specific intramolecular disulfide bonds that are essential for its stability. Using AlphaFold for structural prediction of Tgl2, we found cysteine residues (C31 and C150) that are potentially involved in intramolecular disulfide bridges (Fig. 5 and B, 30, 31). Additionally, we used bioinformatics tools (32–34) to predict the oxidation states of all the cysteine residues and to predict disulfide bridges between them (Fig. 5C). Based on these tools, we selected three cysteine residues – C31, C232, and C256, and replaced them by site-directed mutagenesis with alanine residues, creating HA-Tgl2_{C31A}, HA-Tgl2_{C232A}, and HA-Tgl2_{C256A}, respectively. Next, we transformed them into *tgl2* Δ , *mcp2* Δ /*tgl2* Δ , and *yme1* Δ strains. Surprisingly, we observed that all three mutants could rescue the growth defect of *mcp2* Δ /*tgl2* Δ (Fig. 5D). Thus, it seems that despite their predicted participation in disulfide bridges, these cysteine residues are not essential for the functionality of the protein.

To study the steady-state levels of the three mutants, we isolated crude mitochondrial fractions from *tgl2* Δ and *yme1* Δ yeast and analysed them by Western blotting. We observed that the expression levels and the stability of the cysteine variants were comparable to that of the native protein. Moreover, none of these point mutations had an impact on the homodimerization although C256 and C232 (partially) are exposed on the surface of the protein and could be involved in intermolecular disulfide bridges. (Fig. 5E). Since the Tgl2 complex is cysteine dependent (Fig. 4C), we wanted to analyse if residues C31, C232, and C256 are essential for its formation and/or stability. With that aim, we analysed isolated mitochondria harbouring the cysteine variants of Tgl2 by BN-PAGE (Fig. 5F). We could not observe any difference in

the complex formation or stability between the native protein and the cysteine mutants. Thus, we conclude that these single point mutations by themselves are not sufficient to destabilize either the homodimer or oligomer formed by Tgl2 and therefore have no obvious impact on the functionality of the protein.

The predicted catalytic triad of Tgl2 is required for its functionality

Tgl2 was first categorized as a lipase due to its canonical lipase motif - (G/A)XSXG, of which the serine is the catalytically active residue (Fig. 6A, adapted from (16)). In *in vitro* lipase assays using affinity tag-enriched protein, Ham et al reported that mutating the Serine 144 to Alanine (HA-Tgl2_{S144A}) leads to loss of lipolytic activity of Tgl2 (14). Moreover, prokaryotic and eukaryotic lipases typically contain a catalytic triad consisting of Ser-Asp-His, wherein the serine is often part of the conserved (G/A)XSXG motif. This triad is also analogous to the catalytic centre of serine proteases as well as acyltransferases such as Tgl3 and Lro1 (35–37 and Fig. S3). We used structural data on LipA as well as other bacterial lipases that share homology with Tgl2, to gain more insight into the catalytic triad of Tgl2 (38). *In silico* analysis of the predicted structure of Tgl2 suggest a catalytic triad comprising of Ser144, Asp259, and His281 (Fig. 6B) (30, 31, 38).

We performed site-directed mutagenesis to mutate the catalytically active S144 (14) or D259 to alanine. Next, we tested the ability of the resulting HA-Tgl2_{S144A} and HA-Tgl2_{D259A} constructs to complement the growth phenotype exhibited by *mcp2Δ/tgl2Δ* cells. As expected, we could observe comparable growth behaviours of all the tested strains on fermentable carbon sources. In agreement with the previous reports, HA-Tgl2_{S144A} was unable to complement the growth phenotype exhibited by *mcp2Δ/tgl2Δ* on glycerol-containing medium (Fig. 6C). In addition, HA-Tgl2_{D259A} was also unable to rescue the growth phenotype under these conditions. These findings indicate that the residues S144 and D259 are potentially involved in the catalytic triad of the protein function.

Disruption of the catalytic triad leads to protein instability

HA-Tgl2_{S144A} is a non-functional mutant which can be overexpressed to the same levels as the native protein and could also form the dimeric form of Tgl2 (Fig. 7A). To study the impact of this mutation on the quaternary structure of Tgl2, we solubilized mitochondria isolated from *tgl2Δ* and *yme1Δ* cell harbouring HA-Tgl2 or HA-Tgl2_{S144A} and subjected them to BN-PAGE and immunodecoration with antibodies against the HA-tag and Tom40.

Figure 7B shows that the complex could be detected comparably for both variants. We conclude that while the Ser144 is vital for the catalytic activity of the protein, it has no impact on the stability or structural integrity of the monomeric, dimeric, or oligomeric form of the protein.

To analyse if the catalytically active aspartate is crucial for protein stability, we analysed its steady-state levels in *tgl2Δ* and *yme1Δ* yeast cells. We found that in addition to losing its function, the aspartate mutant is expressed notably less than the native protein in *tgl2Δ* cells yet to the same extent in *yme1Δ* (Fig. 7C). This expression behaviour was similar for the protein complex, as the higher molecular weight complex is detectable only in very little amounts for the mutated protein in *tgl2Δ* cells, but rather similar to the native complex in *yme1Δ* yeast (Fig. 7D). In contrast to the S144A variant, perturbing the catalytic triad in mutating the aspartate residue leads to instability in complex formation in WT-like conditions, suggesting that the aspartate residue is critical for the stability of Tgl2.

These observations are in congruence with previous studies where the catalytically active aspartate residue was shown to be crucial for protein stability in lipases from *G. candidum* as well as human pancreatic lipase and choline esterase. These previous studies have also reported that while mutating the serine residues in the catalytic triad leads to loss of function, it has no impact on protein stability (39).

Genetic interactions of *MCP2*, *TGL2*, and *YME1*

In this study, we assess several different mutants of Tgl2 to gain a better understanding of the protein's structure-function relationship. We use complementation of *mcp2Δ/tgl2Δ* under non-fermentable conditions as a tool to analyse functionality. Of the mutants created in this study, the non-functional variants (HA-Tgl2_{Cys}, Tgl2-HA, HA-Tgl2_{S144A}, and HA-Tgl2_{D259A}) either could not be detected or were detected in very low amounts in *mcp2Δ/tgl2Δ* (Fig. S2). Naturally, this raises the question – are these variants indeed non-functional due to loss of enzymatic capacity or are they unable to complement the growth phenotype simply due to their low expression levels.

Since we could show that Yme1 is responsible for the turnover of Tgl2 (Fig. 4B), we attempted to create the triple mutant strain - *mcp2Δ/tgl2Δ/yme1Δ* to ensure that the mutated Tgl2 variants are not degraded and the growth defect caused by the absence of Mcp2 and Tgl2, can be analysed in the absence of Yme1. Interestingly, the deletion of all three genes always yielded non-viable spores. Figure 8A shows an excerpt from n>100 tetrads dissected.

Of note, we observed that lethality of the triple deletion mutant does not stem from a simple combination of growth defects caused by the three individual genes. All three single deletion mutant cells as well as all combinations of double mutations show no growth defect on glucose containing synthetic medium at normal temperatures. Furthermore, the growth defect of *yme1Δ* cells at elevated temperatures is not worsened by loss of Mcp2 or Tgl2. Finally, on non-fermentable carbon sources where *mcp2Δ/tgl2Δ* cells show the pronounced growth defect, *yme1Δ* cells grow like wild type (Fig. 8B).

Although we so far cannot explain the cause of lethality of the combined deletion of *MCP2*, *TGL2* and *YME1*, we assume that all three proteins share a functional relationship. As expected, when we express functional plasmid borne Tgl2 in heterozygous diploid triple mutant cells prior to tetrad dissection we can retrieve triple deletion cells expressing plasmid borne Tgl2. On the other hand, empty plasmids or plasmids encoding the non-functional Tgl2 variant Ser144A failed to yield triple deletion cells expressing the mutant proteins (data not shown).

Mitochondria lacking Tgl2 have elevated levels of neutral lipids

Previous lipidomics analysis from whole cell extracts, indicated elevated TAG and DAG levels in *mcp2Δ/tgl2Δ* yeast cells (15). Since Tgl2 and Mcp2 are mitochondrial proteins, we wondered if this perturbation is primarily caused by mitochondrial alternations. To that goal, we extracted neutral lipids from isolated mitochondria (WT, *mcp2Δ*, *tgl2Δ*, and *mcp2Δ/tgl2Δ*) and subjected them to thin-layer chromatography (TLC) analysis. We observed a slight increase in TAG levels in organelles from *mcp2Δ/tgl2Δ* (Fig. 9A). To further analyse the lipid composition of the isolated organelles, we trypsinized the mitochondria from WT, *mcp2Δ*, *tgl2Δ*, and *mcp2Δ/tgl2Δ*, to eliminate protein-mediated mitochondrial contact sites, and purified the organelles by a density gradient. The purity of the mitochondria was confirmed by SDS-PAGE and immunodecoration with antibodies against peroxisomal (Pex14), ER (Erv2), and mitochondrial (Tom40 and Hep1) marker proteins. Figure 9B confirms that the mitochondrial fractions are essentially free from ER and/or peroxisome contaminations. Lipidomics analyses of the purified mitochondria revealed elevated TAG and DAG levels in *mcp2Δ/tgl2Δ* (Fig. 9C). Collectively, these results suggest that the combined deletion of TGL2 and MCP2 results in an increase mitochondrial or mitochondria-associated TAGs.

Discussion

The importance of cellular lipid homeostasis is highlighted by its implication for human health (40, 41). Even in simpler model organisms like *S. cerevisiae*, deficiencies in lipid metabolism result in impaired cellular function and, in some cases, severe growth defects (40, 41). There have been significant advancements in the field of lipid metabolism in the last few years wherein the cross talk between mitochondria and other organelles has acquired a crucial role. Reports of protein tethers between the mitochondrial outer membrane (MOM) and membranes of proximal organelles laid the foundation of the concept of ‘contact sites’, which has become a topic of extensive research. The ERMES complex was the first of such mitochondrial tethers to be recognized, and has been now thoroughly elucidated (42–44). ERMES subunits have been shown to bind to and traffic phospholipids between the ER and mitochondria. The loss of these subunits results in severe growth phenotypes and anomalous mitochondrial morphology (45–48).

In a previous study, we characterized a high copy suppressor of ERMES mutants – Mcp2 (now Cqd2) which was more recently suggested to be involved in CoQ metabolism in yeast (19). To better characterize *MCP2/CQD2*, we performed a high throughput screen of *mcp2Δ* and identified *TGL2* as a hit, where the two genes displayed negative genetic interaction, more prominently on non-fermentable carbon sources (15). This growth defect is lost after prolonged growth on fermentable carbon sources – a phenomenon often observed for lipid metabolism defects and ERMES mutants (46, 49, 50). We could also show that both Mcp2 and Tgl2 are located with their functional domains in the IMS. Of the two, Tgl2 is a soluble protein and relies on the disulfide relay pathway for its import into the IMS (15).

In our current study, we further characterized Tgl2 to gain a better understanding of its molecular structure and function. We observed that Tgl2 can form homodimers under non-reducing conditions and suggest that the dimer is a product of intermolecular disulfide bridges between one of the eight cysteine residues of each monomer of the protein. We could also confirm an oligomeric form of the protein containing at least two copies of Tgl2. This complex is also thiol dependent and is susceptible to treatment with stronger detergents. The formation of a structural important disulfide bridge would agree with a more oxidising environment in the IMS, similar to the periplasm of bacteria. Moreover, Tgl2 is not conserved amongst higher eukaryotes and has its closest structural homologues in prokaryotes. These bacterial lipases e.g. LipA from *P. aeruginosa*, were shown to harbour intra- as well as intermolecular disulfide bridges. Furthermore, extracellular lipases of higher eukaryotes like human pancreatic lipase, and lipoprotein lipase also contain disulfide bonds which are often essential for protein function, allowing dimerization that facilitates substrate binding or protein stability (28, 51, 52). Since mutation of all cysteine residues of Tgl2 led to loss of function of the protein we started to mutate three single cysteine residues that according to structure prediction programs are likely to be involved in intra- or intermolecular cysteine bridges. However,

replacing the cysteines 31, 232, or 256 to alanine had no influence on the quaternary structure or function of Tgl2. We cannot exclude the possibility that the function of the cysteine residues is somewhat redundant, and therefore a single replacement can be compensated by the other seven cysteine residues.

The non-functional variants of Tgl2 like Tgl2-HA and Tgl2_{cys}, are nearly undetectable in WT or *tgl2Δ* cells despite their over-expression, indicating a strict quality control mechanism for the protein. A vast majority of the IMS proteins rely on Yme1, an i-AAA protease in the MIM, for their folding and/or degradation (26). Yme1 has an IMS exposed catalytic domain which is suggested to have chaperone-like activity (27). By comparing the steady state levels of native and non-functional variants of Tgl2, we could confirm that its quality control is maintained by Yme1. The undetectable or weakly detectable protein mutants could be observed upon deletion of *YME1*, in amounts similar to those of native Tgl2. We also found a synthetic lethal genetic interaction of *MCP2*, *TGL2*, and *YME1* which suggests a functional relationship beyond the quality control of Tgl2 by Yme1. Further studies are required to understand this observation.

Ham et al. previously characterized the lipase motif of Tgl2. By mutating the conserved serine residue (S144), they could show a loss of *in vitro* lipolytic activity (14). Our observations that despite native-like expression levels, Tgl2_{S144A} is unable to rescue the growth defect of *mcp2Δ/tgl2Δ*, agree with their report. We also characterized the predicted Ser-Asp-His catalytic triad of Tgl2 and showed that disrupting the catalytically active triad by replacing the aspartate by alanine leads to an unstable, poorly expressing variant of the protein (51). Studies pertaining to other lipases and acyltransferases show that while a conservative mutation (aspartate to glutamate) results in only partial loss of function, mutating the aspartate to alanine or valine leads to loss of enzyme activity and stability. Since the carboxylic group is essential for stabilizing interactions with other residues in its vicinity, its loss can lead to protein misfolding and/or instability (37, 39)

The catalytic triad is a feature of several enzymes including proteases, acyltransferases, and lipases (Fig. S3 and (51)). Some members of the Tgl family exhibit lipase as well as acyltransferase activity, therefore Tgl2 could also be involved in transferring fatty acids between substrates rather than hydrolysing TAGs like classical lipases (16, 53).

The lipolytic activity of Tgl2 was shown through *in vitro* lipase assays wherein Tgl2 enriched lysate was used to hydrolyse different TAGs – of which tributyrin was the optimal substrate (14). Of note, tributyrin is not a typical physiological substrate in mitochondria. We performed lipidomics analysis of purified mitochondrial fractions and could detect elevated levels of neutral lipids in fractions isolated from *mcp2Δ/tgl2Δ* yeast cells. This observation aligns with our previous lipidomics analysis from whole cell lysate fractions of the same cells (15). Notably, the neutral lipid content measured in the lipidomics analyses reflected primarily long chain fatty acids, which are the most abundant forms of TAGs and DAGs in yeast cells. In conclusion, our experiments could show that the combined absence of Tgl2 and Mcp2 results in

increased neutral lipid amounts in yeast cells which is mainly caused by an increase in TAGs in mitochondrial fractions. Further experiments are required to clarify whether TAGs indeed occur in between the leaflets of either the MIM or the MOM. We cannot exclude that stronger interaction between LDs and mitochondria, in the absence of Mcp2 and Tgl2, leads to an increased LD co-sedimentation during isolation of mitochondria. The physiological function of Tgl2 in the IMS is currently unclear and further studies are required to confirm whether it behaves as a classical TAG lipase or it evolved to perform a different role. To achieve a comprehensive understanding of Tgl2's function, we tried to identify its physical partners through co-immunoprecipitation experiments followed by mass spectrometry experiments. Despite using different affinity tags and experimental conditions, we were unable to find any proteins of interest in these assays. In a recent mitochondrial complexome study, Tgl2 was shown to have a similar migration behaviour as Ups1 and Ups3, lipid transfer proteins in the IMS (25). To investigate potential Tgl2-Ups1 interactions, we performed BN-PAGE with *ups1Δ* yeast cells expressing HA-Tgl2 but the complex remains unchanged in size and stability (Fig. S1). We applied the same approach to *ups2Δ* and *mdm35Δ*, proteins involved in the lipid transfer complex of the IMS (22, 23), but the complex was still unchanged (Fig. S1).

The closest structural homologue of Tgl2 is a bacterial TAG lipase – LipA, which is located in the periplasm. Given the bacterial ancestry of mitochondria and the similarity of Tgl2 with mostly bacterial lipases, one could speculate that during the course of evolution, the protein was maintained in simpler eukaryotes like yeast but was lost in higher organisms. Taken together, our study sheds new light on the structure-function relationship of the mitochondrial protein Tgl2.

Experimental procedures

Yeast strains and growth conditions

Yeast strains were grown in standard rich medium (YP) or synthetic medium (S) with either glucose, galactose, or glycerol as the carbon source.

Transformation of yeast cells was done using the lithium acetate method. For strains transformed with plasmids, synthetic media with appropriate selection marker(s) were used.

For drop dilution assays, yeast cells were cultured to an OD₆₀₀ of 1.0 and serially diluted in five-fold increments. An aliquot of the serially diluted cultures (5 µL) was spotted onto the corresponding solid medium, and the cells were incubated at 30 or 37°C.

All deletion strains were made using tetrad dissection and confirmed by PCR using primers specific for the genes of interest.

All *S. cerevisiae* strains used in this study are listed in Table 2.

Recombinant DNA techniques

The previously constructed plasmid pGEM-Tgl2 (15) was used as a template for inserting a FLAG tag at the N-terminus of the ORF of Tgl2. The construct pGEM-HATgl2 was created using primers from (15) and this construct served as a template for site-directed mutagenesis reactions. Primer pairs containing the mutation of interest were used to generate a mutated sequence of Tgl2. The PCR products were digested using DpnI and transformed into *E. coli* cells for further screening. After confirmation with sequencing, the mutated constructs were cloned into a yeast expression plasmid.

All primers and plasmids used in this study are listed in Table 1 and 3, respectively.

Isolation of mitochondria

Mitochondria were isolated from yeast cells using a previously published protocol based on differential centrifugation (54). Yeast cultures (2-5 L) were grown at 30°C and harvested at an OD₆₀₀ of 0.8-1.6 by centrifugation (3000 xg, 5 min, RT). The cell pellets were washed, weighed and resuspended in resuspension buffer (100 mM Tris and 10 mM DTT). The cell suspension was incubated at 30°C for 10 min after which the cells were harvested as above. The cell pellets were washed with a spheroplasting buffer (1.2 M Sorbitol and 20 mM Sodium Phosphate, pH 7.2). Next, the cell pellets were resuspended in zymolyase-containing spheroplasting buffer and incubated at 30°C for at least 1 h with constant shaking. The spheroplasts were harvested (1100 xg, 5 min, 2°C), resuspended in Homogenization buffer (0.6 M Sorbitol, 1 mM EDTA, 1 mM PMSF, 0.2% (w/v) fatty-acid free BSA, and 10 mM Tris pH 7.4), and dounced 10-12 times. The lysed spheroplasts were first subjected to a clarifying step (2000 xg, 5 min, 2°C) and then to a high-speed centrifugation step (17,500 xg, 15 min, 2°C). The pellets were washed with the isotonic

SEM buffer (250 mM sucrose, 1 mM EDTA, and 10 mM MOPS/KOH pH 7.2) containing 2 mM PMSF and centrifuged as in the previous step. The pellet obtained after the high-speed spin is the mitochondrial fraction. The pellet was resuspended in SEM buffer, snap-frozen in liquid N₂, and stored at -80°C until further use.

To obtain pure mitochondrial fractions, the mitochondrial pellet obtained after differential centrifugation was subjected to trypsinization (5 µg of trypsin per mg of mitochondrial protein) on ice for 20 min. The reaction was stopped by adding Soybean Trypsin Inhibitor (STI) (10 µg STI per µg of Trypsin) and incubated on ice for 30 min. The trypsinized mitochondria were mixed with 2-3 mL of SEM buffer containing 1 mM PMSF and loaded on a sucrose step gradient (20, 30, 40, 50, and 60% (w/v) sucrose in 10 mM MOPS/KOH pH 7.4, 100 mM KCl, 1 mM EDTA, 1 mM PMSF). The gradients were centrifuged (210,000 xg, 16 h at 4°C) using a swing-out rotor (SW40Ti). The fractions between the 40%-60% phase - the mitochondrial fractions, were collected and diluted with 35 mL SEM buffer containing 2 mM PMSF. A pure mitochondrial pellet was harvested by centrifuging the suspension (17500 xg, 15 min at 4°C). The pellet was resuspended in SEM buffer, snap-frozen, and stored at -80°C until further use.

Alkaline Extraction

Isolated mitochondria (50 µg) were resuspended in 50 µL of 20 mM MOPS/KPH pH 7.5. Next, 50 µL of 0.1 M Sodium carbonate solution of varying pH (11 or 11.5) was added to the samples, which were then incubated on ice for 30 min. The samples were centrifuged (94000 xg, 30 min, 4°C), the pellet was resuspended in sample buffer. The supernatant was subjected to trichloroacetic acid (TCA) precipitation and the resulting pellet was also resuspended in sample buffer. The samples were boiled at 95°C for 10 min and analysed by SDS-PAGE and immunodecoration.

All antibodies used in this study are listed in Table 4.

Isolation of mitochondria by mechanical rupture.

Yeast cultures (100-200mL) were grown at 30°C and harvested at an OD₆₀₀ of 0.8-1.6 by centrifugation (3000 xg, 5 min, RT). The pellet was resuspended in SEM buffer and the cells were disrupted by repeated cycles of vortexing with glass beads at 4°C. The lysed cells were centrifuged (2000 xg, 3 min, 4°C) to remove unbroken cells and the crude mitochondria were pelleted from the supernatant by centrifugation (14000 xg, 12 min 4°C).

Co-Immunoprecipitation

Mitochondria (1 mg) were re-isolated and solubilized in 500 μ L of Tris-buffered saline (TBS) supplemented with protease inhibitor cocktail and 1% (w/v) digitonin. The mitochondria were incubated on an orbital shaker for 30 min at 4°C and the solubilized material was centrifuged (18000 xg, 30 min, 4°C). Magnetic Anti-FLAG beads were incubated with the supernatant on an orbital shaker for 1 h at 4°C. The beads were washed three times with 500 μ L of TBS supplemented with protease inhibitor cocktail, and the bound proteins were eluted using a three-fold excess of FLAG peptide (150 ng/ μ L in TBS).

BN-PAGE

Mitochondria (50 μ g) were solubilized in 50 μ L of SEM buffer supplemented with either Triton X-100 (0.5% (v/v)) or digitonin (1% (w/v)). The solution was incubated for 30 min at 4°C on an orbital shaker and the solubilized fraction was subjected to a clarifying spin (20000 xg, 15 min, 4°C). The supernatant was mixed with the loading dye (5% (w/v) Coomassie blue G, 500 mM 6-amino-N-caproic acid, 100 mM Bis-Tris, pH 7.0) and analysed on a 4-14% acrylamide blue native gel. The gels were blotted onto a PVDF membrane and further analysed by immunodecoration.

Antibody shift assay

Mitochondria (50 μ g) were resuspended in 50 μ L of SEM buffer supplemented with 1% digitonin and incubated on an orbital shaker for 30 min at 4°C. The solubilized mitochondria were subjected to a clarifying spin (20000 xg, 30 min, 4°C) and the supernatant was incubated with 1 μ L of SEM buffer or 0.5 μ L or 1 μ L of anti-HA antibody. The samples were incubated on ice for 30 min and then centrifuged briefly (13000 xg, 10 min, 4°C). The supernatant was mixed with the loading dye as above and analysed by BN-PAGE and immunodecoration.

Extraction and analysis of mitochondrial neutral lipids

Lipid extraction of isolated mitochondria was done according to a published protocol (55).

Briefly, 500 μ g of mitochondria were resuspended in a mixture of chloroform:methanol 1:2 (v/v), vortexed, and incubated on ice for 30 min. Next, 1.25 volumes of chloroform followed by 1.25 volumes of water were added - the samples were vortexed vigorously after each addition. The organic and inorganic phases were separated by centrifuging the samples (1000 xg, 10 min, RT). The lower, organic phase was collected with a Pasteur pipette and the samples were evaporated by SpeedVac. The lipids were resuspended in 30 μ L of chloroform:methanol 1:1 (v/v) and immediately used for TLC.

Neutral lipids were separated by TLC using glass plates of pre-coated 0.25 mm silica gel with fluorescent indicator UV₂₅₄. The silica plates were prepared by washing them with a mixture of chloroform:

methanol 1:1 (v/v) and then allowing them to dry for 15-20 min. The plates were then sprayed with a solution of 2.3% boric acid (w/v) in ethanol and dried in an oven for 15 min at 100°C.

The lipids were spotted gradually (3-5 μ l at a time) until the entire volume was spotted onto the TLC plate. The spots were air dried and then separated by a solvent mixture of chloroform/ethanol/water/trimethylamine (30:35:7:35, v/v/v/v). After the samples have migrated through the whole distance completely, the plate was air dried and the run was repeated to ensure successful separation. The plate was allowed to dry completely and then sprayed with a 0.05% (w/v) primuline solution in 80% (v/v) acetone. The plate was visualised under a UV-lamp.

Sucrose Gradient

A sucrose gradient (0.9/1/1.1/1.2/1.3 M) to separate MIM and MOM vesicles was performed according to a previously published protocol (18). Briefly, Mitochondria (3 mg) were reisolated and resuspended in 10 mL of swelling buffer (20 mM HEPES/KOH pH 7.4, 2 mM EDTA, 2 mM PMSF) and incubated for 1 h at 4°C on an orbital shaker. The sucrose concentration was adjusted to 0.45 M using a High Sucrose buffer (2.3 M Sucrose 20 mM HEPES/KOH pH 7.4, 2mM EDTA, 2 mM PMSF). The suspension was sonicated eight times with 10 second pulses, alternating with a break of 1 min on ice. The sonicated sample was clarified (35000 xg, 30 min, 4°C) and the pellet was resuspended in 15 mL of swelling buffer. The solution was centrifuged (200,000 xg, 2 h, 4°C) to harvest the mitochondrial vesicles. The pellet was resuspended in 400 μ L of low sucrose buffer (0.45 M Sucrose 20 mM HEPES/KOH pH 7.4, 2 mM EDTA, 2 mM PMSF), pipetted up and down several times, and sonicated in a sonifying bath at 4°C for 5 min.

Next, the sample was clarified (35000 xg, 15 min, 4°C) and the pellet was resuspended in 1.5 mL of swelling buffer. The supernatant (350 μ L) was transferred to a new tube and the sucrose concentration was adjusted to 0.85M using the sucrose gradient buffer (2.5 M sucrose, 5 mM MOPS/KOH, 1 mM EDTA, 50 mM KCl). The supernatant was loaded onto a sucrose step gradient assembled using the sucrose gradient buffer and the gradient buffer (5 mM MOPS/KOH, 1 mM EDTA, 50 mM KCl) where each layer has a volume of 625 μ L. The gradient was centrifuged in a SW60 rotor (230000 xg, 16 h, 4°C) such that the lighter MOM vesicles float up while the denser MIM vesicles settle at the bottom. After the centrifugation step, fractions (250 μ L, each) were collected starting from the top of the gradient, resuspended in sampled buffer, and analysed by SDSPAGE and immunoblotting.

Mass spectrometric lipid analysis

Quantitative analysis of lipids was performed by standard nanoelectrospray ionization mass spectrometry (56, 57). Lipids were extracted from 50 µg of yeast mitochondria in the presence of internal standards for the major phospholipid classes and neutral lipids (PC 17:0-14:1, PE 17:0-14:1, PI 17:0-14:1, PS 17:0-14:1, PG 17:0-14:1, 15:0-18:1-d7-PA; Cardiolipin mix I; d5-TG ISTD Mix I; d5-DG ISTD Mix I; d5-DG ISTD Mix II, all from Avanti Polar Lipids). Extraction was performed according to Bligh and Dyer with some optimization for whole yeast cells (52). Lipids were dissolved in 10 mM ammonium acetate in methanol and analyzed in a QTRAP 6500 triple quadrupole mass spectrometer (SCIEX) equipped with a nanoinfusion spray device (TriVersa NanoMate, Advion). Mass spectra were processed by LipidView Software Version 1.2 (SCIEX) for identification and quantification of lipids. Lipid amounts (pmol) were corrected for response differences between internal standards and endogenous lipids.

Data availability

All data contained within the manuscript.

Supporting information

This article contains supporting information.

Author Contributions

VT, TT, and KSD performed experiments and analysed data together with DR. KSD designed the study with advice from DR. VT and KSD wrote the manuscript with advice from TT, MJ, and DR.

Acknowledgements

We thank E. Kracker for technical assistance and F. Beitel and P. A. Campos for their help during their internships. We would also like to thank T. Langer for providing yeast strains and G. Zocher for helping with the structural analysis.

Funding and additional information

This work was supported by the Deutsche Forschungsgemeinschaft (DI 1386/2-2 to KSD).

Conflict of interest

The authors declare that they have no conflict of interest.

References

1. Gray, M. W. (2012) Mitochondrial Evolution. *Cold Spring Harb. Perspect. Biol.* **4**, a011403
2. Margulis, L. (1981) Symbiosis in cell evolution: Life and its environment on the early earth. [online] <https://ntrs.nasa.gov/citations/19820044578> (Accessed February 26, 2024)
3. Enkler, L., Szentgyörgyi, V., Pennauer, M., Prescianotto-Baschong, C., Riezman, I., Wiesyk, A., Avraham, R. E., Spiess, M., Zalckvar, E., Kucharczyk, R., Riezman, H., and Spang, A. (2023) Arf1 coordinates fatty acid metabolism and mitochondrial homeostasis. *Nat. Cell Biol.* **25**, 1157–1172
4. Geltinger, F., Tevini, J., Briza, P., Geiser, A., Bischof, J., Richter, K., Felder, T., and Rinnerthaler, M. (2020) The transfer of specific mitochondrial lipids and proteins to lipid droplets contributes to proteostasis upon stress and aging in the eukaryotic model system *Saccharomyces cerevisiae*. *GeroScience*. **42**, 19–38
5. Hoppins, S., Collins, S. R., Cassidy-Stone, A., Hummel, E., DeVay, R. M., Lackner, L. L., Westermann, B., Schuldiner, M., Weissman, J. S., and Nunnari, J. (2011) A mitochondrial-focused genetic interaction map reveals a scaffold-like complex required for inner membrane organization in mitochondria. *J. Cell Biol.* **195**, 323–340
6. Mesmin, B. (2016) Mitochondrial lipid transport and biosynthesis: A complex balance. *J. Cell Biol.* **214**, 9–11
7. Stephan, T., Brüser, C., Deckers, M., Steyer, A. M., Balzarotti, F., Barbot, M., Behr, T. S., Heim, G., Hübner, W., Ilgen, P., Lange, F., Pacheu-Grau, D., Pape, J. K., Stoldt, S., Huser, T., Hell, S. W., Möbius, W., Rehling, P., Riedel, D., and Jakobs, S. (2020) MICOS assembly controls mitochondrial inner membrane remodeling and crista junction redistribution to mediate cristae formation. *EMBO J.* **39**, e104105
8. Dimmer, K. S., and Rapaport, D. (2017) Mitochondrial contact sites as platforms for phospholipid exchange. *Biochim. Biophys. Acta BBA - Mol. Cell Biol. Lipids.* **1862**, 69–80
9. Tatsuta, T., and Langer, T. (2017) Intramitochondrial phospholipid trafficking. *Biochim. Biophys. Acta BBA - Mol. Cell Biol. Lipids.* **1862**, 81–89
10. Rath, S., Sharma, R., Gupta, R., Ast, T., Chan, C., Durham, T. J., Goodman, R. P., Grabarek, Z., Haas, M. E., Hung, W. H. W., Joshi, P. R., Jourdain, A. A., Kim, S. H., Kotrys, A. V., Lam, S. S., McCoy, J. G., Meisel, J. D., Miranda, M., Panda, A., Patgiri, A., Rogers, R., Sadre, S., Shah, H., Skinner, O. S., To, T.-L., Walker, M. A., Wang, H., Ward, P. S., Wengrod, J., Yuan, C.-C., Calvo, S. E., and Mootha, V. K. (2021) MitoCarta3.0: an updated mitochondrial proteome now with sub-organelle localization and pathway annotations. *Nucleic Acids Res.* **49**, D1541–D1547
11. Vögtle, F.-N., Burkhart, J. M., Rao, S., Gerbeth, C., Hinrichs, J., Martinou, J.-C., Chacinska, A., Sickmann, A., Zahedi, R. P., and Meisinger, C. (2012) Intermembrane Space Proteome of Yeast Mitochondria*. *Mol. Cell. Proteomics.* **11**, 1840–1852
12. Edwards, R., Gerlich, S., and Tokatlidis, K. (2020) The biogenesis of mitochondrial intermembrane space proteins. *Biol. Chem.* **401**, 737–747
13. Herrmann, J. M., and Hell, K. (2005) Chopped, trapped or tacked – protein translocation into the IMS of mitochondria. *Trends Biochem. Sci.* **30**, 205–212
14. Ham, H. J., Rho, H. J., Shin, S. K., and Yoon, H.-J. (2010) The TGL2 Gene of *Saccharomyces cerevisiae* Encodes an Active Acylglycerol Lipase Located in the Mitochondria. *J. Biol. Chem.* **285**, 3005–3013
15. Odendall, F., Backes, S., Tatsuta, T., Weill, U., Schuldiner, M., Langer, T., Herrmann, J. M., Rapaport, D., and Dimmer, K. S. (2019) The mitochondrial intermembrane space-facing proteins Mcp2 and Tgl2 are involved in yeast lipid metabolism. *Mol. Biol. Cell.* **30**, 2681–2694
16. Grillitsch, K., and Daum, G. (2011) Triacylglycerol lipases of the yeast. *Front. Biol.* **6**, 219–230
17. Van Heusden, G. P. H., Nebohâcová, M., Overbeeke, T. L. A., and Steensma, H. Y. (1998) The *Saccharomyces cerevisiae* TGL2 gene encodes a protein with lipolytic activity and can complement an *Escherichia coli* diacylglycerol kinase disruptant. *Yeast.* **14**, 225–232

18. Tan, T., Özbalci, C., Brügger, B., Rapaport, D., and Dimmer, K. S. (2013) Mcp1 and Mcp2, two novel proteins involved in mitochondrial lipid homeostasis. *J. Cell Sci.* 10.1242/jcs.121244
19. Kemmerer, Z. A., Robinson, K. P., Schmitz, J. M., Manicki, M., Paulson, B. R., Jochem, A., Hutchins, P. D., Coon, J. J., and Pagliarini, D. J. (2021) UbiB proteins regulate cellular CoQ distribution in *Saccharomyces cerevisiae*. *Nat. Commun.* **12**, 4769
20. Horvath, S. E., Böttinger, L., Vögtle, F.-N., Wiedemann, N., Meisinger, C., Becker, T., and Daum, G. (2012) Processing and Topology of the Yeast Mitochondrial Phosphatidylserine Decarboxylase 1. *J. Biol. Chem.* **287**, 36744–36755
21. Miyata, N., Watanabe, Y., Tamura, Y., Endo, T., and Kuge, O. (2016) Phosphatidylserine transport by Ups2-Mdm35 in respiration-active mitochondria. *J. Cell Biol.* **214**, 77–88
22. Potting, C., Wilmes, C., Engmann, T., Osman, C., and Langer, T. (2010) Regulation of mitochondrial phospholipids by Ups1/PRELI-like proteins depends on proteolysis and Mdm35. *EMBO J.* **29**, 2888–2898
23. Tamura, Y., Endo, T., Iijima, M., and Sesaki, H. (2009) Ups1p and Ups2p antagonistically regulate cardiolipin metabolism in mitochondria. *J. Cell Biol.* **185**, 1029–1045
24. Hu, J., Dong, L., and Outten, C. E. (2008) The Redox Environment in the Mitochondrial Intermembrane Space Is Maintained Separately from the Cytosol and Matrix*. *J. Biol. Chem.* **283**, 29126–29134
25. Schulte, U., Den Brave, F., Haupt, A., Gupta, A., Song, J., Müller, C. S., Engelke, J., Mishra, S., Mårtensson, C., Ellenrieder, L., Priesnitz, C., Straub, S. P., Doan, K. N., Kulawiak, B., Bildl, W., Rampelt, H., Wiedemann, N., Pfanner, N., Fakler, B., and Becker, T. (2023) Mitochondrial complexome reveals quality-control pathways of protein import. *Nature.* **614**, 153–159
26. Schreiner, B., Westerburg, H., Forné, I., Imhof, A., Neupert, W., and Mokranjac, D. (2012) Role of the AAA protease Yme1 in folding of proteins in the intermembrane space of mitochondria. *Mol. Biol. Cell.* **23**, 4335–4346
27. Leonhard, K., Stiegler, A., Neupert, W., and Langer, T. (1999) Chaperone-like activity of the AAA domain of the yeast Yme1 AAA protease. *Nature.* **398**, 348–351
28. Liebeton, K., Zacharias, A., and Jaeger, K.-E. (2001) Disulfide Bond in *Pseudomonas aeruginosa* Lipase Stabilizes the Structure but Is Not Required for Interaction with Its Foldase. *J. Bacteriol.* **183**, 597
29. Papadopoulos, A., Busch, M., Reiners, J., Hachani, E., Baeumers, M., Berger, J., Schmitt, L., Jaeger, K.-E., Kovacic, F., Smits, S. H. J., and Kedrov, A. (2022) The periplasmic chaperone Skp prevents misfolding of the secretory lipase A from *Pseudomonas aeruginosa*. *Front. Mol. Biosci.* [online] <https://www.frontiersin.org/articles/10.3389/fmolb.2022.1026724> (Accessed February 20, 2024)
30. Jumper, J., Evans, R., Pritzel, A., Green, T., Figurnov, M., Ronneberger, O., Tunyasuvunakool, K., Bates, R., Žídek, A., Potapenko, A., Bridgland, A., Meyer, C., Kohl, S. A. A., Ballard, A. J., Cowie, A., Romera-Paredes, B., Nikolov, S., Jain, R., Adler, J., Back, T., Petersen, S., Reiman, D., Clancy, E., Zielinski, M., Steinegger, M., Pacholska, M., Berghammer, T., Bodenstein, S., Silver, D., Vinyals, O., Senior, A. W., Kavukcuoglu, K., Kohli, P., and Hassabis, D. (2021) Highly accurate protein structure prediction with AlphaFold. *Nature.* **596**, 583–589
31. Varadi, M., Anyango, S., Deshpande, M., Nair, S., Natassia, C., Yordanova, G., Yuan, D., Stroe, O., Wood, G., Laydon, A., Žídek, A., Green, T., Tunyasuvunakool, K., Petersen, S., Jumper, J., Clancy, E., Green, R., Vora, A., Lutfi, M., Figurnov, M., Cowie, A., Hobbs, N., Kohli, P., Kleywegt, G., Birney, E., Hassabis, D., and Velankar, S. (2022) AlphaFold Protein Structure Database: massively expanding the structural coverage of protein-sequence space with high-accuracy models. *Nucleic Acids Res.* **50**, D439–D444
32. Cheng, J., Saigo, H., and Baldi, P. (2006) Large-scale prediction of disulphide bridges using kernel methods, two-dimensional recursive neural networks, and weighted graph matching. *Proteins Struct. Funct. Bioinforma.* **62**, 617–629

33. Ferrè, F., and Clote, P. (2005) DiANNA: a web server for disulfide connectivity prediction. *Nucleic Acids Res.* **33**, W230–W232
34. Ferrè, F., and Clote, P. (2005) Disulfide connectivity prediction using secondary structure information and diresidue frequencies. *Bioinformatics.* **21**, 2336–2346
35. Athenstaedt, K., and Daum, G. (2003) YMR313c/TGL3 Encodes a Novel Triacylglycerol Lipase Located in Lipid Particles of *Saccharomyces cerevisiae**. *J. Biol. Chem.* **278**, 23317–23323
36. Choudhary, V., Jacquier, N., and Schneider, R. (2011) The topology of the triacylglycerol synthesizing enzyme Lro1 indicates that neutral lipids can be produced within the luminal compartment of the endoplasmic reticulum. *Commun. Integr. Biol.* **4**, 781–784
37. Jaeger, K.-E., Ransac, S., Dijkstra, B. W., Colson, C., van Heuvel, M., and Misset, O. (1994) Bacterial lipases☆. *FEMS Microbiol. Rev.* **15**, 29–63
38. Noble, M. E., Cleasby, A., Johnson, L. N., Egmond, M. R., and Frenken, L. G. (1993) The crystal structure of triacylglycerol lipase from *Pseudomonas glumae* reveals a partially redundant catalytic aspartate. *FEBS Lett.* **331**, 123–128
39. Østerlund, T., Contreras, J. A., and Holm, C. (1997) Identification of essential aspartic acid and histidine residues of hormone-sensitive lipase: apparent residues of the catalytic triad. *FEBS Lett.* **403**, 259–262
40. Vendruscolo, M. (2022) Lipid Homeostasis and Its Links With Protein Misfolding Diseases. *Front. Mol. Neurosci.* 10.3389/fnmol.2022.829291
41. Yoon, H., Shaw, J. L., Haigis, M. C., and Greka, A. (2021) Lipid metabolism in sickness and in health: Emerging regulators of lipotoxicity. *Mol. Cell.* **81**, 3708–3730
42. AhYoung, A. P., Jiang, J., Zhang, J., Khoi Dang, X., Loo, J. A., Zhou, Z. H., and Egea, P. F. (2015) Conserved SMP domains of the ERMES complex bind phospholipids and mediate tether assembly. *Proc. Natl. Acad. Sci.* 10.1073/pnas.1422363112
43. Kornmann, B., and Walter, P. (2010) ERMES-mediated ER-mitochondria contacts: molecular hubs for the regulation of mitochondrial biology. *J. Cell Sci.* **123**, 1389–1393
44. Kawano, S., Tamura, Y., Kojima, R., Bala, S., Asai, E., Michel, A. H., Kornmann, B., Riezman, I., Riezman, H., Sakae, Y., Okamoto, Y., and Endo, T. (2018) Structure–function insights into direct lipid transfer between membranes by Mmm1-Mdm12 of ERMES. *J. Cell Biol.* **217**, 959–974
45. Youngman, M. J., Hobbs, A. E. A., Burgess, S. M., Srinivasan, M., and Jensen, R. E. (2004) Mmm2p, a mitochondrial outer membrane protein required for yeast mitochondrial shape and maintenance of mtDNA nucleoids. *J. Cell Biol.* **164**, 677–688
46. Burgess, S. M., Delannoy, M., and Jensen, R. E. (1994) MMM1 encodes a mitochondrial outer membrane protein essential for establishing and maintaining the structure of yeast mitochondria. *J. Cell Biol.* **126**, 1375–1391
47. Dimmer, K. S., Fritz, S., Fuchs, F., Messerschmitt, M., Weinbach, N., Neupert, W., and Westermann, B. (2002) Genetic Basis of Mitochondrial Function and Morphology in *Saccharomyces cerevisiae*. *Mol. Biol. Cell.* **13**, 847–853
48. Kornmann, B., Currie, E., Collins, S. R., Schuldiner, M., Nunnari, J., Weissman, J. S., and Walter, P. (2009) An ER-Mitochondria Tethering Complex Revealed by a Synthetic Biology Screen. *Science.* **325**, 477–481
49. John Peter, A. T., Herrmann, B., Antunes, D., Rapaport, D., Dimmer, K. S., and Kornmann, B. (2017) Vps13-Mcp1 interact at vacuole–mitochondria interfaces and bypass ER–mitochondria contact sites. *J. Cell Biol.* **216**, 3219–3229
50. Sogo, L. F., and Yaffe, M. P. (1994) Regulation of mitochondrial morphology and inheritance by Mdm10p, a protein of the mitochondrial outer membrane. *J. Cell Biol.* **126**, 1361–1373
51. Brady, L., Brzozowski, A. M., Derewendat, Z. S., Dodson, E., Dodson, G., Tolley, S., Turkenburg, J. P., Christiansent, L., Hüge-Jensent, B., Nørskovt, L., Thimt, L., and Menge, U. (1990) A serine protease triad forms the catalytic centre of a triacylglycerol lipase
52. Gunn, K. H., and Neher, S. B. (2023) Structure of dimeric lipoprotein lipase reveals a pore adjacent to the active site. *Nat. Commun.* **14**, 2569

53. Klug, L., and Daum, G. (2014) Yeast lipid metabolism at a glance. *FEMS Yeast Res.* **14**, 369–388
54. Daum, G., Böhni, P. C., and Schatz, G. (1982) Import of proteins into mitochondria. Cytochrome b2 and cytochrome c peroxidase are located in the intermembrane space of yeast mitochondria. *J. Biol. Chem.* **257**, 13028–13033
55. Bligh, E. G., and Dyer, W. J. (1959) A rapid method of total lipid extraction and purification. *Can. J. Biochem. Physiol.* **37**, 911–917
56. Tatsuta, T. (2017) Quantitative Analysis of Glycerophospholipids in Mitochondria by Mass Spectrometry. *Methods Mol. Biol. Clifton NJ.* **1567**, 79–103
57. Özbalci, C., Sachsenheimer, T., and Brügger, B. (2013) Quantitative Analysis of Cellular Lipids by Nano-Electrospray Ionization Mass Spectrometry. *Methods Mol. Biol. Clifton NJ.* **1033**, 3–20

Figure Legends

Fig. 1 Tgl2 forms a homodimer that is sensitive to reducing agents.

(A) Tgl2 forms a higher molecular weight adduct under non-reducing conditions. Cells lacking *TGL2* (*tgl2Δ*) were transformed with a plasmid encoding HA-Tgl2 and grown to mid-logarithmic phase. Mechanical lysis was used to isolate whole cell (W), cytosolic (C), and mitochondrial (M) fractions. The samples were mixed with sample buffer with or without β -mercaptoethanol (β -ME) and analysed by SDS-PAGE and immunodecoration with antibodies against the HA-tag, as well as Tom20 (mitochondrial marker) and BmhI (cytosolic marker). The higher molecular weight adduct is marked by an arrowhead. (B) The higher molecular weight adduct is more pronounced upon shorter isolation protocols. Cells expressing HA-Tgl2 were grown to mid-logarithmic phase and mitochondrial fractions were isolated afterwards either mechanical lysis (1) or spheroplasting (2). The samples were analysed by non-reducing SDS-PAGE and immunodecoration. Quantification of the adduct was done with Tom20 as a loading control and the total Tgl2 amounts were taken as 100%. The graph represents the mean values \pm SD of four independent experiments. (C) The adduct is a homodimer of Tgl2. Mitochondria were isolated from *tgl2Δ* cells expressing either HA-Tgl2 or co-expressing HA-Tgl2 and FLAG-Tgl2. The organelles were solubilized and subjected to co-immunoprecipitation with anti-FLAG beads. Samples from input (I), unbound (U, 5%), wash (W, 5%) and eluate fractions (E, 50%) were analyzed by SDS-PAGE and immunodecoration with antibodies against the FLAG-tag. (D) Tgl2 dimer is soluble. Mitochondria containing HA-Tgl2 were subjected to alkaline extraction at different pH values. The supernatant (S) and pellet (P) fractions were analysed by SDS-PAGE and immunodecoration with the indicated antibodies. Tom20 (membrane integrated protein), Hep1 (soluble matrix protein), Mcr1 (a protein with two isoforms, long 34 kDa form embedded in the MOM and shorter soluble form in the IMS).

Fig. 2 Tgl2 associates with the mitochondrial inner membrane.

(A) The majority of Tgl2 is found in mitochondrial vesicles. Mitochondrial vesicles were obtained after swelling and sonication of mitochondria from cells containing HA-Tgl2. The indicated control fractions were collected after swelling, vesicle generation, and clarifying spins. The sample was sonicated to form vesicles followed by clarifying spin to yield supernatant – SV and pellet – PV fractions. The vesicles in PV was sonicated again and subjected to a slower clarifying spin resulting in SG (supernatant) and PG (pellet). Fraction SG was further subjected to a sucrose gradient to separate the MOM and MIM vesicles. The fractions were analysed by SDS-PAGE and immunodecoration. (B) Tgl2 associates with MIM vesicles. The mitochondrial vesicles from S4 fraction (depicted in panel A) were separated by sucrose density

centrifugation. Fractions were collected and analysed by SDS-PAGE and immunodecorated with the indicated antibodies, Cox2 (MIM protein) and Tom20 (MOM protein). (C) Tgl2 and Cox2 containing fractions coincide. Intensities corresponding to Tgl2, Cox2, and Tom20 were quantified and normalized to the total content of each protein.

Fig. 3 Tgl2 is a component of a higher molecular weight complex

(A) Tgl2 forms a higher molecular weight complex. Mitochondria containing HA-Tgl2 were solubilized with either digitonin or TritonX-100 (Tx-100) and subjected to BN-PAGE (4-14%) and immunodecoration with antibodies against either HA-tag or Tom40, as a loading control. (B) Tgl2 complex contains at least 2 copies of the protein. Mitochondria containing either only HA-Tgl2 or HA-Tgl2 and FLAG-Tgl2 were solubilized with digitonin. The lysate was incubated with 0, 0.5, or 1 μ L anti-HA antibody (α -HA) and analysed by BN-PAGE (4-14%) and immunodecoration with anti-FLAG antibody.

Fig. 4 The MIM protease Yme1 mediates the quality control of Tgl2

(A) C-terminally tagged Tgl2 and Tgl2 variant with all its cysteines mutated to serine do not rescue the growth defect of *mcp2 Δ /tgl2 Δ* . WT or *mcp2 Δ /tgl2 Δ* cells were transformed with an empty vector (\emptyset) or a plasmid encoding the indicated variants were grown to logarithmic phase, and dropped on SG-Leu plates in a 1:5 dilution series. Plates were incubated at 30°C and imaged after 5 days. (B) WT or *yme1 Δ* cells encoding the indicated Tgl2 variants were grown to mid-logarithmic phase and whole cell (W), cytosolic (C), or mitochondrial (M) fractions were isolated by mechanical lysis. The samples were analysed by SDS-PAGE and immunodecoration with antibodies against HA and Tom20 as a loading control. (C) Mitochondria isolated from either WT or *yme1 Δ* cells expressing the indicated Tgl2 variants were solubilized with digitonin and analysed by BN-PAGE (4-14%) and immunodecoration with antibodies against HA or Tom40, as a loading control. (D) Aliquots (5%) of the solubilized mitochondria described in (C) were taken after the clarifying spin and analysed by SDS-PAGE and immunodecoration against HA and Tom20, as a loading control.

Fig. 5 Analysis of the contribution of single cysteine residues of Tgl2

(A) Tgl2 has 8 cysteine residues that can potentially form intra or intermolecular disulfide bridges. Predicted structure of Tgl2 with the cysteine residues highlighted in red (functional group buried) or yellow (functional group exposed). (B) Schematic representation of the cysteine residues of Tgl2 marked with blue

arrows and the canonical lipase motif marked in green (Created with Biorender). (C) Prediction of putative disulfide bonds within Tgl2 using DiANNA and DIPro. The cysteine pairs are in decreasing order of probability of disulfide bond formation. (D) WT or *mcp2Δ/tgl2Δ* cells were transformed with an empty vector (\emptyset) or a plasmid encoding the indicated variants were grown to logarithmic phase, and dropped on SD-Leu or SG-Leu plates in a 1:5 dilution series. Plates were incubated at 30°C and imaged after several days. (E) *tgl2Δ* cells expressing the indicated variants of Tgl2 were grown to mid-logarithmic phase and the crude mitochondrial fractions were isolated. The samples were analysed by SDS-PAGE and immunodecoration with the indicated antibodies. (F) Mitochondria from *tgl2Δ* cells expressing the indicated protein variants were solubilized with digitonin and analysed by BN-PAGE (4-14%) and immunodecoration with antibodies against HA or Tom40.

Fig. 6 The predicted catalytic triad of Tgl2 is required for its functionality

(A) Tgl2 belongs to the Tgl family of yeast lipases and has a characteristic lipase motif (green) with a catalytically active serine (yellow arrow). Adapted from (16). (B) The predicted catalytic triad of Tgl2 (Ser-Asp-His). The crystal structure of LipA (left) with the intramolecular disulfide bond highlighted in yellow and the catalytic triad consisting of S82, D229, and H251 highlighted in blue ((29, 30) was employed to predict the structure of Tgl2 (right) with its cysteine residues in yellow and the predicted catalytic triad (S144-D259-H281) in blue. (C) WT or *mcp2Δ/tgl2Δ* cells transformed with the indicated variants were grown to logarithmic phase, and dropped on either SD-Leu or SG-Leu plates in a 1:5 dilution series. Plates were incubated at 30°C and imaged after several days.

Fig. 7 Disruption of the catalytic triad leads to protein instability

(A) and (C) WT and *yme1Δ* cells expressing the indicated Tgl2 variants were grown to mid-logarithmic phase and crude mitochondrial fractions were isolated by mechanical lysis. The samples were analysed by SDS-PAGE and immunodecoration with antibodies against HA and Tom20, as a loading control. (B) and (D) Mitochondria isolated from WT and *yme1Δ* cells expressing the indicated Tgl2 variants were solubilized with digitonin and analysed by BN-PAGE (4-14%) and immunodecoration with antibodies against HA and Tom40.

Fig. 8 Genetic interactions of MCP2, TGL2, and YME1

(A) Excerpt of 11 out of more than 100 dissected tetrads of the heterozygous triple deletion mutant (*mcp2Δ/MCP2 - tgl2Δ/TGL2 - yme1Δ/YME1*). The table below the haploid clones shows the genotype

analysis, *m*: *mcp2Δ*, *t*: *tgl2Δ*, *y*: *yme1Δ*, WT: wild type, (3Δ): triple deletion – not viable. (B) Growth analysis of single and double deletion strains of the three genes. Growth at either 30°C or 37°C was analysed by drop dilution assay of 1:5 serial dilutions on synthetic medium containing either glucose (SD) or glycerol (SG).

Fig. 9 Mitochondrial fractions from *mcp2Δ/tgl2Δ* cells show increased TAG levels.

(A) Neutral lipids were extracted from mitochondria of the indicated cells and analysed by thin-layer chromatography. The lipids were stained with a primuline solution and visualised under UV-light. The migration behaviour of standard neutral lipids is indicated on the left. (B) Mitochondria were isolated from the indicated strains, treated with trypsin and further purified by sucrose gradient. Crude and purified mitochondria (100 µg) were analysed by SDS-PAGE and immunodecoration. Tom40 and Hep1, mitochondrial markers, Pex14, peroxisomal marker, and Erv2, ER marker. (C) Pure mitochondria from (B) were analysed by mass spectrometric analysis. The amounts of TAGs and DAGs versus total PL is shown as a mean with SD bars (n = 3, * p < 0.05, GraphPad T-test calculator).

Tables

Table 1: Primers used in this study

Name	Sequence	Remarks
FLAG-Tgl2-For	GGGGAATTCATGGACTACAAAGACGATGACGACAAG AAAAATGATAATAAAGCTAATGATATAATAATA	Insert FLAG tag at the N terminus of Tgl2
Tgl2S144A-For	CTAATCGCACACGCAATGGGGGGAC	Mutate Ser (TCA) to Alanine (GCA) at position 144
Tgl2S144A-Rev	GTCCCCCATTGCGTGTGCGATTAG	
Tgl2 _{D259A} -For	GGTTGCCCAACGCTGGCCTTGTAACCATA	Mutate Asp (GAT) to Alanine (GCT) at position 259
Tgl2 _{D259A} -Rev	TATGGTTACAAGGCCAGCGTTGGGGCAACC	
Tgl2 _{Cys31Ala} -For	AAAAATCCTATTGTATTTGCCCATGGTTTATCAGGATTT	Mutate Cys(TGC) to Ala(GCC) at position 31
Tgl2 _{Cys31Ala} -Rev	AAATCCTGATAAACCATGGGCAAATACAATAGGATTTTT	
Tgl2 _{Cys232Ala} -For	TCTTATTTTTCGTATGGAGCCTCCTTTGTGCCTAAGTG	Substitution of Cys(TGC) to Ala(GCC) at position 232
Tgl2 _{Cys232Ala} -Rev	CACTTAGGCACAAAGGAGGCTCCATACGAAAAATAAGA	
Tgl2 _{Cys256Ala} -For	AGGTCTAAAGGTGCCCCAACGATGGCCT	Substitution of Cys(TGC) to Ala(GGC) at position 256
Tgl2 _{Cys256Ala} -Rev	AGGCCATCGTTGGGGGCACCTTTAGACCT	

Table 2: *S. cerevisiae* strains used in this study

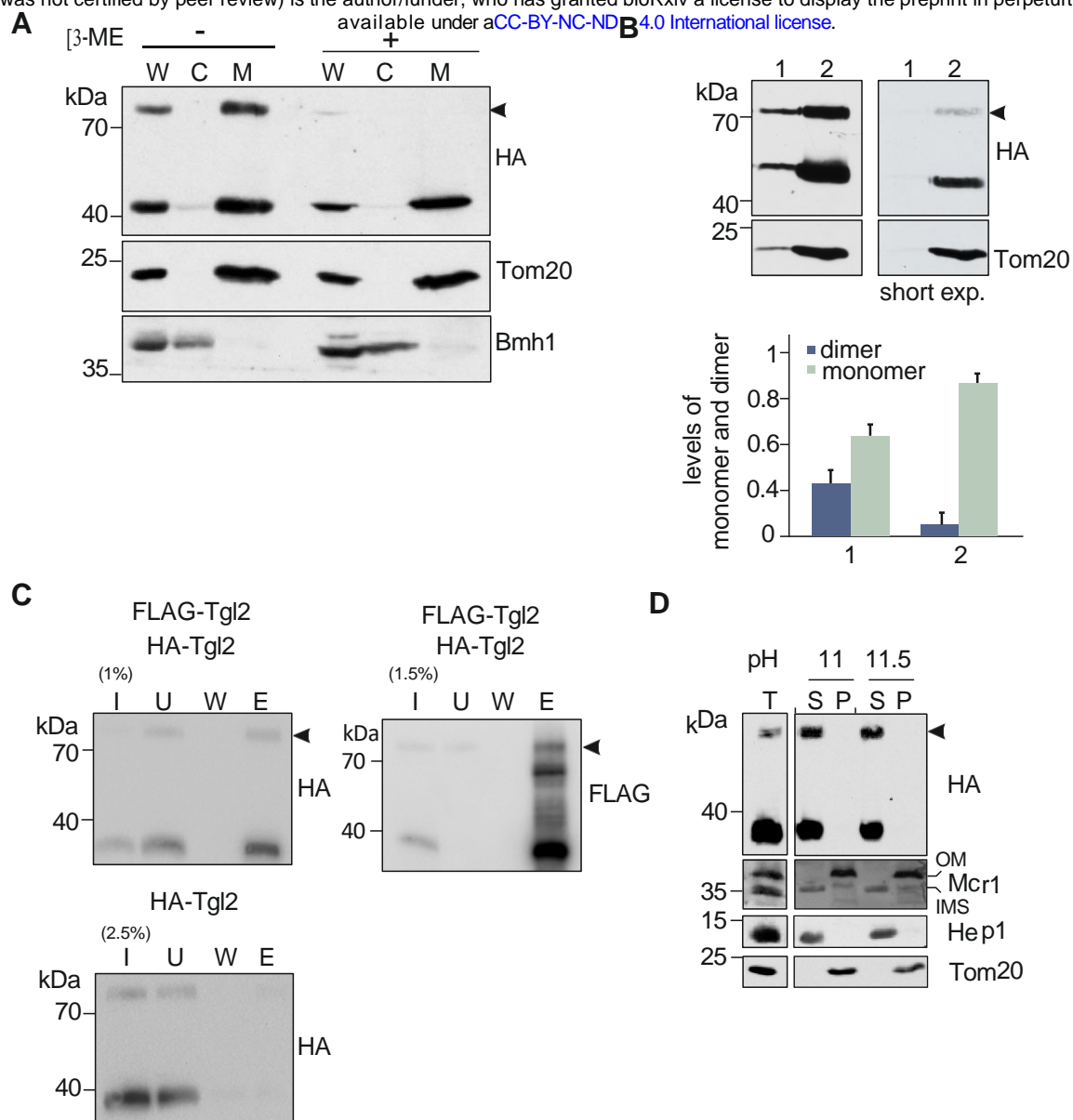
Name	Genotype	Reference
W303a	MAT a; <i>ade2-1</i> ; <i>can1-100</i> ; <i>his3-11</i> ; <i>leu2-3,112</i> ; <i>trp1Δ2</i> ; <i>ura3-52</i>	(Thomas & Rothstein, 1989)
W303α	MAT α; <i>ade2-1</i> ; <i>can1-100</i> ; <i>his3-11</i> ; <i>leu2-3,112</i> ; <i>trp1Δ2</i> ; <i>ura3-52</i>	(Thomas & Rothstein, 1989)
YKD432	W303a; <i>mcp2Δ::HIS3MX6</i>	(Tan et al., 2013)
YKD898	W303a; <i>tgl2Δ::KanMX4</i>	(Odendall et al., 2019)
YKD1009	W303a; <i>mcp2Δ::HIS3MX6</i> ; <i>tgl2Δ::KanMX4</i>	(Odendall et al., 2019)
YKD552	W303a; <i>yme1Δ::KanMX6</i>	Gift from T. Langer
YKD492	W303a; <i>gep4Δ::KanMX4</i>	(Odendall et al., 2019)
YKD472	W303a; <i>psd1Δ::KanMX4</i>	(Odendall et al., 2019)
YTT158	W303a; <i>ups2Δ::Nat</i>	(Potting et al., 2010)
YTT159	W303a; <i>ups1Δ::Nat</i>	(Potting et al., 2010)
YKD806	W303a; <i>mdm35Δ::HIS3MX6</i>	Lab stock
YKD180	W303a; <i>mdm31Δ::KANMX4</i>	(Dimmer et al., 2002)
YKD182	W303a; <i>mdm32Δ::HIS3MX6</i>	(Dimmer et al., 2002)
YKD175	W303a; <i>fzo1Δ::HIS3MX6</i>	Lab stock
BY4741	MATa <i>his3Δ1 leu 2Δ0 met15Δ0 ura3Δ0</i>	Lab stock
YMS306	BY4741; <i>om45Δ::KANMX4</i>	Euroscarf
YKD986	W303a; <i>tgl1Δ::KANMX4</i>	Lab stock
YKD991	W303a; <i>tgl3Δ::KANMX4</i>	Lab stock
YDP038	W303a; <i>fis1Δ::KANMX4</i>	Lab stock
YFO002	W303a; <i>rho⁰</i>	Lab stock
YDA283	BY4741; <i>crd1Δ::HIS3MX6</i>	Euroscarf
YDA107	BY4741; <i>taz1Δ::KANMX4</i>	Euroscarf

Table 3: List of plasmids used in this study

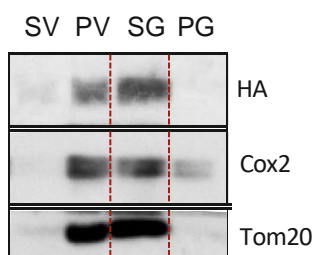
Name	Promoter	Markers	Coding Sequence
pYX142-HA-Tgl2	TPI	LEU2, Amp ^R	Tgl2 with N-terminal HA-Tag
pYX142-Tgl2-HA	TPI	LEU2, Amp ^R	Tgl2 with C-terminal HA-Tag
pYX142-HA-Tgl2 _{Cys}	TPI	LEU2, Amp ^R	Tgl2 with N-terminal HA-Tag, all cysteines mutated to serine
pGEM4-HA-Tgl2	T7	Amp ^R	Tgl2 with N-terminal HA-Tag
pYX122-FLAG-Tgl2	TPI	HIS3, Amp ^R	Tgl2 with N-terminal FLAG-Tag
pYX142-HA-Tgl2 _{S144A}	TPI	LEU2, Amp ^R	Tgl2 with N-terminal HA-Tag, S144A mutation
pYX142-HA-Tgl2 _{C31A}	TPI	LEU2, Amp ^R	Tgl2 with N-terminal HA-Tag, C31A mutation
pYX142-HA-Tgl2 _{C232A}	TPI	LEU2, Amp ^R	Tgl2 with N-terminal HA-Tag, C232A mutation
pYX142-HA-Tgl2 _{C256A}	TPI	LEU2, Amp ^R	Tgl2 with N-terminal HA-Tag, C256A mutation
pYX142-HA-Tgl2 _{D259A}	TPI	LEU2, Amp ^R	Tgl2 with N-terminal HA-Tag, D259A mutation

Table 4: List of antibodies used in this study

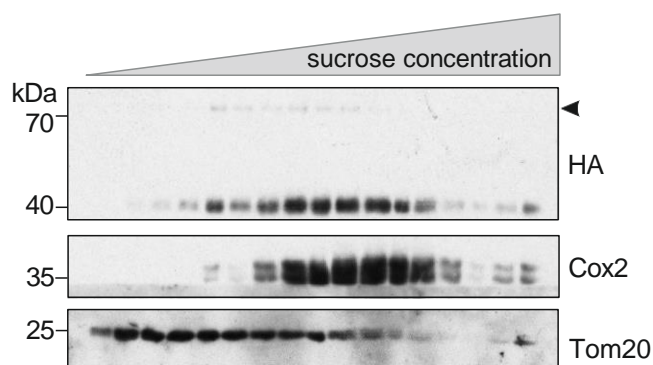
Antibody	Dilution	Source
Polyclonal rat anti-HA	1:1000	Roche
Polyclonal rabbit anti-Erv2	1:1000	Lab of Roland Lill
Polyclonal rabbit anti-Hep1	1:2000	Lab stocks
Polyclonal rabbit anti-Pex14	1:10000	Lab stocks
Polyclonal rabbit anti-Bmh1	1:10,000	Lab stocks
Polyclonal rabbit anti-Tom20	1:4000	Lab stocks
Polyclonal rabbit anti-Tom40	1:4000	Lab stocks
Polyclonal rabbit anti-Tom70	1:2000	Lab stocks
Polyclonal rabbit anti-FLAG	1:2000	ThermoFischer
Horseradish peroxidase coupled goat anti-rabbit	1:10000	1721019 (Bio-rad)
Horseradish peroxidase coupled goat anti-rat	1:5000	ab6845 (Abcam)



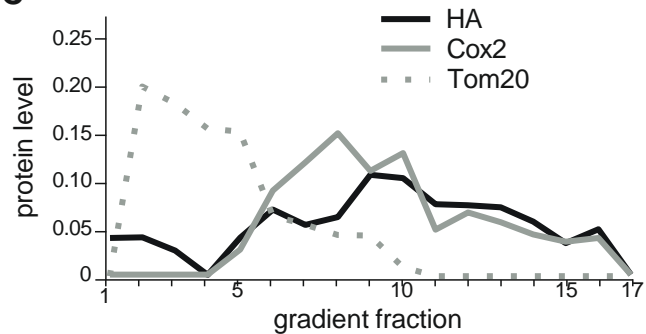
A

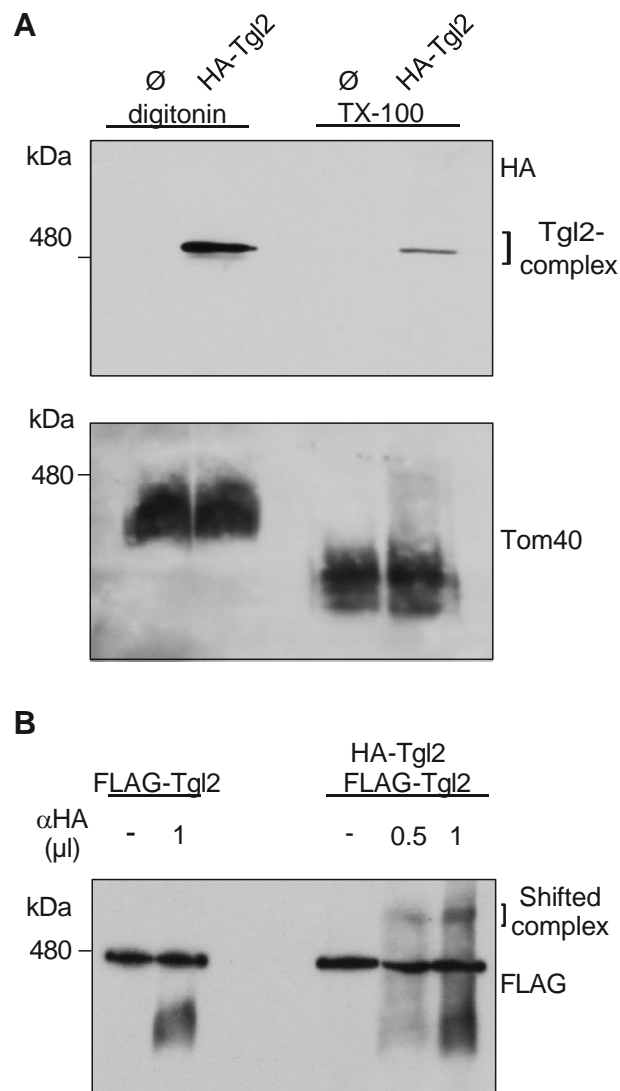


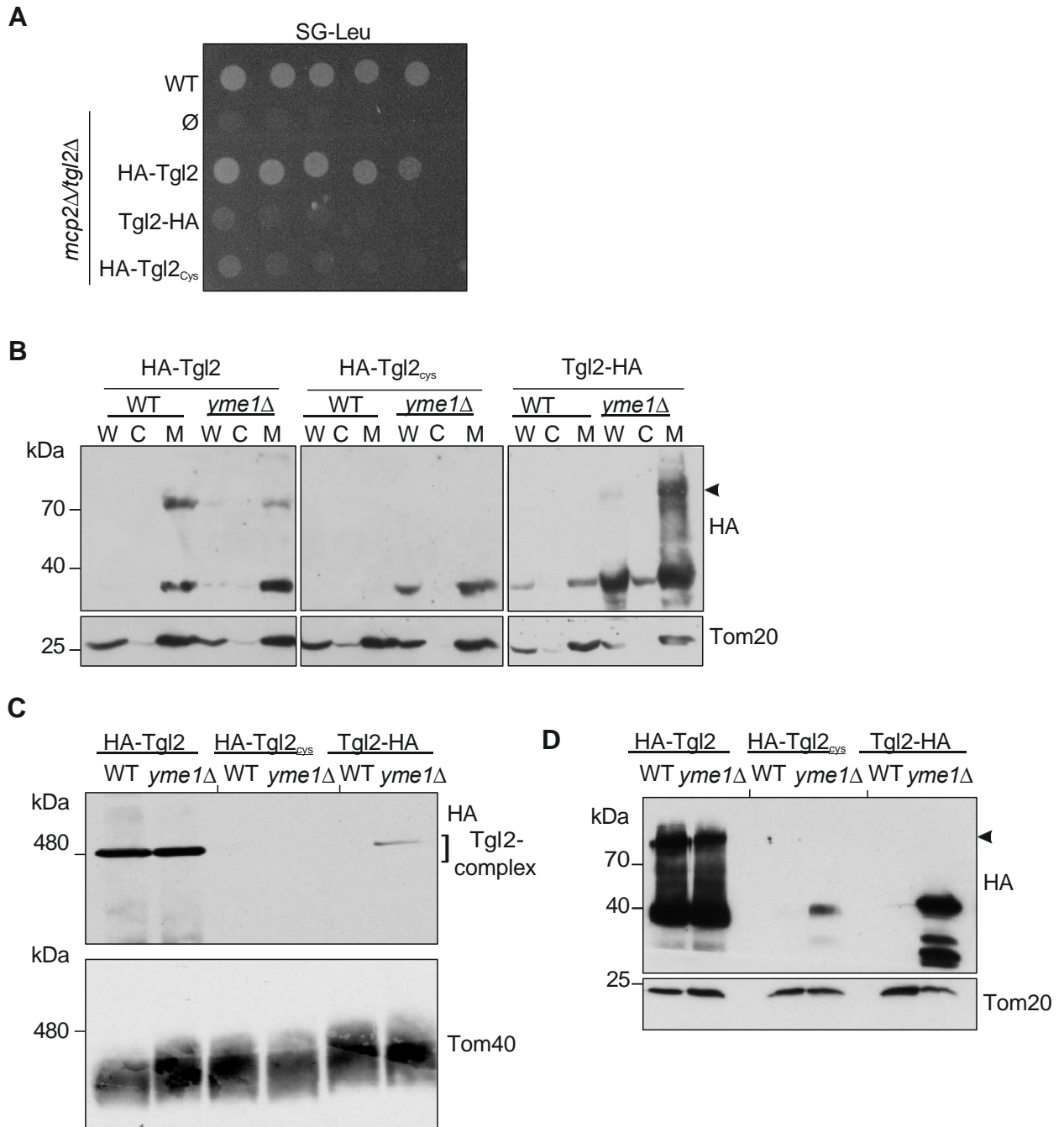
B

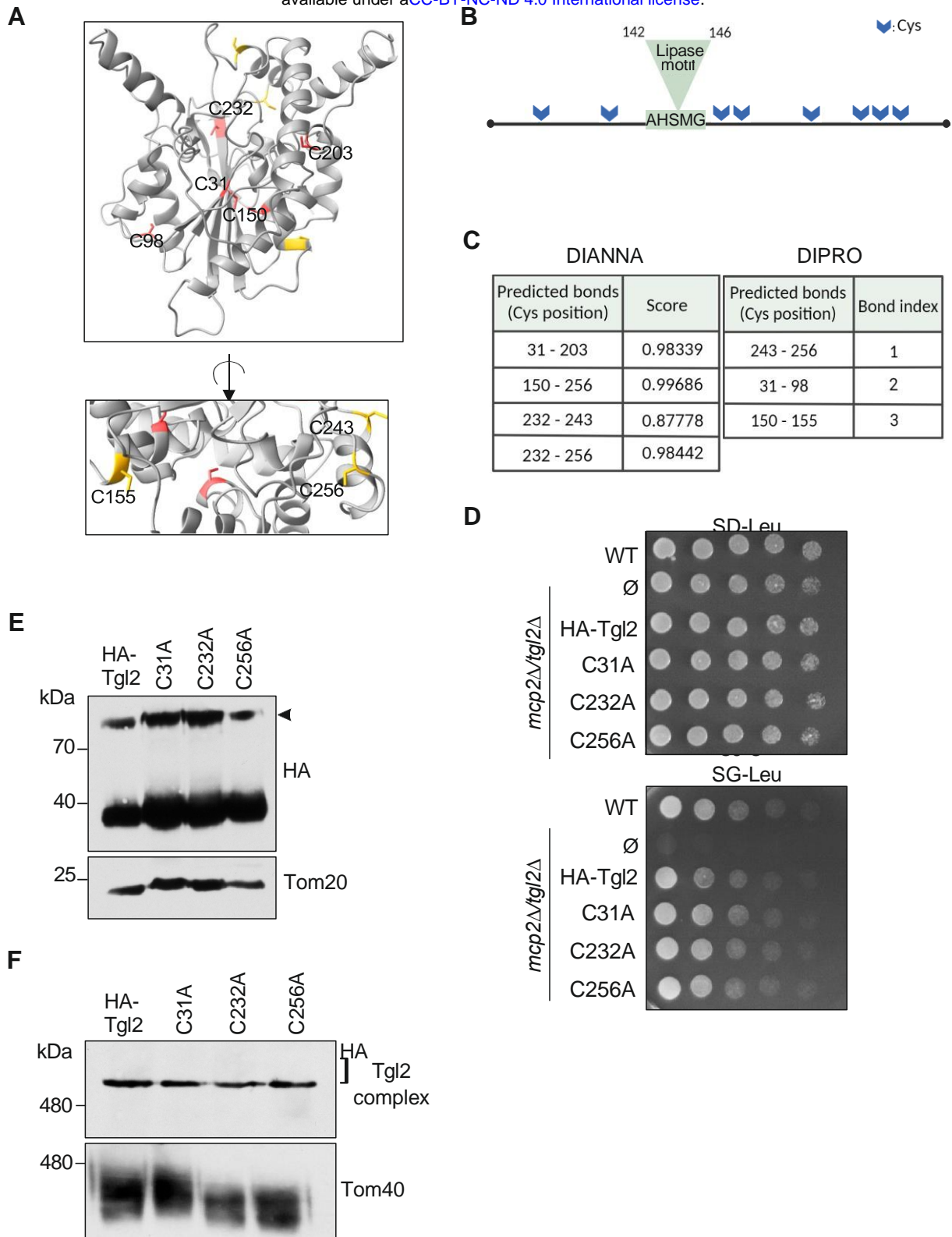


C

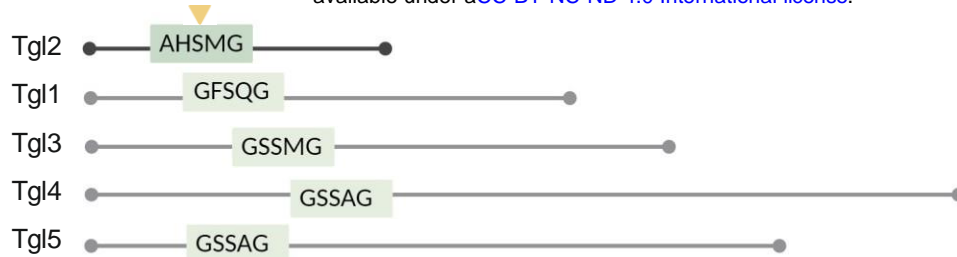




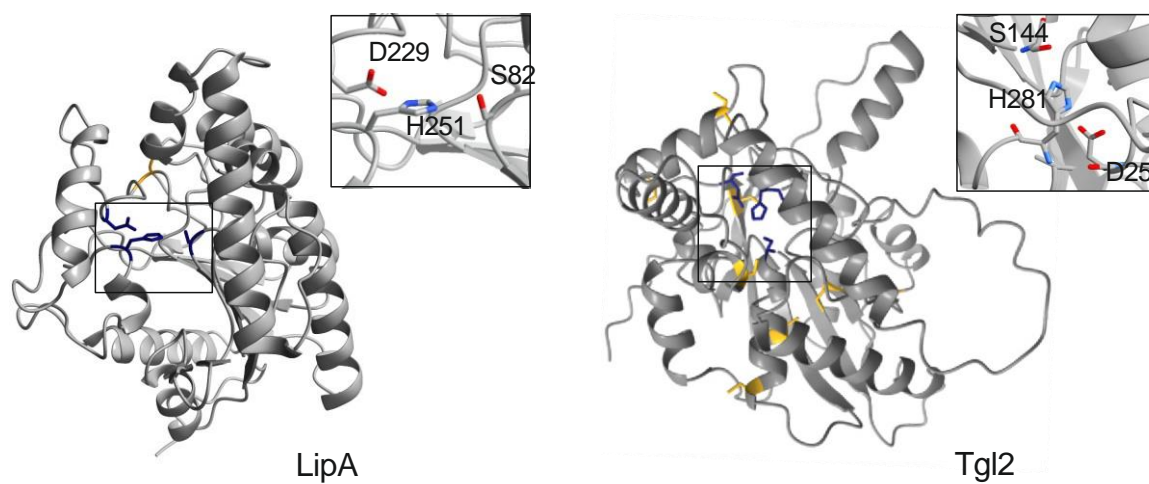




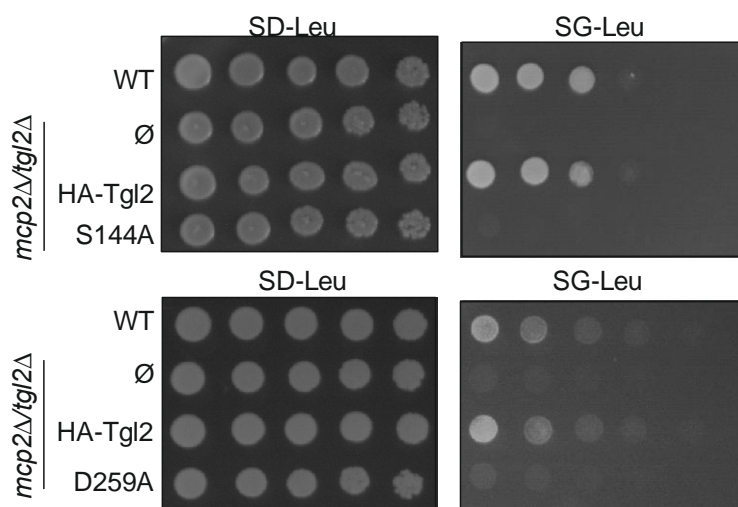
A

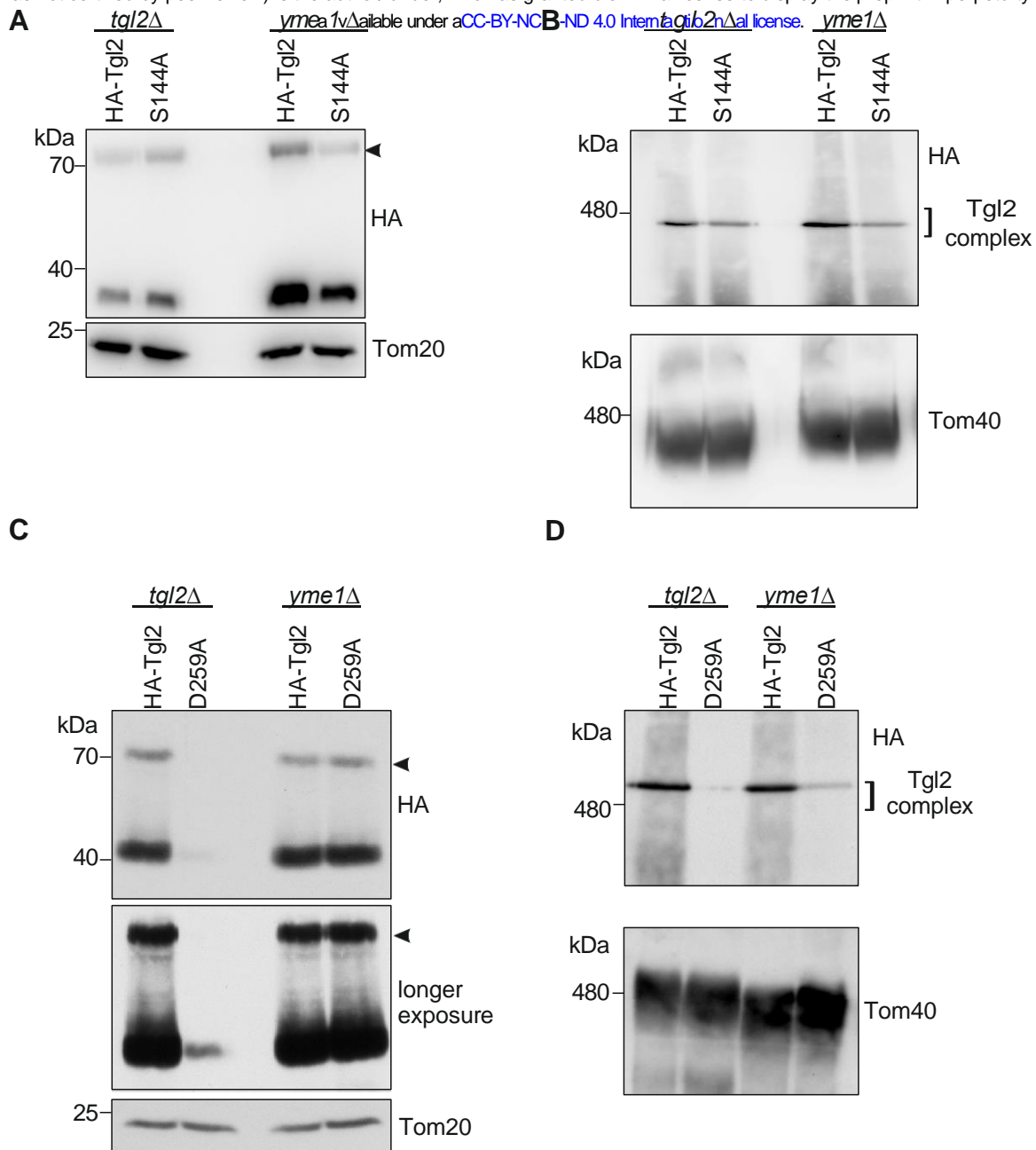


B

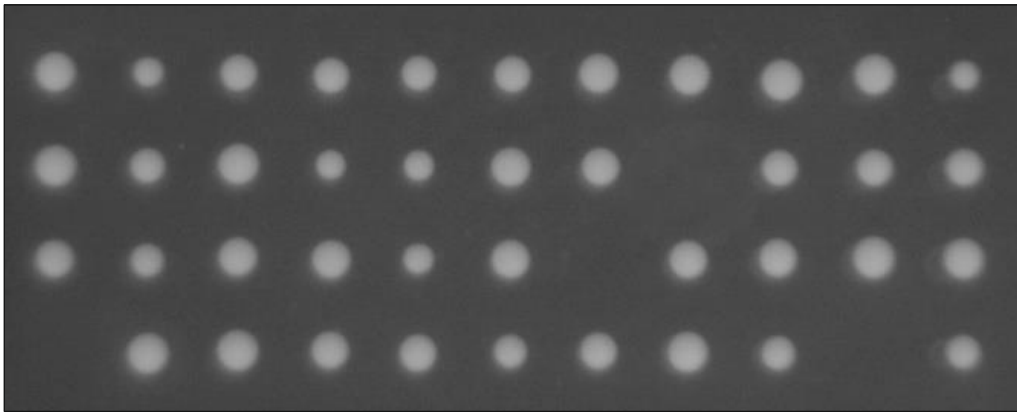


C



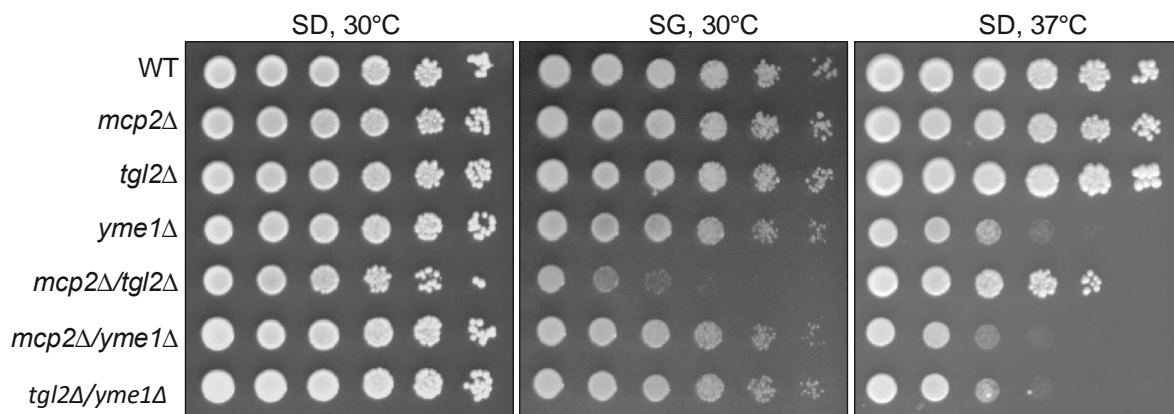


A

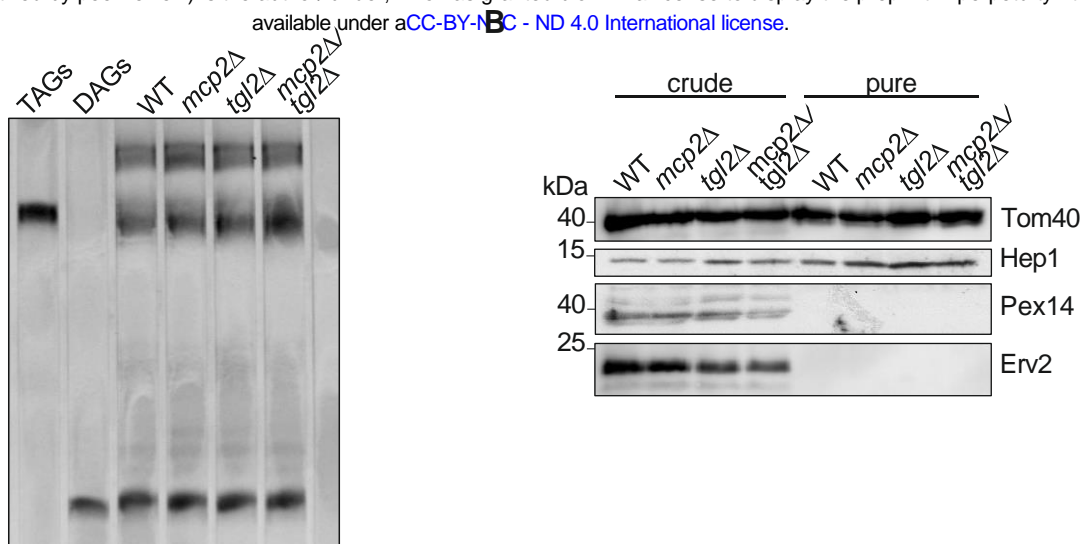


WT	<i>m t</i>	<i>m y</i>	<i>t y</i>	<i>y</i>	<i>t y</i>	<i>t</i>	<i>t</i>	<i>t</i>	<i>t</i>	<i>m t</i>
<i>t</i>	<i>y</i>	<i>t</i>	<i>m t</i>	<i>m t</i>	<i>m</i>	<i>m</i>	(3Δ)	<i>m y</i>	<i>m y</i>	<i>y</i>
<i>m y</i>	<i>m y</i>	<i>t y</i>	<i>m</i>	<i>m t</i>	<i>y</i>	(3Δ)	<i>y</i>	<i>y</i>	WT	<i>t</i>
(3Δ)	<i>t</i>	<i>m</i>	<i>y</i>	<i>y</i>	<i>m t</i>	<i>y</i>	<i>m</i>	<i>m t</i>	(3Δ)	<i>m y</i>

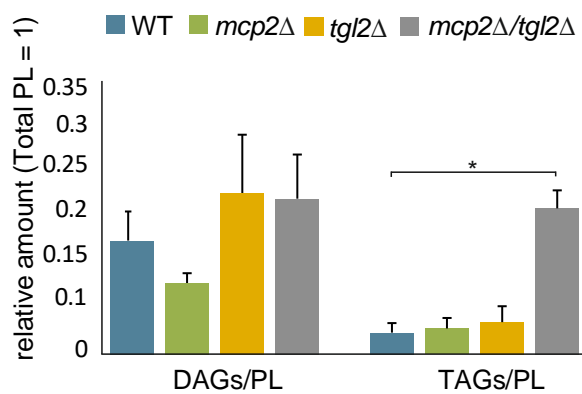
B





A



C



Yeast mitochondria can process *de novo* designed β -barrel proteins

Anasuya Moitra, Vitasta Tiku  and Doron Rapaport 

Interfaculty Institute of Biochemistry, University of Tuebingen, Tuebingen, Germany

Keywords

de novo designed proteins; mitochondria; outer membrane; TOB/SAM complex; β -barrel proteins

Correspondence

D. Rapaport, Interfaculty Institute of Biochemistry, University of Tuebingen, Auf der Morgenstelle 34, 72076 Tuebingen, Germany
 Tel: +49 7071 2974184
 E-mail: doron.rapaport@uni-tuebingen.de

(Received 29 December 2022, revised 18 August 2023, accepted 4 September 2023)

doi:10.1111/febs.16950

Mitochondrial outer membrane β -barrel proteins are encoded in the nucleus, translated in the cytosol and then targeted to and imported into the respective organelles. Detailed studies have uncovered the mechanisms involved in the import of these proteins and identified the targeting signals and the cytosolic factors that govern their proper biogenesis. Recently, *de novo* designed eight-stranded β -barrel proteins (Tmb2.3 and Tmb2.17) were shown to fold and assemble into lipid membranes. To better understand the general aspects of the biogenesis of β -barrel proteins, we investigated the fate of these artificial proteins upon their expression in yeast cells. We demonstrate that although these proteins are *de novo* designed and are not related to *bona fide* mitochondrial β -barrel proteins, they were targeted to mitochondria and integrated into the organelle outer membrane. We further studied whether this integration requires components of the yeast mitochondrial import machinery like Tom20, Tom70, Tob55/Sam50 and Mas37/Sam37. Whereas it seems that none of the import receptors was required for the biogenesis of the artificial β -barrel proteins, we observed a strong dependency on the TOB/SAM complex. Collectively, our findings demonstrate that the mitochondrial outer membrane is the preferential location in yeast cells for any membrane-embedded β -barrel protein.

Introduction

Membrane-embedded β -barrel proteins are found in a myriad of organisms. They are a class of outer membrane (OM) proteins that form a barrel-shaped hydrophilic pore in the membrane. This structure can be composed of 8–26 H-bonded, mostly antiparallel β -strands [1,2]. These proteins perform a variety of functions ranging from active transporters of solutes, through enzymes or structural proteins to protein translocators and membrane insertion machinery [3]. β -barrel proteins are found in the OM of Gram-negative bacteria and the two endosymbiont organelles, namely mitochondria and chloroplasts [4–6]. This relationship matches the evolutionary origins of mitochondria and

chloroplasts from α -proteobacterium and a photosynthetic cyanobacterium, respectively. Over the course of evolution, most of the organellar genes were transferred to the nucleus with the mitochondrial and chloroplast genome retaining the codes for only a few key components [7,8]. Thus, the mitochondrial and chloroplast β -barrel proteins are transcribed in the nucleus and translated on cytosolic ribosomes. Then, they need to be targeted to the correct subcellular organelle and ultimately integrated with the help of dedicated import machineries into the respective OM.

The biogenesis pathways for β -barrel proteins are evolutionarily conserved [9]. Precursors of bacterial

Abbreviations

BN-PAGE, blue native polyacrylamide gel electrophoresis; HA, hemagglutinin; OM, outer membrane; PK, proteinase K; SAM, sorting and assembly machinery; TMB, transmembrane barrel; TOB, topogenesis of mitochondrial outer membrane β -barrel proteins; TOM, translocase of the mitochondrial outer membrane; WCL, whole cell lysate.

b-barrel proteins are synthesised in the cytoplasm with signal sequences, which are recognised by Sec chaperones, who in turn guide them through the SecYEG translocon across the inner membrane. Signal sequences are next cleaved in the periplasm and the periplasmic chaperones SurA and Skp mediate the transfer of these proteins to the b-barrel assembly machinery (BAM) that ultimately assembles the protein into the bacterial OM [10,11]. Mitochondrial b-barrel proteins are synthesised on cytosolic ribosomes and transported to the mitochondrial OM surface in an import-competent conformation by chaperones of the Hsp70 and Hsp40 families [12]. They are subsequently delivered to the mitochondria where a hydrophobic b-hairpin element can interact with the Tom20 receptor, and the precursors cross the OM via the Tom40 pore [13–17]. The combined contribution of several b-hairpin motifs with a highly hydrophobic face is crucial for efficient mitochondrial targeting of b-barrel proteins [17,18]. The import and assembly of the b-barrel precursors is facilitated by the translocase of the outer membrane (TOM) [19–21] and topogenesis of outer membrane b-barrel/sorting and assembly machinery (TOB/SAM) complexes together with the small translocase of inner membrane (sTIM) chaperones [22–31]. Chloroplast b-barrel proteins like OEP21, OEP24 and OEP37 are imported into chloroplasts with the help of translocase of the outer membrane of chloroplast (TOC) and are inserted into the plastid OM via interactions with OEP80, which is related to BamA or Tob55/Sam50 of the BAM or TOB/SAM complex in bacteria and mitochondria, respectively [32,33].

Such conserved mechanisms prompted studies to investigate the evolutionary lineage of these pathways. Bacterial and chloroplast b-barrel proteins have been shown to be targeted and integrated into mitochondria upon their expression in yeast cells [17,34–37]. This opened the realm of possibilities for the potential of yeast cells to assemble and integrate novel b-barrel proteins. A recent study from the Baker Lab showed that *de novo* designed synthetic eight-stranded b-barrel proteins (that were named Tmb2.3 and Tmb2.17) could fold and assemble into synthetic lipid membranes [38]. To better understand the basic principles of the biogenesis of b-barrel proteins, we investigated whether such artificial b-barrel proteins could be expressed in yeast cells and integrated into the yeast mitochondria. We further explored the role of yeast mitochondrial import and assembly components in the proper biogenesis of such b-barrel proteins.

Our results show that these *de novo* designed b-barrels, although not related to *bona fide*

mitochondrial b-barrel proteins, can be targeted to and integrated into the yeast mitochondrial OM. We demonstrate that one of them can even form higher oligomers that depend on the TOB/SAM complex. Collectively, our findings suggest that the strong evolutionary conservation of pathways and machineries that deal with b-barrel proteins allows processing of yet completely artificial members of this family.

Results

TMBs can localise to and integrate into the mitochondrial outer membrane

To better understand the biogenesis of b-barrel proteins, we aimed to study the targeting and assembly of *de novo* designed members of this family. To this end, we utilised two recently reported artificial b-barrel proteins that were named Tmb2.3 and Tmb2.17 [38]. To facilitate their expression in yeast (*Saccharomyces cerevisiae*), we created artificial genes with codon usage optimised to that of *S. cerevisiae*. To allow detection of the translated proteins, both DNA segments included at their 3' end a sequence encoding a HA tag. The resulting coding sequences were cloned into the yeast expression vector pYX142 where the expression is under the control of the *TPI* (triosephosphate isomerase, a housekeeping enzyme) promoter.

Next, wild-type (WT) yeast cells were transformed with either the empty vector or the vector coding for either Tmb2.3-HA or Tmb2.17-HA. To test whether the expression of these b-barrel proteins affects the growth of the corresponding cells, growth curves of liquid cultures were obtained and drop-dilution assays were performed. Both approaches showed that the expression of these TMBs does not have any influence on the growth of yeast cells (Fig. 1A,B).

Confirming the lack of a toxic effect, we next aimed to ascertain the subcellular location to which these proteins are targeted. To address this question, we performed subcellular fractionation of the above cells. As a confirmation of the successful separation of the different fractions, the mitochondrial OM protein Porin, the ER protein Erv2, and the cytosolic protein hexokinase were detected in their respective fractions. Interestingly, while Tmb2.3-HA was predominantly localised to mitochondria, Tmb2.17-HA was found in both the ER and mitochondrial fractions (Fig. 2). These findings demonstrate that at least one of the TMBs behaved similarly to bacterial and chloroplast b-barrel proteins that were also targeted to mitochondria upon their expression in yeast cells [34,35].

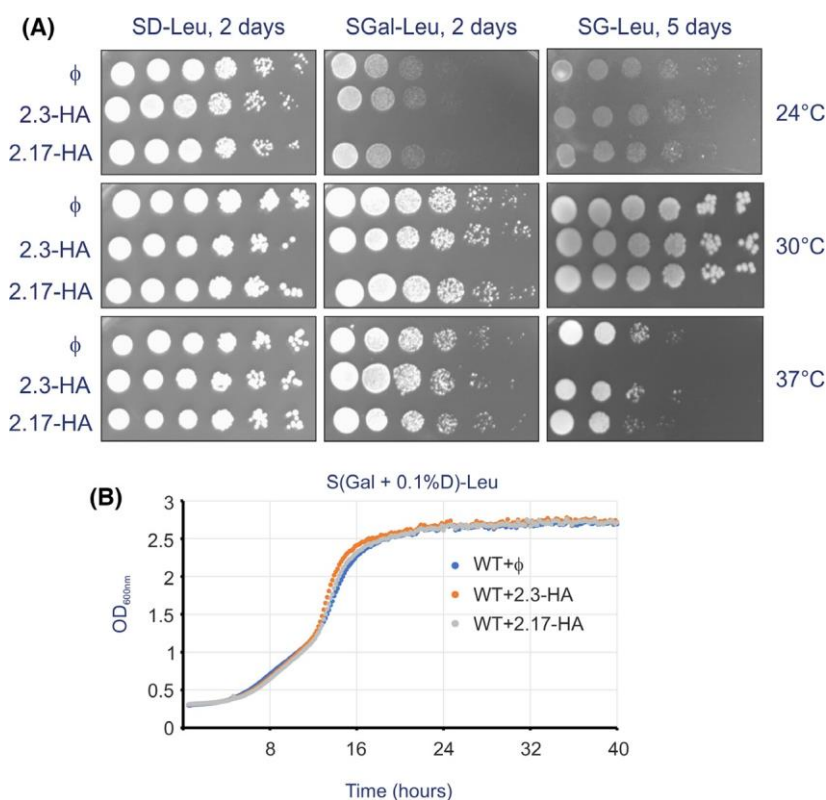


Fig. 1. Expression of both transmembrane barrels (TMBs) does not affect the growth of yeast cells. (A) Wild-type (WT) yeast cells were transformed with an empty plasmid (ϕ) or with a plasmid encoding for either Tmb2.3-HA (2.3-HA) or Tmb2.17-HA (2.17-HA). The growth of the cells was analysed by drop-dilution assay on synthetic medium containing glucose (SD), galactose (SGal) or glycerol (SG) as carbon source. Plates were incubated for the indicated number of days at 24, 30 or 37 °C before pictures were taken. (B) Cells transformed as in A were grown in S(Gal+0.1%D)-Leu liquid media at 30 °C in a 96-well plate and growth was monitored by measuring the OD at 600 nm. The plot shows the mean values of OD of three technical replicates for each strain ($n = 3$).

Next, we investigated the membrane integration ability of these TMBs by subjecting mitochondria harbouring either Tmb2.3-HA or Tmb2.17-HA, to alkaline extraction. *Bona fide* membrane proteins like the OM proteins Tom20 and Tom40 and mitochondrial inner membrane (IM) protein Pic2 were found in the

pellet (P) fraction, whereas the soluble matrix protein Hsp60 was detected in the supernatant (S). Both Tmb2.3-HA and Tmb2.17-HA were found in the pellet fraction indicating that they are membrane-embedded proteins (Fig. 3A,B).

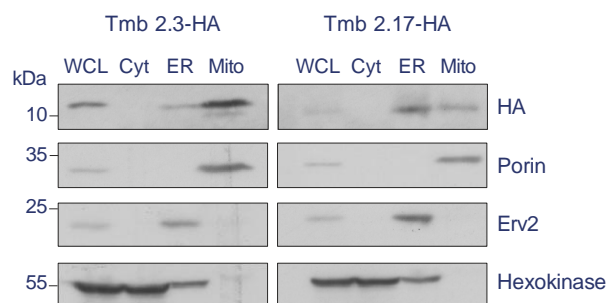


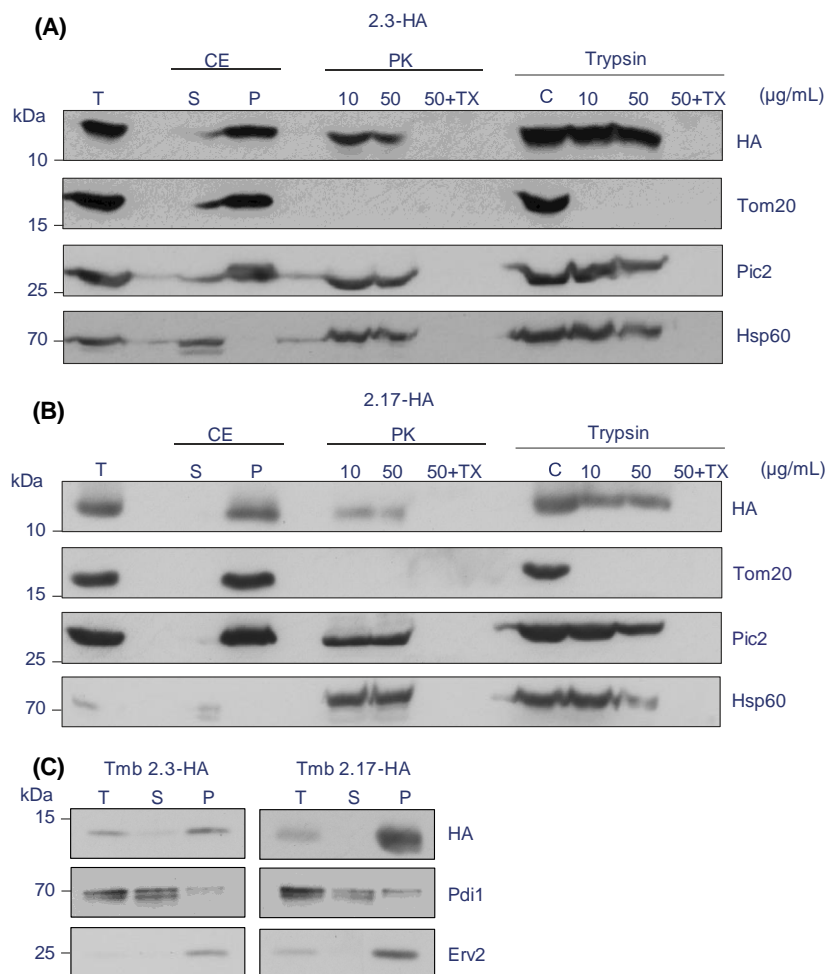
Fig. 2. Tmb2.3 and Tmb2.17 are targeted mainly to mitochondria upon expression in yeast cells. Wild-type (WT) yeast cells expressing either Tmb2.3-HA (left panel) or Tmb2.17-HA (right panel) were subjected to subcellular fractionation, followed by analysis of the whole cell lysate (WCL), cytosol (Cyt), endoplasmic reticulum (ER)/microsomes and mitochondria (Mito) fractions by SDS-PAGE and immunodecoration with the indicated antibodies. Erv2 and Porin/VDAC are ER and mitochondrial marker proteins, respectively, while hexokinase is used as a cytosolic marker. A representative of three similar experiments is shown ($n = 3$).

To assess the topology of the TMBs and determine in which mitochondrial membrane they reside, mitochondria containing these TMBs were subjected to treatment with the proteases Proteinase K (PK) or trypsin. OM proteins with an exposed cytosolic domain like Tom20 were completely digested by these proteases, whereas IM and matrix proteins like Pic2 and Hsp60, respectively, were protected from the proteases. Both TMBs were partially susceptible to PK and better protected from trypsin (Fig. 3A,B). As a control, the addition of 1% Triton-X-100 to the reaction, which leads to the solubilisation of the mitochondrial membranes, resulted in the complete degradation of the proteins by the proteases (Fig. 3A,B). Thus, we can conclude that both TMBs are embedded into the mitochondrial OM with a topology that exposes part of them to the cytosol.

Since we observed that a portion of both TMBs is localised to the ER (Fig. 2), we wondered if these molecules are associated with the membrane of this compartment. To that aim, we performed a carbonate extraction of the ER fraction and found that both

Fig. 3. Both transmembrane barrels (TMBs) are embedded in the mitochondrial outer membrane. (A and B) Mitochondria isolated from wild-type (WT) yeast cells expressing either Tmb2.3-HA (A) or Tmb2.17-HA (B) were left untreated (Total, T), subjected to carbonate extraction (CE) to obtain supernatant (S) and pellet (P) fractions, or were treated with either 10 or 50 $\mu\text{g}/\text{mL}$ of Proteinase K (PK) or Trypsin in the presence or absence of 1% Triton-X-100 (TX). In the control lane (C), mitochondria were treated with 50 $\mu\text{g}/\text{mL}$ of Trypsin, that had been preincubated with trypsin inhibitor. Samples were finally analysed by SDS-PAGE and immunoblotting. Tom20 is a mitochondrial OM protein exposed to the cytosol; Pic2 is embedded in the mitochondrial inner membrane; Hsp60 is a soluble mitochondrial matrix protein. (C) The ER fraction isolated from WT yeast cells

expressing either Tmb2.3-HA (left panel) or Tmb2.17-HA (right panel) were left untreated (T) or subjected to carbonate extraction to obtain supernatant (S) and pellet (P) fractions. Pdi1, a soluble ER protein; Erv2, an ER membrane protein. For each part, a representative of three similar experiments is shown ($n = 3$).



proteins are in the pellet portion of this procedure (Fig. 3C). Although these findings suggest the potential of both TMBs to associate with the ER membrane, their conformation at this membrane is unknown.

The biogenesis of the artificial TMBs does not depend on the import receptors Tom20 and Tom70

Next, we wanted to examine the possible import machineries that these proteins utilise to arrive and thrive in the mitochondria. b-barrel proteins have been shown to interact with the TOM complex receptors [39]. Recently, it was shown that a hydrophobic b-hairpin element could interact with Tom20, and a chaperone-bound b-barrel precursor could bind to Tom70 to enable the precursor to enter via the Tom40 pore [12,17]. Hence, we wanted to check whether the rather small TMBs also depend on these receptors for their entry into mitochondria. To address this issue,

WT, *tom20D* and *tom70/71D* yeast cells were transformed with an empty vector (ϕ) or a vector encoding either Tmb2.3-HA or Tmb2.17-HA. Then, we obtained from the transformed cells fractions corresponding to mitochondria (Mito), whole cell lysate (WCL) and cytosol (Cyt). Subsequently, we analysed the proteins of these fractions by SDS-PAGE and immunoblotting.

Surprisingly, the steady-state levels of both Tmb2.3-HA and Tmb2.17-HA seem to be even higher in the mitochondrial fraction of cells lacking the Tom20 receptor (Fig. 4A,B, respectively). Tom40 and Hexokinase are used as mitochondrial and cytosolic controls, respectively, and their levels remain unchanged. Of note, the levels of the Tom70 receptor, which might compensate for the loss of Tom20, are also unaltered in cells deleted for Tom20 (Fig. 4). Hence, it appears that Tom20 is not required for the proper import of the TMBs to mitochondria.

Similar observations were made when the other import receptors Tom70 and its paralog Tom71 were

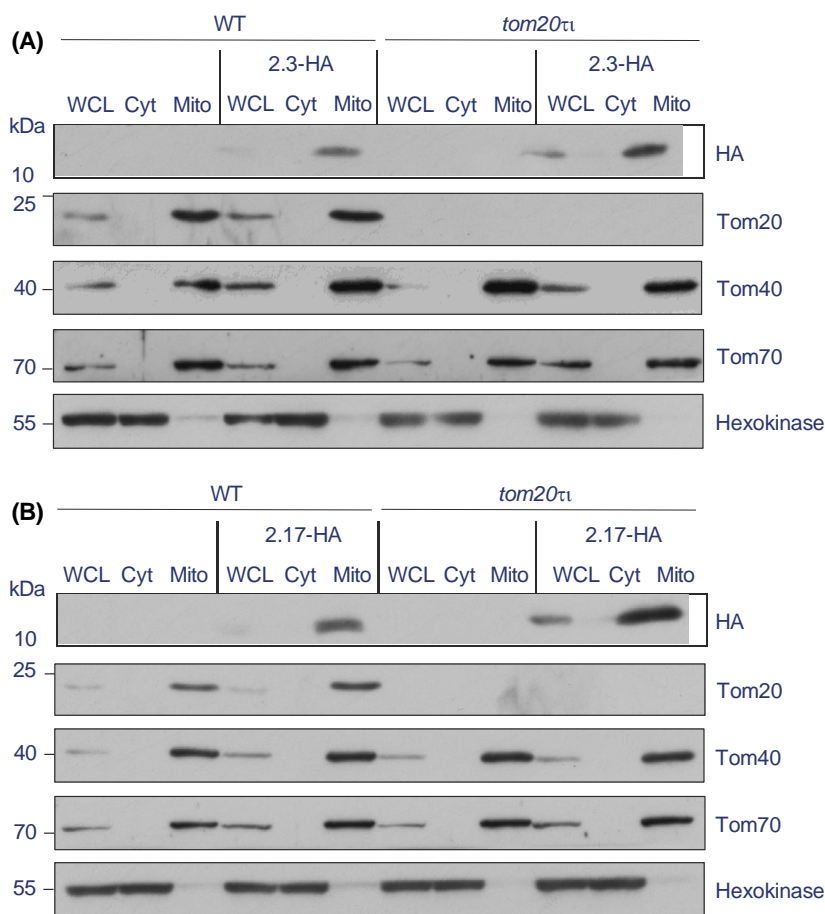


Fig. 4. Steady-state levels of both transmembrane barrels (TMBs) in yeast cells do not depend on Tom20. (A and B) Wild-type (WT) and *tom20 Δ* yeast cells were transformed with an empty plasmid (u) or with a plasmid encoding for either Tmb2.3-HA (A) or Tmb2.17-HA (B). Whole cell lysate (WCL), cytosol (Cyt) and mitochondrial (Mito) fractions isolated from the transformed cells were subjected to SDS-PAGE and immunoblotting with the indicated antibodies. Tom40 and Tom70 are mitochondrial OM proteins. For each part, a representative of three similar experiments is shown ($n = 3$).

deleted. The levels of both TMBs were somewhat higher in the *tom70/71 Δ* yeast cells (Fig. 5). However, the steady-state levels of Tom20 were slightly higher in the mutated organelles and this could potentially compensate for the loss of Tom70/71. Thus, we can conclude that the TMBs can be targeted to the mitochondria in the absence of either Tom20 or the Tom70/71 receptors.

The assembly of the TMBs depends to a variable extent on the TOB/SAM complex

Once the b-barrel protein precursors reach the mitochondrial surface, they are initially processed by the TOM complex [40]. Then, they reach the IMS where they are bound by the small TIM chaperones to prevent aggregation [41]. Finally, the b-barrel precursors are integrated into the mitochondrial OM via the TOB/SAM complex, which consists of Mas37/Sam37, Tob38/Sam35 and Tob55/Sam50 [22,25–28,31]. Thus, we wanted to assess whether the absence of certain critical components of the TOB/SAM complex could affect the assembly of the artificial TMBs.

To that goal, we transformed plasmids encoding either Tmb2.3-HA or Tmb2.17-HA into WT or cells lacking Mas37/Sam37. The cells were grown at 24 °C to avoid accumulation of suppressors at elevated temperatures as Mas37/Sam37 is crucial for the proper function of the TOB/SAM complex. Subcellular fractions were obtained and the steady-state levels of both TMBs analysed by SDS-PAGE and immunoblotting. We observed that the mitochondrial levels of both Tmb2.3-HA and Tmb2.17-HA were significantly lower in *mas37/sam37 Δ* cells as compared to those in control samples (Fig. 6A,B, respectively). This behaviour is similar to that of a canonical mitochondrial b-barrel protein like Tom40 (Fig. 6). As expected, the levels of the ER protein Erv2 or the cytosolic chaperone Hsp82 were unaltered (Fig. 6A,B). A possible explanation for the reduced mitochondrial amounts of both TMBs is mistargeting to another compartment in the absence of Mas37/Sam37. However, the results depicted in Fig. 6 demonstrate that considerable mistargeting to either ER or cytosol did not take place.

Next, we wanted to examine the role of Mas37/Sam37 in the assembly of these TMBs in the mitochondrial OM.

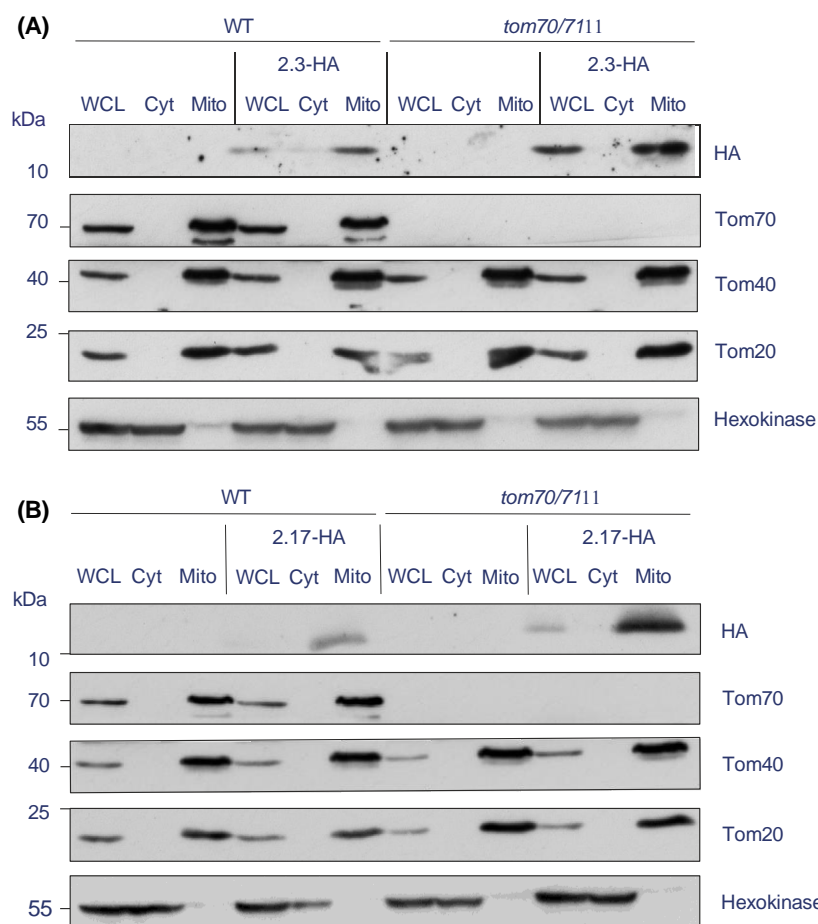


Fig. 5. Tom70 is not involved in the biogenesis of both transmembrane barrels (TMBs). (A, B) Wild-type (WT) and *tom70D*/*tom71D* cells were transformed with an empty plasmid (u) or with a plasmid encoding either Tmb2.3-HA (A) or Tmb2.17-HA (B). Whole cell lysate (WCL), cytosol (Cyt) and mitochondrial (Mito) fractions isolated from the transformed cells were subjected to SDS-PAGE and immunoblotting with the indicated antibodies. For each part, a representative of three similar experiments is shown ($n = 3$).

Therefore, mitochondria isolated from WT or *mas37/sam37D* cells expressing the TMBs were subjected to BN-PAGE followed by immunoblotting. In the control organelles, Tmb2.3-HA could form high molecular weight oligomers, while Tmb2.17-HA was mostly present as monomers. Interestingly, in the organelles lacking Mas37/Sam37, Tmb2.3-HA could no longer assemble into higher oligomers and was found to exist, similar to Tmb2.17-HA, only as monomers (Fig. 6C, left panel). As a control, the TOM complex, which was immunodecorated at about 400 kDa with antibodies against Tom40, was detected as expected in lower levels upon deletion of *MAS37/SAM37* (Fig. 6C, right panel). These findings suggest that Tmb2.3-HA can assemble into higher oligomers in a TOB/SAM complex dependent manner.

Observing this effect of Mas37/Sam37, we wanted to assess the importance of Tob55/Sam50, the central component of the TOB/SAM complex, for the biogenesis of the TMBs. A complete knockdown of Tob55/Sam50 is detrimental for yeast cells. Hence, we transformed an empty vector (u) or vector encoding either Tmb2.3-HA or Tmb2.17-HA into cells expressing

Tob55/Sam50 under the control of the inducible *GAL10* promoter. To ensure the expression of Tob55/Sam50, the cells were initially grown at 30 °C in selective lactate medium with galactose. Then, to deplete Tob55/Sam50, the cells were harvested and resuspended in glucose-containing medium. Cells were then harvested at various time points after a shift from galactose- to glucose-containing medium, mitochondria were isolated, and the steady-state levels of the TMBs analysed by SDS-PAGE and immunoblotting.

We observed that the levels of Tob55/Sam50 were depleted after about 51 h on glucose-containing medium (Fig. 7A,B). Consequently, Porin/VDAC, a quintessential mitochondrial OM b-barrel protein, that depends on Tob55/Sam50 for optimum assembly, was depleted after 71 h while steady-state levels of the matrix protein Aconitase, whose biogenesis is independent of Tob55/Sam50, remained unaffected (Fig. 7A, B). Similar to Porin, Tmb2.3-HA levels decreased upon Tob55/Sam50 depletion (Fig. 7A). Unexpectedly, Tmb2.17-HA levels even slightly increased in the mitochondria from Tob55/Sam50-depleted cells (Fig. 7B).

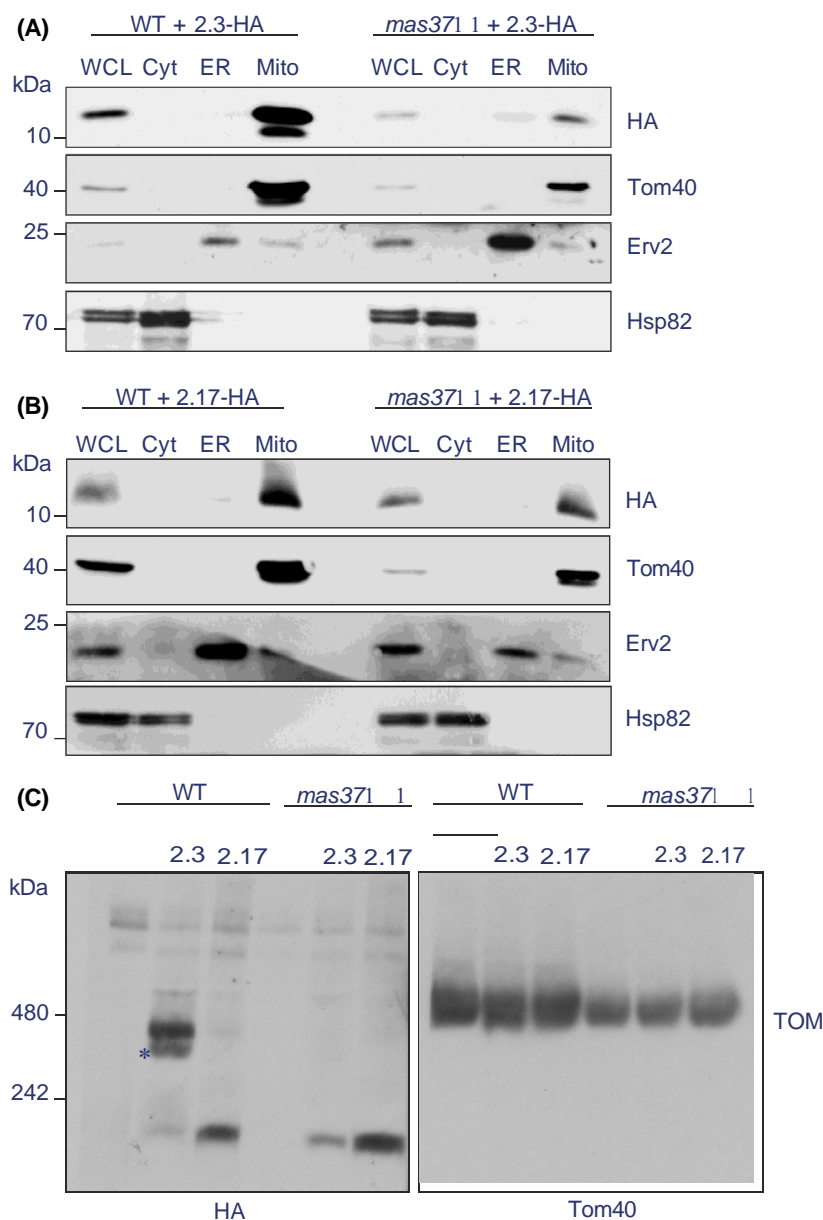


Fig. 6. Membrane integration of both transmembrane barrels (TMBs) requires Mas37/Sam37. (A and B) Wild-type (WT) and *mas37/sam37Δ* yeast cells were transformed with an empty plasmid (ϕ) or with a plasmid encoding for either Tmb2.3-HA (A) or Tmb2.17-HA (B). Whole cell lysate (WCL), cytosol (Cyt), endoplasmic reticulum (ER) and mitochondrial (Mito) fractions isolated from the transformed cells were subjected to SDS-PAGE and

immunoblotting with the indicated antibodies. Erv2 is an ER membrane protein, while Hsp82 is used as a cytosolic marker. (C) Mitochondria isolated as in A and B were analysed by BN-PAGE and immunoblotting with antibodies against either the HA tag (left panel) or Tom40 (right panel). Tom40 is a known substrate of Mas37/Sam37. A high molecular weight form of Tmb2.3-HA and the TOM complex are indicated by an asterisk or 'TOM', respectively. For each part, a representative of three similar experiments is shown ($n = 3$).

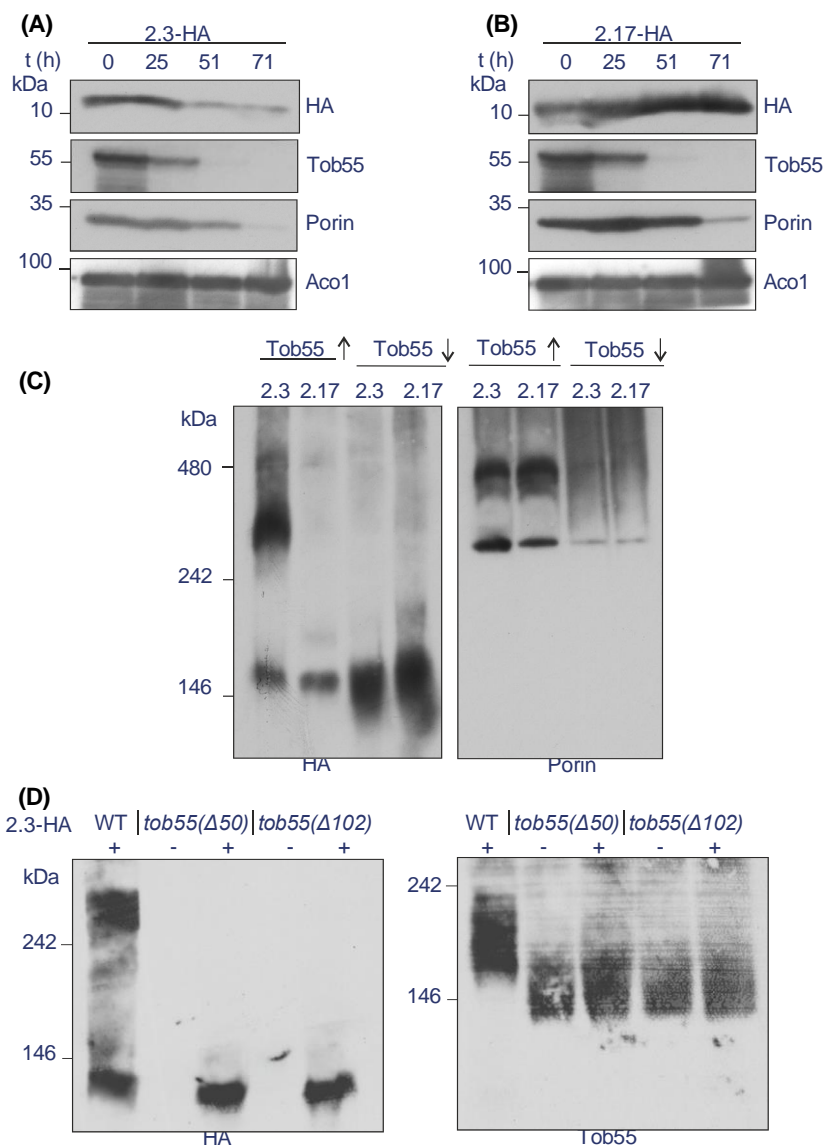
These findings led us to ask whether Tob55/Sam50 was crucial also for the assembly of the higher oligomers of Tmb2.3-HA. As we observed before, BN-PAGE analysis revealed that Tmb2.3-HA could form higher oligomers in the presence of Tob55/Sam50, while Tmb2.17-HA was mostly present as monomers (Fig. 7C, left panel). Of note, upon depletion of Tob55/Sam50, Tmb2.3-HA could no longer assemble into higher oligomers and was found to exist only as monomers. In agreement with the analysis by SDS-PAGE, Tmb2.17-HA monomers were detected in increased amounts in the organelles depleted for Tob55/Sam50 (Fig. 7C, left panel). As expected, Porin

also formed higher oligomers in the presence of Tob55/Sam50, but their levels were substantially decreased upon Tob55/Sam50 depletion (Fig. 7C, right panel).

To further test the involvement of the TOB/SAM complex in the formation of the oligomeric species of Tmb2.3-HA, we express the latter protein in cells harbouring Tob55/Sam50 with truncations of either 50 or 102 amino acid residues at the N terminus [42]. Analysing mitochondria isolated from these cells by BN-PAGE revealed that these truncations prevent the formation of the oligomeric form of Tmb2.3-HA (Fig. 7D). These findings clearly demonstrate that the

Fig. 7. Depletion of Tob55/Sam50 affects the assembly of Tmb2.3 but not that of Tmb2.17. (A and B) Plasmids encoding Tmb2.3-HA or Tmb2.17-HA were transformed into yeast cells expressing Tob55/Sam50 under the control of the

GAL10 promoter. To induce the depletion of Tob55/Sam50, cells were shifted at $t = 0$ from galactose- to glucose-containing medium and harvested at the indicated time points after this shift. Mitochondria were isolated and proteins were analysed by SDS-PAGE and immunoblotting with antibodies against the indicated proteins. Aconitase (Aco1) is a mitochondrial matrix protein. (C) Mitochondria were isolated from cells described above grown on galactose (Tob55/Sam50 \uparrow) or depleted for Tob55/Sam50 by growth for 71 h on glucose-containing medium (Tob55/Sam50 \downarrow). Samples were analysed by BN-PAGE and immunodecoration with antibodies against either the HA tag (left panel) or Porin/VDAC (right panel). Porin/VDAC is a b-barrel protein embedded in the mitochondrial OM and a known substrate of Tob55/Sam50. (D) Mitochondria were isolated from the indicated Tmb2.3-HA expressing cells harbouring either native Tob55/Sam50 or its N-terminally truncated variants. Samples were analysed by BN-PAGE and immunodecoration with antibodies against either the HA tag (left panel) or Tob55/Sam50 (right panel). For each part, a representative of three similar experiments is shown ($n = 3$).



N-terminal region of Tob55/Sam50 is required for proper assembly of Tmb2.3-HA.

Taken together, these data indicate the differential involvement of the TOB/SAM complex in the biogenesis and assembly of the artificial TMBs. Whereas the complex facilitates the membrane integration and oligomerisation of Tmb2.3-HA, it appears to be dispensable for the biogenesis of Tmb2.17-HA.

Single amino acid mutation in the b-signal does not significantly alter the biogenesis of both TMBs

The distinct behaviour of both TMBs prompted us to search for reasons for this difference. We have

previously demonstrated that a hydrophobic b-hairpin can serve as a mitochondrial targeting signal [17]. Hence, a clear difference in the hydrophobicity of the b-hairpins of both TMBs might explain the difference in their subcellular distribution. To clarify this option, we analysed the hydrophobicity patterns of the eight b-strands of both TMBs (Fig. 8). However, despite local variations in the hydrophobicity pattern between the two proteins, we could not identify a major difference that can explain their distinctive localisation (Fig. 8).

Previous studies showed that the last C-terminal b-strand of mitochondrial b-barrel proteins contains a stretch of amino acids that facilitate their interaction with the TOB/SAM complex [26]. These residues were

(A)

Tmb2.3 (13541 Da) (NMR PDB 6X1K)

 β strand

MQDGPGLTLDVFAAGWN TDN TIEITGGATYQ LSPYIMVKAGYGW NNSSLN RFEFGGG
 LQYKVPDL EPYAWAGATYN TDN TLVPAAGAGFRYK VSPEV KLVVEYGW NNSSLQ FL
 QAGLSYRIQP

Tmb2.17 (13415 Da) (Crystal Structure PDB 6X9Z)

 β strand

MEQKPGT LMVYVVGYN TDNT VDWGGAQYA VSPY LFLDVGYGWN NSS LNFLEVGG
 GVS YKVSPL EPYVKAGFEYN TDNT KPTAGAGALYR VSPN LALMVEYGW NNSSL QK
 VAIGIAYKVKD

(B)

	Tmb 2.3	Tmb 2.17
Strand 1 face A	-0.58	0.18
face B	2.62	3.02
Strand 2 face A	-1.58	-0.28
face B	1.82	1.70
Strand 3 face A	-0.70	-1.00
face B	1.66	1.92
Strand 4 face A	-2.20	0.25
face B	2.25	1.66
Strand 5 face A	1.72	-2.68
face B	0.50	1.61
Strand 6 face A	0.56	-1.01
face B	1.22	1.16
Strand 7 face A	-0.90	-0.05
face B	1.45	1.92
Strand 8 face A	-1.28	-0.92
face B	2.03	1.68

(C)

Hairpin	Tmb 2.3	Tmb 2.17
hp1	2.22	2.36
hp2	1.74	1.81
hp3	1.92	1.79
hp4	1.28	1.64
hp5	0.89	1.39
hp6	1.31	1.51
hp7	1.74	1.80

Fig. 8. Analysis of the amino acid sequence and hydrophobicity patterns of the transmembrane barrel (TMBs). (A) The amino acid sequence of the two TMBs along with the annotation of the eight b-strands according to the published structures from Vorobieva *et al.* [38]. (B) The average hydrophobicity of the hydrophilic face (face A) and the hydrophobic face (face B) of each of the eight b-strands of Tmb2.3 and Tmb2.17 was calculated by summing up the hydrophobicity values of the residues either facing the lipid environment (face B) or the b-barrel lumen (face A) and dividing it by the number of the residues in that strand. The values are colour coded, with blue, white and red representing the highest, median and the lowest hydrophobicity values, respectively. (C) The average hydrophobicity of the hydrophobic face of the b-hairpins of Tmb2.3 and Tmb2.17 was calculated by summing up the hydrophobicity values of the residues facing the lipid environment from both b-strands that form each b-hairpin (hp) and dividing it by the number of the residues. The values are colour coded as in B.

termed the **b**-signal and comprised of the following motif: Po-X-G-X-X-Hy-X-Hy-X, where Po stands for a polar residue, G for Glycine, and Hy represents a hydrophobic residue. Deletion or mutation of the **b**-signal did not interfere with the initial targeting of newly synthesised **b**-barrel proteins to mitochondria.

We wanted to investigate whether sequences similar to such a **b**-signal present within the TMBs, could explain their differential dependence on the TOB/SAM complex. To this end, we analysed the amino acid sequence of both TMBs. They showed a 60% sequence identity (using Clustal Omega [43], data not shown). The amino acid sequence and the annotation of the eight **b**-strands are shown in Fig. 8A (adapted from [38]). The analysis revealed that Tmb2.3 indeed contained a canonical **b**-signal, whereas Tmb2.17 had only a partial

consensus sequence. Tmb2.17 lacked the polar residue at the N terminus of the **b**-signal (Q115 in Tmb2.3, A115 in Tmb2.17) (Fig. 9A, wild-type TMBs).

Considering this difference, we wanted to assess whether this residue (Q115) of the **b**-signal was crucial for the assembly of the TMBs into higher oligomeric forms. Thus, we performed site-directed mutagenesis to swap this residue between the two TMBs. In this way, the glutamine residue of Tmb2.3 was replaced by alanine, resulting in the construct Tmb2.3_{Q115A}-HA. Reciprocally, the alanine residue of Tmb2.17 was changed to glutamine obtaining the variant Tmb2.17_{A115Q}-HA (Fig. 9A, mutant TMBs). Then, WT yeast cells were transformed with vectors encoding these mutant TMBs and the transformants were grown on S(Gal+0.1%D)-Leu media and subjected to subcellular fractionation. The results

(A) β -signal residue β -signal motif

Po-X-G-X-X-Hy-X-Hy-X

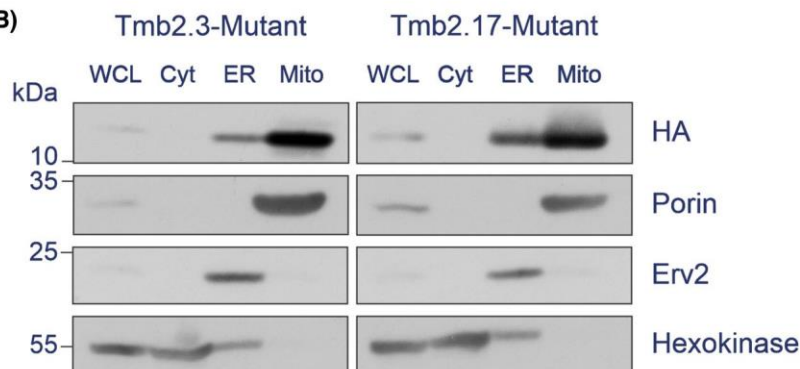
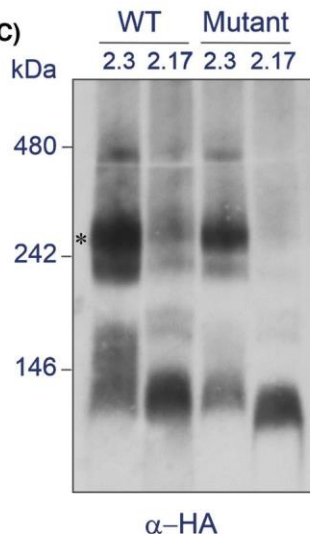
wildtypeTmb 2.3 115 **Q** A **G** L S **Y** R **I** Q¹²³Tmb 2.17 115 **A** I **G** I A **Y** K **V** K¹²³**mutant**Tmb 2.3 115 **A** A **G** L S **Y** R **I** Q¹²³Tmb 2.17 115 **Q** I **G** I A **Y** K **V** K¹²³**(B)****(C)**

Fig. 9. Single amino acid mutation in the b-signal does not alter the subcellular localisation or assembly of Tmb2.3 and Tmb2.17. (A) Conserved mitochondrial b-signal motif (top) and the corresponding b-signal motif in the TMBs (bottom). The b-signal residues are in red and the mutated residues in bold. Po, polar; Hy, hydrophobic. (B) Wild-type (WT) yeast cells expressing Tmb2.3_{Q115A}-HA and Tmb2.17_{A115Q}-HA (mutants) were subjected to subcellular fractionation, followed by analysis of the whole cell lysate (WCL), cytosol (Cyt), endoplasmic reticulum (ER) and mitochondria (Mito) fractions by SDS-PAGE and immunodecoration with the indicated antibodies. Erv2 and Porin/VDAC are ER and mitochondrial marker proteins, respectively, while hexokinase is used as a cytosolic marker. (C) Mitochondria isolated from WT cells expressing either wild-type or mutant transmembrane barrel (TMBs) were subjected to BN-PAGE and immunoblotting with antibodies against the HA tag. A high molecular weight form of Tmb2.3-HA is indicated by an asterisk. For each part, a representative of three similar experiments is shown ($n = 3$).

revealed that the mutations did not interfere with the initial targeting of the TMBs. Tmb2.3_{Q115A}-HA was still predominantly mitochondrial, while Tmb2.17_{A115Q}-HA was distributed between the ER and mitochondria (Fig. 9B). BN-PAGE analysis followed by immunoblotting of mitochondria isolated from cells expressing either the control or mutant TMBs showed that replacement of Q115 by alanine led to a minor decrease in the levels of the higher oligomeric forms of Tmb2.3_{Q115A}-HA compared with the original Tmb2.3-HA (Fig. 9C). The

introduction of glutamine residue at position 115 of Tmb2.17-HA did not cause it to form higher oligomers (Fig. 9C). Overall, it seems that a single amino acid mutation in the b-signal motif of the TMBs does not have an observable effect on their overall biogenesis.

Discussion

The evolutionary conservation of the biogenesis pathways of b-barrel proteins allowed us in the past to

express and target bacterial and chloroplast b-barrel proteins into yeast mitochondria [17,34–37]. Recently, Vorobieva *et al.* designed synthetic eight-stranded b-barrel proteins, namely Tmb2.3 and Tmb2.17, that could be assembled into a barrel structure in liposomes [38]. To better understand the general principles of the biogenesis of b-barrel proteins, we wanted to test whether such artificially designed proteins could also be recognised by and assembled into yeast mitochondria. Subcellular fractionation experiments revealed that both Tmb2.3 and Tmb2.17 could be targeted to the mitochondria, with 2.17 also showing partial ER localisation. Similar observations were also made when bacterial secretins like PulD, InvG or SsaC were expressed in yeast cells [37]. Of note, Tmb2.3-HA was more efficiently localised to mitochondria in comparison with Tmb2.17-HA. b-barrel proteins are targeted and assembled into the mitochondria based on the hydrophobicity and the sequence of the last few b-hairpins [17,18,26]. However, we could not pinpoint the precise differences between both proteins that cause this divergent behaviour. It is interesting to note that both TMBs, although they contain only 8 b-strands, were integrated properly into the mitochondrial OM, demonstrating the capacity of the organelle to deal with any type of membrane-embedded b-barrel proteins. These observations are in line with our previous findings that yeast mitochondria can deal, among other bacterial b-barrel proteins, also with OmpA, which also contains only 8 b-strands [34].

Interestingly, when we assessed the role of the TOM complex receptors in the biogenesis of the TMBs, we observed that in the absence of either one of the receptors (Tom20 or Tom70), the mitochondrial steady-state levels of the TMBs were enhanced. Similar observations were made for the secretins InvG-HA and SsaC-HA where the absence of Tom20 or Tom70 led to increased amounts of the protein in the mitochondria, respectively [37]. This behaviour might be explained by the small size of the artificial TMBs that have only 8 b-strands as compared to the 16 or 19 strands of *bona fide* mitochondrial b-barrel proteins. As Tom70, in addition to its receptor function, is also the docking site for cytosolic chaperones that escort the newly synthesised b-barrel substrates, the smaller size of the substrates might reduce the need for such an escort and hence also the relevance of the chaperone docking site. An alternative, but not mutually exclusive, option is a compensating function of the remaining receptor in the absence of its counterpart. Also, a possible role of Tom22 in the absence of either Tom20 or Tom70 remains to be investigated.

Collectively, we can conclude that the absence of a single receptor does not impair the biogenesis of the TMBs.

After the initial recognition at the mitochondrial surface, followed by the actual translocation through the Tom40 pore, b-barrel proteins are assembled into the mitochondrial OM with the help of sTIM chaperones and the TOB/SAM complex [22–28,31,41,44]. We investigated the role of the TOB/SAM complex in the assembly of the artificial TMBs. In the absence of Mas37/Sam37, the mitochondrial steady-state levels of the TMBs decreased, similar to the effect on *bona fide* mitochondrial b-barrel protein like Tom40. It is known that the absence of Mas37/Sam37 decreases the stability of the TOB/SAM complex, thus affecting the efficiency of integration of the TMBs into the mitochondrial OM. Additional decrease in Tom40 levels, which by itself is a substrate of the TOB/SAM complex, may also contribute to the lower steady-state levels of the TMBs. BN-PAGE analysis of mitochondria from *mas37/sam37D* cells or from cells either depleted for Tob55/Sam50 or with N-terminal truncations of this protein demonstrated the importance of the TOB/SAM complex not only for the general import of Tmb2.3-HA, but also for its optimal assembly into oligomeric structures. In contrast to Tmb2.3-HA, Tmb2.17-HA existed as lower monomeric forms under all tested conditions. Although it appears as an appealing possibility, we failed to demonstrate that the inability of Tmb2.17-HA to form higher oligomers could be attributed to the absence of a *bona fide* mitochondrial b-signal in its sequence.

Our findings surprisingly indicate that different b-barrel proteins can be dependent to a variable extent on the proper function of the TOB/SAM complex. Such distinctions could be related to dissimilarities in their sequence (60% identity), variabilities in the hydrophobicity patterns of the b-strands, differences in their thermodynamic stability and/or different sequences of the classical b-signal at the last b-strand. This variability also raises the question of how Tmb2.17-HA can integrate into the mitochondrial OM in the absence of a functional TOB/SAM complex, and future studies should address such apparent TOB/SAM-independent membrane integration.

Collectively, our study demonstrates that *de novo* designed TMBs can be targeted to mitochondria upon their expression in eukaryotic cells. Their biogenesis is independent of the TOM receptors and differentially dependent on the TOB/SAM complex. These findings shed new light on the general principles of the biogenesis of b-barrel proteins.

Materials and methods

Yeast strains and growth conditions

Standard genetic techniques were used for the growth and manipulation of yeast strains. The *Saccharomyces cerevisiae* strains used in this study are listed in Table S1. Yeast cells were usually grown at 30 °C on synthetic selective (S) medium (0.67% [w/v] yeast nitrogen base without amino acids) containing galactose (Gal, 2%) + glucose (D, 0.1%) as carbon source. A mixture of the required amino acids, omitted for Leu to select for transformants with the pYX142 plasmid, was added as well. Cells deleted for *MAS37/SAM37* (*mas37/sam37D*) were grown at 24 °C to avoid accumulation of suppressors [24]. Transformation of yeast cells was performed by the lithium acetate method [45].

For experiments with cells depleted for *TOB55/SAM50*, a strain where *TOB55/SAM50* expression is under the control of the inducible *GAL10* promoter was used [46]. Cells of this strain were initially grown at 30 °C on synthetic depleted (S) medium containing lactate (Lac, 2%) + galactose (Gal, 0.1%) as carbon source and amino acid mixture as above. After a few days of growth on this medium, cells were shifted to S media containing 0.1% glucose instead of 0.1% galactose. Cells were harvested at the indicated time points after the shift from galactose- to glucose-containing medium.

Some experiments were performed with cells containing N-terminally truncated variants of Tob55/Sam50. These strains are deleted for the endogenous *TOB55/SAM50* and contain the yeast expression plasmid pYX132 encoding either the native protein or truncated variant of *TOB55/SAM50* where the first 50 [*TOB55(D50)*] or 102 [*TOB55(D102)*] N-terminal amino acid residues were removed [42]. Cells of these strains were grown at 30 °C in synthetic selective medium containing galactose (Gal, 2%) + glucose (D, 0.1%) as carbon source and amino acid mixture omitted for Trp to select for pYX132 plasmid. The cells of the above strains, when expressing pYX142 encoded Tmb2.3-HA, were grown as above with an amino acid mixture depleted of both Trp and Leu.

Analysis of growth of yeast cells

For drop-dilution assay, cells were grown overnight in liquid cultures and then diluted and grown further on SD-Leu liquid media to an OD_{600nm} of 1.0. Then, a serial dilution of the cultures in fivefold increments was performed, followed by spotting 5 IL of each diluted culture on solid selective media plates and further growth at 24, 30 or 37 °C for 2–5 days.

To analyse the growth of liquid cultures, cells were inoculated for overnight cultures in 3–5 mL of SD-Leu liquid media and 1 OD_{600nm} unit of cells were harvested on the following day. The cells were resuspended in 1 mL sterile

water. Then, to obtain a starting culture of 0.1 OD_{600nm} of cells per well, 20 IL of cell suspension and 180 IL of the desired medium [S(Gal+0.1%D)-Leu] were pipetted into each well of a round-bottomed 96-well plate. The plate was sealed with a semi-permeable membrane and placed in the SPECTROstar Nano microplate reader. Cells were allowed to grow at 30 °C for up to 72 h, with the OD at 600 nm measured every 10 min after 30 s double orbital shaking at 300 r.p.m. Data obtained were analysed by the MARS software and plotted by Excel.

Recombinant DNA techniques

The DNA sequences encoding Tmb2.3 and Tmb2.17 [38] were synthesised by Eurofins Genomics (Ebersberg, Germany) after optimisation for the codon usage of *S. cerevisiae*. These DNA segments were amplified by PCR with primers containing 5^o EcoRI and 3^o HindIII restriction sites, 5^o yeast Kozak sequence, and a DNA sequence encoding C-terminal HA tag. Subsequently, the PCR products were subcloned into the yeast expression vector pYX142 where the expressed gene is under the control of the *TPI* promoter. To create single amino acid mutations in the b-signal motif of the TMBs, forward and reverse primers were used for site-directed mutagenesis by the standard whole plasmid mutagenesis method. The mutations Q115A and A115Q were introduced using as template pYX142-Tmb2.3-HA or pYX142-Tmb2.17-HA, respectively. Tables S2 and S3 contain the lists of primers and plasmids used in this study, respectively.

Isolation of mitochondria

Mitochondrial fractions were obtained according to an established protocol [47]. Yeast cells were grown in liquid media to logarithmic phase, harvested and resuspended in resuspension buffer (100 mM Tris, 10 mM DTT). Cells were harvested again and resuspended in spheroblasting buffer (1.2 M Sorbitol, 20 mM KPI, pH 7.2) without zymolyase, followed by harvesting. These pellets were gently dissolved in spheroblasting buffer with zymolyase (4.5 mg/g of cells) and incubated at 30 °C for 1 h while shaking at 120 r.p.m. The obtained spheroblasts were dissolved in homogenisation buffer (0.6 M Sorbitol, 10 mM Tris, pH 7.4, 1 mM EDTA, 0.2% fatty acid-free BSA) with 1 mM phenylmethylsulfonyl fluoride (PMSF) and homogenised with a douncer to obtain the whole cell lysate. Cell debris was removed by a clarifying spin (600 g, 5 min, 4 °C), followed by isolation of crude mitochondria (18 000 g, 10 min, 4 °C). The supernatant obtained in this step represents the cytosolic fraction of this separation. Mitochondria were washed once in SEM buffer (250 mM Sucrose, 1 mM EDTA, 10 mM MOPS, pH 7.2) containing 2 mM PMSF and pelleted again (18 000 g, 10 min, 4 °C).

Subcellular fractionation

Mitochondrial fraction and whole cell lysate were obtained as described above. To acquire the cytosolic fraction, the postmitochondrial fraction was clarified by spinning (18 000 g, 15 min, 4 °C) and the supernatant subjected to high-speed centrifugation (200 000 g, 1 h, 4 °C). The resulting supernatant constituted the cytosolic fraction. The sticky, transparent pellet was resuspended in 3 mL SEM buffer containing 2 mM PMSF, homogenised with a douncer and centrifuged at 18 000 g for 20 min at 4 °C. The supernatant of this step constituted of the ER/microsomes fraction.

To obtain highly pure mitochondria, the mitochondrial fraction obtained as described above was layered on a Percoll gradient and centrifuged (80 000 g, 45 min, 4 °C). Mitochondria in the brownish layer at the bottom interface were collected with a Pasteur pipette and washed once in SEM buffer containing 1 mM PMSF and pelleted again (18 000 g, 10 min, 4 °C). The whole cell lysate, ER and cytosolic fractions were precipitated by using chloroform/methanol precipitation method, and all samples, including mitochondria were dissolved in 29 sample buffer (125 mM Tris pH 6.8, 4% SDS, 20% glycerol, 10% 2-mercaptoethanol, 2 mg/mL bromophenol blue) to a concentration of 2 mg/mL. Samples were heated at 95 °C for 10 min and further analysed by SDS-PAGE and immunoblotting.

Protease protection assay

Mitochondria (100 lg) were resuspended in 200 IL of SEM buffer and incubated on ice for 30 min in the presence or absence of 1% Triton-X-100. This was followed by addition of either 10 or 50 lg/mL of proteinase K (PK) or trypsin and further incubation on ice for 30 min. PK was then inhibited by supplementing the reaction with 2 mM PMSF, while trypsin was inhibited by addition of 1 mg/mL of soybean trypsin inhibitor (STI), followed by incubation on ice for 10 min. In the control samples (C), mitochondria were incubated on ice for 30 min with 50 lg/mL of trypsin (in the absence of 1% Triton-X-100), that had been preincubated (10 min) with STI, to block the proteolytic activity of trypsin and serve as an indicator of the inhibitor's efficacy. Samples without Triton were then centrifuged (18 000 g, 15 min, 4 °C), whereas the Triton solubilised samples were subjected to trichloroacetic acid (TCA) precipitation. The precipitated samples and the pellets from samples without Triton were resuspended in 40 IL 29 sample buffer, heated at 95 °C for 10 min and subjected to SDS-PAGE and immunoblotting.

Alkaline (carbonate) extraction

Isolated mitochondria (100 lg) were resuspended in 100 IL of 100 mM Na₂CO₃, pH 11.5 and incubated on ice for

30 min. To separate the membranous pellet fraction and the soluble supernatant fraction, samples were centrifuged (76 000 g, 30 min, 4 °C). Soluble supernatant fractions were subjected to TCA precipitation and the precipitated samples as well as the original pellets were resuspended in 40 IL 29 sample buffer, heated at 95 °C for 10 min and subjected to SDS-PAGE and immunoblotting.

Western blotting and immunodecoration

For analysis of steady-state levels of various proteins, mitochondrial fractions or whole cell lysate and cytosolic fractions (after their precipitation using chloroform/methanol) were dissolved in 29 sample buffer to a concentration of 2 mg/mL. All samples were heated at 95 °C for 10 min and further analysed on 12.5% SDS-PAGE and transferred onto nitrocellulose membranes via semi-dry western blotting. Membranes were blocked with 5% skimmed milk (in TBS buffer), incubated with primary antibodies, washed and then incubated with horseradish peroxidase-conjugated goat anti-rabbit or goat anti-rat secondary antibodies. The antibodies used in this study are listed in Table S4.

Blue native (BN)-PAGE

Isolated mitochondria (100 lg) were washed with SEM buffer and spun (20 000 g, 10 min, 4 °C). The pellets were solubilised with a digitonin-containing buffer (1% digitonin in 20 mM Tris, 0.1 mM EDTA, 50 mM NaCl, 10% glycerol, pH 7.4) for 30 min on ice, followed by a clarifying spin (13 000 g, 10 min, 4 °C). The supernatant was mixed with 109 sample buffer (5% [w/v] Coomassie brilliant blue G-250, 100 mM Bis-Tris, 500 mM 6-aminocaproic acid, pH 7.0) and analysed on a gel containing 6%–14% gradient of acrylamide. Proteins were blotted onto polyvinylidene fluoride (PVDF) membrane and detected by immunodecoration. Not available from the instrument specifications (Thermo Scientific, Thermo Fisher Scientific, Carlsbad, CA, USA) was used as molecular weight markers.

Author contributions

AM designed and performed the majority of experiments, analysed the data, prepared the figures and wrote the manuscript. VT designed and performed some experiments and helped in preparing the figures. DR designed experiments, analysed the data, supervised the overall project, acquired funding and wrote the manuscript.

Acknowledgements

We thank Elena Kracker for excellent technical assistance and Dr. Klaudia K. Maruszczak for technical help, critical inputs and insightful discussions. We thank Dr. Kai S.

Dimmer for helpful suggestions and critical comments on the manuscript. Our work is supported by the Deutsche Forschungsgemeinschaft (RA1028/8-2 to DR) and the IMPRS 'From Molecules to Organisms' (AM). Open Access funding enabled and organized by Projekt DEAL.

Conflict of interest statement

The authors declare that the research was conducted in the absence of any commercial or financial relationships that could be construed as a potential conflict of interest.

Peer review

The peer review history for this article is available at <https://www.webofscience.com/api/gateway/wos/peer-review/10.1111/febs.16950>.

Data availability statement

The data that supports the findings of this study are available in Figs 1–9 and the supplementary material of this article. Further raw data that support the findings of this study are available from the corresponding author [doron.rapaport@uni-tuebingen.de] upon reasonable request.

References

- Paschen SA, Neupert W & Rapaport D (2005) Biogenesis of b-barrel membrane proteins of mitochondria. *Trends Biochem Sci* 30, 575–582.
- Pereira J & Lupas AN (2018) The origin of mitochondria-specific outer membrane b-barrels from an ancestral bacterial fragment. *Genome Biol Evol* 10, 2759–2765.
- Wimley WC (2003) The versatile b-barrel membrane protein. *Curr Opin Struct Biol* 13, 404–411.
- Gray MW, Burger G & Lang BF (1999) Mitochondrial Evolution. *Science* 283, 1476–1481.
- Schleiff E, Eichacker LA, Eckart K, Becker T, Mirus O, Stahl T & Soll J (2003) Prediction of the plant b-barrel proteome: a case study of the chloroplast outer envelope. *Protein Sci* 12, 748–759.
- Young MJ, Bay DC, Hausner G & Court DA (2007) The evolutionary history of mitochondrial porins. *BMC Evol Biol* 7, 31.
- Gray MW (1999) Evolution of organellar genomes. *Curr Opin Genet Dev* 9, 678–687.
- Soll J & Schleiff E (2004) Protein import into chloroplasts. *Nat Rev Mol Cell Biol* 5, 198–208.
- Diederichs KA, Buchanan SK & Botos I (2021) Building better barrels - b-barrel biogenesis and insertion in bacteria and mitochondria. *J Mol Biol* 433, 166894.
- Ulrich T & Rapaport D (2015) Biogenesis of beta-barrel proteins in evolutionary context. *Int J Med Microbiol* 305, 259–264.
- Lundquist K, Billings E, Bi M, Wellnitz J & Noinaj N (2021) The assembly of b-barrel membrane proteins by BAM and SAM. *Mol Microbiol* 115, 425–435.
- Jores T, Lawatscheck J, Beke V, Franz-Wachtel M, Yunoki K, Fitzgerald JC, Macek B, Endo T, Kalbacher H, Buchner J *et al.* (2018) Cytosolic Hsp70 and Hsp40 chaperones enable the biogenesis of mitochondrial b-barrel proteins. *J Cell Biol* 217, 3091–3108.
- Rapaport D & Neupert W (1999) Biogenesis of Tom40, core component of the TOM complex of mitochondria. *J Cell Biol* 146, 321–331.
- Schleiff E, Silviu JR & Shore GC (1999) Direct membrane insertion of voltage-dependent anion-selective channel protein catalyzed by mitochondrial Tom20. *J Cell Biol* 145, 973–978.
- Krimmer T, Rapaport D, Ryan MT, Meisinger C, Kassenbrock CK, Blachly-Dyson E, Forte M, Douglas MG, Neupert W, Nargang FE *et al.* (2001) Biogenesis of porin of the outer mitochondrial membrane involves an import pathway via receptors and the general import pore of the TOM complex. *J Cell Biol* 152, 289–300.
- Yamano K, Yatsukawa Y, Esaki M, Hobbs AE, Jensen RE & Endo T (2008) Tom20 and Tom22 share the common signal recognition pathway in mitochondrial protein import. *J Biol Chem* 283, 3799–3807.
- Jores T, Klinger A, Groß LE, Kawano S, Flinner N, Duchardt-Ferner E, Wöhrner J, Kalbacher H, Endo T, Schleiff E *et al.* (2016) Characterization of the targeting signal in mitochondrial b-barrel proteins. *Nat Commun* 7, 12036.
- Klinger A, Gosch V, Bodensohn U, Ladig R & Schleiff E (2019) The signal distinguishing between targeting of outer membrane b-barrel protein to plastids and mitochondria in plants. *Biochim Biophys Acta Mol Cell Res* 1866, 663–672.
- Bausewein T, Mills DJ, Langer JD, Nitschke B, Nussberger S & Kuhlbrandt W (2017) Cryo-EM structure of the TOM Core complex from *Neurospora crassa*. *Cell* 170, 693–700.e7.
- Araiso Y, Tsutsumi A, Qiu J, Imai K, Shiota T, Song J, Lindau C, Wenz L-S, Sakaue H, Yunoki K *et al.* (2019) Structure of the mitochondrial import gate reveals distinct preprotein paths. *Nature* 575, 395–401.
- Tucker K & Park E (2019) Cryo-EM structure of the mitochondrial protein-import channel TOM complex at near-atomic resolution. *Nat Struct Mol Biol* 26, 1158–1166.
- Wiedemann N, Kozjak V, Chacinska A, Schönfisch B, Rospert S, Ryan MT, Pfanner N & Meisinger C (2003) Machinery for protein sorting and assembly in the mitochondrial outer membrane. *Nature* 424, 565–571.
- Wiedemann N, Truscott KN, Pfannschmidt S, Guiard B, Meisinger C & Pfanner N (2004) Biogenesis of THE

- protein import channel Tom40 of THE mitochondrial outer membrane: INTERMEMBRANE SPACE COMPONENTS ARE INVOLVED IN AN EARLY STAGE OF THE ASSEMBLY PATHWAY*. *J Biol Chem* 279, 18188–18194.
- 24 Habib SJ, Waizenegger T, Lech M, Neupert W & Rapaport D (2005) Assembly of the TOB complex of mitochondria*. *J Biol Chem* 280, 6434–6440.
 - 25 Habib SJ, Waizenegger T, Niewianda A, Paschen SA, Neupert W & Rapaport D (2006) The N-terminal domain of Tob55 has a receptor-like function in the biogenesis of mitochondrial b-barrel proteins. *J Cell Biol* 176, 77–88.
 - 26 Kutik S, Stojanovski D, Becker L, Becker T, Meinecke M, Kru€ger V, Prinz C, Meisinger C, Guiard B, Wagner R *et al.* (2008) Dissecting membrane insertion of mitochondrial b-barrel proteins. *Cell* 132, 1011–1024.
 - 27 Ho€hr AIC, Lindau C, Wirth C, Qiu J, Stroud DA, Kutik S, Guiard B, Hunte C, Becker T, Pfanner N *et al.* (2018) Membrane protein insertion through a mitochondrial b-barrel gate. *Science* 359, eaah6834.
 - 28 Takeda H, Tsutsumi A, Nishizawa T, Lindau C, Busto JV, Wenz L-S, Ellenrieder L, Imai K, Straub SP, Mossmann W *et al.* (2021) Mitochondrial sorting and assembly machinery operates by b-barrel switching. *Nature* 590, 163–169.
 - 29 Jores T & Rapaport D (2017) Early stages in the biogenesis of eukaryotic b-barrel proteins. *FEBS Lett* 591, 2671–2681.
 - 30 Moitra A & Rapaport D (2021) The biogenesis process of VDAC – from early cytosolic events to its final membrane integration. *Front Physiol* 12, 732742.
 - 31 Waizenegger T, Habib SJ, Lech M, Mokranjac D, Paschen SA, Hell K, Neupert W & Rapaport D (2004) Tob38, a novel essential component in the biogenesis of beta-barrel proteins of mitochondria. *EMBO Rep* 5, 704–709.
 - 32 Gross LE, Klinger A, Spies N, Ernst T, Flinner N, Simm S, Ladig R, Bodensohn U & Schleiff E (2021) Insertion of plastidic b-barrel proteins into the outer envelopes of plastids involves an intermembrane space intermediate formed with Toc75-V/OEP80. *Plant Cell* 33, 1657–1681.
 - 33 Lee J, Kim DH & Hwang I (2014) Specific targeting of proteins to outer envelope membranes of endosymbiotic organelles, chloroplasts, and mitochondria. *Front Plant Sci* 5, 173.
 - 34 Walther DM, Papic D, Bos MP, Tommassen J & Rapaport D (2009) Signals in bacterial beta-barrel proteins are functional in eukaryotic cells for targeting to and assembly in mitochondria. *Proc Natl Acad Sci USA* 106, 2531–2536.
 - 35 Ulrich T, Gross LE, Sommer MS, Schleiff E & Rapaport D (2012) Chloroplast b-barrel proteins are assembled into the mitochondrial outer membrane in a process that depends on the TOM and TOB complexes. *J Biol Chem* 287, 27467–27479.
 - 36 Ulrich T, Oberhettinger P, Schu€tz M, Holzer K, Ramms AS, Linke D, Autenrieth IB & Rapaport D (2014) Evolutionary conservation in biogenesis of b-barrel proteins allows mitochondria to assemble a functional bacterial trimeric autotransporter protein*. *J Biol Chem* 289, 29457–29470.
 - 37 Natarajan J, Moitra A, Zabel S, Singh N, Wagner S & Rapaport D (2019) Yeast can express and assemble bacterial secretins in the mitochondrial outer membrane. *Microb Cell* 7, 15–27.
 - 38 Vorobieva AA, White P, Liang B, Horne JE, Bera AK, Chow CM, Gerben S, Marx S, Kang A, Stiving AQ *et al.* (2021) *De novo* design of transmembrane b barrels. *Science* 371, eabc8182.
 - 39 Wiedemann N & Pfanner N (2017) Mitochondrial machineries for protein import and assembly. *Annu Rev Biochem* 86, 685–714.
 - 40 Neupert W & Herrmann JM (2007) Translocation of proteins into mitochondria. *Annu Rev Biochem* 76, 723–749.
 - 41 Wein€aupl K, Lindau C, Hessel A, Wang Y, Schu€tze C, Jores T, Melchionda L, Scho€nfisch B, Kalbacher H, Bersch B *et al.* (2018) Structural basis of membrane protein chaperoning through the mitochondrial intermembrane space. *Cell* 175, 1365.e25–1379.e25.
 - 42 Habib SJ, Waizenegger T, Niewianda A, Paschen SA, Neupert W & Rapaport D (2007) The N-terminal domain of Tob55 has a receptor-like function in the biogenesis of mitochondrial beta-barrel proteins. *J Cell Biol* 176, 77–88.
 - 43 Madeira F, Pearce M, Tivey ARN, Basutkar P, Lee J, Edbali O, Madhusoodanan N, Kolesnikov A & Lopez R (2022) Search and sequence analysis tools services from EMBL-EBI in 2022. *Nucleic Acids Res* 50, W276–W279.
 - 44 Kozjak V, Wiedemann N, Milenkovic D, Lohaus C, Meyer HE, Guiard B, Meisinger C & Pfanner N (2003) An essential role of Sam50 in the protein sorting and assembly machinery of the mitochondrial outer membrane. *J Biol Chem* 278, 48520–48523.
 - 45 Gietz RD & Woods RA (2006) Yeast transformation by the LiAc/SS carrier DNA/PEG method. *Methods Mol Biol* 313, 107–120.
 - 46 Paschen SA, Waizenegger T, Stan T, Preuss M, Cyrklaff M, Hell K, Rapaport D & Neupert W (2003) Evolutionary conservation of biogenesis of beta-barrel membrane proteins. *Nature* 426, 862–866.
 - 47 Daum G, Bo€hni PC & Schatz G (1982) Import of proteins into mitochondria. Cytochrome b2 and cytochrome c peroxidase are located in the intermembrane space of yeast mitochondria. *J Biol Chem* 257, 13028–13033.

Supporting information

Additional supporting information may be found online in the Supporting Information section at the end of the article.

Table S1. Yeast strains used in this study.

Table S2. Primers used in this study.

Table S3. Plasmids used in this study.

Table S4. Antibodies used in this study.